Un mécanisme commun peut-il sous-tendre l'horloge moléculaire de la microglie et l'activité neuronale dans le contrôle du métabolisme et de la mémoire ?

Xiao-Lan Wang

UNIVERSITÉ DE STRASBOURG

France

UNIVERSITÉ D'AMSTERDAM

Pays-Bas

ÉCOLE DOCTORALE DES SCIENCES DE LA VIE DE LA SANTE (ED414)

Laboratoire de Neurosciences Cognitives et Adaptatives

THÈSE présentée par : Xiaolan Wang

soutenue le : **18 May 2021**

pour obtenir le grade de : **Docteur de l'université de Strasbourg**
&
Docteur de l'université d'Amsterdam

Discipline/ Spécialité : Sciences du vivant/Neurosciences

Un mécanisme commun peut-il sous-tendre l'horloge moléculaire de la microglie et l'activité neuronale dans le contrôle du métabolisme et de la mémoire ?

THÈSE dirigée par (co-tutelle) :	
BOUTILLIER Anne-Laurence	Directeur de Recherche CNRS, Université de Strasbourg
KALSBEEK Andries	Professeur, Université d'Amsterdam
Co-promoter :	
YI Chun-Xia	Docteur, Université d'Amsterdam
RAPPORTEURS EXTERNES :	
BLUM David	Directeur de Recherche INSERM, Université de Lille
KOROSI Aniko	Docteur, Université d'Amsterdam
EXAMINATEUR INTERNE :	
DUPUIS Luc	Directeur de Recherche INSERM, Université de Strasbourg
AUTRES MEMBRES DU JURY :	
MATHIS Chantal	Directeur de Recherche CNRS, Université de Strasbourg
LA FLEUR Suzanne	Professeur, Université d'Amsterdam

Cleanup at the right time: a common mechanism underlies the molecular clock of microglia and neuronal activity in metabolic and memory control

This project was financially supported by the Neurotime Erasmus Mundus Fellowship for PhD ; University of Strasbourg, CNRS and ANR-18-CE16-0008 (to ALB).

Cleanup at the right time: a common mechanism underlies the molecular clock of microglia and neuronal activity in metabolic and memory control

ACADEMISCH PROEFSCHRIFT

ter verkrijging van de graad van doctor

aan de Universiteit van Amsterdam

op gezag van de Rector Magnificus

prof. dr. ir. K.I.J. Maex

ten overstaan van een door het college voor promoties ingestelde commissie

in het openbaar te verdedigen in het

Laboratoire de Neurosciences Cognitives et Adaptatives de Strasbourg

op dinsdag 18 mei 2021, te 13.30 uur

door

XIAOLAN WANG

geboren te Nanyang

PROMOTIECOMMISSIE:

Promotor(es) :	Prof. Dr. A. Kalsbeek	AMC-UvA
	Dr. A. Boutillier	Université de Strasbourg
Copromotor(es) :	Dr. C. Yi	AMC-UvA
Overige leden :	Prof. Dr. S.E. la Fleur	AMC-UvA
	Dr. A. Korosi	AMC-UvA
	Dr. L. Dupuis	Université de Strasbourg
	Dr. C. Mathis	Université de Strasbourg
	Dr. D. Blum	Université de Lille

Faculteit der Geneeskunde

Dit proefschrift is tot stand gekomen in het kader van het NeuroTime programma, een Erasmus Mundus Joint Doctorate, met als doel het behalen van een gezamenlijk doctoraat. Het proefschrift is voorbereid in: het Nederlands Herseninstituut en in het Amsterdam Universitair Medisch Centrum (AUMC), Faculteit der Geneeskunde, van de Universiteit van Amsterdam; en in het Laboratorium voor Cognitieve en Adaptieve Neurowetenschap (LNCA) van de Université de Strasbourg.

This thesis has been written within the framework of the NeuroTime program, an Erasmus Mundus Joint Doctorate, with the purpose of obtaining a joint doctorate degree. The thesis was prepared in: the Netherlands Institute for Neuroscience (NIN) and in the Amsterdam University Medical Center (AUMC), Faculty of Medicine at the University of Amsterdam; and in the Laboratoire de Neurosciences Cognitives et Adaptative (LNCA) of the Université de Strasbourg.

Contents

Principal Abbreviations

AAV	adeno-associated virus
AgRP	agouti-related peptide
AM	amygdala
AMPA	α-amino-3-hydroxy-5-methyl-4-isoxazolepropionic acid
AP	area postrema
ARC	Arcuate nucleus
ARNTL	Aryl hydrocarbon receptor nuclear translocator-like protein 1
BBB	blood brain barrier
BDNF	brain-derived neurotrophic factor
bHLH	basic helix-loop-helix
Bmal1	brain and muscle ARNT-like 1
CART	cocaine- and amphetamine-regulated transcript
CC	corpus callosum
CCK	cholecystokinin
CCL2	chemokine ligand 2
CCX	cerebral cortex
Clock	circadian locomotor output cycles Kaput
CNS	central nervous system
CR	complement receptor
CRH	corticotropin-releasing hormone
Cry1	cryptochrome 1
Cry2	cryptochrome 2
CSF1	Colony-stimulating factor-1
Csf1r	Colony-stimulating factor-1 receptor 1
CVO	circumventricular organ
CX3CL1	C-X3-C motif chemokine ligand 1
CX3CR1	C-X3-C motif chemokine receptor 1
DIO	diet-induced obesity
DMN	dorsomedial nucleus
ECM	extracellular matrix
ECS	endocannabinoid systems
FX	fornix
GABA	gamma-aminobutyric acid

GIT	gastrointestinal tract
GLP-1	glucagon-like peptide-1
HFD	high-fat diet
HCHF	high-carbohydrate high-fat diet
HO-1	heme oxygenase
Iba1	ionized calcium binding adaptor molecule 1
IGF-1	insulin-like growth factor 1
IL-10	interleukin-10
IL-1β	interleukin-1β
IL-34	interleukin-34
IL-4	interleukin-4
IL-6	interleukin-6
InsR	insulin receptors
LepRs	leptin receptors
LH	lateral hypothalamus
LHA	lateral hypothalamic area
LPL	lipoprotein lipase
LPS	Lipopolysaccharide
LTP	long-term potentiation
MBH	mediobasal hypothalamus
ME	median eminence
mGlutR2	glutamate metabotropic receptor 2
MMP	matrix metallopeptidase
NA	neuraminidase
NLRs	NOD-like receptors
NO	nitric oxide
NPAS2	Neuronal PAS domain containing protein 2
NPCs	neural precursor cells
NPY	neuropeptide Y
Nr1d1	nuclear receptor subfamily 1, group D, member 1
Nr1d2	nuclear receptor subfamily 1, group D, member 2
Nr1f1	nuclear receptor subfamily 1, group F, member 1
NT	neurotensin
NTS	nucleus of the solitary tract
OC	optic chiasm

OX1 orexin receptor 1
OXM oxyntomodulin
Per1 period 1
Per2 period 2
PFA perifornical area
POMC proopiomelanocortin
PP pancreatic polypeptide
PVN paraventricular nucleus
PVT the paraventricular thalamus
PYY peptide tyrosine tyrosine,
ROS reactive oxygen species
SCN suprachiasmatic nucleus
SE septum
SFAs saturated fatty acids
SGZ subgranular zone
Sirt1 sirtuin 1
SVZ subventricular zone
TGF-β Transforming growth factor beta 1
TH thalamus
TLR4 toll-like receptor-4
TNFα Tumor necrosis factor alpha
TREM2 triggering receptor expressed on myeloid cells 2
TRH thyrotrophin-releasing factor
TTFLs transcription-translation feedback loops
VMN ventromedial nucleus
VTA ventral tegmental area
α-MSH alpha-melanocyte-stimulating hormone

General Framework of the Thesis

General Framework of the Thesis

The brain acts as the control center throughout the body and precisely regulates biological functions via particular cells in specific brain regions. For example, the hippocampal pyramidal neurons are involved in regulating learning and memory processes and the hypothalamic anorexigenic proopiomelanocortin (POMC) neurons play a key role in the control of energy homeostasis. Signal transmission within neural circuits is an essential characteristic of brain functioning. Axons transmit signals from one neuron to others via specialized junctions called synapses. Neurons and synapses are the structural foundation of brain functions, but their formation is affected by the complex behaviors and changes in their micro-environment. For example, learning activity induces synaptic modification, which is the primary mechanism for memory formation (Caroni et al., 2014a; Wu et al., 2015) and high-fat diet (HFD) induced obese rodents and humans show a decreased number of POMC neurons (Thaler et al., 2012c). However, neurons are not the only cells driving brain functions and our knowledge on the role of these other cell types, among which glial cells such as astrocytes and microglia, in these functions, is rapidly increasing.

The maintenance of an optimal micro-environment and neural circuits relies on microglia, the extremely dynamic and sensitive innate immune cells in the brain, even in the resting state. For example, microglia continuously extend and retract their processes to scan the brain parenchyma, interact with dendritic spines, and sense neuronal activity; increased neuronal activity will trigger the enhanced movement of microglial processes (Dissing-Olesen et al., 2014; Nimmerjahn et al., 2005). As the major immune cell in the brain, microglia not only phagocytose apoptotic cells, cellular debris, unwanted synapses, and pathogens, but they also release inflammatory cytokines (such as IL-1β, IL-6, TNFa, and IL-10) and neurotrophic factors (such as BDNF, IGF-1, and TGF-β) to affect neuronal populations and connections. Thus, microglia provide surveillance and scavenging functions to optimize the surrounding micro-environment and shape neural circuits.

The microglial phagocytosis of synapses plays an active role in synapses maturation (Paolicelli et al., 2011b; Schafer et al., 2012) and disruption of this process results in deficits in synaptic connectivity (Mallya et al., 2019; Schafer et al., 2013; Schafer and Stevens, 2013). Recent evidence shows that microglia also has an important role in synapse formation and neurogenesis during CNS development (Miyamoto et al., 2016b; Weinhard et al., 2018a). We have reported that microglial activation is involved in the HFD-induced loss of hypothalamic

anorexigenic POMC neurons (Gao et al., 2017a). Aberrant microglial phagocytosis is associated with obesity, as well as neurodegenerative and psychiatric diseases (Gao et al., 2017a; Zhan et al., 2014). Moreover, microglial activity shows a daily variation, with higher activity during the daily active phase in lean rats (Yi et al., 2017a). Also, the microglial immune response to lipopolysaccharide (LPS) is time-dependent (Fonken et al., 2015a). Furthermore, microglia phagocytose more synapses at the onset of the light phase than at the onset of the dark phase, which is in line with synaptic protein expression in the prefrontal cortex (Choudhury et al., 2020a).

The circadian timing system is an internal timekeeping system, which plays a crucial role in the control of cellular processes, and subsequently affects overall physiological functions (Bass and Takahashi, 2010b; Early et al., 2018b; Gabriel and Zierath, 2019b). For example, skeletal muscle clock gene deficiency disturbs nutrient utilization and leads to metabolic disorders (Gabriel and Zierath, 2019a; Schiaffino et al., 2016; Stenvers et al., 2019a). Clock genes in macrophages and microglia modulate the production of cytokines, following an immune challenge (Griffin et al., 2019; Nakazato et al., 2017; Sato et al., 2014). It has been known that immune activity is highly dependent on cellular metabolic processes (Geltink et al., 2018; Vijayan et al., 2019; Wang et al., 2019a); reduced glucose or lipid utilization inhibits microglial activation and inflammation (Gao et al., 2017b; Wang et al., 2019a).

In the first study presented in this thesis manuscript, we investigated the hypothesis that the intrinsic clock - Bmal1 plays an important role in regulating microglial functions, and finally affects synaptic plasticity in the hippocampus during learning and memory processes and energy homeostasis as controlled by the hypothalamus. We generated microglia-specific Bmal1 knockdown (microglia$^{Bmal1\text{-KD}}$) mice and evaluated the metabolic phenotype and memory performance. We also tested microglial phagocytic capacity and neuronal morphology under HFD and during cognitive processes in these mice.

In the second study presented in this thesis manuscript, we investigated the hypothesis that Bmal1 may regulate microglial immune function through modulation of cellular metabolism. We used global Bmal1 knocked out mice and studied the expression of clock genes, inflammation-related genes, and cellular metabolic-related genes in isolated microglial cells. Next, we evaluated the expression of these genes in Bmal1 knockdown microglial BV-2 cells under LPS and palmitic acid-induced inflammation.

In the third study presented in this thesis manuscript, we investigated the hypothesis that Rev-erbα, a nuclear receptor has profound effects on molecular clock, metabolism and also

plays an important role in neuroinflammation. SR9011, an agonist of Rev-erbα disrupts circadian rhythm by altering intracellular clock machinery. We hypothesized that SR9011 had a detrimental impact on microglial immunometabolic functions. To evaluate the effect of SR9011 on microglial immunometabolism, we checked the immune response, phagocytic activity, and mitochondria function on primary microglia which were isolated from 1-3 days old Sprague-Dawley rat pups.

Disruption of immunometabolism is a key process involved in the progression of obesity. HFD leads to microglial activation. However, how HFD affects the daily rhythmicity of microglial circadian, immune, and metabolic function is still unknown. Therefore, in the fourth study presented in this thesis manuscript, we investigated the hypothesized that HFD disturbs microglial immunometabolism in a day/night-dependent manner in obese rats. Obesity was induced in Wistar rats by feeding them HFD *ad libitum* for 8 weeks. Microglia were isolated from HFD-and chow-fed control animals at six-time points during 24 h [every 4 h starting 2 h after lights on]. The circadian clock, inflammatory functions, substrate utilization, and energy production were evaluated using quantitative RT-PCR.

Microglia play an important role in the regulation of synaptic plasticity and its activation-induced neuroinflammation contributes to memory impairment in Alzheimer's disease. Histone acetylations are also key players in memory processes and in regulating the neuroprotection/neurodegeneration balance. Lastly, in the fifth study, we investigated the gliosis and epigenetic changes in post-mortem brains from Alzheimer's disease patients. Two brain regions were investigated: the F2 area of the frontal cortex and the hippocampus.

References

Bass, J., and Takahashi, J.S. (2010). Circadian integration of metabolism and energetics. Science *330*, 1349-1354.

Caroni, P., Chowdhury, A., and Lahr, M. (2014). Synapse rearrangements upon learning: from divergent-sparse connectivity to dedicated sub-circuits. Trends in Neurosciences *37*, 604-614.

Choudhury, M.E., Miyanishi, K., Takeda, H., Islam, A., Matsuoka, N., Kubo, M., Matsumoto, S., Kunieda, T., Nomoto, M., Yano, H.*, et al.* (2020). Phagocytic elimination of synapses by microglia during sleep. Glia *68*, 44-59.

Dissing-Olesen, L., LeDue, J.M., Rungta, R.L., Hefendehl, J.K., Choi, H.B., and MacVicar, B.A. (2014). Activation of Neuronal NMDA Receptors Triggers Transient ATP-Mediated Microglial Process Outgrowth. Journal of Neuroscience *34*, 10511-10527.

Early, J.O., Menon, D., Wyse, C.A., Cervantes-Silva, M.P., Zaslona, Z., Carroll, R.G., Palsson-McDermott, E.M., Angiari, S., Ryan, D.G., Corcoran, S.E.*, et al.* (2018). Circadian clock protein BMAL1 regulates IL-1beta in macrophages via NRF2. Proc Natl Acad Sci U S A *115*, E8460-E8468.

Fonken, L.K., Frank, M.G., Kitt, M.M., Barrientos, R.M., Watkins, L.R., and Maier, S.F. (2015). Microglia inflammatory responses are controlled by an intrinsic circadian clock. Brain Behav Immun *45*, 171-179.

Gabriel, B.M., and Zierath, J.R. (2019a). Circadian rhythms and exercise - re-setting the clock in metabolic disease. Nat Rev Endocrinol *15*, 197-206.

Gao, Y., Vidal-Itriago, A., Kalsbeek, M.J., Layritz, C., Garcia-Caceres, C., Tom, R.Z., Eichmann, T.O., Vaz, F.M., Houtkooper, R.H., van der Wel, N.*, et al.* (2017a). Lipoprotein Lipase Maintains Microglial Innate Immunity in Obesity. Cell Rep *20*, 3034-3042.

Geltink, R.I.K., Kyle, R.L., and Pearce, E.L. (2018). Unraveling the Complex Interplay Between T Cell Metabolism and Function. Annual Review of Immunology, Vol 36 *36*, 461-488.

Griffin, P., Dimitry, J.M., Sheehan, P.W., Lananna, B.V., Guo, C., Robinette, M.L., Hayes, M.E., Cedeno, M.R., Nadarajah, C.J., Ezerskiy, L.A.*, et al.* (2019). Circadian clock protein Rev-erba regulates neuroinflammation. P Natl Acad Sci USA *116*, 5102-5107.

Mallya, A.P., Wang, H.D., Lee, H.N.R., and Deutch, A.Y. (2019). Microglial Pruning of Synapses in the Prefrontal Cortex During Adolescence. Cereb Cortex *29*, 1634-1643.

Miyamoto, A., Wake, H., Ishikawa, A.W., Eto, K., Shibata, K., Murakoshi, H., Koizumi, S., Moorhouse, A.J., Yoshimura, Y., and Nabekura, J. (2016). Microglia contact induces synapse formation in developing somatosensory cortex. Nat Commun *7*, 12540.

Nakazato, R., Hotta, S., Yamada, D., Kou, M., Nakamura, S., Takahata, Y., Tei, H., Numano, R., Hida, A., Shimba, S.*, et al.* (2017). The intrinsic microglial clock system regulates interleukin-6 expression. Glia *65*, 198-208.

Nimmerjahn, A., Kirchhoff, F., and Helmchen, F. (2005). Resting microglial cells are highly dynamic surveillants of brain parenchyma in vivo. Science *308*, 1314-1318.

Paolicelli, R.C., Bolasco, G., Pagani, F., Maggi, L., Scianni, M., Panzanelli, P., Giustetto, M., Ferreira, T.A., Guiducci, E., Dumas, L.*, et al.* (2011). Synaptic pruning by microglia is necessary for normal brain development. Science *333*, 1456-1458.

Sato, S., Sakurai, T., Ogasawara, J., Takahashi, M., Izawa, T., Imaizumi, K., Taniguchi, N., Ohno, H., and Kizaki, T. (2014). A circadian clock gene, Rev-erbalpha, modulates the inflammatory function of macrophages through the negative regulation of Ccl2 expression. J Immunol *192*, 407-417.

Schafer, D.P., Lehrman, E.K., Kautzman, A.G., Koyama, R., Mardinly, A.R., Yamasaki, R., Ransohoff, R.M., Greenberg, M.E., Barres, B.A., and Stevens, B. (2012). Microglia sculpt postnatal neural circuits in an activity and complement-dependent manner. Neuron *74*, 691-705.

Schafer, D.P., Lehrman, E.K., and Stevens, B. (2013). The "quad-partite" synapse: microglia-synapse interactions in the developing and mature CNS. Glia *61*, 24-36.

Schafer, D.P., and Stevens, B. (2013). Phagocytic glial cells: sculpting synaptic circuits in the developing nervous system. Curr Opin Neurobiol *23*, 1034-1040.

Schiaffino, S., Blaauw, B., and Dyar, K.A. (2016). The functional significance of the skeletal muscle clock: lessons from Bmal1 knockout models. Skelet Muscle *6*, 33.

Stenvers, D.J., Scheer, F., Schrauwen, P., la Fleur, S.E., and Kalsbeek, A. (2019). Circadian clocks and insulin resistance. Nat Rev Endocrinol *15*, 75-89.

Thaler, J.P., Yi, C.X., Schur, E.A., Guyenet, S.J., Hwang, B.H., Dietrich, M.O., Zhao, X.L., Sarruf, D.A., Izgur, V., Maravilla, K.R.*, et al.* (2012). Obesity is associated with hypothalamic injury in rodents and humans (vol 122, pg 153, 2012). Journal of Clinical Investigation *122*, 778-778.

Vijayan, V., Pradhan, P., Braud, L., Fuchs, H.R., Gueler, F., Motterlini, R., Foresti, R., and Immenschuh, S. (2019). Human and murine macrophages exhibit differential metabolic responses to lipopolysaccharide - A divergent role for glycolysis. Redox Biol *22*, 101147.

Wang, L., Pavlou, S., Du, X., Bhuckory, M., Xu, H., and Chen, M. (2019). Glucose transporter 1 critically controls microglial activation through facilitating glycolysis. Mol Neurodegener *14*, 2.

Weinhard, L., di Bartolomei, G., Bolasco, G., Machado, P., Schieber, N.L., Neniskyte, U., Exiga, M., Vadisiute, A., Raggioli, A., Schertel, A.*, et al.* (2018). Microglia remodel synapses by presynaptic trogocytosis and spine head filopodia induction. Nat Commun *9*, 1228.

Wu, Y., Dissing-Olesen, L., MacVicar, B.A., and Stevens, B. (2015). Microglia: Dynamic Mediators of Synapse Development and Plasticity. Trends Immunol *36*, 605-613.

Yi, C.X., Walter, M., Gao, Y., Pitra, S., Legutko, B., Kalin, S., Layritz, C., Garcia-Caceres, C., Bielohuby, M., Bidlingmaier, M.*, et al.* (2017). TNFalpha drives mitochondrial stress in POMC neurons in obesity. Nat Commun *8*, 15143.

Zhan, Y., Paolicelli, R.C., Sforazzini, F., Weinhard, L., Bolasco, G., Pagani, F., Vyssotski, A.L., Bifone, A., Gozzi, A., Ragozzino, D.*, et al.* (2014). Deficient neuron-microglia signaling results in impaired functional brain connectivity and social behavior. Nat Neurosci *17*, 400-406.

General Introduction

1. Learning and Memory

1.1. Brief History

Learning and memory are closely connected and depend on each other. Learning is a process of acquiring new information and modifying subsequent behavior. Memory is a process of encoding, storage, and retrieval of information. Memory provides the framework to link new knowledge, which is essential to learning. The question of what is the nature of memory has existed for thousands of years back to the ancient philosophers. However, a truly systematic, quantified, and rigorous assessment of the memory only started from the end of the nineteenth century. Whether memory is stored in the brain and where exactly each memory is stored were first asked by neuropsychologists such as Carl Lashley (1890–1958). Lashley trained rats to run through a maze and then removed parts of their brain (1950). After recovery from the surgery, probe test was performed into the maze. However, no matter what part of the brain was removed, the lesioned rats still performed better than control rats that were the first time in the maze. How much tissue had been removed was more important than where is the lesion. Lashley concluded that memory traces, which he called engrams, were not localized in one part of the brain but were distributed throughout the cortex (Radvansky, 2017). Also Donald Hebb (1904-1985), one of the pioneers of computational neuroscience, tried to understand how the learning and memory works. According to Hebb's theory - Hebbian learning, memories are encoded in the nervous system in a two-stage process. During the first stage, neural excitation would reverberate around in cell assemblies and stimulate the corresponding cells for a while. During the second stage, the interconnections among the neurons would physically change, such as some connections becoming stronger (Hebb and Konzett 1949). This hypothesis is similar to the current idea of long-term potentiation (LTP).

1.2. Memory Process

As mention earlier the memory process includes encoding, storage, and retrieval of the information. Encoding is the first step, but also present throughout the memory process. It links the information to existing knowledge. This information is stored sequentially in three memory systems: sensory memory, short-term memory, and long-term memory. Sensory memory is generated automatically, and has a huge capacity to process information, but lasts

less than a second. Some of the sensory memory can transfer to short-term memory, which has a limited capacity and retains the information for 30-45 seconds. During this period, part of the information can be retrieved. Working memory is a kind of short-term memory, including not only temporary storage of the information but also manipulation of the information (Kent, 2016). The prefrontal cortex plays a fundamental role in the working memory (Figure 1).

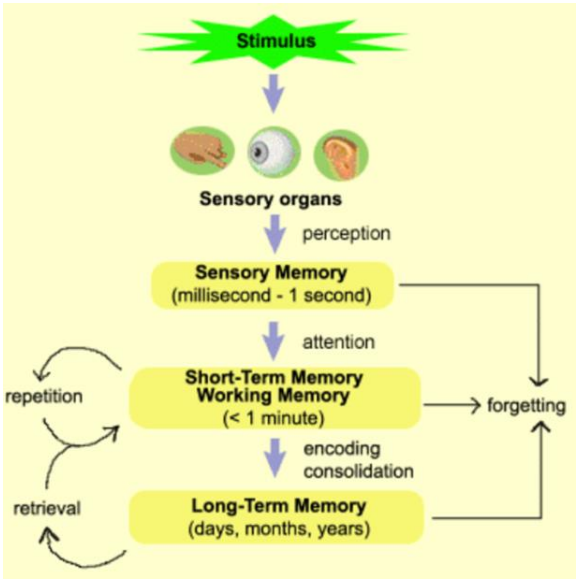

Figure 1. Memory process and forms of storage. The information is stored as sensory memory, short-term memory, and long-term memory according to chronological sequence. Adapted from thebrain.mcgill.ca.

Repetition of the information in short-term memory can finally transfer it to long-term memory. Long-term memory has unlimited storage capacity and information can remain for a long time, sometimes even the entire life. However, information can also be forgotten. The hippocampus, medial temporal lobes, and other structures that are connected to the limbic system are involved in the consolidation of long-term memory. The process of getting information out of the memory is known as retrieval, including recognition and recall, which are used to answer questions, perform tasks, make decisions, and interact with others. During this process, information stored in the long-term memory presents as working memory. The recognition process is initiated by a cue or even a part of the object that has previously been experienced. Recognition compares new information with previous information. The recall is the retrieval of information from memory without a cue, such as answer questions.

1.3. Different Types of Long-Term Memory

Evidence has shown that long-term memory comes in different types and their formation depends on different brain regions (Thompson and Kim, 1996). For example, one of the most famous cases is Henry Gustav Molaison, known widely as H.M., who had brain surgery to remove bilaterally the medial temporal lobes (MTLs) to cure his epilepsy in 1953. However, the surgery caused anterograde amnesia (inability to form new long-term memories), and incomplete retrograde amnesia (partial loss of memory before his surgery). But H.M. could still recall memories from his childhood and exhibited intact working memories and motor learning abilities (Sagar et al., 1985; Schmolck et al., 2002). Another patient - Clive Wearing, who had hippocampal damage caused by a herpes simplex encephalitis infection, showed severe anterograde amnesia and retrograde amnesia but still kept his motor skills. Brain imaging studies also show that different types of recall activate different brain areas (Bontempi et al., 1999; Frankland et al., 2004). These cases indicate that there are different forms of long-term memory and that the hippocampus plays an essential role in memory formation.

Long-term memory can be divided into declarative/explicit and non-declarative/implicit memory, based on conscious and unconscious recall, respectively. Declarative memory refers to things you know that you can tell others and consists of episodic (remembering events such as yesterday's dinner) and semantic (knowing facts such as the capital of China) memory. Non-declarative memory refers to things you know that you can show by doing. For example, knowing how to ride a bicycle (skill learning), being more likely to use a word that you recently heard (priming), salivating when you see a favorite food (non-associative learning), and so on (Raslau et al., 2014) (Figure 2).

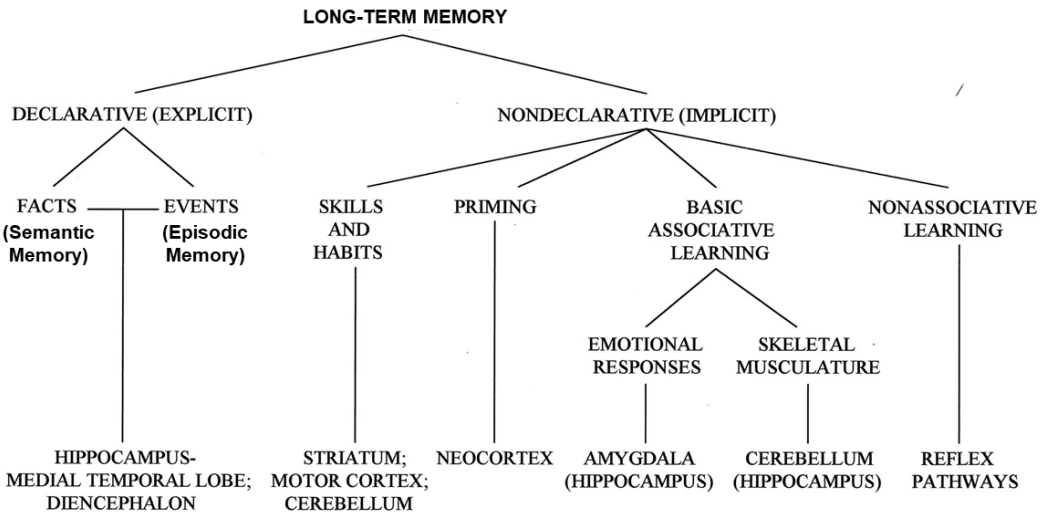

Figure 2. Classification of long-term memory and related brain regions. Modified from (Thompson and Kim, 1996).

Spatial memory belongs to episodic memory, which is responsible for recording events about the environment (content) and spatial orientation (place) (Cassel and Pereira de Vasconcelos, 2015). It is used to navigate the surrounding environment. Spatial memory also has representations within the working and short-term memory. Research indicates that the hippocampus, especially the dorsal part, is required for the spatial memory process (Hebert and Dash, 2004; Liu and Bilkey, 2001), including processing short-term memory, transferring memory from the short-term to long-term and memory retrieval (Bannerman et al., 2002; Lee and Kesner, 2003; Moser and Moser, 1998). The Morris water maze (MWM) is a frequently used task to evaluate spatial memory in rodents.

1.4. Hippocampal Neural Circuits in Memory Formation

The hippocampus plays an important role in the consolidation of long-term memory, especially spatial memory that regulates navigation (Broadbent et al., 2004). It locates in the medial temporal lobe under the cerebral cortex in primates and contains two parts: the hippocampus proper (also known as Ammon's horn) and the dentate gyrus (DG). The hippocampus proper is made up of four regions within the Cornu Ammon (CA, an earlier name of the hippocampus): CA1, CA2, CA3, and CA4. Usually, CA4 is called hilus and

considered as a part of DG. According to the distinct functions and anatomy, the hippocampus also can be divided into dorsal, intermediate, and ventral parts. The dorsal hippocampus regulates primarily cognitive functions, while the ventral part relates to stress, emotion, and affect. Furthermore, gene expression analysis shows that the dorsal hippocampus correlates with cortical regions involved in information processing, and the ventral part correlates with regions involved in emotion and stress (related to the amygdala and hypothalamus) (Fanselow and Dong, 2010).

A coronal section of the brain shows different layers of the hippocampus. CA1 and CA2 have four layers: oriens, pyramidal, radiatum, and lacunosum-moleculare; while CA3 has one more layer -lucidum stratum- than CA1 and CA2. The DG contains the molecular layer (ML), granular layer, and inner polymorphic layer (in hilus). Between hilus and the granular layer is a region -subgranular zone- which is the site of neurogenesis to form new granulecells. Different neuronal cell types are neatly organized into different layers in the hippocampus. Pyramidal neurons lie in the pyramidal layer; granule cells and mossy cell are located in the granular layer and hilus, respectively.

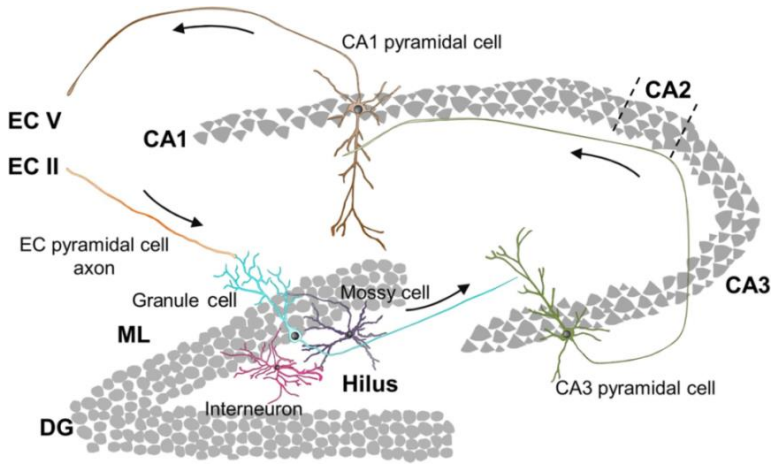

Figure 3. Hippocampal tri-synaptic circuit. Information transmits from EC II via the DG to CA3 and then to CA1. Modified from (Rodriguez-Iglesias et al., 2019).

The main input to the hippocampus is through layers II and III of the entorhinal cortex (EC), which is located in the medial temporal lobe. The major output of the hippocampus is to the subiculum (Sub) via CA1. Information can directly reach apical dendrites of CA1 from EC III via the perforant path. The indirect pathway is the tri-synaptic circuit, which was initially described by Santiago Ramon y Cajal in the early twentieth century, using the Golgi staining

method. In this circuit, EC II sends the signals from the parahippocampal gyrus to the granule cells of the DG via the perforant path. Then, the signals are transmitted to CA3 through mossy fibers. The axon collaterals of CA3 pyramidal cells, which are called Schaffer collaterals, send the signals to the apical dendrites of CA1 pyramidal cells. Finally, the axons from the CA1 pyramidal neurons project to the EC V, completing the tri-synaptic circuit (Figure 3 and 4) (Nolan et al., 2004).

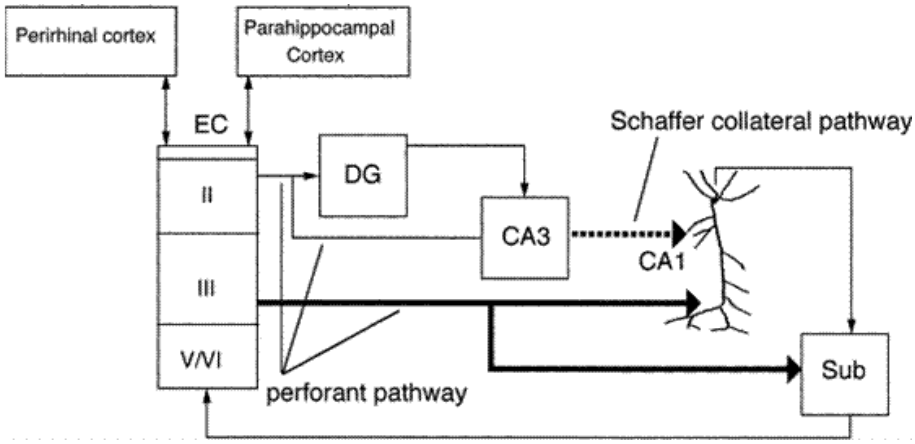

Figure 4. Schematic of hippocampal neuronal circuits. Information through EC II and EC III flows to CA1 via trisynaptic circuit and direct input (bold line), respectively. The dashed line indicates the Schaffer collateral pathway, which represents the input from the axon collaterals of CA3 to the proximal dendrites of CA1 pyramidal neurons. Modified from (Nolan et al., 2004).

1.5. The Molecular Mechanism of Long-Term Memory Consolidation

Neural circuits are made up of groups of neurons that are connected through synapses. During the signal transmission, synapses can be strengthened or weakened according to the neuronal activity. The ability for synapses to modify their strength is called synaptic plasticity, which is the neurochemical foundation of learning and memory (Citri and Malenka, 2008). The achievement of synaptic plasticity depends on neurotransmitters released by a presynaptic neuron into the synaptic cleft, and the

response of receptors on the postsynaptic neuron to those neurotransmitters. Short-term synaptic plasticity lasts less than a few minutes, while long-term plasticity is maintained from minutes to hours. Long-term potentiation (LTP) and long-term depression (LTD) are two kinds of long-term plasticity that occur at excitatory synapses. LTP is a persisting synaptic strengthening based on the increased response of postsynaptic neurons after the intense stimulation of the specific presynaptic neurons. LTD is the opposite process to LTP. These processes are considered as the major mechanisms underlying the memory process (Nicoll, 2017).

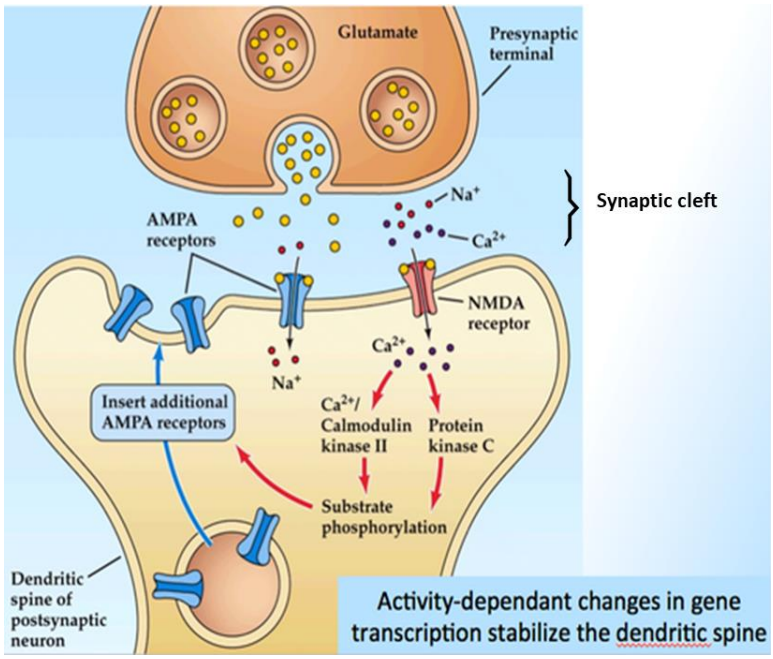

Figure 5. Synaptic responses during LTP. The activated presynaptic neuron releases neurotransmitter-glutamate, which binds to AMPA and NMDA receptors of the postsynaptic neuron. Then Na^+ enters the cell through the AMPA channel, which leads to postsynaptic neuron depolarization. Sufficient depolarization and glutamate binding enable Ca^{2+} entry through the NMDA receptor, which triggers a signaling cascade, and finally leads to synaptic stabilization. Modified from https://quizlet.com/87954137/learning -and memory-Flash cards.

During hippocampal LTP, the excitatory neurotransmitter glutamate is capable to modify the synaptic strength by binding to glutamate receptors, such as AMPA and N-methyl-D-aspartate (NMDA), which are paired with sodium and calcium channels,

respectively. Synaptic plasticity depends on the postsynaptic release of calcium ions (Ca^{2+}). During the resting potential, the calcium channel is blocked by magnesium ions (Mg^{2+}), which can be withdrawn by postsynaptic depolarization. Thus, after the high-frequency stimulation leading to glutamate release, AMPA receptors are activated, which allows sodium ions (Na^{+}) into the cell and depolarizes the postsynaptic dendrite. This depolarization leads to the withdrawal of Mg^{2+} from NMDA receptors. When the depolarization and glutamate are present simultaneously, the NMDA receptor lets Ca^{2+} enter the dendrite, and finally triggers LTP. Ca^{2+} acts as an important intracellular messenger and initiates a typical cascade of biochemical reactions that increase synapse efficiency for an extended period (Figure 5). Except for the postsynaptic signaling cascade, it has been postulated that retrograde signals (such as nitric oxide) acting back on the presynaptic terminal to increase the amount of glutamate released also contribute to the maintenance of LTP. Neuronal activity-induced LTP finally results in synaptic stabilization. However, during hippocampal LTD, the most common neurotransmitter is L-glutamate, which acts on the NMDA receptors, metabotropic glutamate receptors (mGluRs), and endocannabinoids. This process selectively weakens specific synapses to make space to encode new information.

1.6. Synaptic Rearrangement during Long-Term Memory Consolidation

A neuron continuously modifies its structures to fit the experiences (Hua and Smith, 2004). Synaptic plasticity is an essential foundation for the refinement of neural circuits and memory consolidation processes (Zhou et al., 2003). The neural circuit remodeling process includes new synapse formation, synaptic strengthening, and selective synapse elimination. Skill learning accelerates the synaptic rearrangement process (Caroni et al., 2014b). Plasticity starts from pre-existing synapses at the time of acquisition (Knott et al., 2006; Xu et al., 2009). New synapses can be formed within 1 hour after the acquisition and are immature synapses. During this process, acquisition initiates the first signaling cascade, including post-translational modifications (such as protein kinase RNA-like endoplasmic reticulum kinase (pERK) and phosphorylated cAMP-response element-binding protein (pCREB), within minutes), translation of pre-existing genes for encoding plasticity (such as c-Fos and Arc, within minutes and peaking at around 90 minutes), and transcription of plasticity genes (such as BDNF and Arc, within 1-3 hours) (Ressler et al., 2002). These early plasticity responses are

followed by a second wave of plasticity-post-translational modifications (such as pERK and pCREB, peaking at 9 hours), which leads to structural and functional maturation of new synapses (12-15 hours) (Bekinschtein et al., 2007; Cane et al., 2014; Meyer et al., 2014b). Long-term memory consolidation lasts several days, accompanied by synapse elimination (most occurs during the first 1.5 days) and long-term retention of some of the new synapses (Barnes and Cheetham, 2014; Hofer et al., 2009; Xu et al., 2009; Yang et al., 2009a). The timeline of the long-term memory consolidation process varies for different types of learning. Moreover, this process is affected by sleep, local network events such as ripples, replay, and rehearsal (Figure 6).

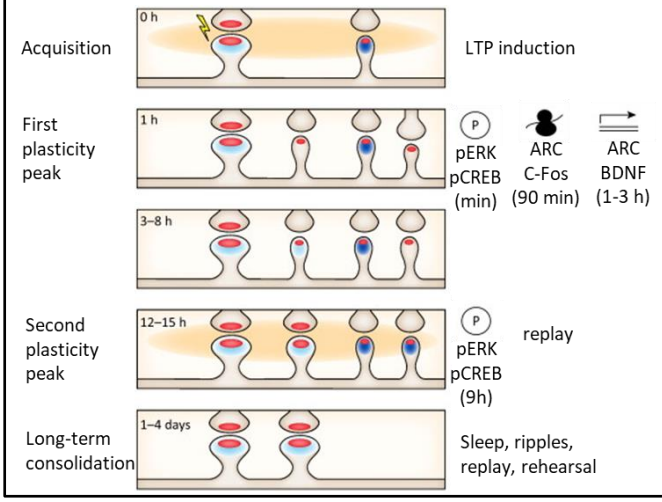

Figure 6: Timeline of plasticity processes and synaptic rearrangement upon leaning. The dynamic process of synapses upon learning. Red oval: pre- and post-synaptic density; pale blue: strong post-synapse; dark blue: weak post -synapse; yellow arrow: long-term potentiation induction. Modified from (Caroni et al., 2014a).

The dendritic spine is the postsynaptic component on the neuronal dendrite. Spines receive and isolate synaptic inputs, store synaptic strength (Koch and Zador, 1993; Yuste and Denk, 1995b), as well as transmit electrical signals to neuronal cell bodies (Araya et al., 2006a; Araya et al., 2006b; Segev and Rall, 1988). The result of plasticity finally is reflected in the number and morphology of spines (Govindarajan et al., 2011; Harvey and Svoboda, 2007). The actin cytoskeleton directly determines the highly dynamic character of spines. It has been shown that 10-20% of spines can spontaneously appear or disappear on the pyramidal cells of the cerebral cortex, and the majority of spines change their shape within seconds to minutes. The dendritic spine consists of two compartments: a bulbous head that is contacting the axon and a constricted neck that connects to the dendrite (Koh et al., 2002). According to the head width and spine length, dendritic spines are classified in four different subtypes, including filopodia, stubby, thin, and mushroom types (Risher et al., 2014; Son et al., 2011) (Figure 7). Filopodia have long necks and generally do not have clear heads; whereas in stubby spines,

the neck is either missing or very small. Mushroom spines have large bulbous heads and clear short necks; thin spines have small heads and thin long necks. It has been shown that spine head diameter is correlated with the area of postsynaptic density (PSD), which contains postsynaptic receptors, scaffold proteins, and many signaling molecules (Arellano et al., 2007; Matsuzaki et al., 2004). Filopodia are immature spines without PSD and are usually highly dynamic newly generated protrusions (De Roo et al., 2008; Fiala et al., 1998). Thin spines don't express AMPA receptors but do express NMDA receptors, which allow Ca^{2+} to enter postsynaptic neurons upon appropriate stimulation (Zito et al., 2009). Stubby and mushroom-shape spines are more stable and mature, containing large PSD (Steiner et al., 2008). Thus, the size of the spine head represents the spine function and maturation (Matsuzaki et al., 2001). The distribution of different types of spines varies in different brain regions and neurons and is also affected by learning, aging, and species (Yuste and Denk, 1995a).

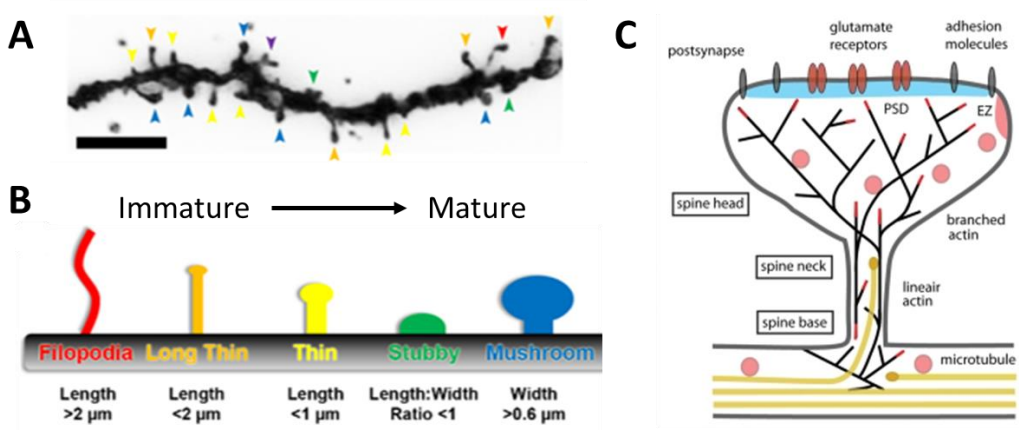

Figure 7: Characteristics of dendritic spines. A. A Golgi stained secondary dendritic branch of a pyramidal neuron in the cortex. Different spine types are indicated by arrowheads. **A** and **B** are color matched. Scale bar: 5 µm. **B.** Illustration of different types of spines and their geometric characteristics. Modified from (Risher et al., 2014). **C.** Schematic of the mushroom spine, which includes PSD (blue), glutamate receptors (reddish-brown), adhesion molecules (grey), actin (black lines), and microtubule (yellow) cytoskeleton, and organelles. Adapted from (Hotulainen and Hoogenraad, 2010).

Synaptic stabilization is determined by pre- and postsynaptic structures such as the axonal button, dendritic spine, and PSD (Yoshihara et al., 2009). On the molecular level, scaffold proteins of the PSD, such as PSD-95 and Homer1c, have been shown to correlate with the

stabilization of synaptic enlargement (Meyer et al., 2014a). Except these, there are a lot of additional factors that play important roles in regulating synaptic plasticity and long-term memory consolidation, such as circadian rhythms (Jasinska et al., 2019), microglia (Ikegami et al., 2019; Schafer et al., 2012), astrocytes (Clarke and Barres, 2013), growth factors (Park and Poo, 2013), trans-synaptic cell adhesion molecules (Missaire and Hindges, 2015; Missler et al., 2012), and so on.

1.7. System Consolidation of Long-Term Memory

Studies on humans (such as those by H.M. and Clive Wearing) and animals show that disrupting hippocampal function preferentially affects recent, rather than remote, memories (Anagnostaras et al., 1999; Clark et al., 2002; Gaskin et al., 2003; Maren et al., 1997). Based on these examples of retrograde amnesia, the system consolidation of long-term memory has established. This consolidation is a time-dependent reorganization of brain regions that support memory (Dudai et al., 2015). The hippocampus acts as a temporary store for new information, and permanent storage depends on a broadly distributed cortical network (Frankland and Bontempi, 2005).

The first model of system consolidation was provided by Marr (Marr, 1970, 1971). He proposed that daily information is temporarily retained in the hippocampus and transferred to the cortex when the hippocampal neural network is reactivated during sleep (Mcclelland et al., 1995; Squire and Alvarez, 1995). Recently, memory replay has been recorded in extensive cortical and subcortical areas in rodents and the motor cortex of humans (Eichenlaub et al., 2020; Euston et al., 2007; Wilber et al., 2017). According to Marr's theory, hippocampal memory reactivation is the core mechanism in consolidation models, which reinstates activity in different cortical networks. This coordination across hippocampal-cortical networks strengthens the cortico-cortical connections. Eventually, new memories become independent of the hippocampus and integrate with pre-existing cortical memories. Memories retain longer in the cortex than in the hippocampus (Figure 8).

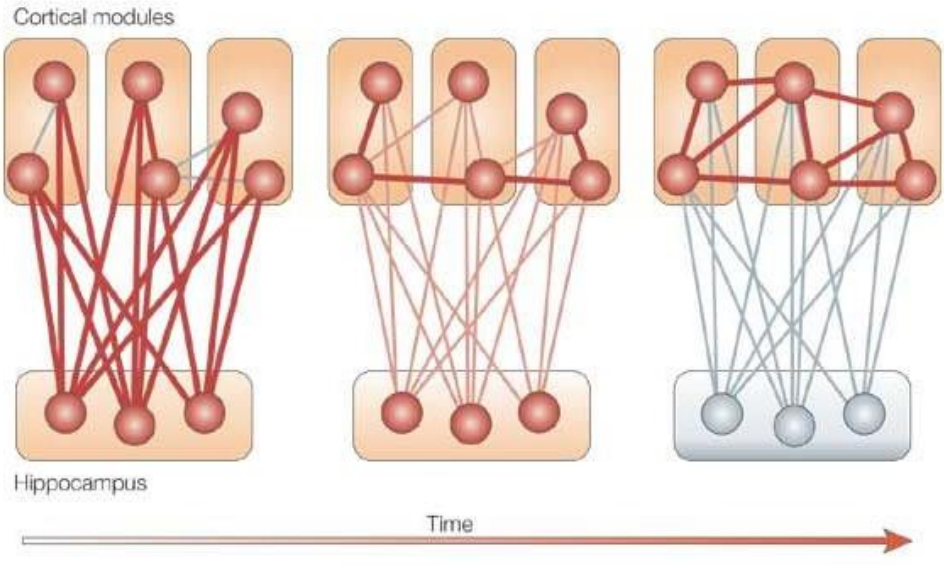

Figure 8. Standard system consolidation model. Information is initially encoded in different cortical modules that representing various components of an experience, and then transferred to the hippocampus where information is integrated. Reactivation of the hippocampal-cortical network strengthens cortico-cortical connections. Finally, new memories integrate with existed cortical memories and become independent of the hippocampus. Adapted from (Frankland and Bontempi, 2005).

The multiple trace theory was proposed in 1997 as an alternative to the standard consolidation models (Nadel and Moscovitch, 1997). It also assumes that memory reactivation initiates a process of reorganization. However, this model predicts that memories are encoded in hippocampal-cortical networks, and that retrieval of contextually rich episodic memories and spatial detail always requires the hippocampus.

Moreover, imaging and inactivation studies have indicated that the prefrontal cortex also plays a critical role during remote memory recall. Firstly, the prefrontal cortex consists of several highly interconnected regions (Miller, 1996; Uylings et al., 2003), which provide an ideal situation to integrate and synthesize information from distributed cortical modules (Miyashita, 2004). Secondly, the prefrontal cortex may directly or indirectly inhibit the hippocampal function to minimize the re-encoding of redundant information (Miller and Cohen, 2001; Moody et al., 1998; Tomita et al., 1999) (Figure 9).

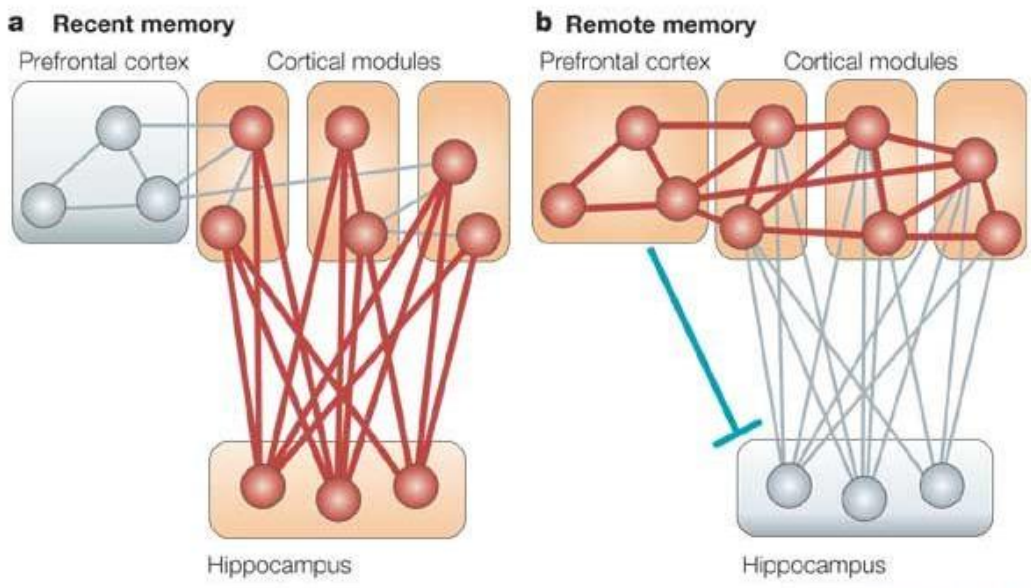

Figure 9. The prefrontal cortex is involved in remote memory recall. a. Memories are encoded in the hippocampal-cortical network. b. The prefrontal cortex involves new memories integration and inhibits the hippocampal function. Adapted from (Frankland and Bontempi, 2005).

2. Central Nervous System Control of Energy Homeostasis

2.1. Systemic Control of Energy Homeostasis

Energy homeostasis is the biological process that maintains the energy balance by regulating food intake and energy expenditure (Bray et al., 2012). This process is controlled by afferent signals from the periphery to the CNS about the state of peripheral energy stores, efferent signals that affect energy intake and expenditure, and the integration of these central and peripheral signals. Central and peripheral physiological signals involved in maintaining energy homeostasis, include neuronal networks in the hypothalamus, the brainstem, reward, and endocannabinoid systems in the brain, and satiety and adiposity signals from peripheral organs (Abdalla, 2017; Ferrario et al., 2016a; Morton et al., 2006). These behavioral, sensory, autonomic, nutritional, and endocrine mechanisms also influence food intake (Abdalla, 2017).

Satiety is affected by short-term signals from the gastrointestinal tract (GIT) and long-term signals from the adipose tissue (Morton et al., 2006; Zac-Varghese et al., 2010). Via vagal and spinal nerves, signals from the GIT are transmitted to the nucleus of the solitary tract (NTS) in the brainstem. Adiposity signals, such as leptin (secreted by adipocytes) and insulin (secreted by the endocrine pancreas in proportion to adiposity), interact with different neuronal circuits in the hypothalamus and midbrain that control food intake. For example, leptin diminishes the perception of food reward -the palatability of food, while it enhances the response to satiety signals generated during food consumption; thus, leptin inhibits feeding and leads to meal termination via direct and indirect actions (Morton et al., 2006) (Figure 10).

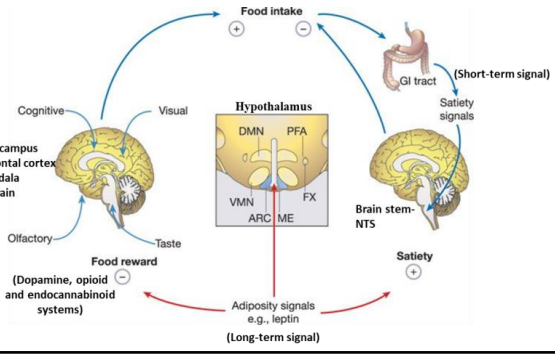

Figure 10. Schematic illustration of CNS and systemic regulation of food intake. ARC, arcuate nucleus (in blue); DMN, dorsomedial nucleus; FX, fornix; ME, median eminence; PFA, perifornical area; VMN, ventromedial nucleus. Modified from (Morton et al., 2006).

2.2. Hypothalamic Control of Energy Homeostasis

A growing number of findings have demonstrated a more extended role for the CNS in the control of energy homeostasis, and have revealed the important role of specifically hypothalamic circuits in regulating systemic metabolism, food intake, and body weight (Myers and Olson, 2012). The hypothalamus is part of the limbic system and forms the ventral part of the diencephalon. In the coronal plane, the hypothalamus is often divided into 3 areas (periventricular, medial, and lateral), which contain several small nuclei with a variety of functions and link the nervous system to the endocrine system via the pituitary gland. Since the early 1940s, hypothalamic lesion experiments have identified specific functional areas of the hypothalamus, and thus linked the function of the hypothalamus to energy homeostasis (Brobeck, 1946). For example, lesions of the ventromedial hypothalamus (VMH) or dorsomedial hypothalamus (DMH) resulted in profound hyperphagia and obesity (Ferrario et al., 2016b); whereas, damage of the lateral hypothalamic area (LHA) led to reduced food intake (hypophagia) (Anand and Brobeck, 1951). Subsequent studies expanded our knowledge of specific nuclei and neuronal circuits in the arcuate nucleus (ARC), the paraventricular nucleus (PVN), DMN, VMN, and LHA that control energy homeostasis (Sawchenko, 1998) (Figure 11).

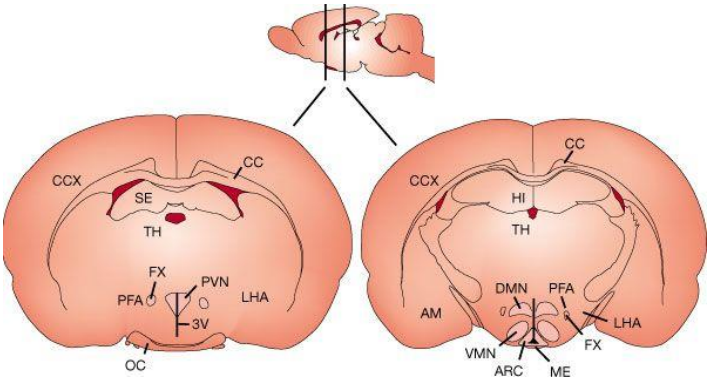

Figure 11. Diagrams of the rat brain in the sagittal and coronal plane, showing major hypothalamic regions involved in the regulation of food intake. AM, amygdala; CC, corpus callosum; CCX, cerebral cortex; SE, septum; TH, thalamus; HI, hippocampus; FX, fornix; PFA, zona incerta, perifornical area; 3V, third ventricle; OC, optic chiasm; ME, median eminence. Adapted from (Schwartz et al., 2000).

The hypothalamus responds to circulating signals connected to changes in body homeostasis and energy balance, such as leptin, ghrelin, insulin, and glucose, which enter the hypothalamus mainly through the ARC. ARC neurons transform these metabolic signals into neuronal signals and thus are considered as first-order neurons. Axons of these neurons

project widely onto diverse second-order neurons that are involved in the regulation of energy intake and body weight. In this way, different territories and cell types within the hypothalamus are assembled in an integrated manner to support the organism's ability and physiological homeostasis (Burbridge et al., 2016; Palkovits, 2003) (Figure 12).

Arcuate nucleus (ARC)

The ARC is the key hypothalamic region regulating energy homeostasis (Abdalla, 2017). It is located in the mediobasal hypothalamus (MBH), where it abuts the third ventricle and median eminence (ME). The ME is one of the circumventricular organs (CVOs) that are comprised of extensive and highly permeable capillaries to facilitate the diffusion of specific molecules found in the blood. This characteristic allows peripheral metabolic signals to be sensed by adjacent neuronal dendrites that extend from the ARC (Djogo et al., 2016). Thus, the integration between the hypothalamus and peripheral signals is established in the ME and ARC. The first-order neurons in these structures integrate metabolic signals and transform them into neuronal signals.

Two important populations of neurons in the ARC are the orexigenic agouti-related peptide (AgRP)/neuropeptide Y (NPY) neurons and the anorexigenic proopiomelanocortin (POMC) neurons (Krashes et al., 2011; Luquet et al., 2005; Morton et al., 2006; Palkovits, 2003; Schwartz et al., 2000). NPY and AgRP are co-localized in the ARC (Hahn et al., 1998). Activation of the AgRP/NPY neurons stimulates food intake and reduces energy expenditure, thereby increasing body weight, whereas activation of POMC neurons has the opposite effect on food intake, energy expenditure and body weight (Ellacott and Cone, 2004; Lechan and Fekete, 2006; Toda et al., 2017a). In addition to the inhibition of POMC neurons by the local release of gamma-aminobutyric acid (GABA) (Liu et al., 2003), the orexigenic effect of NPY is mediated by stimulation of the hypothalamic neuropeptide Y receptors-Y1R and Y5R (Abdalla, 2017; Pralong et al., 2002), whereas AgRP behaves as a selective antagonist at melanocortin MC3R and MC4R receptors in the PVN (Nijenhuis et al., 2001). The ARC POMC neurons promote energy expenditure and satiety by releasing the co-localized alpha-melanocyte-stimulating hormone (α-MSH) and cocaine- and amphetamine-regulated transcript (CART) peptides. α-MSH is a POMC-derived peptide and binds to melanocortin receptors -MC3R and MC4R- in the PVN and the nucleus of the solitary tract (NST) (Koch et al., 2015; Lau and Herzog, 2014; Mountjoy, 2010; Pinto et al., 2004; Wang et al., 2000). Within the PVN, CART significantly stimulates the secretion of corticotropin-releasing hormone (CRH) and thyrotrophin-releasing factor (TRH) to reduce food intake in addition to its role as a regulator of the hypothalamic-pituitary-adrenal/

thyroid axis (Bray et al., 1990; Kow and Pfaff, 1991; Stanley et al., 2001). In the DMN and LHA CART may also be involved in the activation of the orexigenic effect, which suggests that CART can be both orexigenic and anorexigenic, depending on the neural circuit that is stimulated (Hou et al., 2010). Neuropeptides such as α-MSH, CRH, TRH, and CART all are part of the melanocortin pathway that promotes a negative energy balance by activation of the MC3R and MC4R receptors in the brain. POMC gene expression in the ARC can also be increased by a peripheral peptide such as neurotensin (NT) from the GIT (Ratner et al., 2016). In addition, POMC neurons also secrete β-endorphin into the PVN, which promotes feeding in response to cannabinoids in sated mice (Koch et al., 2015).

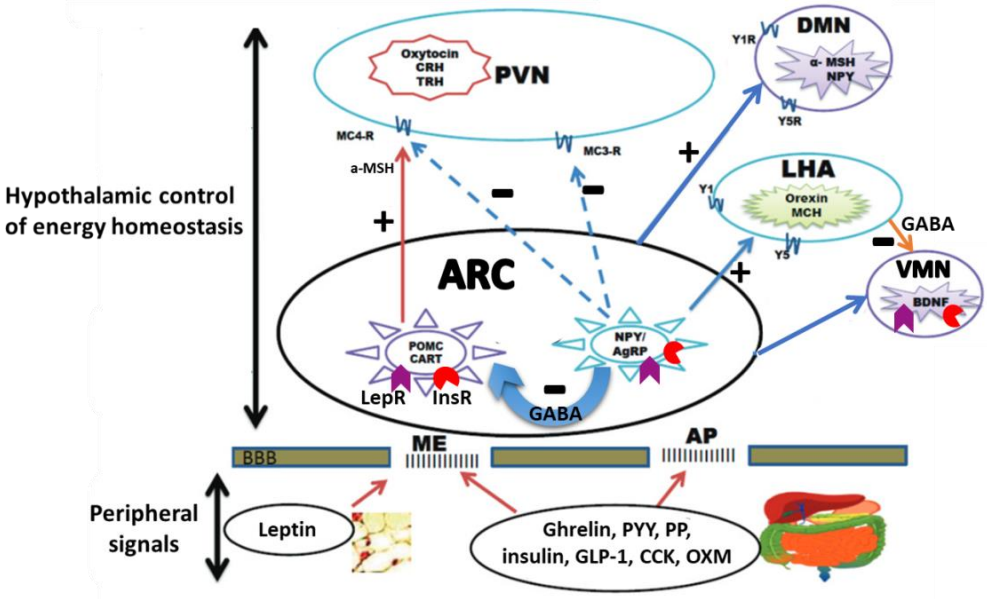

Figure 12. Hypothalamic regulation of energy homeostasis in response to peripheral signals. Peripheral signals: leptin is secreted mainly by the adipose tissue; ghrelin is an orexigenic gut peptide secreted mainly from the stomach; PYY, peptide tyrosine tyrosine, is released from cells in the ileum and colon; PP, pancreatic polypeptide, is a hormone released from the pancreas; insulin is a peptide secreted from beta cells of the pancreas after a meal; GLP-1, glucagon-like peptide-1 is produced in the pancreas; CCK, cholecystokinin, a gut hormone; OXM, oxyntomodulin, is released from the intestine; AP, area postrema; BBB, blood-brain barrier; Y1R & Y5R, neuropeptide Y receptors 1 & 5. Modified from (Abdalla, 2017).

Axons from ARC NPY/AgRP and POMC/CART neurons are highly connected with hypothalamic dendrites from PVN, VMN, DMN, PFA, and LH neurons, thus neurons from these latter regions

are considered as second-order neurons (Elmquist et al., 1999; Elmquist et al., 1998b). But except for releasing neuropeptides in the hypothalamus to control food intake and energy expenditure, the axons of ARC neurons also directly project to different other brain areas to regulate energy homeostasis. For example, AgRP axons specifically project to the paraventricular thalamus (PVT) to initiate acute feeding (Betley et al., 2013) and POMC neurons in the rostral ARC project to autonomic brainstem regions (Toda et al., 2017a).

Both NPY/AgRP and POMC/CART neurons show a high expression of leptin receptors (LepRs) and insulin (InsR) (Elmquist et al., 1998a; Taniguchi et al., 2006; Varela and Horvath, 2012), which provide a functional foundation for the control of energy homeostasis and blood glucose levels (Toda et al., 2017a). The response of POMC neurons to metabolic factors also shows regional differences, for instance, neurons in the medial ARC are more sensitive to glucose, while those in the lateral ARC are more responsive to leptin (Lam et al., 2017).

Table 1. Molecules implicated in the control of energy homeostasis

Orexigenic	Anorexigenic
NPY/AgRP; β-endorphin; Orexin; MCH; Dopamine; Noradrenaline	α-MSH/CART; CRH; TRH; Neurotensin; Oxytocin; BDNF; Serotonin

Paraventricular nucleus (PVN)

As indicated by its name the PVN is located adjacent to the third ventricle. It contains magnocellular neurosecretory cells, parvocellular neurosecretory cells that project to the ME, and several populations of other peptide-containing parvocellular cells (Qin et al., 2018). The magnocellular PVN cells release the peptide hormones oxytocin and vasopressin in the systemic circulation via the posterior pituitary. Centrally oxytocin also binds to the oxytocin receptor that is expressed in the nucleus accumbens core in rats (Herisson et al., 2016). Parvocellular neurosecretory neurons release CRH and TRH from their terminals into the primary capillary plexus of the hypothalamo-hypophyseal portal system within the ME. Oxytocin, CRH, and TRH inhibit food intake, increase energy expenditure, and reduce glucose levels (Fekete et al., 2000; Morton et al., 2012; Ott et al., 2013).

Lateral hypothalamus (LH)

The LH includes the LHA and perifornical area (PFA), which is the primary orexinergic nucleus and contains neurons that produce the orexigenic neuropeptides orexin (orexin-A and -B) and melanin-concentrating hormone (MCH) (Broberger et al., 1998; Dhuria et al., 2016). The LHA

has both kinds of neurons, but the PFA only contains orexin neurons and no MCH-producing neurons (Yi et al., 2009). Orexin A enhances food intake when injected into certain hypothalamic nuclei such as LHA, PVN, DMN, or PFA. Orexin B-producing neurons increase food intake by projecting to the dopamine-producing neurons in the ventral tegmental area (VTA), which is a key structure of the reward system (Borgland et al., 2008). The LH receives both NPY-and α-MSH-containing projections from the ARC and also exerts a GABAergic inhibitory tone onto VMH neurons (Viggiano et al., 2004). It has been noted that the cannabinoid receptor 1 (CB1) is localized on orexinergic projection neurons in the LH. The CB1 and orexin receptor 1 (OX1) may physically and functionally join together (CB1-OX1 receptor heterodimer) to regulate energy homeostasis (Flores et al., 2013).

Ventromedial nucleus (VMN)

The VMN can sense glucose levels, which makes the VMN an important place to examine the hypothalamic circuits that control overall metabolism (Barnes et al., 2011; Chan et al., 2007; Levin et al., 2011). Some VMN neurons express the LepR and InsR to control energy balance (Dhillon et al., 2006; Elias et al., 2000; Klockener et al., 2011). Moreover, BDNF, which is involved in regulating the energy balance through MC4R signaling, is also highly expressed in the VMN (Xu et al., 2003); central infusion of BDNF reduces food intake and excessive weight gain in rodents (Pelleymounter et al., 1995; Xu et al., 2003). The VMN also receives NPY/AgRP and POMC neuronal projections from the ARC.

Dorsomedial nucleus (DMN)

Almost all major nuclei and areas of the hypothalamus send information to the DMH. The DMN receives a high density of projections from NPY and POMC/α-MSH neurons. Lesions of the DMN results in hyperphagia and obesity (Bernardis and Bellinger, 1986).

Monoamine neurotransmitters and food intake

Serotonin, also known as 5-hydroxytryptamine (5-HT), analogs have an anorexic effect and are widely used as anti-obesity drugs (for example, dexfenfluramine and sibutramine) (Leibowitz and Alexander, 1998). The serotonin receptors 5-HT2C and 5-HT2B are thought to mediate most of the weight-loss actions of these 5-HT agonists. The melanocortin signaling pathway is also involved in the anorexic effects of serotonin, and disruption of the 5-HT2C receptor increases food intake and body weight (Lam et al., 2008; Zhou et al., 2007). Dopaminergic neurons control the activity of nearby AgRP and POMC cells in the ARC and show an orexigenic effect (Zhang and van den Pol, 2016). The mesolimbic dopamine pathways, also known as the reward pathway,

contributes to consuming palatable foods (Pothos et al., 1995). Noradrenaline is often co-localized with NPY and also shows an orexigenic effect (Leibowitz et al., 1984). However, there is controversy on the effects of dopamine and noradrenaline on feeding behavior.

Furthermore, the reward system, such as the mesolimbic dopamine system, endogenous opioids (such as β-endorphins, μ-opioid), and the endocannabinoid systems (ECS) play an important role in the control of feeding behavior. Extensive brain circuits including the hippocampus, amygdala, prefrontal cortex, and midbrain, are involved in this reward-related feeding. The endocannabinoid system also promotes energy storage via the cannabinoid receptors (CB1 and CB2) and increasing hypothalamic endocannabinoid levels (Horvath, 2003; Jamshidi and Taylor, 2001; Quarta et al., 2011).

In conclusion, energy homeostasis is controlled by a complex system, which needs to coordinate and integrate central and peripheral signals. Many different neuronal populations, peptides, hormones, neurotransmitters, and neuronal circuits are involved in the control of this process. Moreover, it has been found that also astrocytes and microglial cells in the brain play an important role in the regulation of energy balance.

3. Microglia

3.1. Brief History

Microglia were first described in the 1880s by Franz Nissl and F. Robertson during histological staining. Activated microglia and ramified microglial clusters were first noticed in 1897 by Victor Babeş when studying a rabies brain infection. However, they didn't know what cells those were. Until around 1920, microglia were first named by Pío del Río Hortega, a student of Santiago Ramón y Cajal. Using a silver staining technique and a light microscope, Hortega observed the treelike processes of microglia and predicted their phagocytic function in the central nervous system (CNS) (Nayak et al., 2014). After many years of research on microglia, Rio Hortega became considered as the "Father of Microglia". For a long period, microgliologists have been validating Hortega's postulates. Hickey and Kimura showed that perivascular microglia in the CNS are bone-marrow-derived and act as the antigen-presenting cells *in vivo* in 1988 (Hickey and Kimura, 1988), conferring that microglia are similar to macrophages (Figure 13).

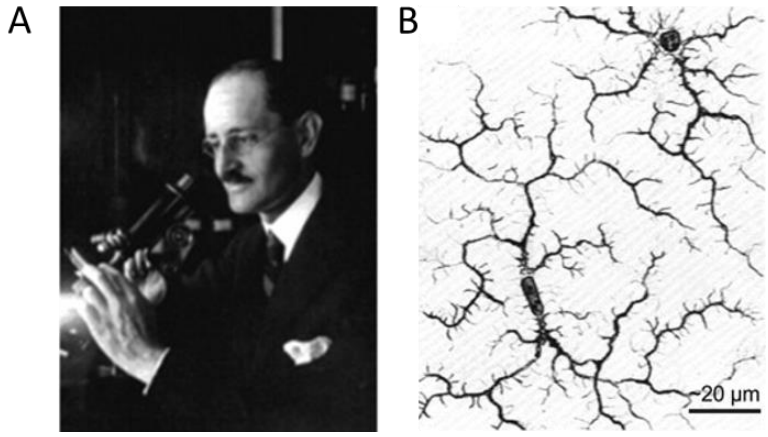

Figure 13. A. Portrait of Pío del Río Hortega (1882-1945), "father of microglia". B. Ramified microglia, drawing by Del Rio-Hortega, 1919. Adapted from https://cienciaycientificos.blogspot.com/2011/08/pio-del-rio-hortega-el-otro-gran.html; and https://www.researchgate.net/figure/Evolving-views-of-resting-microglia-from-the-pioneer-observation-of-silver-carbonate_fig1_221895742.

3.2. Development

For a long time, it has been assumed that microglia originate from hematopoietic stem cells in the bone marrow. Recent studies have further demonstrated that microglia are derived from primitive myeloid precursors in the early fetal development stage (before embryonic day 8) and migrate from the embryonic yolk sac into the developing neural tube, where they proliferate, colonize the entire parenchyma and are maintained throughout the lifespan (Ginhoux et al., 2010). However, it has still not been clarified what is guiding microglia to the brain during embryonic development. Following the migration of these progenitors to the CNS, the blood-brain barrier (BBB) forms and effectively isolates the microglia from the periphery (Mildner et al., 2007). Thus, under normal conditions the infiltration of peripheral monocytes or macrophages into the CNS is impossible. However, according to the anatomical and functional specificity, it is postulated that the mediobasal hypothalamus (MBH) either lie outside the BBB or have a porous BBB with increased infiltration, allowing peripheral myeloid cells to infiltrate into this brain region (Olofsson et al., 2013; Valdearcos et al., 2017a).

Microglia are longevity and self-renewing cells, with a low turnover rate under homeostatic conditions across the lifespan, but in Alzheimer's mice, the proliferation rate shows a threefold increase (Fuger et al., 2017). The development, proliferation, maintenance, and survival of microglia mainly rely on colony-stimulating factor 1 receptor (CSF1R), a tyrosine kinase transmembrane receptor that is expressed by microglia, as well as macrophages, and osteoclasts. CSF1R null mice show microglia deficiency and rarely survive to adulthood (Erblich et al., 2011). Furthermore, the pharmacological blockade of CSF1R drastically reduces microglial cell numbers in adult mice (Dai et al., 2002; Elmore et al., 2014), while the microglia-depleted brain completely repopulates with new microglia within 1 week after withdrawing the CSF1R inhibitor (Elmore et al., 2014). CSF1R continually interacts with two natural ligands, colony-stimulating factor 1 (CSF1) and interleukin-34 (IL-34) (Lin et al., 2008; Wang et al., 2012). CSF1 is secreted by neurons, as well as glial cells, including microglia (Bradley and Metcalf, 1966; Elmore et al., 2014; Metcalf, 2010); IL-34 is secreted by neurons throughout the brain except for the cerebellum.

3.3. Distribution and Morphology

Microglia account for 10-15% of all cells in the brain and are not uniformly distributed throughout the CNS parenchyma, their density shows a wide variation between different brain regions (Tan et al., 2020). Within the whole brain, the gray matter has more microglia than white matter (Lawson et al., 1990). The hippocampus, olfactory telencephalon, basal ganglia, and substantia nigra have more microglia than other brain regions. In comparison, microglial density is lowest in fiber tracts, cerebellum, and much of the brainstem. The cerebral cortex, thalamus, and hypothalamus show an average cell density (Lawson et al., 1990). Moreover, the morphology of microglia throughout development shows high plasticity, which dependents on age, neuronal activity, as well as brain region. For example, in basal conditions, cells from the hippocampus of an adult rat are highly branched with thin extensions and small round or oval somas, whereas cells in the hypothalamic ARC show low homogeneity and appear hypertrophied, with shorter and thicker branches (Figure 14).

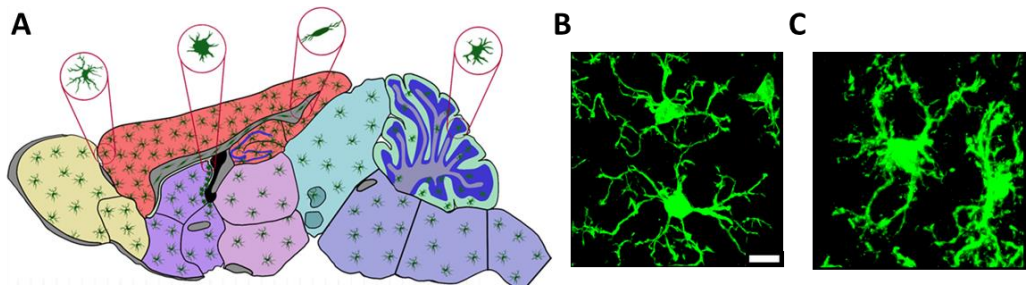

Figure 14: Microglial morphology in the brain. A. Microglia show regional heterogeneity. Adapted from (Tan et al., 2020). B-C. Immunofluorescent staining of microglia in basal conditions in the hippocampal stratum radiatum (B) and the hypothalamic ARC (C). Scale bar: 10 µm.

According to their shape, microglial cells have been categorized into three broadly distinct subtypes in the healthy brain: round/amoeboid-like microglia, microglia with thick long processes, or microglia with thin ramified processes (Lawson et al., 1990). Microglia can change the volume of the cell body and the length and complexity of the processes to deal with different situations. This phenomenon is observed not only in pathological situations but also in physiological conditions during brain development (Ayoub and Salm, 2003; Streit et al., 1999). For instance, when ramified microglia are activated, they can transform into swollen ramified cells with a larger cell body and shorter, thick processes. Microglia also can be a small

and round cell shape, as well as exhibit amoeboid-like morphology (Fernandez-Arjona et al., 2017). Microglial morphologies are associated with their functional states (Fernandez-Arjona et al., 2017). Microglia with an increased phagocytic capacity usually show a less ramified morphology, reduced branches, and decreased cell volume (Ayata et al., 2018a). In the acute neuroinflammatory process, hippocampal microglia display reduced ramifications and hypothalamic microglia present a significant drop in branch length around swollen soma 4h after stimulation (Fernandez-Arjona et al., 2017).

3.4. Functions

Microglia are highly motile resident immune cells of the CNS and sensitive to the microenvironment (Davalos et al., 2005). It has been estimated that in the homeostatic mice brain, the brain parenchyma is completely screened by resting microglia every few hours (Nimmerjahn et al., 2005), which plays an important role in maintaining normal brain function (Wake et al., 2009). Microglia are brain resident macrophages and act as the first line of immune defense but are distinct from their peripheral counterparts. Microglia are not only involved in immune surveillance but also are responsible for the CNS homeostasis. Based on recent comprehensive gene expression profiling and functional studies, microglial functions are divided into sensing the surrounding environment, conducting physiological housekeeping, and protecting the brain against injurious stimuli (Hickman et al., 2018a; Hickman et al., 2013). These three essential functions are crucial in maintaining a healthy microenvironment in the CNS during various stages of development, from embryonic stages to adulthood and aging.

Microglia continually extend and retract their highly ramified thin processes to survey the surrounding microenvironment even in their resting state. The average speed of extension and retraction of processes is 1.47 ± 0.10 μm/min and 1.47 ± 0.08 μm/min, respectively (Nimmerjahn et al., 2005). Microglia processes also display highly motile filopodia-like protrusions and typically are bulbous at their terminal endings, which indicates that the microglia engulf tissue components or cell debris. Such protrusions are short-lived and show a high turnover rate with an average lifetime of 3.9 ± 0.2 min, however, the total sites per cell that show protrusive activity and the average total length of microglial processes are rather constant over time (Nimmerjahn et al., 2005). This high motility is a prerequisite for microglia to perform their housekeeping and defense functions. Microglial housekeeping functions include effectively clearing up cellular debris and apoptotic cells, synaptic remodeling, and

neurogenesis to maintain optimal brain circuits under physiological conditions (Ji et al., 2013; Ming and Song, 2011; Miyamoto et al., 2016b; Paolicelli et al., 2011b).

Moreover, microglia are able to defend against infectious agents, neuronal damage, and the pathogenic protein aggregates produced in neurodegenerative diseases (Davalos et al., 2005; Gonzalez-Scarano and Baltuch, 1999; Subhramanyam et al., 2019a), by phagocytosing and initiating immune responses (Aloisi, 2001). To deal with a neuronal injury or other insults, microglia will be activated and show pro-inflammatory phenotype (M1) or anti-inflammatory phenotype (M2) (Subhramanyam et al., 2019a). Microglia produce pro-inflammatory cytokines (TNFα, IL-1β, IL-6), chemokine ligand 2 (CCL2), superoxide, reactive oxygen species (ROS), nitric oxide (NO), and matrix metallopeptidase 12 (MMP12) in response to injury or infection, which subsequently induce inflammation and neuronal loss. While microglia also secrete anti-inflammatory cytokines (IL-10 and IL-4) to antagonize the pro-inflammatory responses and facilitate phagocytosis, reconstruct the extracellular matrix (ECM), as well as repair tissue (Subhramanyam et al., 2019a). Microglia also produce neurotropic factors, such as transforming growth factor beta 1 (TGF-β) and insulin-like growth factor 1 (IGF-1) to support neuronal cell health and survival (Olah et al., 2011; Orihuela et al., 2016; Walker et al., 2014) (Figure 15).

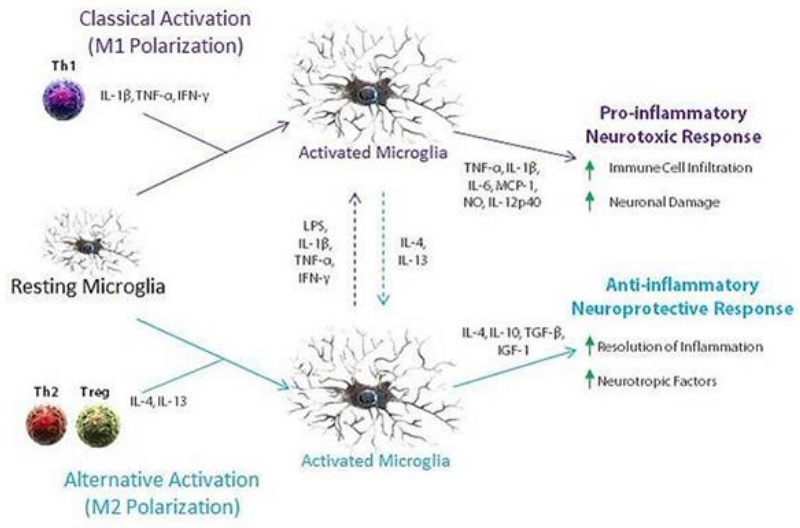

Figure 15. Schematic of microglial polarization and functions. Upon classical activation, resting microglia polarize into a pro-inflammatory (M1) or anti-inflammatory phenotype (M2), leading to neurotoxic and neuroprotective effect, respectively. Adapted from https://www.biolegend.com/en-us/bio-bits/microglia-in-inflammation-and-survival.

Besides, microglia express a variety of inducible receptors that may promote migration, as well as induce or downregulate immune functions and phagocytosis of microglia (Aloisi, 2001; Das and Chinnathambi, 2019; Hickman et al., 2018a; Subhramanyam et al., 2019a). These receptors include complement receptors (CRs) (such as CR1 and CR3) (Heneka et al., 2015), chemokine receptors (such as C-X3-C motif chemokine receptor 1 (CX3CR1) and CXCR4) (El Khoury et al., 2007), cytokine receptors (such as IFN-α/β, IFN-γ, TNF-α, IL-1β, and IL-10), TGF-β, Toll-like receptors (TLRs) (such as TLR4 and TLR1/2), NOD-like receptors (NLRs) (such as the NLRP3 inflammasome) (Heneka et al., 2015), scavenger receptors (such as CD36, SR1, and MARCO) (Areschoug and Gordon, 2009), TAM receptor tyrosine kinases Mer and AxL (Lemke, 2013), and other receptors. CX3CR1 also known as the fractalkine receptor is specifically expressed by all microglia, as well as the monocytes from embryonic development throughout adulthood. CX3CR1 can interact with C-X3-C motif chemokine ligand 1 (CX3CL1), which is a chemokine expressed by neurons, that regulates neuronal networks and functions. The TAM receptor binds the ligands Gas6 and protein S to drive the microglial phagocytosis of the apoptotic cells (Fourgeaud et al., 2016). Except for immune receptors, microglia express multiple other receptors to monitor neuronal activity, which guides microglia processes toward neuronal synapses to sculpt dendritic spine density (Pocock and Kettenmann, 2007), eliminate the damaged neurons, and promote synaptic formation or neuronal regeneration. For instance, the activating microglial α-amino-3-hydroxy-5-methyl-4-isoxazolepropionic acid (AMPA) receptor inhibits TNF-α release (Hagino et al., 2004), and activation of the glutamate metabotropic receptor 2 (mGlutR2) promotes TNF-α release and neurotoxicity (Taylor et al., 2005). Moreover, microglia can release neurotrophic factors such as BDNF, TGF-β, and IGF-1 to support neuronal survival (Figure 16).

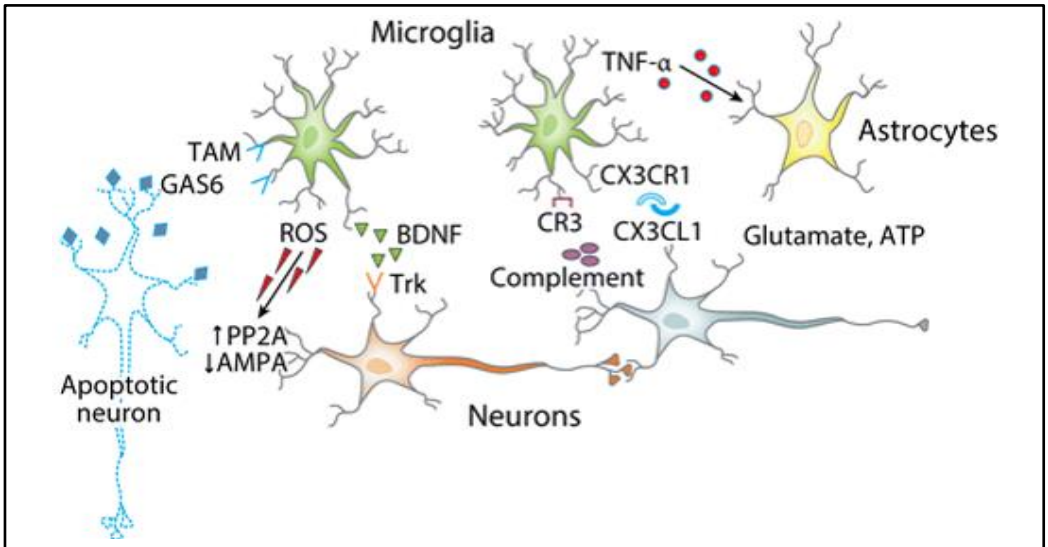

Figure 16: Microglia regulation of brain circuits. Microglia phagocytose apoptotic neurons via the TAM receptor. Microglia regulate the neuronal circuits by expressing CX3CR1 and CR3, releasing ROS and BDNF, and affecting the functions of astrocytes. Adapted from (Colonna and Butovsky, 2017).

However, microglia are double-edged swords. Excessive microglial activation damages the surrounding healthy neural tissue, and factors (such as ATP) secreted by the dead or dying neurons, in turn, exacerbate the chronic activation of microglia. These processes cause persistent neuroinflammation, which in turn induces neurotoxicity and neuronal loss (Hide et al., 2000). This case has been observed in many neurodegenerative diseases such as Alzheimer's disease (AD), Parkinson's disease (PD), Huntington's disease and amyotrophic lateral sclerosis (ALS) (Fu et al., 2014; Hickman et al., 2018a; Rajendran and Paolicelli, 2018; Tang and Le, 2016). Aging microglia display reduced ramification and short, tortuous, swollen processes (Sierra et al., 2007), which is paralleled by a reduced expression of M1 markers and increased expression of M2 markers and genes involved in neuroprotection, suggesting that aging microglia shift towards a neuroprotective or phagocytic phenotype (Hickman et al., 2013). This switch may also contribute to the development of neurodegenerative diseases.

3.5. Sex Difference

Evidence shows that microglia show sex differences from cell number and morphology to functions, which may have a profound influence on behavioral phenotypes or even

neuropsychiatric diseases. In early postnatal development male mice have more microglia than females in the cortex, hippocampus, and amygdala, areas critical for cognition, learning, and memory. At this stage, microglia are large round amoeboid cells and have the potential to produce more cytokines and chemokines compared with the adult brain. Thus, in the event of neonatal infection male mice are more vulnerable and have an increased risk of cognitive deficits (Schwarz and Bilbo, 2012). Specifically, males show an increased prevalence of autism associated with the early infection; in contrast, females have more disorders that present after adolescence, such as depression and anxiety disorders. Moreover, female microglia show significantly higher phagocytic capacity compared to males (Nelson et al., 2017), while male microglia show more migration than females (Yanguas-Casas et al., 2018).

4. Microglia Functions in Learning and Memory

Recently, evidence has been provided that microglia also have an important role in synaptic formation and neurogenesis during CNS development (Miyamoto et al., 2016b; Weinhard et al., 2018a). During development, there is an overproduction of neuron-synapse connections, many of which will be eliminated to allow for the strengthening of more productive connections and more efficient neural networks (Caroni et al., 2014a). Pruning the unwanted or weak synapses is a necessary process for appropriate brain connectivity during brain development (Jiang and Nardelli, 2016; Kettenmann et al., 2013; Tremblay et al., 2011a). Microglia phagocytosis of synapses plays an active role in synapses maturation (Paolicelli et al., 2011b; Schafer et al., 2012) and disruption of this process results in deficits in synaptic connectivity (Mallya et al., 2019; Schafer et al., 2013; Schafer and Stevens, 2013). Moreover, microglia engulf cell bodies to ensure a proper cell number, which further contributes to the specific behavioral formation (VanRyzin et al., 2019). The following part focuses on microglial functions in the refinement of neural circuits, which affect learning and memory processes across CNS development and in homeostasis.

4.1. Microglia and Neural Circuits during Development

4.1.1. Microglia engulf synapses

During brain development, neurons form an excess of synaptic connections, many of which are eliminated during synapse pruning to establish functional brain connectivity (Tremblay et al., 2011b). Synaptic density is highest during early postnatal development in the human frontal cortex (Huttenlocher, 1979) and significantly reduces with aging (Huttenlocher, 1979; Kabaso et al., 2009). In mice, the peak of synaptic density in the hippocampus is around the fourth postnatal week. Emerging work implicates microglia and immune-related molecules as key players in the refinement of immature synapses (Schafer et al., 2013; Sierra et al., 2013). High-resolution imaging studies have established that microglia engulf pre and post-synaptic elements (such as axonal terminals and dendritic spines) during CNS development (Paolicelli et al., 2011b; Schafer et al., 2012). A recent study provides direct evidence that microglia partially phagocytose presynaptic material in living brain tissue at P15 (Ralston et al., 2014). Disruption of microglial function leads to negative influences on synapses formation and neuronal connections.

Several mechanisms are involved in synaptic stripping, most of which share the immune system. Microglial CX3CR1 interacts with neuronal CX3CL1 to affect synaptic maturation (Ransohoff and Stevens, 2011). The transient reduction in microglia activity from P8 to P28 leads to increased spine density and abundant excitatory synapses during the second and third postnatal weeks in the *Cx3cr1* knockout mice (Paolicelli et al., 2011b), which leads to deficits in social interaction and increased repetitive behavior that has been associated with autism and other neurodevelopmental and neuropsychiatric disorders (Paolicelli et al., 2011b; Zhan et al., 2014). A similar delay of synapse maturation was seen in the barrel cortex in *Cx3cr1* deleted mice (Hoshiko et al., 2012). Cx3cr1 deficient mice also exhibit increased microglial activation and pro-inflammatory phenotype in other specific brain regions, which leads to the impairment of synaptic plasticity and triggers cognitive deficits and mood disorders (Bordeleau et al., 2019; Rogers et al., 2011).

Moreover, microglia recognize the classical complement cascade proteins (C1q and C3), which localize to the unwanted immature synapses and participate in the synaptic pruning via CR3 (Stephan et al., 2012). In the mouse visual system, the reduced microglial engulfment results in significantly increased synapse density in retinal ganglion cells and a deficit in eye-specific segregation at P10 in CR3 or C3 KO mice (Schafer et al., 2012). Besides, microglia mediate synaptic pruning via the triggering receptor expressed on myeloid cells 2 (TREM2), which is mainly expressed on microglia in the brain. TREM2 deficient mice have increased synapse density and display sociability defects very much comparable to autism in humans (Filipello et al., 2018). These findings indicate that synapse elimination and rearrangement promote a mature neuronal circuitry formation in the healthy brain.

However, increased microglial synaptic elimination may also result in spine number reduction and cognitive deficits. For instance, in adult microglia specific polycomb repressive complex 2 (PRC2) KO mice, increased microglial clearance activity results in reduced spine density in the striatal medium spiny neurons, accompanied by enhanced anxiety behavior and mild cognition and memory deficits in novel object recognition and fear conditioning task (Ayata et al., 2018b). Increased microglial density and exacerbated microglial activity in the hippocampus lead to reduced dendritic spine density in newborn neurons of the subgranular zone that may contribute to the depression-like behavior and impaired long-term recognition memory in adult microglia-specific VPS35 deficient mice (Appel et al., 2018). Microglia-like cells derived from schizophrenia patients show excessive synaptic pruning *in vitro,* which may explain the reduced synapse density found in postmortem cortical tissue of schizophrenia patients (Sellgren et al., 2019). Therefore, the antibiotic minocycline which can reduce microglial

activation and engulfment of synapse structures may have therapeutic benefits in schizophrenia patients (Sellgren et al., 2019; Tikka et al., 2001).

Thus, appropriate microglial phagocytic capacity during development is crucial for synaptic pruning and subsequently mature neuronal connectivity formation.

4.1.2. Microglia phagocytose cell bodies

In different brain regions, microglia phagocytic content contains cell nuclei fragments, indicating that microglia engulf cell bodies to maintain CNS homeostasis (Ayata et al., 2018a; VanRyzin et al., 2019). It shows that in the adult hippocampal subgranular zone (SGZ), where neurogenesis occurs, only a small amount of neuroblasts can survive and integrate into neural circuits; the majority of newborn cells are eliminated through apoptosis-coupled phagocytosis by microglia (Sierra et al., 2010). Microglia also engulf the apoptotic neurons in the developing and adult mouse cerebellum (Ashwell, 1990; Ayata et al., 2018a). Moreover, microglia phagocytose live neural progenitor cells (NPCs) (Cunningham et al., 2013; Sellgren et al., 2017) and remove viable neurons during neuronal development to limit the overproduction of cortical neurons (Brown and Neher, 2014). Except these, microglial also phagocytose ALDH1L1, which is an early astrocyte marker, indicating the engulfment of astrocytic material in the early developing amygdala, which subsequently affects the neural circuitry and mice behavior (VanRyzin et al., 2019). These data suggest that microglia not only play a critical role in removing apoptotic cells and cell debris to maintain a healthy microenvironment for neuronal survival, but also regulate the live cells to ensure the proper cell number and brain circuits.

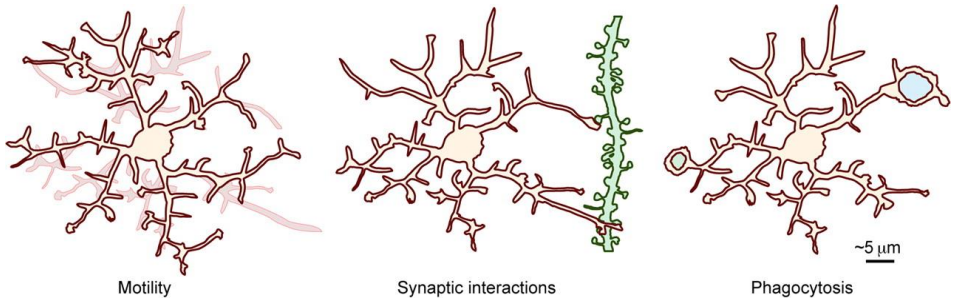

Figure 17: Microglia sculpt neural circuits in the healthy brain. Highly motile microglial processes continuously survey the surrounding environment (left). Microglia interact with synaptic elements (middle; green: dendritic branch and spines) and contribute to remodeling of neuronal circuits by phagocytosing synaptic elements and cell bodies (right; cellular inclusions, blue and green). Adapted from (Tremblay et al., 2011a).

4.2. Microglia in Synaptic Formation and Maturation

Except for synapse and cell body elimination, microglia also participate in synaptic formation and neurogenesis, which play a crucial role in brain circuits' maturation (Reshef et al., 2017). Microglia increase spine length and spine head filopodia (Schatzle et al., 2011) formation in postsynaptic sites, providing direct evidence that microglia contacts involve structural synaptic plasticity (Weinhard et al., 2018a). This phenomenon is also observed in pyramidal neurons in the developing somatosensory cortex. Transient genetic ablation of microglia around P8 leads to a reduced spine density in P11 in layer II/III neurons, further demonstrating that microglia promote the filopodia and functional mature synapses formation and subsequently contribute to the maturation of specific neuronal circuits (Miyamoto et al., 2016b). Transient microglial depletion in the late postnatal period (P19) or young adulthood (P30) causes a significant decrease in both spine formation and elimination in layer V pyramidal neurons in the motor cortex in mice, and leads to deficits in multiple learning tasks and learning-induced synaptic remodeling (Parkhurst et al., 2013).

Besides, microglia impact synapse formation, strength, and plasticity through releasing soluble factors such as inflammatory cytokines, ROS, and NO as well as neurotrophic factors (Vezzani and Viviani, 2015). Co-cultures of hippocampal neurons and microglia show that microglia induce neuronal synapses formation via releasing IL-10 that can interact with IL-10 receptors expressed on hippocampal neurons (Lim et al., 2013). It has also been suggested that a physiological level of IL-1β is necessary for the induction and maintenance of LTP. IL-1R deficient mice show absent LTP in perforant path granule cells and CA1 pyramidal cells (Avital et al., 2003), but excessive IL-1β has an inhibitory effect on LTP (Bellinger et al., 1993). Specific microglia BDNF depletion repeats many of the phenotypes generated by microglia depletion, indicating that microglia BDNF is an important factor for synaptic remodeling associated with motor learning and memory (Parkhurst et al., 2013). Moreover, microglia mediate LTD via the CR3-NADPH oxidase-ROS-AMPA receptor endocytosis cascade that depresses synaptic transmission (Collingridge and Peineau, 2014; Zhang et al., 2014a). These results show that microglia effects on functional synaptic formation involve multiple pathways.

4.3. Microglia and Neurogenesis

Microglia are necessary for maintaining the proper neuronal cell number in neural networks throughout life (de Miranda et al., 2017). Postnatal neurogenesis, which mainly occurs in the subventricular zone (SVZ) of the lateral ventricles and subgranular zone (SGZ) of the hippocampus plays a critical role in learning and memory (Clelland et al., 2009; Ernst et al., 2014; Sahay et al., 2011). Microglial activation in the SVZ from P1 to P10 is necessary to enhance neurogenesis and oligodendrogenesis via releasing cytokines, while the suppression of microglial activation inhibits neurogenesis in rats. *In vitro* studies show that neurogenesis can be increased by activating microglia or adding cytokines (IL-4, low concentration of IL-1β, IFN-γ, or IFN- γ) in the NPCs culture medium (Butovsky et al., 2006; Shigemoto-Mogami et al., 2014). Microglia also release IGF1 to support neuronal survival (Ueno et al., 2013). These reports indicate that microglia are closely relevant to neurogenesis and neuronal survival.

Furthermore, CX3CL1-CX3CR1 signaling involves exercise-induced activation of NPCs in the hippocampus, but NPCs activity is suppressed in the aged brain (Vukovic et al., 2012). Replacement of microglia in aged mice (24 months) restores microglial tissue characteristics to those found in young adult animals (4 months), without changing immune reactivity. The microglial repopulation reverses the hippocampal neuronal complexity, and fully rescues the age-induced deficits in LTP and spatial memory in mice (Elmore et al., 2018). Thus, microglia repopulation may be a new strategy to improve the functions of the aged brain.

Altogether, these data indicate that microglia play a crucial role in shaping the brain microenvironment and neural wiring to maintain homeostasis across the lifespan (Figure 18).

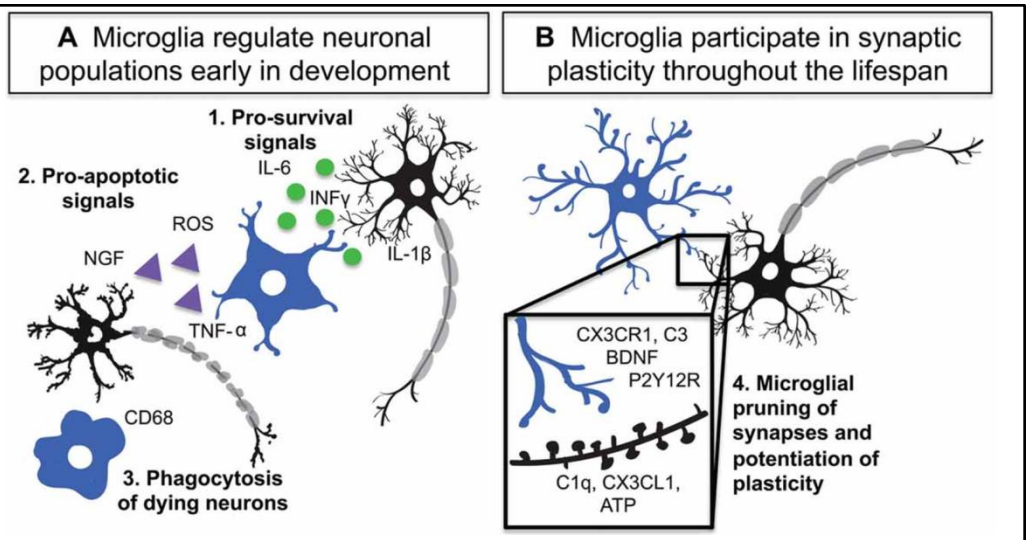

Figure 18. Microglia regulate neuronal circuit development and maintenance. A. Microglia regulate neuronal populations. **B.** microglia participate in synaptic plasticity and pruning throughout the lifespan. Adapted from(Wong et al., 2017).

5. Microglia and Energy Metabolism

Microglia serve as the brain resident macrophages. An increasing number of studies show the involvement of microglia in regulating physiological homeostasis (Gao et al., 2014). Elimination of microglia from the fetal brain leads to decreased litter size and accumulation of hypothalamic apoptotic cells, especially POMC neurons, throughout the development, accompanied by accelerated body weight gain from P5 (Rosin et al., 2018). Even transient removal of microglia results in permanent loss of POMC neurons and this effect is irreversible (Elmore et al., 2014; Rosin et al., 2018). These studies indicate that microglia play an important role in regulating hypothalamic neuronal circuits and energy homeostasis. Indeed, active microglia are found more often adjacent to POMC neurons than to NPY neurons in the hypothalamus (Gao et al., 2017b), and thus may have a more powerful influence on POMC cells.

Hypothalamic inflammation has been linked to the impairment of brain circuits controlling energy balance, as well as the development and progression of obesity and (pre)diabetes in both humans and rodents (Avalos et al., 2018; Baufeld et al., 2016; Jais and Bruning, 2017; Le Thuc et al., 2017). HFD consumption induces low-grade hypothalamic inflammation, neuronal stress, and leptin resistance (De Souza et al., 2005), which is accompanied by rapid glial cell accumulation, especially the microglia (Thaler et al., 2012a; Valdearcos et al., 2014b) (Figure 19). It has been shown that 3 weeks of HFD consumption significantly increases hypothalamic microglial cell numbers in association with increased body weight in rodents. Other studies have proposed that inhibiting microglial activation and inflammation in the ARC is sufficient to protect against diet-induced hypothalamic inflammation and prevent obesity (Andre et al., 2017; Valdearcos et al., 2014b).

Recently, the underlying signaling pathways via which microglial activation impacts the hypothalamic control of energy balances have been demonstrated across various animal models. The hypercaloric diet-induced obese mice show persistently activated microglia in the MBH with increased secretion of TNFα, which increases mitochondrial stress of POMC neurons and contributes to the development of obesity; specific knocking down of the TNFα downstream signals in the MBH of DIO mice reduces obesity (Yi et al., 2017a). High-fat feeding induces a hypothalamic inflammatory response and impairs the insulin-signaling pathway, which is mediated by the activation of hypothalamic c-Jun N-terminal kinase (JNK) and nuclear factor-kappaB (NF-κB) (De Souza et al., 2005; Zhang et al., 2008). Specific inhibition of

hypothalamic c-Jun N-terminal kinase restores insulin signaling and reduces caloric intake and weight gain in HFD fed rats (De Souza et al., 2005). Moreover, depleting microglia or selective silencing of microglial NF-κB-mediated signaling in the genetic mouse model (microglial-specific IKKβ KO) reduces microgliosis (microglial activation and accumulation) and greatly limits diet-induced hyperphagia and weight gain. Additionally, activating microglia through cell-specific deletion of the negative NF-κB regulator A20 induces spontaneous microgliosis in MBH, reduces energy expenditure, and increases both food intake and weight gain even independent of HFD challenge (Valdearcos et al., 2017a). Besides, adeno-associated virus (AAV)-mediated specific overexpression of IκBα in the ARC, which inhibits NF-κB nuclear translocation specifically downstream of IKKβ/NF-κB signaling, attenuates HFD-induced body weight gain, body fat mass accumulation, and increases energy expenditure. Inhibition of the microglial toll-like receptor-4 (TLR4) prevents the central orexigenic AgRP/NPY neuronal response and feeding behavior (Reis et al., 2015). These studies demonstrate that microglial inflammation is sufficient and necessary for the development of DIO and suggests that microglial pro-inflammatory signals induce neuronal stress and ultimately impair neuronal networks involved in the regulation of energy balance, even in the absence of HFD. Inhibition of hypothalamic inflammatory pathways may protect against diet-induced obesity.

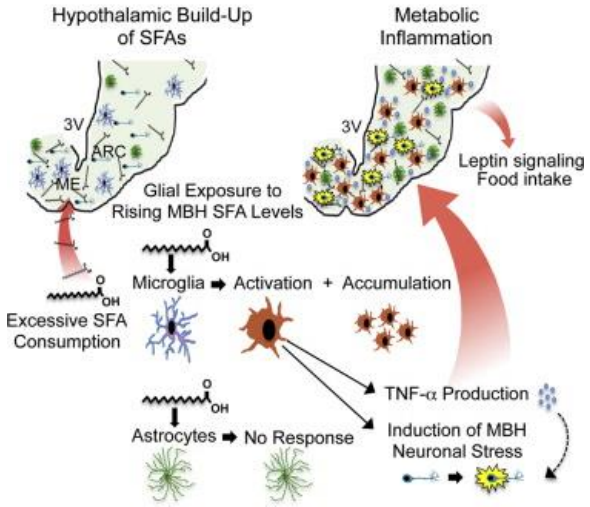

Figure 19. Hypothalamic microglial inflammatory signaling mediates HFD-induced energy imbalance. Hypothalamic microglia sense the increased saturated fat acids (SFAs) and orchestrate local inflammation. In this context, microglia mediate the impact of SFAs on neuronal stress, leptin responsiveness, and regulate food intake. Adapted from (Valdearcos et al., 2014a).

Except for inhibiting hypothalamic inflammation, AAV-mediated overexpression of IL-10 ameliorates hyperphagia and obesity, as well as restores POMC gene expression in DIO mice. Furthermore, IL-10 treatment markedly attenuates the HFD-induced leptin resistance by inhibiting IKKs activation and SOCS3 expression in the ARC of DIO mice (Nakata et al., 2017). Quercetin, a polyphenolic flavonoid, which is known to protect against obesity-induced oxidative stress and inflammation in peripheral tissues (Kim et al., 2015; Le et al., 2014), reduces hypothalamic inflammation by inhibiting the microglia-mediated inflammatory responses in DIO mice and also upregulates the expression of the anti-oxidant enzyme heme oxygenase (HO-1) in the hypothalamus. These findings indicate that increasing the anti-inflammatory effect or preventing oxidative stress in the hypothalamus may provide new therapeutic strategies for the treatment of metabolic disorders, including obesity (Yang et al., 2017).

Moreover, microglial phagocytosis mediates the maintenance of hypothalamic neural circuits. It has been reported that the myeloid cell leptin receptor-deficient mice show impaired microglial phagocytic capacity, decreased POMC neurons, and less α-MSH projections from the ARC to PVN, as well as increased food intake and body weight gain (Gao et al., 2018b). Lacking lipoprotein lipase (LPL) in microglia reduces phagocytosis and leads to a reduction of POMC neurons, and more weight gain than controls when challenged with a high-carbohydrate high-fat (HCHF) diet in adult mice (Gao et al., 2017b). Moreover, microglia release neurotrophic factors to support the surrounding neurons that regulate appetite; mice with BDNF deficiency in microglia show hyperphagia and obesity (Urabe et al., 2013). Thus, proper microglial functions are necessary for maintaining the appropriate hypothalamic neuronal circuits to regulate metabolism.

It should be noted that also clear sex differences are present in the development of metabolic complications associated with obesity (Shi et al., 2009). In humans, metabolic disorders and obesity are less present in premenopausal women as compared to men, however, metabolic dysfunction and obesity significantly increase in women following menopause (Ford, 2005). In rodents, males are more susceptible to diet-induced obesity and hypothalamic inflammation than females (Argente-Arizon et al., 2018; Dorfman et al., 2017; Hong et al., 2009). Microglial sex differences play a decisive role in hypothalamic inflammation and energy homeostasis, which may depend on the CX3CR1-CX3CL1 pathway that mediates the resistance of female mice to become obese under HFD feeding (Dorfman et al., 2017). It has been shown that HFD feeding results in the reduction of both CX3CR1 and CX3CL1 in male mice, but not in females. Moreover, CX3CR1 deficient female mice show hypothalamic microglial accumulation and

activation and gain a comparative amount of body weight compared with males when fed with HFD (Dorfman et al., 2017).

In conclusion, microglia are necessary for the proper development and maintenance of hypothalamic neuronal circuits that are involved in the regulation of physiological homeostasis, via releasing soluble factors and phagocytosis. However, excessive microglial activation leads to hypothalamic inflammation, which has been linked to the development and progression of obesity. Therefore, optimizing microglia functions may be an effective strategy to prevent and treat the hypothalamic inflammation, neuronal loss, and metabolic disorders.

6. Circadian Clocks

The circadian timing system is an internal timekeeping system, which regulates various physiological events, including the sleep-wake cycle, the feeding-fasting cycle, body temperature, activity, metabolism, immune response, and cognition, repeating these physiological processes with a daily rhythm of approximately 24 hours (Gerstner and Yin, 2010; Kalsbeek et al., 2014; Snider et al., 2018; Stenvers et al., 2019b). To stay in synchrony with the environmental 24-hour rhythm, these circadian rhythms have to be reset by environmental cues, also known as Zeitgebers (from German, "time givers"), such as light, temperature, feeding, and oxygen. Circadian rhythms coordinate cellular functions, tissue functions, behavioral and mental changes to align them with the external light/dark cycle. Long-term disruption of these circadian rhythms, such as caused by shift work, will lead to a series of significant adverse health consequences, for example, metabolic disease, immune dysfunction, cognitive deficit, sleep and bipolar disorder, and cardiovascular disease (Xie et al., 2019). It has been reported that also insufficient and delayed sleep are risk factors for overweight or obesity in children and adolescents (Miller et al., 2018).

The circadian system is organized in a hierarchy of multiple oscillators at the organism, cellular, and molecular level. In mammals, the central pacemaker is located in the hypothalamic suprachiasmatic nucleus (SCN), which aligns all clocks with the external light/dark cycles via its neural and humoral outputs. The SCN is made up of multiple populations of oscillating neurons that are integrated to act as a single circadian unit, resulting in a coordinated circadian output signal. For the central clock, the predominant Zeitgeber is light, which is sensed by retinal ganglion cells that project directly to the SCN. SCN lesions impair hippocampal-dependent memory, such as long-term novel object recognition (Shimizu et al., 2016), contextual memory, and Morris water maze performance (Phan et al., 2011). At the molecular level, the core clock machinery relies on a number of autoregulatory transcription-translation feedback loops (TTFLs) (Dudek and Meng, 2014). The transcriptional activator Bmal1 (brain and muscle ARNT-like 1)/Clock (circadian locomotor output cycles Kaput) complex drives the genes that contain an E-box sequence in their promoter regions, including the *Per1/2/3* (period circadian clock 1/2/3) and *Cry1/2* (cryptochrome 1/2) genes, in turn, their products can inhibit the activity of the Bmal1/Clock complex (Barca-Mayo et al., 2017; Dudek and Meng, 2014; Gekakis et al., 1998). A sub-loop including the nuclear hormone receptors *Ror*α (RAR-related orphan receptor alpha, activator) and *Rev-erb*α (repressor) fine-tunes the expression of *Bmal1*. Moreover, recent studies have shown that except for this autoregulation, core clock genes control the rhythmic

expression of 10%-43% other genes in cells or tissues, via specific regulatory elements [E-box, D-box and RORE (Ror/Rev-erb-binding element)] in their promoters (Figure 20) (Duffield, 2003; Reppert and Weaver, 2002; Sato et al., 2004; Zhang et al., 2014b).

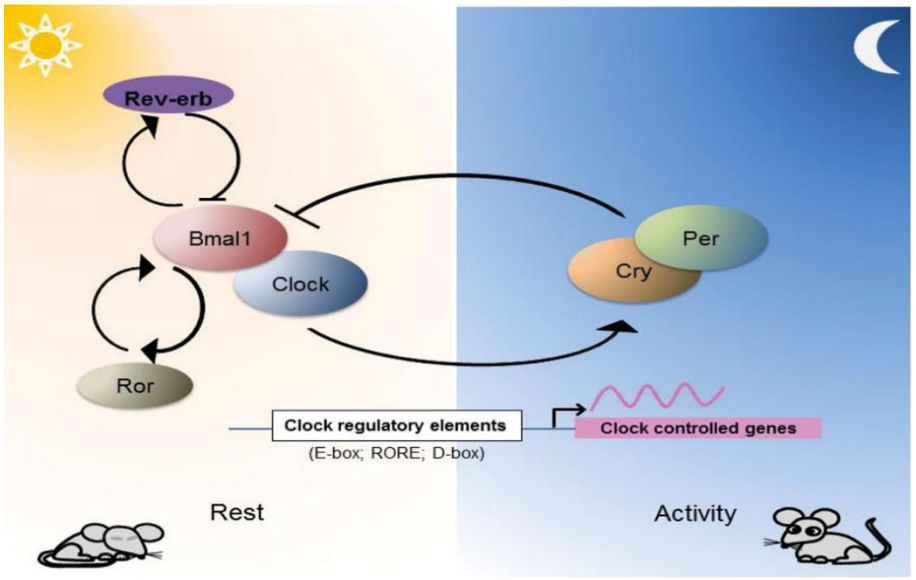

Figure 20. A simplified representation of the core clock components that contribute to mammalian circadian oscillations. The *Bmal1* and *Clock* complex is highly expressed during the light phase, while *Per* and *Cry* are mainly expressed in the dark phase. The Bmal1/Clock complex promotes the transcription of genes containing clock regulatory elements (E-box, RORE, D-box), which include the Per, Cry, Ror, and Rev-erb. These genes expression adjust the activity of the Bmal1/Clock complex. Adapted from (Dudek and Meng, 2014).

The molecular clocks drive the circadian rhythm of gene and protein expression in many tissues (Bass and Takahashi, 2010b; Early et al., 2018b; Loizides-Mangold et al., 2017; Rahman et al., 2015; Stenvers et al., 2019b). Moreover, a growing body of literature shows that the endogenous circadian clock plays a crucial role in the control of many cellular processes that affect overall physiology (Barca-Mayo et al., 2019; Bass and Takahashi, 2010a) (Figure 21). For example, skeletal muscle clock gene deficiency disturbs nutrient utilization and leads to metabolic disorders (Gabriel and Zierath, 2019a; Schiaffino et al., 2016; Stenvers et al., 2019a). Hippocampal dependent cognitive performance is also controlled by the circadian clock (Hasegawa et al., 2019). Furthermore, non-transcriptional elements, such as redox oscillations and protein phosphorylation cycles are also essential for cellular circadian rhythms (Edgar et al., 2012; O'Neill and Reddy, 2011; Ray et al., 2020; Rey and Reddy, 2015; Wu and Reddy, 2014).

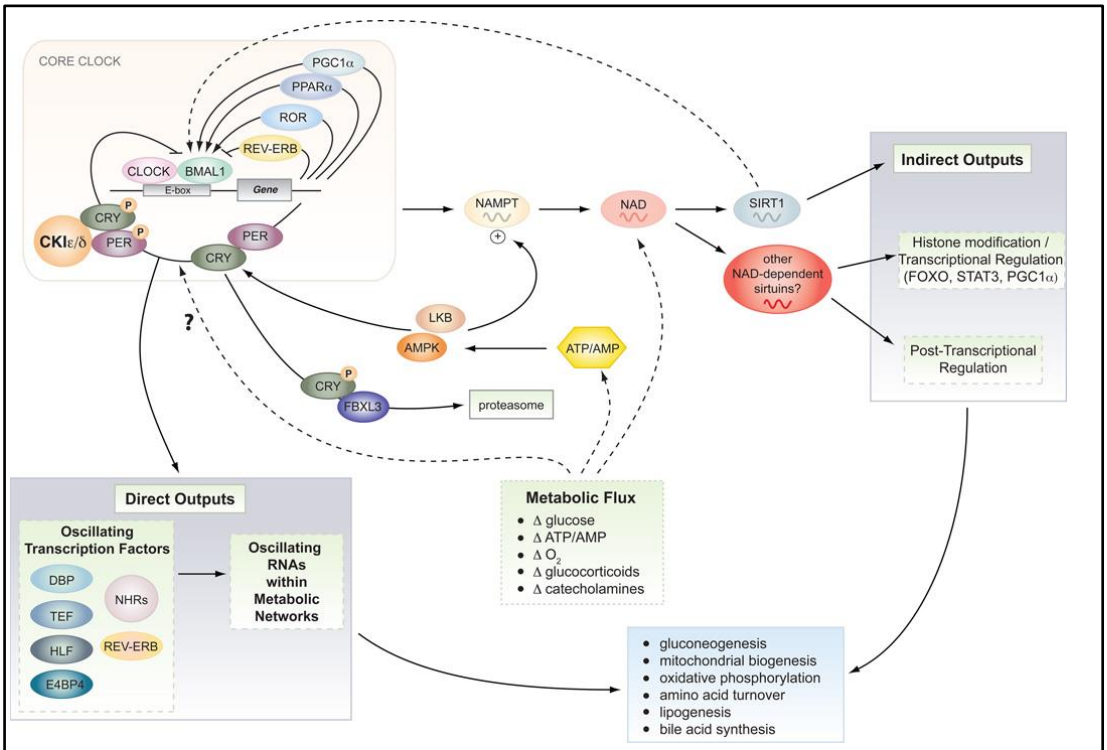

Figure 21. Direct and indirect outputs of the core clock mechanism. The core clocks synchronize diverse metabolic processes through both direct and indirect outputs including gluconeogenesis, lipogenesis, amino acid turnover, mitochondrial biogenesis, and oxidative metabolism. The clock also receives reciprocal input from nutrient signaling pathways, which function as rheostats to couple circadian cycles to metabolic flux especially in peripheral tissues. Adapted from (Bass and Takahashi, 2010b).

Bmal1

Bmal1, also known as Aryl hydrocarbon receptor nuclear translocator-like protein 1 (ARNTL) and MOP3, is a transcription factor with a basic helix-loop-helix (bHLH), two PAS domains, and a trans-activating domain (Hogenesch et al., 1997). Via the PAS domain, Bmal1 binds with a second bHLH-PAS protein-Clock (or its paralog, NPAS2, Neuronal PAS domain-containing protein 2) to form a heterodimer in the nucleus. Via the bHLH domain, the Bmal1/Clock heterodimer binds to E-box elements in the promoter regions of *Per* (*Per1* and *Per2*), *Cry* (*Cry1*, *Cry2*, and *Cry3*), *Rev-Erbα*, and *ROR* genes and regulates the transcription of these genes. Moreover, as a member of the PAS superfamily, BMAL1/CLOCK (or NPAS2) may have the capacity to sense environmental and developmental signals, such as hypoxia, light, temperature (Gu et al., 2000).

Bmal1 plays an important role in the regulation of glucose homeostasis, lipogenesis, cholesterol homeostasis, metabolism, and the immune response (Kitchen et al., 2020b; Lee et al., 2012; Marcheva et al., 2010; Oishi et al., 2017; Rudic et al., 2004). Experiments with genetically modified animals have identified *Bmal1* as a candidate gene for susceptibility to hypertension, type II diabetes, and obesity (Pappa et al., 2013; Richards et al., 2014; Woon et al., 2007). Global *Bmal1* knockout mice are arrhythmic in constant darkness and show reduced locomotor activity in light/dark cycles (Bunger et al., 2000). This animal model also shows widespread astrocytosis and discrete degeneration of presynaptic axonal terminals in the brain (Musiek et al., 2013a). Conditional ablation of *Bmal1* in peripheral organs, such as liver, pancreas, adipose tissue or skeletal muscle reveals profound and diverse disorders and pathologies (Alvarez et al., 2008; Lamia et al., 2008; Loizides-Mangold et al., 2017; Marcheva et al., 2010; Schiaffino et al., 2016; Shimba et al., 2005), highlighting the importance of local clocks in tissue and whole-body homeostasis. The molecules involved in the circadian clock machinery are present in all cell types. Specific astrocytic deletion of Bmal1 results in cognitive deficiency and metabolic imbalance in mice (Barca-Mayo et al., 2019; Barca-Mayo et al., 2017). Microglial activity shows a circadian variation in mice (Yi et al., 2017a). It has been reported that age-related microglial circadian disruption sensitizes the neuroinflammatory response in the hippocampus (Fonken et al., 2016), while specific microglial Bmal1 deficient mice show reduced expression of IL-6 in the brain, with a significant attenuation of neuronal damage following middle cerebral artery occlusion (Nakazato et al., 2017).

Clock

Clock, a bHLH-PAS transcription activator, affects both the persistence and period of circadian rhythms. In constant darkness, the deletion of exon 19 of the *Clock* gene leads to a lengthened circadian period and arrhythmicity in heterozygous and homozygous mice, respectively (Herzog et al., 1998; Vitaterna et al., 1994). Surprisingly, mice totally deficient of Clock display completely normal circadian rhythms in locomotor activity as the Clock paralog-NPAS2 substitutes for Clock in this process (Debruyne, 2008; Debruyne et al., 2006; DeBruyne et al., 2007). But *Clock* mutant mice show an attenuated diurnal feeding rhythm, hyperphagia, obesity, and metabolic syndrome (Turek et al., 2005). Moreover, *Clock* mutations have been implicated in sleep disorders, mood disorders, breast cancers, and colorectal cancers (Alhopuro et al., 2010; McClung, 2007; Naylor et al., 2000; Turek et al., 2005).

Per1, Per2, and Per3

The family of Period genes includes 3 members: *Per1*, *Per2*, and *Per3*, and the proteins encoded by these genes dimerize with Cry1 and Cry2 proteins. This Per/Cry heterodimer inhibits its own transcription via translocation into the nucleus upon phosphorylation and suppressing Bmal1/Clock activation. Moreover, *Sirt1* (sirtuin 1), an NAD(+)-dependent protein deacetylase, regulates Per proteins deacetylation and degradation by binding the Bmal1/Clock heterodimer in a circadian manner (Asher et al., 2008). *Per1* and *Per2* are necessary for the daily resetting of the circadian clock via normal environmental light cues; light exposure increases *Per1* expression and also stabilizes *Per2* expression in mice (Miyake et al., 2000). Per3 may have a stabilizing effect on Per1 and Per2 (Zhang et al., 2016a).

The Period family also plays an important role in the regulation of the daily rhythms of locomotor activity, metabolism, cancer formation, and behavior in mammals. Per1 and Per2 double knockout mice show complete circadian arrhythmicity (Bae et al., 2001; Zheng et al., 2001). Per2 shows protective functions in heart attacks and liver diseases (Benegiamo et al., 2013; Eckle et al., 2012). *Per1* and *Per2* genes also play a key role in tumor growth; lowered *Per1* and *Per2* expression is linked with promoting tumor progression (Liu et al., 2014; Winter et al., 2007; Yang et al., 2009b). For example, *Per2* expression is significantly lower in human patients with lymphoma and acute myeloid leukemia (Ko and Takahashi, 2006).

Cry1 and Cry2

Cry1 and Cry2 play a crucial role in the generation and maintenance of circadian rhythms as light-independent inhibitors of Bmal1/Clock components of the circadian clock (Griffin et al., 1999). Cry1 and Cry2 are closely associated with energy balance (Barclay et al., 2013; Griebel et al., 2014).

Rev-erba and RORα

The Rev-erba proteins are members of the nuclear receptor family of intracellular transcription factors, including Rev-erba alpha (Rev-erbα) and Rev-erba beta (Rev-erbβ), which are encoded by the *Nr1d1* (nuclear receptor subfamily 1, group D, member 1) and *Nr1d2* (nuclear receptor subfamily 1, group D, member 2) genes, respectively. RORα, also known as Nr1f1 (nuclear receptor subfamily 1, group F, member 1) is also a nuclear receptor. Rev-erbα, Rev-erbβ, and RORα fine-tune their target physiologic networks, such as circadian rhythms, metabolic homeostasis, and inflammation (Delezie and Challet, 2011; Forman et al., 1994; Ko and Takahashi, 2006; Lo et al., 2016). For example, the deletion of the *Rev-erbα* leads to

diet-induced obesity and alters glucose and lipid metabolism, which increases the risk for these mice to become diabetic (Delezie et al., 2012).

References

Abdalla, M.M. (2017). Central and peripheral control of food intake. Endocr Regul *51*, 52-70.

Alhopuro, P., Bjorklund, M., Sammalkorpi, H., Turunen, M., Tuupanen, S., Bistrom, M., Niittymaki, I., Lehtonen, H.J., Kivioja, T., Launonen, V.*, et al.* (2010). Mutations in the circadian gene CLOCK in colorectal cancer. Mol Cancer Res *8*, 952-960.

Aloisi, F. (2001). Immune function of microglia. Glia *36*, 165-179.

Alvarez, J.D., Hansen, A., Ord, T., Bebas, P., Chappell, P.E., Giebultowicz, J.M., Williams, C., Moss, S., and Sehgal, A. (2008). The circadian clock protein BMAL1 is necessary for fertility and proper testosterone production in mice. J Biol Rhythm *23*, 26-36.

Anagnostaras, S.G., Maren, S., and Fanselow, M.S. (1999). Temporally graded retrograde amnesia of contextual fear after hippocampal damage in rats: within-subjects examination. J Neurosci *19*, 1106-1114.

Anand, B.K., and Brobeck, J.R. (1951). Hypothalamic control of food intake in rats and cats. Yale J Biol Med *24*, 123-140.

Andre, C., Guzman-Quevedo, O., Rey, C., Remus-Borel, J., Clark, S., Castellanos-Jankiewicz, A., Ladeveze, E., Leste-Lasserre, T., Nadjar, A., Abrous, D.N.*, et al.* (2017). Inhibiting Microglia Expansion Prevents Diet-Induced Hypothalamic and Peripheral Inflammation. Diabetes *66*, 908-919.

Appel, J.R., Ye, S., Tang, F., Sun, D., Zhang, H., Mei, L., and Xiong, W.C. (2018). Increased Microglial Activity, Impaired Adult Hippocampal Neurogenesis, and Depressive-like Behavior in Microglial VPS35-Depleted Mice. J Neurosci *38*, 5949-5968.

Araya, R., Eisenthal, K.B., and Yuste, R. (2006a). Dendritic spines linearize the summation of excitatory potentials. P Natl Acad Sci USA *103*, 18799-18804.

Araya, R., Jiang, J., Eisenthal, K.B., and Yuste, R. (2006b). The spine neck filters membrane potentials. P Natl Acad Sci USA *103*, 17961-17966.

Arellano, J.I., Benavides-Piccione, R., DeFelipe, J., and Yuste, R. (2007). Ultrastructure of dendritic spines: correlation between synaptic and spine morphologies. Front Neurosci-Switz *1*, 131-143.

Areschoug, T., and Gordon, S. (2009). Scavenger receptors: role in innate immunity and microbial pathogenesis. Cell Microbiol *11*, 1160-1169.

Argente-Arizon, P., Diaz, F., Ros, P., Barrios, V., Tena-Sempere, M., Garcia-Segura, L.M., Argente, J., and Chowen, J.A. (2018). The Hypothalamic Inflammatory/Gliosis Response to Neonatal Overnutrition Is Sex and Age Dependent. Endocrinology *159*, 368-387.

Asher, G., Gatfield, D., Stratmann, M., Reinke, H., Dibner, C., Kreppel, F., Mostoslavsky, R., Alt, F.W., and Schibler, U. (2008). SIRT1 regulates circadian clock gene expression through PER2 deacetylation. Cell *134*, 317-328.

Ashwell, K. (1990). Microglia and cell death in the developing mouse cerebellum. Brain Res Dev Brain Res *55*, 219-230.

Avalos, Y., Kerr, B., Maliqueo, M., and Dorfman, M. (2018). Cell and molecular mechanisms behind diet-induced hypothalamic inflammation and obesity. J Neuroendocrinol *30*, e12598.

Avital, A., Goshen, I., Kamsler, A., Segal, M., Iverfeldt, K., Richter-Levin, G., and Yirmiya, R. (2003). Impaired interleukin-1 signaling is associated with deficits in hippocampal memory processes and neural plasticity. Hippocampus *13*, 826-834.

Ayata, P., Badimon, A., Strasburger, H.J., Duff, M.K., Montgomery, S.E., Loh, Y.E., Ebert, A., Pimenova, A.A., Ramirez, B.R., Chan, A.T.*, et al.* (2018a). Epigenetic regulation of brain region-specific microglia clearance activity. Nat Neurosci *21*, 1049-1060.

Ayoub, A.E., and Salm, A.K. (2003). Increased morphological diversity of microglia in the activated hypothalamic supraoptic nucleus. J Neurosci *23*, 7759-7766.

Bae, K., Jin, X., Maywood, E.S., Hastings, M.H., Reppert, S.M., and Weaver, D.R. (2001). Differential functions of mPer1, mPer2, and mPer3 in the SCN circadian clock. Neuron *30*, 525-536.

Bannerman, D.M., Deacon, R.M.J., Offen, S., Friswell, J., Grubb, M., and Rawlins, J.N.P. (2002). Double dissociation of function within the hippocampus: Spatial memory and hyponeophagia. Behavioral Neuroscience *116*, 884-901.

Barca-Mayo, O., Boender, A.J., Armirotti, A., and De Pietri Tonelli, D. (2019). Deletion of astrocytic BMAL1 results in metabolic imbalance and shorter lifespan in mice. Glia.

Barca-Mayo, O., Pons-Espinal, M., Follert, P., Armirotti, A., Berdondini, L., and De Pietri Tonelli, D. (2017). Astrocyte deletion of Bmal1 alters daily locomotor activity and cognitive functions via GABA signalling. Nat Commun *8*, 14336.

Barclay, J.L., Shostak, A., Leliavski, A., Tsang, A.H., Johren, O., Muller-Fielitz, H., Landgraf, D., Naujokat, N., van der Horst, G.T., and Oster, H. (2013). High-fat diet-induced hyperinsulinemia and tissue-specific insulin resistance in Cry-deficient mice. Am J Physiol Endocrinol Metab *304*, E1053-1063.

Barnes, M.B., Lawson, M.A., and Beverly, J.L. (2011). Rate of fall in blood glucose and recurrent hypoglycemia affect glucose dynamics and noradrenergic activation in the ventromedial hypothalamus. Am J Physiol Regul Integr Comp Physiol *301*, R1815-1820.

Barnes, S.J., and Cheetham, C.E.J. (2014). A Role for Short-Lived Synapses in Adult Cortex? Journal of Neuroscience *34*, 7044-7046.

Bass, J., and Takahashi, J.S. (2010a). Circadian integration of metabolism and energetics. Science *330*, 1349-1354.

Baufeld, C., Osterloh, A., Prokop, S., Miller, K.R., and Heppner, F.L. (2016). High-fat diet-induced brain region-specific phenotypic spectrum of CNS resident microglia. Acta Neuropathol *132*, 361-375.

Bekinschtein, P.A., Cammarota, M., Muller, I.L., Bevilaqua, L.R., Izquierdo, I., and Medina, J.H. (2007). Persistence of long-term memory storage requires a late protein synthesis- and BDNF-dependent phase in the hippocampus. Journal of Neurochemistry *102*, 22-22.

Bellinger, F.P., Madamba, S., and Siggins, G.R. (1993). Interleukin 1 beta inhibits synaptic strength and long-term potentiation in the rat CA1 hippocampus. Brain Res *628*, 227-234.

Benegiamo, G., Mazzoccoli, G., Cappello, F., Rappa, F., Scibetta, N., Oben, J., Greco, A., Williams, R., Andriulli, A., Vinciguerra, M., *et al.* (2013). Mutual Antagonism between Circadian Protein Period 2 and Hepatitis C Virus Replication in Hepatocytes. PLoS One *8*.

Bernardis, L.L., and Bellinger, L.L. (1986). Effect of palatable diet on growth, caloric intake and endocrine-metabolic profile in weanling rats with dorsomedial hypothalamic lesions. Appetite *7*, 219-230.

Betley, J.N., Cao, Z.F., Ritola, K.D., and Sternson, S.M. (2013). Parallel, redundant circuit organization for homeostatic control of feeding behavior. Cell *155*, 1337-1350.

Bontempi, B., Laurent-Demir, C., Destrade, C., and Jaffard, R. (1999). Time-dependent reorganization of brain circuitry underlying long-term memory storage. Nature *400*, 671-675.

Bordeleau, M., Carrier, M., Luheshi, G.N., and Tremblay, M.E. (2019). Microglia along sex lines: From brain colonization, maturation and function, to implication in neurodevelopmental disorders. Semin Cell Dev Biol.

Borgland, S.L., Storm, E., and Bonci, A. (2008). Orexin B/hypocretin 2 increases glutamatergic transmission to ventral tegmental area neurons. Eur J Neurosci *28*, 1545-1556.

Bradley, T.R., and Metcalf, D. (1966). The growth of mouse bone marrow cells in vitro. Aust J Exp Biol Med Sci *44*, 287-299.

Bray, G.A., Fisler, J., and York, D.A. (1990). Neuroendocrine Control of the Development of Obesity - Understanding Gained from Studies of Experimental Animal-Models. Front Neuroendocrin *11*, 128-181.

Bray, G.A., Smith, S.R., DeJonge, L., de Souza, R., Rood, J., Champagne, C.M., Laranjo, N., Carey, V., Obarzanek, E., Loria, C.M*., et al.* (2012). Effect of diet composition on energy expenditure during weight loss: the POUNDS LOST Study. Int J Obes (Lond) *36*, 448-455.

Broadbent, N.J., Squire, L.R., and Clark, R.E. (2004). Spatial memory, recognition memory, and the hippocampus. Proc Natl Acad Sci U S A *101*, 14515-14520.

Brobeck, J.R. (1946). Mechanism of the development of obesity in animals with hypothalamic lesions. Physiol Rev *26*, 541-559.

Broberger, C., De Lecea, L., Sutcliffe, J.G., and Hokfelt, T. (1998). Hypocretin/orexin- and melanin-concentrating hormone-expressing cells form distinct populations in the rodent lateral hypothalamus: relationship to the neuropeptide Y and agouti gene-related protein systems. J Comp Neurol *402*, 460-474.

Brown, G.C., and Neher, J.J. (2014). Microglial phagocytosis of live neurons. Nat Rev Neurosci *15*, 209-216.

Bunger, M.K., Wilsbacher, L.D., Moran, S.M., Clendenin, C., Radcliffe, L.A., Hogenesch, J.B., Simon, M.C., Takahashi, J.S., and Bradfield, C.A. (2000). Mop3 is an essential component of the master circadian pacemaker in mammals. Cell *103*, 1009-1017.

Burbridge, S., Stewart, I., and Placzek, M. (2016). Development of the Neuroendocrine Hypothalamus. Compr Physiol *6*, 623-643.

Butovsky, O., Ziv, Y., Schwartz, A., Landa, G., Talpalar, A.E., Pluchino, S., Martino, G., and Schwartz, M. (2006). Microglia activated by IL-4 or IFN-gamma differentially induce neurogenesis and oligodendrogenesis from adult stem/progenitor cells. Mol Cell Neurosci *31*, 149-160.

Cane, M., Maco, B., Knott, G., and Holtmaat, A. (2014). The Relationship between PSD-95 Clustering and Spine Stability In Vivo (pg 2075, 2014). Journal of Neuroscience *34*, 6717-6717.

Caroni, P., Chowdhury, A., and Lahr, M. (2014a). Synapse rearrangements upon learning: from divergent-sparse connectivity to dedicated sub-circuits. Trends in Neurosciences *37*, 604-614.

Cassel, J.C., and Pereira de Vasconcelos, A. (2015). Importance of the ventral midline thalamus in driving hippocampal functions. Prog Brain Res *219*, 145-161.

Chan, O., Lawson, M., Zhu, W., Beverly, J.L., and Sherwin, R.S. (2007). ATP-sensitive K(+) channels regulate the release of GABA in the ventromedial hypothalamus during hypoglycemia. Diabetes *56*, 1120-1126.

Choudhury, M.E., Miyanishi, K., Takeda, H., Islam, A., Matsuoka, N., Kubo, M., Matsumoto, S., Kunieda, T., Nomoto, M., Yano, H.*, et al.* (2020). Phagocytic elimination of synapses by microglia during sleep. Glia *68*, 44-59.

Citri, A., and Malenka, R.C. (2008). Synaptic plasticity: multiple forms, functions, and mechanisms. Neuropsychopharmacology *33*, 18-41.

Clark, R.E., Broadbent, N.J., Zola, S.M., and Squire, L.R. (2002). Anterograde amnesia and temporally graded retrograde amnesia for a nonspatial memory task after lesions of hippocampus and subiculum. J Neurosci *22*, 4663-4669.

Clarke, L.E., and Barres, B.A. (2013). Emerging roles of astrocytes in neural circuit development. Nat Rev Neurosci *14*, 311-321.

Clelland, C.D., Choi, M., Romberg, C., Clemenson, G.D., Jr., Fragniere, A., Tyers, P., Jessberger, S., Saksida, L.M., Barker, R.A., Gage, F.H.*, et al.* (2009). A functional role for adult hippocampal neurogenesis in spatial pattern separation. Science *325*, 210-213.

Collingridge, G.L., and Peineau, S. (2014). Strippers Reveal Their Depressing Secrets: Removing AMPA Receptors. Neuron *82*, 3-6.

Colonna, M., and Butovsky, O. (2017). Microglia Function in the Central Nervous System During Health and Neurodegeneration. Annu Rev Immunol *35*, 441-468.

Cunningham, C.L., Martinez-Cerdeno, V., and Noctor, S.C. (2013). Microglia regulate the number of neural precursor cells in the developing cerebral cortex. J Neurosci *33*, 4216-4233.

Dai, X.M., Ryan, G.R., Hapel, A.J., Dominguez, M.G., Russell, R.G., Kapp, S., Sylvestre, V., and Stanley, E.R. (2002). Targeted disruption of the mouse colony-stimulating factor 1 receptor gene results in osteopetrosis, mononuclear phagocyte deficiency, increased primitive progenitor cell frequencies, and reproductive defects. Blood *99*, 111-120.

Das, R., and Chinnathambi, S. (2019). Microglial priming of antigen presentation and adaptive stimulation in Alzheimer's disease. Cell Mol Life Sci.

Davalos, D., Grutzendler, J., Yang, G., Kim, J.V., Zuo, Y., Jung, S., Littman, D.R., Dustin, M.L., and Gan, W.B. (2005). ATP mediates rapid microglial response to local brain injury in vivo. Nat Neurosci *8*, 752-758.

de Miranda, A.S., Zhang, C.J., Katsumoto, A., and Teixeira, A.L. (2017). Hippocampal adult neurogenesis: Does the immune system matter? J Neurol Sci *372*, 482-495.

De Roo, M., Klauser, P., Mendez, P., Poglia, L., and Muller, D. (2008). Activity-dependent PSD formation and stabilization of newly formed spines in hippocampal slice cultures. Cerebral Cortex *18*, 151-161.

De Souza, C.T., Araujo, E.P., Bordin, S., Ashimine, R., Zollner, R.L., Boschero, A.C., Saad, M.J., and Velloso, L.A. (2005). Consumption of a fat-rich diet activates a proinflammatory response and induces insulin resistance in the hypothalamus. Endocrinology *146*, 4192-4199.

Debruyne, J.P. (2008). Oscillating perceptions: the ups and downs of the CLOCK protein in the mouse circadian system. J Genet *87*, 437-446.

Debruyne, J.P., Noton, E., Lambert, C.M., Maywood, E.S., Weaver, D.R., and Reppert, S.M. (2006). A clock shock: mouse CLOCK is not required for circadian oscillator function. Neuron *50*, 465-477.

DeBruyne, J.P., Weaver, D.R., and Reppert, S.M. (2007). CLOCK and NPAS2 have overlapping roles in the suprachiasmatic circadian clock. Nature Neuroscience *10*, 543-545.

Delezie, J., and Challet, E. (2011). Interactions between metabolism and circadian clocks: reciprocal disturbances. Year in Diabetes and Obesity *1243*, 30-46.

Delezie, J., Dumont, S., Dardente, H., Oudart, H., Grechez-Cassiau, A., Klosen, P., Teboul, M., Delaunay, F., Pevet, P., and Challet, E. (2012). The nuclear receptor REV-ERB alpha is required for the daily balance of carbohydrate and lipid metabolism. Faseb Journal *26*, 3321-3335.

Dhillon, H., Zigman, J.M., Ye, C.P., Lee, C.E., McGovern, R.A., Tang, V.S., Kenny, C.D., Christiansen, L.M., White, R.D., Edelstein, E.A*., et al.* (2006). Leptin directly activates SF1 neurons in the VMH, and this action by leptin is required for normal body-weight homeostasis. Neuron *49*, 191-203.

Dhuria, S.V., Fine, J.M., Bingham, D., Svitak, A.L., Burns, R.B., Baillargeon, A.M., Panter, S.S., Kazi, A.N., Frey, W.H., 2nd, and Hanson, L.R. (2016). Food consumption and activity levels increase in rats following intranasal Hypocretin-1. Neurosci Lett *627*, 155-159.

Dissing-Olesen, L., LeDue, J.M., Rungta, R.L., Hefendehl, J.K., Choi, H.B., and MacVicar, B.A. (2014). Activation of Neuronal NMDA Receptors Triggers Transient ATP-Mediated Microglial Process Outgrowth. Journal of Neuroscience *34*, 10511-10527.

Djogo, T., Robins, S.C., Schneider, S., Kryzskaya, D., Liu, X., Mingay, A., Gillon, C.J., Kim, J.H., Storch, K.F., Boehm, U.*, et al.* (2016). Adult NG2-Glia Are Required for Median Eminence-Mediated Leptin Sensing and Body Weight Control. Cell Metab *23*, 797-810.

Dorfman, M.D., Krull, J.E., Douglass, J.D., Fasnacht, R., Lara-Lince, F., Meek, T.H., Shi, X., Damian, V., Nguyen, H.T., Matsen, M.E.*, et al.* (2017). Sex differences in microglial CX3CR1 signalling determine obesity susceptibility in mice. Nat Commun *8*, 14556.

Dudai, Y., Karni, A., and Born, J. (2015). The Consolidation and Transformation of Memory. Neuron *88*, 20-32.

Dudek, M., and Meng, Q.J. (2014). Running on time: the role of circadian clocks in the musculoskeletal system. Biochem J *463*, 1-8.

Duffield, G.E. (2003). DNA microarray analyses of circadian timing: the genomic basis of biological time. J Neuroendocrinol *15*, 991-1002.

Early, J.O., Menon, D., Wyse, C.A., Cervantes-Silva, M.P., Zaslona, Z., Carroll, R.G., Palsson-McDermott, E.M., Angiari, S., Ryan, D.G., Corcoran, S.E.*, et al.* (2018). Circadian clock protein BMAL1 regulates IL-1beta in macrophages via NRF2. Proc Natl Acad Sci U S A *115*, E8460-E8468.

Eckle, T., Hartmann, K., Bonney, S., Reithel, S., Mittelbronn, M., Walker, L.A., Lowes, B.D., Han, J., Borchers, C.H., Buttrick, P.M.*, et al.* (2012). Adora2b-elicited Per2 stabilization promotes a HIF-dependent metabolic switch crucial for myocardial adaptation to ischemia. Nat Med *18*, 774-782.

Edgar, R.S., Green, E.W., Zhao, Y., van Ooijen, G., Olmedo, M., Qin, X., Xu, Y., Pan, M., Valekunja, U.K., Feeney, K.A.*, et al.* (2012). Peroxiredoxins are conserved markers of circadian rhythms. Nature *485*, 459-464.

Eichenlaub, J.B., Jarosiewicz, B., Saab, J., Franco, B., Kelemen, J., Halgren, E., Hochberg, L.R., and Cash, S.S. (2020). Replay of Learned Neural Firing Sequences during Rest in Human Motor Cortex. Cell Reports *31*.

El Khoury, J., Toft, M., Hickman, S.E., Means, T.K., Terada, K., Geula, C., and Luster, A.D. (2007). Ccr2 deficiency impairs microglial accumulation and accelerates progression of Alzheimer-like disease. Nat Med *13*, 432-438.

Elias, C.F., Kelly, J.F., Lee, C.E., Ahima, R.S., Drucker, D.J., Saper, C.B., and Elmquist, J.K. (2000). Chemical characterization of leptin-activated neurons in the rat brain. J Comp Neurol *423*, 261-281.

Ellacott, K.L., and Cone, R.D. (2004). The central melanocortin system and the integration of short- and long-term regulators of energy homeostasis. Recent Prog Horm Res *59*, 395-408.

Elmore, M.R.P., Hohsfield, L.A., Kramar, E.A., Soreq, L., Lee, R.J., Pham, S.T., Najafi, A.R., Spangenberg, E.E., Wood, M.A., West, B.L.*, et al.* (2018). Replacement of microglia in the aged brain reverses cognitive, synaptic, and neuronal deficits in mice. Aging Cell *17*, e12832.

Elmore, M.R.P., Najafi, A.R., Koike, M.A., Dagher, N.N., Spangenberg, E.E., Rice, R.A., Kitazawa, M., Matusow, B., Nguyen, H., West, B.L.*, et al.* (2014). Colony-Stimulating Factor 1 Receptor Signaling Is Necessary for Microglia Viability, Unmasking a Microglia Progenitor Cell in the Adult Brain. Neuron *82*, 380-397.

Elmquist, J.K., Bjorbaek, C., Ahima, R.S., Flier, J.S., and Saper, C.B. (1998a). Distributions of leptin receptor mRNA isoforms in the rat brain. J Comp Neurol *395*, 535-547.

Elmquist, J.K., Elias, C.F., and Saper, C.B. (1999). From lesions to leptin: hypothalamic control of food intake and body weight. Neuron *22*, 221-232.

Elmquist, J.K., Maratos-Flier, E., Saper, C.B., and Flier, J.S. (1998b). Unraveling the central nervous system pathways underlying responses to leptin. Nat Neurosci *1*, 445-450.

Erblich, B., Zhu, L., Etgen, A.M., Dobrenis, K., and Pollard, J.W. (2011). Absence of colony stimulation factor-1 receptor results in loss of microglia, disrupted brain development and olfactory deficits. PLoS One *6*, e26317.

Ernst, A., Alkass, K., Bernard, S., Salehpour, M., Perl, S., Tisdale, J., Possnert, G., Druid, H., and Frisen, J. (2014). Neurogenesis in the striatum of the adult human brain. Cell *156*, 1072-1083.

Euston, D.R., Tatsuno, M., and McNaughton, B.L. (2007). Fast-forward playback of recent memory sequences in prefrontal cortex during sleep. Science *318*, 1147-1150.

Fanselow, M.S., and Dong, H.W. (2010). Are the dorsal and ventral hippocampus functionally distinct structures? Neuron *65*, 7-19.

Fekete, C., Legradi, G., Mihaly, E., Huang, Q.H., Tatro, J.B., Rand, W.M., Emerson, C.H., and Lechan, R.M. (2000). alpha-melanocyte-stimulating hormone is contained in nerve terminals innervating thyrotropin-releasing hormone-synthesizing neurons in the hypothalamic paraventricular nucleus and

prevents fasting-induced suppression of prothyrotropin-releasing hormone gene expression. Journal of Neuroscience *20*, 1550-1558.

Fernandez-Arjona, M.D.M., Grondona, J.M., Granados-Duran, P., Fernandez-Llebrez, P., and Lopez-Avalos, M.D. (2017). Microglia Morphological Categorization in a Rat Model of Neuroinflammation by Hierarchical Cluster and Principal Components Analysis. Front Cell Neurosci *11*, 235.

Ferrario, C.R., Labouebe, G., Liu, S., Nieh, E.H., Routh, V.H., Xu, S., and O'Connor, E.C. (2016a). Homeostasis Meets Motivation in the Battle to Control Food Intake. J Neurosci *36*, 11469-11481.

Ferrario, C.R., Labouebe, G., Liu, S., Nieh, E.H., Routh, V.H., Xu, S.J., and O'Connor, E.C. (2016b). Homeostasis Meets Motivation in the Battle to Control Food Intake. Journal of Neuroscience *36*, 11469-11481.

Fiala, J.C., Feinberg, M., Popov, V., and Harris, K.M. (1998). Synaptogenesis via dendritic filopodia in developing hippocampal area CA1. J Neurosci *18*, 8900-8911.

Filipello, F., Morini, R., Corradini, I., Zerbi, V., Canzi, A., Michalski, B., Erreni, M., Markicevic, M., Starvaggi-Cucuzza, C., Otero, K.*, et al.* (2018). The Microglial Innate Immune Receptor TREM2 Is Required for Synapse Elimination and Normal Brain Connectivity. Immunity *48*, 979-+.

Flores, A., Maldonado, R., and Berrendero, F. (2013). Cannabinoid-hypocretin cross-talk in the central nervous system: what we know so far. Front Neurosci-Switz *7*.

Fonken, L.K., Frank, M.G., Kitt, M.M., Barrientos, R.M., Watkins, L.R., and Maier, S.F. (2015). Microglia inflammatory responses are controlled by an intrinsic circadian clock. Brain Behav Immun *45*, 171-179.

Fonken, L.K., Kitt, M.M., Gaudet, A.D., Barrientos, R.M., Watkins, L.R., and Maier, S.F. (2016). Diminished circadian rhythms in hippocampal microglia may contribute to age-related neuroinflammatory sensitization. Neurobiol Aging *47*, 102-112.

Ford, E.S. (2005). Prevalence of the metabolic syndrome defined by the International Diabetes Federation among adults in the U.S. Diabetes Care *28*, 2745-2749.

Forman, B.M., Chen, J., Blumberg, B., Kliewer, S.A., Henshaw, R., Ong, E.S., and Evans, R.M. (1994). Cross-Talk among Ror-Alpha-1 and the Rev-Erb Family of Orphan Nuclear Receptors. Mol Endocrinol *8*, 1253-1261.

Fourgeaud, L., Traves, P.G., Tufail, Y., Leal-Bailey, H., Lew, E.D., Burrola, P.G., Callaway, P., Zagorska, A., Rothlin, C.V., Nimmerjahn, A.*, et al.* (2016). TAM receptors regulate multiple features of microglial physiology. Nature *532*, 240-+.

Frankland, P.W., and Bontempi, B. (2005). The organization of recent and remote memories. Nat Rev Neurosci *6*, 119-130.

Frankland, P.W., Bontempi, B., Talton, L.E., Kaczmarek, L., and Silva, A.J. (2004). The involvement of the anterior cingulate cortex in remote contextual fear memory. Science *304*, 881-883.

Fu, R., Shen, Q., Xu, P., Luo, J.J., and Tang, Y. (2014). Phagocytosis of microglia in the central nervous system diseases. Mol Neurobiol *49*, 1422-1434.

Fuger, P., Hefendehl, J.K., Veeraraghavalu, K., Wendeln, A.C., Schlosser, C., Obermuller, U., Wegenast-Braun, B.M., Neher, J.J., Martus, P., Kohsaka, S.*, et al.* (2017). Microglia turnover with aging and in an Alzheimer's model via long-term in vivo single-cell imaging. Nat Neurosci *20*, 1371-1376.

Gabriel, B.M., and Zierath, J.R. (2019a). Circadian rhythms and exercise - re-setting the clock in metabolic disease. Nat Rev Endocrinol *15*, 197-206.

Gao, Y., Ottaway, N., Schriever, S.C., Legutko, B., Garcia-Caceres, C., de la Fuente, E., Mergen, C., Bour, S., Thaler, J.P., Seeley, R.J.*, et al.* (2014). Hormones and diet, but not body weight, control hypothalamic microglial activity. Glia *62*, 17-25.

Gao, Y., Vidal-Itriago, A., Kalsbeek, M.J., Layritz, C., Garcia-Caceres, C., Tom, R.Z., Eichmann, T.O., Vaz, F.M., Houtkooper, R.H., van der Wel, N.*, et al.* (2017a). Lipoprotein Lipase Maintains Microglial Innate Immunity in Obesity. Cell Rep *20*, 3034-3042.

Gao, Y., Vidal-Itriago, A., Milanova, I., Korpel, N.L., Kalsbeek, M.J., Tom, R.Z., Kalsbeek, A., Hofmann, S.M., and Yi, C.X. (2018). Deficiency of leptin receptor in myeloid cells disrupts hypothalamic metabolic circuits and causes body weight increase. Mol Metab *7*, 155-160.

Gaskin, S., Tremblay, A., and Mumby, D.G. (2003). Retrograde and anterograde object recognition in rats with hippocampal lesions. Hippocampus *13*, 962-969.

Gekakis, N., Staknis, D., Nguyen, H.B., Davis, F.C., Wilsbacher, L.D., King, D.P., Takahashi, J.S., and Weitz, C.J. (1998). Role of the CLOCK protein in the mammalian circadian mechanism. Science *280*, 1564-1569.

Geltink, R.I.K., Kyle, R.L., and Pearce, E.L. (2018). Unraveling the Complex Interplay Between T Cell Metabolism and Function. Annual Review of Immunology, Vol 36 *36*, 461-488.

Gerstner, J.R., and Yin, J.C. (2010). Circadian rhythms and memory formation. Nat Rev Neurosci *11*, 577-588.

Ginhoux, F., Greter, M., Leboeuf, M., Nandi, S., See, P., Gokhan, S., Mehler, M.F., Conway, S.J., Ng, L.G., Stanley, E.R.*, et al.* (2010). Fate Mapping Analysis Reveals That Adult Microglia Derive from Primitive Macrophages. Science *330*, 841-845.

Gonzalez-Scarano, F., and Baltuch, G. (1999). Microglia as mediators of inflammatory and degenerative diseases. Annu Rev Neurosci *22*, 219-240.

Govindarajan, A., Israely, I., Huang, S.Y., and Tonegawa, S. (2011). The Dendritic Branch Is the Preferred Integrative Unit for Protein Synthesis-Dependent LTP. Neuron *69*, 132-146.

Griebel, G., Ravinet-Trillou, C., Beeske, S., Avenet, P., and Pichat, P. (2014). Mice deficient in cryptochrome 1 (Cry1(-/-)) exhibit resistance to obesity induced by a high-fat diet. Frontiers in Endocrinology *5*.

Griffin, E.A., Jr., Staknis, D., and Weitz, C.J. (1999). Light-independent role of CRY1 and CRY2 in the mammalian circadian clock. Science *286*, 768-771.

Griffin, P., Dimitry, J.M., Sheehan, P.W., Lananna, B.V., Guo, C., Robinette, M.L., Hayes, M.E., Cedeno, M.R., Nadarajah, C.J., Ezerskiy, L.A.*, et al.* (2019). Circadian clock protein Rev-erba regulates neuroinflammation. P Natl Acad Sci USA *116*, 5102-5107.

Gu, Y.Z., Hogenesch, J.B., and Bradfield, C.A. (2000). The PAS superfamily: sensors of environmental and developmental signals. Annu Rev Pharmacol Toxicol *40*, 519-561.

Hagino, Y., Kariura, Y., Manago, Y., Amano, T., Wang, B., Sekiguchi, M., Nishikawa, K., Aoki, S.U., Wada, K., and Noda, M. (2004). Heterogeneity and potentiation of AMPA type of glutamate receptors in rat cultured microglia. Glia *47*, 68-77.

Hahn, T.M., Breininger, J.F., Baskin, D.G., and Schwartz, M.W. (1998). Coexpression of Agrp and NPY in fasting-activated hypothalamic neurons. Nat Neurosci *1*, 271-272.

Harvey, C.D., and Svoboda, K. (2007). Locally dynamic synaptic learning rules in pyramidal neuron dendrites. Nature *450*, 1195-U1193.

Hasegawa, S., Fukushima, H., Hosoda, H., Serita, T., Ishikawa, R., Rokukawa, T., Kawahara-Miki, R., Zhang, Y., Ohta, M., Okada, S.*, et al.* (2019). Hippocampal clock regulates memory retrieval via Dopamine and PKA-induced GluA1 phosphorylation. Nat Commun *10*, 5766.

Hebert, A.E., and Dash, P.K. (2004). Nonredundant roles for hippocampal and entorhinal cortical plasticity in spatial memory storage. Pharmacol Biochem Be *79*, 143-153.

Heneka, M.T., Golenbock, D.T., and Latz, E. (2015). Innate immunity in Alzheimer's disease. Nat Immunol *16*, 229-236.

Herisson, F.M., Waas, J.R., Fredriksson, R., Schioth, H.B., Levine, A.S., and Olszewski, P.K. (2016). Oxytocin Acting in the Nucleus Accumbens Core Decreases Food Intake. Journal of Neuroendocrinology *28*.

Herzog, E.D., Takahashi, J.S., and Block, G.D. (1998). Clock controls circadian period in isolated suprachiasmatic nucleus neurons. Nat Neurosci *1*, 708-713.

Hickey, W.F., and Kimura, H. (1988). Perivascular microglial cells of the CNS are bone marrow-derived and present antigen in vivo. Science *239*, 290-292.

Hickman, S., Izzy, S., Sen, P., Morsett, L., and El Khoury, J. (2018). Microglia in neurodegeneration. Nat Neurosci *21*, 1359-1369.

Hickman, S.E., Kingery, N.D., Ohsumi, T.K., Borowsky, M.L., Wang, L.C., Means, T.K., and El Khoury, J. (2013). The microglial sensome revealed by direct RNA sequencing. Nat Neurosci *16*, 1896-1905.

Hide, I., Tanaka, M., Inoue, A., Nakajima, K., Kohsaka, S., Inoue, K., and Nakata, Y. (2000). Extracellular ATP triggers tumor necrosis factor-alpha release from rat microglia. J Neurochem *75*, 965-972.

Hofer, S.B., Mrsic-Flogel, T.D., Bonhoeffer, T., and Hubener, M. (2009). Experience leaves a lasting structural trace in cortical circuits. Nature *457*, 313-U314.

Hogenesch, J.B., Chan, W.K., Jackiw, V.H., Brown, R.C., Gu, Y.Z., PrayGrant, M., Perdew, G.H., and Bradfield, C.A. (1997). Characterization of a subset of the basic-helix-loop-helix-PAS superfamily that interacts with components of the dioxin signaling pathway. Journal of Biological Chemistry *272*, 8581-8593.

Hong, J., Stubbins, R.E., Smith, R.R., Harvey, A.E., and Nunez, N.P. (2009). Differential susceptibility to obesity between male, female and ovariectomized female mice. Nutr J *8*.

Horvath, T.L. (2003). Endocannabinoids and the regulation of body fat: the smoke is clearing. Journal of Clinical Investigation *112*, 323-326.

Hoshiko, M., Arnoux, I., Avignone, E., Yamamoto, N., and Audinat, E. (2012). Deficiency of the microglial receptor CX3CR1 impairs postnatal functional development of thalamocortical synapses in the barrel cortex. J Neurosci *32*, 15106-15111.

Hotulainen, P., and Hoogenraad, C.C. (2010). Actin in dendritic spines: connecting dynamics to function. J Cell Biol *189*, 619-629.

Hou, J., Zheng, D.Z., Zhou, J.Y., and Zhou, S.W. (2010). Orexigenic effect of cocaine- and amphetamine-regulated transcript (CART) after injection into hypothalamic nuclei in streptozotocin-diabetic rats. Clin Exp Pharmacol P *37*, 989-995.

Hua, J.Y., and Smith, S.J. (2004). Neural activity and the dynamics of central nervous system development. Nat Neurosci *7*, 327-332.

Huttenlocher, P.R. (1979). Synaptic density in human frontal cortex - developmental changes and effects of aging. Brain Res *163*, 195-205.

Ikegami, A., Haruwaka, K., and Wake, H. (2019). Microglia: Lifelong modulator of neural circuits. Neuropathology *39*, 173-180.

Jais, A., and Bruning, J.C. (2017). Hypothalamic inflammation in obesity and metabolic disease. J Clin Invest *127*, 24-32.

Jamshidi, N., and Taylor, D.A. (2001). Anandamide administration into the ventromedial hypothalamus stimulates appetite in rats. Brit J Pharmacol *134*, 1151-1154.

Jasinska, M., Jasek-Gajda, E., Woznicka, O., Lis, G.J., Pyza, E., and Litwin, J.A. (2019). Circadian clock regulates the shape and content of dendritic spines in mouse barrel cortex. PLoS One *14*, e0225394.

Ji, K., Akgul, G., Wollmuth, L.P., and Tsirka, S.E. (2013). Microglia actively regulate the number of functional synapses. PLoS One *8*, e56293.

Jiang, X., and Nardelli, J. (2016). Cellular and molecular introduction to brain development. Neurobiol Dis *92*, 3-17.

Kabaso, D., Coskren, P.J., Henry, B.I., Hof, P.R., and Wearne, S.L. (2009). The Electrotonic Structure of Pyramidal Neurons Contributing to Prefrontal Cortical Circuits in Macaque Monkeys Is Significantly Altered in Aging. Cereb Cortex *19*, 2248-2268.

Kalsbeek, A., la Fleur, S., and Fliers, E. (2014). Circadian control of glucose metabolism. Mol Metab *3*, 372-383.

Kent, P.L. (2016). Working Memory: A Selective Review. Appl Neuropsychol Child *5*, 163-172.

Kettenmann, H., Kirchhoff, F., and Verkhratsky, A. (2013). Microglia: new roles for the synaptic stripper. Neuron *77*, 10-18.

Kim, C.S., Kwon, Y., Choe, S.Y., Hong, S.M., Yoo, H., Goto, T., Kawada, T., Choi, H.S., Joe, Y., Chung, H.T.*, et al.* (2015). Quercetin reduces obesity-induced hepatosteatosis by enhancing mitochondrial oxidative metabolism via heme oxygenase-1. Nutr Metab (Lond) *12*, 33.

Kitchen, G.B., Cunningham, P.S., Poolman, T.M., Iqbal, M., Maidstone, R., Baxter, M., Bagnall, J., Begley, N., Saer, B., Hussell, T.*, et al.* (2020). The clock gene Bmal1 inhibits macrophage motility, phagocytosis, and impairs defense against pneumonia. Proc Natl Acad Sci U S A *117*, 1543-1551.

Klockener, T., Hess, S., Belgardt, B.F., Paeger, L., Verhagen, L.A., Husch, A., Sohn, J.W., Hampel, B., Dhillon, H., Zigman, J.M.*, et al.* (2011). High-fat feeding promotes obesity via insulin receptor/PI3K-dependent inhibition of SF-1 VMH neurons. Nat Neurosci *14*, 911-918.

Knott, G.W., Holtmaat, A., Wilbrecht, L., Welker, E., and Svoboda, K. (2006). Spine growth precedes synapse formation in the adult neocortex in vivo. Nature Neuroscience *9*, 1117-1124.

Ko, C.H., and Takahashi, J.S. (2006). Molecular components of the mammalian circadian clock. Hum Mol Genet *15 Spec No 2*, R271-277.

Koch, C., and Zador, A. (1993). The Function of Dendritic Spines - Devices Subserving Biochemical Rather Than Electrical Compartmentalization. Journal of Neuroscience *13*, 413-422.

Koch, M., Varela, L., Kim, J.G., Kim, J.D., Hernandez-Nuno, F., Simonds, S.E., Castorena, C.M., Vianna, C.R., Elmquist, J.K., Morozov, Y.M.*, et al.* (2015). Hypothalamic POMC neurons promote cannabinoid-induced feeding. Nature *519*, 45-50.

Koh, I.Y., Lindquist, W.B., Zito, K., Nimchinsky, E.A., and Svoboda, K. (2002). An image analysis algorithm for dendritic spines. Neural Comput *14*, 1283-1310.

Kow, L.M., and Pfaff, D.W. (1991). The effects of the TRH metabolite cyclo(His-Pro) and its analogs on feeding. Pharmacol Biochem Behav *38*, 359-364.

Krashes, M.J., Koda, S., Ye, C., Rogan, S.C., Adams, A.C., Cusher, D.S., Maratos-Flier, E., Roth, B.L., and Lowell, B.B. (2011). Rapid, reversible activation of AgRP neurons drives feeding behavior in mice. J Clin Invest *121*, 1424-1428.

Lam, B.Y.H., Cimino, I., Polex-Wolf, J., Nicole Kohnke, S., Rimmington, D., Iyemere, V., Heeley, N., Cossetti, C., Schulte, R., Saraiva, L.R.*, et al.* (2017). Heterogeneity of hypothalamic pro-opiomelanocortin-expressing neurons revealed by single-cell RNA sequencing. Mol Metab *6*, 383-392.

Lam, D.D., Przydzial, M.J., Ridley, S.H., Yeo, G.S., Rochford, J.J., O'Rahilly, S., and Heisler, L.K. (2008). Serotonin 5-HT2C receptor agonist promotes hypophagia via downstream activation of melanocortin 4 receptors. Endocrinology *149*, 1323-1328.

Lamia, K.A., Storch, K.F., and Weitz, C.J. (2008). Physiological significance of a peripheral tissue circadian clock. Proc Natl Acad Sci U S A *105*, 15172-15177.

Lau, J., and Herzog, H. (2014). CART in the regulation of appetite and energy homeostasis. Front Neurosci *8*, 313.

Lawson, L.J., Perry, V.H., Dri, P., and Gordon, S. (1990). Heterogeneity in the distribution and morphology of microglia in the normal adult mouse brain. Neuroscience *39*, 151-170.

Le, N.H., Kim, C.S., Park, T., Park, J.H.Y., Sung, K., Lee, D.G., Hong, S.M., Choe, S.Y., Goto, T., Kawada, T.*, et al.* (2014). Quercetin Protects against Obesity-Induced Skeletal Muscle Inflammation and Atrophy. Mediat Inflamm.

Le Thuc, O., Stobbe, K., Cansell, C., Nahon, J.L., Blondeau, N., and Rovere, C. (2017). Hypothalamic Inflammation and Energy Balance Disruptions: Spotlight on Chemokines. Front Endocrinol (Lausanne) *8*, 197.

Lechan, R.M., and Fekete, C. (2006). The TRH neuron: a hypothalamic integrator of energy metabolism. Prog Brain Res *153*, 209-235.

Lee, I., and Kesner, R.P. (2003). Time-dependent relationship between the dorsal hippocampus and the prefrontal cortex in spatial memory. Journal of Neuroscience *23*, 1517-1523.

Lee, Y.J., Han, D.H., Pak, Y.K., and Cho, S.H. (2012). Circadian regulation of low density lipoprotein receptor promoter activity by CLOCK/BMAL1, Hes1 and Hes6. Exp Mol Med *44*, 642-652.

Leibowitz, S.F., and Alexander, J.T. (1998). Hypothalamic serotonin in control of eating behavior, meal size, and body weight. Biol Psychiatry *44*, 851-864.

Leibowitz, S.F., Roossin, P., and Rosenn, M. (1984). Chronic Norepinephrine Injection into the Hypothalamic Paraventricular Nucleus Produces Hyperphagia and Increased Body-Weight in the Rat. Pharmacol Biochem Be *21*, 801-808.

Lemke, G. (2013). Biology of the TAM receptors. Cold Spring Harb Perspect Biol *5*, a009076.

Levin, B.E., Magnan, C., Dunn-Meynell, A., and Le Foll, C. (2011). Metabolic Sensing and the Brain: Who, What, Where, and How? Endocrinology *152*, 2552-2557.

Lim, S.H., Park, E., You, B., Jung, Y., Park, A.R., Park, S.G., and Lee, J.R. (2013). Neuronal synapse formation induced by microglia and interleukin 10. PLoS One *8*, e81218.

Lin, H., Lee, E., Hestir, K., Leo, C., Huang, M., Bosch, E., Halenbeck, R., Wu, G., Zhou, A., Behrens, D.*, et al.* (2008). Discovery of a cytokine and its receptor by functional screening of the extracellular proteome. Science *320*, 807-811.

Liu, B., Xu, K., Jiang, Y.F., and Li, X.L. (2014). Aberrant expression of Per1, Per2 and Per3 and their prognostic relevance in non-small cell lung cancer. Int J Clin Exp Patho *7*, 7863-7871.

Liu, H., Kishi, T., Roseberry, A.G., Cai, X., Lee, C.E., Montez, J.M., Friedman, J.M., and Elmquist, J.K. (2003). Transgenic mice expressing green fluorescent protein under the control of the melanocortin-4 receptor promoter. J Neurosci *23*, 7143-7154.

Liu, P., and Bilkey, D.K. (2001). The effect of excitotoxic lesions centered on the hippocampus or perirhinal cortex in object recognition and spatial memory tasks. Behav Neurosci *115*, 94-111.

Lo, B.C., Gold, M.J., Hughes, M.R., Antignano, F., Valdez, Y., Zaph, C., Harder, K.W., and McNagny, K.M. (2016). The orphan nuclear receptor ROR alpha and group 3 innate lymphoid cells drive fibrosis in a mouse model of Crohn's disease. Sci Immunol *1*.

Loizides-Mangold, U., Perrin, L., Vandereycken, B., Betts, J.A., Walhin, J.P., Templeman, I., Chanon, S., Weger, B.D., Durand, C., Robert, M.*, et al.* (2017). Lipidomics reveals diurnal lipid oscillations in human skeletal muscle persisting in cellular myotubes cultured in vitro. Proc Natl Acad Sci U S A *114*, E8565-E8574.

Luquet, S., Perez, F.A., Hnasko, T.S., and Palmiter, R.D. (2005). NPY/AgRP neurons are essential for feeding in adult mice but can be ablated in neonates. Science *310*, 683-685.

Mallya, A.P., Wang, H.D., Lee, H.N.R., and Deutch, A.Y. (2019). Microglial Pruning of Synapses in the Prefrontal Cortex During Adolescence. Cereb Cortex *29*, 1634-1643.

Marcheva, B., Ramsey, K.M., Buhr, E.D., Kobayashi, Y., Su, H., Ko, C.H., Ivanova, G., Omura, C., Mo, S., Vitaterna, M.H.*, et al.* (2010). Disruption of the clock components CLOCK and BMAL1 leads to hypoinsulinaemia and diabetes. Nature *466*, 627-631.

Maren, S., Aharonov, G., and Fanselow, M.S. (1997). Neurotoxic lesions of the dorsal hippocampus and Pavlovian fear conditioning in rats. Behavioural Brain Research *88*, 261-274.

Marr, D. (1970). A theory for cerebral neocortex. Proc R Soc Lond B Biol Sci *176*, 161-234.

Marr, D. (1971). Simple memory: a theory for archicortex. Philos Trans R Soc Lond B Biol Sci *262*, 23-81.

Matsuzaki, M., Ellis-Davies, G.C.R., Nemoto, T., Miyashita, Y., Iino, M., and Kasai, H. (2001). Dendritic spine geometry is critical for AMPA receptor expression in hippocampal CA1 pyramidal neurons. Nature Neuroscience *4*, 1086-1092.

Matsuzaki, M., Honkura, N., Ellis-Davies, G.C., and Kasai, H. (2004). Structural basis of long-term potentiation in single dendritic spines. Nature *429*, 761-766.

Mcclelland, J.L., Mcnaughton, B.L., and Oreilly, R.C. (1995). Why There Are Complementary Learning-Systems in the Hippocampus and Neocortex - Insights from the Successes and Failures of Connectionist Models of Learning and Memory. Psychol Rev *102*, 419-457.

McClung, C.A. (2007). Circadian genes, rhythms and the biology of mood disorders. Pharmacol Therapeut *114*, 222-232.

Metcalf, D. (2010). The colony-stimulating factors and cancer. Nat Rev Cancer *10*, 425-434.

Meyer, D., Bonhoeffer, T., and Scheuss, V. (2014a). Balance and stability of synaptic structures during synaptic plasticity. Neuron *82*, 430-443.

Meyer, D., Bonhoeffer, T., and Scheuss, V. (2014b). Balance and Stability of Synaptic Structures during Synaptic Plasticity (vol 82, pg 430, 2014). Neuron *82*, 1188-1188.

Mildner, A., Schmidt, H., Nitsche, M., Merkler, D., Hanisch, U.K., Mack, M., Heikenwalder, M., Bruck, W., Priller, J., and Prinz, M. (2007). Microglia in the adult brain arise from Ly-6ChiCCR2+ monocytes only under defined host conditions. Nat Neurosci *10*, 1544-1553.

Miller, E.K., and Cohen, J.D. (2001). An integrative theory of prefrontal cortex function. Annu Rev Neurosci *24*, 167-202.

Miller, M.A., Kruisbrink, M., Wallace, J., Ji, C., and Cappuccio, F.P. (2018). Sleep duration and incidence of obesity in infants, children, and adolescents: a systematic review and meta-analysis of prospective studies. Sleep *41*.

Miller, R. (1996). Neural assemblies and laminar interactions in the cerebral cortex. Biol Cybern *75*, 253-261.

Ming, G.L., and Song, H. (2011). Adult neurogenesis in the mammalian brain: significant answers and significant questions. Neuron *70*, 687-702.

Missaire, M., and Hindges, R. (2015). The role of cell adhesion molecules in visual circuit formation: from neurite outgrowth to maps and synaptic specificity. Dev Neurobiol *75*, 569-583.

Missler, M., Sudhof, T.C., and Biederer, T. (2012). Synaptic cell adhesion. Cold Spring Harb Perspect Biol *4*, a005694.

Miyake, S., Sumi, Y., Yan, L., Takekida, S., Fukuyama, T., Ishida, Y., Yamaguchi, S., Yagita, K., and Okamura, H. (2000). Phase-dependent responses of Per1 and Per2 genes to a light-stimulus in the suprachiasmatic nucleus of the rat. Neurosci Lett *294*, 41-44.

Miyamoto, A., Wake, H., Ishikawa, A.W., Eto, K., Shibata, K., Murakoshi, H., Koizumi, S., Moorhouse, A.J., Yoshimura, Y., and Nabekura, J. (2016). Microglia contact induces synapse formation in developing somatosensory cortex. Nat Commun *7*, 12540.

Miyashita, Y. (2004). Cognitive memory: Cellular and network machineries and their top-down control. Science *306*, 435-440.

Moody, S.L., Wise, S.P., di Pellegrino, G., and Zipser, D. (1998). A model that accounts for activity in primate frontal cortex during a delayed matching-to-sample task. Journal of Neuroscience *18*, 399-410.

Morton, G.J., Cummings, D.E., Baskin, D.G., Barsh, G.S., and Schwartz, M.W. (2006). Central nervous system control of food intake and body weight. Nature *443*, 289-295.

Morton, G.J., Thatcher, B.S., Reidelberger, R.D., Ogimoto, K., Wolden-Hanson, T., Baskin, D.G., Schwartz, M.W., and Blevins, J.E. (2012). Peripheral oxytocin suppresses food intake and causes weight loss in diet-induced obese rats. Am J Physiol Endocrinol Metab *302*, E134-144.

Moser, M.B., and Moser, E.I. (1998). Distributed encoding and retrieval of spatial memory in the hippocampus. J Neurosci *18*, 7535-7542.

Mountjoy, K.G. (2010). Functions for pro-opiomelanocortin-derived peptides in obesity and diabetes. Biochem J *428*, 305-324.

Musiek, E.S., Lim, M.M., Yang, G., Bauer, A.Q., Qi, L., Lee, Y., Roh, J.H., Ortiz-Gonzalez, X., Dearborn, J.T., Culver, J.P*., et al.* (2013). Circadian clock proteins regulate neuronal redox homeostasis and neurodegeneration. J Clin Invest *123*, 5389-5400.

Myers, M.G., Jr., and Olson, D.P. (2012). Central nervous system control of metabolism. Nature *491*, 357-363.

Nadel, L., and Moscovitch, M. (1997). Memory consolidation, retrograde amnesia and the hippocampal complex. Curr Opin Neurobiol *7*, 217-227.

Nakata, M., Yamamoto, S., Okada, T., and Yada, T. (2017). AAV-mediated IL-10 gene transfer counteracts inflammation in the hypothalamic arcuate nucleus and obesity induced by high-fat diet. Neuropeptides *62*, 87-92.

Nakazato, R., Hotta, S., Yamada, D., Kou, M., Nakamura, S., Takahata, Y., Tei, H., Numano, R., Hida, A., Shimba, S.*, et al.* (2017). The intrinsic microglial clock system regulates interleukin-6 expression. Glia *65*, 198-208.

Nayak, D., Roth, T.L., and McGavern, D.B. (2014). Microglia development and function. Annu Rev Immunol *32*, 367-402.

Naylor, E., Bergmann, B.M., Krauski, K., Zee, P.C., Takahashi, J.S., Vitaterna, M.H., and Turek, F.W. (2000). The circadian clock mutation alters sleep homeostasis in the mouse. J Neurosci *20*, 8138-8143.

Nelson, L.H., Warden, S., and Lenz, K.M. (2017). Sex differences in microglial phagocytosis in the neonatal hippocampus. Brain Behav Immun *64*, 11-22.

Nicoll, R.A. (2017). A Brief History of Long-Term Potentiation. Neuron *93*, 281-290.

Nijenhuis, W.A.J., Oosterom, J., and Adan, R.A.H. (2001). AgRP(83-132) acts as an inverse agonist on the human-melanocortin-4 receptor. Mol Endocrinol *15*, 164-171.

Nimmerjahn, A., Kirchhoff, F., and Helmchen, F. (2005). Resting microglial cells are highly dynamic surveillants of brain parenchyma in vivo. Science *308*, 1314-1318.

Nolan, M.F., Malleret, G., Dudman, J.T., Buhl, D.L., Santoro, B., Gibbs, E., Vronskaya, S., Buzsaki, G., Siegelbaum, S.A., Kandel, E.R.*, et al.* (2004). A behavioral role for dendritic integration: HCN1 channels constrain spatial inputs to distal dendrites memory and plasticity at of CA1 pyramidal neurons. Cell *119*, 719-732.

O'Neill, J.S., and Reddy, A.B. (2011). Circadian clocks in human red blood cells. Nature *469*, 498-503.

Oishi, Y., Hayashi, S., Isagawa, T., Oshima, M., Iwama, A., Shimba, S., Okamura, H., and Manabe, I. (2017). Bmal1 regulates inflammatory responses in macrophages by modulating enhancer RNA transcription. Sci Rep *7*, 7086.

Olah, M., Biber, K., Vinet, J., and Boddeke, H.W. (2011). Microglia phenotype diversity. CNS Neurol Disord Drug Targets *10*, 108-118.

Olofsson, L.E., Unger, E.K., Cheung, C.C., and Xu, A.W. (2013). Modulation of AgRP-neuronal function by SOCS3 as an initiating event in diet-induced hypothalamic leptin resistance. Proc Natl Acad Sci U S A *110*, E697-706.

Orihuela, R., McPherson, C.A., and Harry, G.J. (2016). Microglial M1/M2 polarization and metabolic states. Br J Pharmacol *173*, 649-665.

Ott, V., Finlayson, G., Lehnert, H., Heitmann, B., Heinrichs, M., Born, J., and Hallschmid, M. (2013). Oxytocin reduces reward-driven food intake in humans. Diabetes *62*, 3418-3425.

Palkovits, M. (2003). Hypothalamic regulation of food intake. Ideggyogy Sz *56*, 288-302.

Paolicelli, R.C., Bolasco, G., Pagani, F., Maggi, L., Scianni, M., Panzanelli, P., Giustetto, M., Ferreira, T.A., Guiducci, E., Dumas, L.*, et al.* (2011). Synaptic pruning by microglia is necessary for normal brain development. Science *333*, 1456-1458.

Pappa, K.I., Gazouli, M., Anastasiou, E., Iliodromiti, Z., Antsaklis, A., and Anagnou, N.P. (2013). The major circadian pacemaker ARNT-like protein-1 (BMAL1) is associated with susceptibility to gestational diabetes mellitus. Diabetes Res Clin Pr *99*, 151-157.

Park, H., and Poo, M.M. (2013). Neurotrophin regulation of neural circuit development and function. Nat Rev Neurosci *14*, 7-23.

Parkhurst, C.N., Yang, G., Ninan, I., Savas, J.N., Yates, J.R., Lafaille, J.J., Hempstead, B.L., Littman, D.R., and Gan, W.B. (2013). Microglia Promote Learning-Dependent Synapse Formation through Brain-Derived Neurotrophic Factor. Cell *155*, 1596-1609.

Pelleymounter, M.A., Cullen, M.J., and Wellman, C.L. (1995). Characteristics of BDNF-induced weight loss. Exp Neurol *131*, 229-238.

Phan, T.X., Chan, G.C., Sindreu, C.B., Eckel-Mahan, K.L., and Storm, D.R. (2011). The diurnal oscillation of MAP (mitogen-activated protein) kinase and adenylyl cyclase activities in the hippocampus depends on the suprachiasmatic nucleus. J Neurosci *31*, 10640-10647.

Pinto, S., Roseberry, A.G., Liu, H., Diano, S., Shanabrough, M., Cai, X., Friedman, J.M., and Horvath, T.L. (2004). Rapid rewiring of arcuate nucleus feeding circuits by leptin. Science *304*, 110-115.

Pocock, J.M., and Kettenmann, H. (2007). Neurotransmitter receptors on microglia. Trends Neurosci *30*, 527-535.

Pothos, E.N., Creese, I., and Hoebel, B.G. (1995). Restricted eating with weight loss selectively decreases extracellular dopamine in the nucleus accumbens and alters dopamine response to amphetamine, morphine, and food intake. J Neurosci *15*, 6640-6650.

Pralong, F.P., Gonzales, C., Voirol, M.J., Palmiter, R.D., Brunner, H.R., Gaillard, R.C., Seydoux, J., and Pedrazzini, T. (2002). The neuropeptide Y Y1 receptor regulates leptin-mediated control of energy homeostasis and reproductive functions. FASEB J *16*, 712-714.

Qin, C., Li, J., Tang, K. (2018). Nucleus of the Hypothalamus: Development, Function, and Human Diseases. Endocrinology *159*, 3458-3472.

Quarta, C., Mazza, R., Obici, S., Pasquali, R., and Pagotto, U. (2011). Energy balance regulation by endocannabinoids at central and peripheral levels. Trends Mol Med *17*, 518-526.

Radvansky, G.A. (2017). Human memory. Book, chapter 1, p20.

Rahman, S.A., Castanon-Cervantes, O., Scheer, F.A., Shea, S.A., Czeisler, C.A., Davidson, A.J., and Lockley, S.W. (2015). Endogenous circadian regulation of pro-inflammatory cytokines and chemokines in the presence of bacterial lipopolysaccharide in humans. Brain Behav Immun *47*, 4-13.

Rajendran, L., and Paolicelli, R.C. (2018). Microglia-Mediated Synapse Loss in Alzheimer's Disease. Journal of Neuroscience *38*, 2911-2919.

Ralston, K.S., Solga, M.D., Mackey-Lawrence, N.M., Somlata, Bhattacharya, A., and Petri, W.A., Jr. (2014). Trogocytosis by Entamoeba histolytica contributes to cell killing and tissue invasion. Nature *508*, 526-530.

Ransohoff, R.M., and Stevens, B. (2011). How Many Cell Types Does It Take to Wire a Brain? Science *333*, 1391-1392.

Raslau, F.D., Klein, A.P., Ulmer, J.L., Mathews, V., and Mark, L.P. (2014). Memory part 1: overview. AJNR Am J Neuroradiol *35*, 2058-2060.

Ratner, C., Skov, L.J., Raida, Z., Bachler, T., Bellmann-Sickert, K., Le Foll, C., Sivertsen, B., Dalboge, L.S., Hartmann, B., Beck-Sickinger, A.G.*, et al.* (2016). Effects of Peripheral Neurotensin on Appetite Regulation and Its Role in Gastric Bypass Surgery. Endocrinology *157*, 3482-3492.

Ray, S., Valekunja, U.K., Stangherlin, A., Howell, S.A., Snijders, A.P., Damodaran, G., and Reddy, A.B. (2020). Circadian rhythms in the absence of the clock gene Bmal1. Science *367*, 800-806.

Reis, W.L., Yi, C.X., Gao, Y., Tschop, M.H., and Stern, J.E. (2015). Brain innate immunity regulates hypothalamic arcuate neuronal activity and feeding behavior. Endocrinology *156*, 1303-1315.

Reppert, S.M., and Weaver, D.R. (2002). Coordination of circadian timing in mammals. Nature *418*, 935-941.

Reshef, R., Kudryavitskaya, E., Shani-Narkiss, H., Isaacson, B., Rimmerman, N., Mizrahi, A., and Yirmiya, R. (2017). The role of microglia and their CX3CR1 signaling in adult neurogenesis in the olfactory bulb. Elife *6*.

Ressler, K.J., Paschall, G., Zhou, X.L., and Davis, M. (2002). Regulation of synaptic plasticity genes during consolidation of fear conditioning. Journal of Neuroscience *22*, 7892-7902.

Rey, G., and Reddy, A.B. (2015). Interplay between cellular redox oscillations and circadian clocks. Diabetes Obes Metab *17*, 55-64.

Richards, J., Diaz, A.N., and Gumz, M.L. (2014). Clock genes in hypertension: novel insights from rodent models. Blood Press Monit *19*, 249-254.

Risher, W.C., Ustunkaya, T., Singh Alvarado, J., and Eroglu, C. (2014). Rapid Golgi analysis method for efficient and unbiased classification of dendritic spines. PLoS One *9*, e107591.

Rodriguez-Iglesias, N., Sierra, A., and Valero, J. (2019). Rewiring of Memory Circuits: Connecting Adult Newborn Neurons With the Help of Microglia. Front Cell Dev Biol *7*, 24.

Rogers, J.T., Morganti, J.M., Bachstetter, A.D., Hudson, C.E., Peters, M.M., Grimmig, B.A., Weeber, E.J., Bickford, P.C., and Gemma, C. (2011). CX3CR1 deficiency leads to impairment of hippocampal cognitive function and synaptic plasticity. J Neurosci *31*, 16241-16250.

Rosin, J.M., Vora, S.R., and Kurrasch, D.M. (2018). Depletion of embryonic microglia using the CSF1R inhibitor PLX5622 has adverse sex-specific effects on mice, including accelerated weight gain, hyperactivity and anxiolytic-like behaviour. Brain Behavior and Immunity *73*, 682-697.

Rudic, R.D., McNamara, P., Curtis, A.M., Boston, R.C., Panda, S., Hogenesch, J.B., and Fitzgerald, G.A. (2004). BMAL1 and CLOCK, two essential components of the circadian clock, are involved in glucose homeostasis. PLoS Biol *2*, e377.

Sagar, H.J., Cohen, N.J., Corkin, S., and Growdon, J.H. (1985). Dissociations among Processes in Remote Memory. Ann Ny Acad Sci *444*, 533-535.

Sahay, A., Scobie, K.N., Hill, A.S., O'Carroll, C.M., Kheirbek, M.A., Burghardt, N.S., Fenton, A.A., Dranovsky, A., and Hen, R. (2011). Increasing adult hippocampal neurogenesis is sufficient to improve pattern separation. Nature *472*, 466-U539.

Sato, S., Sakurai, T., Ogasawara, J., Takahashi, M., Izawa, T., Imaizumi, K., Taniguchi, N., Ohno, H., and Kizaki, T. (2014). A circadian clock gene, Rev-erbalpha, modulates the inflammatory function of macrophages through the negative regulation of Ccl2 expression. J Immunol *192*, 407-417.

Sato, T.K., Panda, S., Miraglia, L.J., Reyes, T.M., Rudic, R.D., McNamara, P., Naik, K.A., Fitzgerald, G.A., Kay, S.A., and Hogenesch, J.B. (2004). A functional genomics strategy reveals rora as a component of the mammalian circadian clock. Neuron *43*, 527-537.

Sawchenko, P.E. (1998). Toward a new neurobiology of energy balance, appetite, and obesity: the anatomists weigh in. J Comp Neurol *402*, 435-441.

Schafer, D.P., Lehrman, E.K., Kautzman, A.G., Koyama, R., Mardinly, A.R., Yamasaki, R., Ransohoff, R.M., Greenberg, M.E., Barres, B.A., and Stevens, B. (2012). Microglia sculpt postnatal neural circuits in an activity and complement-dependent manner. Neuron *74*, 691-705.

Schafer, D.P., Lehrman, E.K., and Stevens, B. (2013). The "quad-partite" synapse: Microglia-synapse interactions in the developing and mature CNS. Glia *61*, 24-36.

Schafer, D.P., and Stevens, B. (2013). Phagocytic glial cells: sculpting synaptic circuits in the developing nervous system. Curr Opin Neurobiol *23*, 1034-1040.

Schatzle, P., Ster, J., Verbich, D., McKinney, R.A., Gerber, U., Sonderegger, P., and Mateos, J.M. (2011). Rapid and reversible formation of spine head filopodia in response to muscarinic receptor activation in CA1 pyramidal cells. J Physiol *589*, 4353-4364.

Schiaffino, S., Blaauw, B., and Dyar, K.A. (2016). The functional significance of the skeletal muscle clock: lessons from Bmal1 knockout models. Skelet Muscle *6*, 33.

Schmolck, H., Kensinger, E.A., Corkin, S., and Squire, L.R. (2002). Semantic knowledge in patient H.M. and other patients with bilateral medial and lateral temporal lobe lesions. Hippocampus *12*, 520-533.

Schwartz, M.W., Woods, S.C., Porte, D., Jr., Seeley, R.J., and Baskin, D.G. (2000). Central nervous system control of food intake. Nature *404*, 661-671.

Schwarz, J.M., and Bilbo, S.D. (2012). Sex, glia, and development: Interactions in health and disease. Horm Behav *62*, 243-253.

Segev, I., and Rall, W. (1988). Computational Study of an Excitable Dendritic Spine. J Neurophysiol *60*, 499-523.

Sellgren, C.M., Gracias, J., Watmuff, B., Biag, J.D., Thanos, J.M., Whittredge, P.B., Fu, T., Worringer, K., Brown, H.E., Wang, J.*, et al.* (2019). Increased synapse elimination by microglia in schizophrenia patient-derived models of synaptic pruning. Nat Neurosci *22*, 374-385.

Sellgren, C.M., Sheridan, S.D., Gracias, J., Xuan, D., Fu, T., and Perlis, R.H. (2017). Patient-specific models of microglia-mediated engulfment of synapses and neural progenitors. Mol Psychiatry *22*, 170-177.

Shi, H., Seeley, R.J., and Clegg, D.J. (2009). Sexual differences in the control of energy homeostasis. Front Neuroendocrinol *30*, 396-404.

Shigemoto-Mogami, Y., Hoshikawa, K., Goldman, J.E., Sekino, Y., and Sato, K. (2014). Microglia enhance neurogenesis and oligodendrogenesis in the early postnatal subventricular zone. J Neurosci *34*, 2231-2243.

Shimba, S., Ishii, N., Ohta, Y., Ohno, T., Watabe, Y., Hayashi, M., Wada, T., Aoyagi, T., and Tezuka, M. (2005). Brain and muscle Arnt-like protein-1 (BMAL1), a component of the molecular clock, regulates adipogenesis. Proc Natl Acad Sci U S A *102*, 12071-12076.

Shimizu, K., Kobayashi, Y., Nakatsuji, E., Yamazaki, M., Shimba, S., Sakimura, K., and Fukada, Y. (2016). SCOP/PHLPP1beta mediates circadian regulation of long-term recognition memory. Nat Commun *7*, 12926.

Sierra, A., Abiega, O., Shahraz, A., and Neumann, H. (2013). Janus-faced microglia: beneficial and detrimental consequences of microglial phagocytosis. Frontiers in Cellular Neuroscience *7*.

Sierra, A., Encinas, J.M., Deudero, J.J.P., Chancey, J.H., Enikolopov, G., Overstreet-Wadiche, L.S., Tsirka, S.E., and Maletic-Savatic, M. (2010). Microglia Shape Adult Hippocampal Neurogenesis through Apoptosis-Coupled Phagocytosis. Cell Stem Cell *7*, 483-495.

Sierra, A., Gottfried-Blackmore, A.C., McEwen, B.S., and Bulloch, K. (2007). Microglia derived from aging mice exhibit an altered inflammatory profile. Glia *55*, 412-424.

Snider, K.H., Sullivan, K.A., and Obrietan, K. (2018). Circadian Regulation of Hippocampal-Dependent Memory: Circuits, Synapses, and Molecular Mechanisms. Neural Plast *2018*, 7292540.

Son, J., Song, S., Lee, S., Chang, S., and Kim, M. (2011). Morphological change tracking of dendritic spines based on structural features. J Microsc *241*, 261-272.

Squire, L.R., and Alvarez, P. (1995). Retrograde-Amnesia and Memory Consolidation - a Neurobiological Perspective. Current Opinion in Neurobiology *5*, 169-177.

Stanley, S.A., Small, C.J., Murphy, K.G., Rayes, E., Abbott, C.R., Seal, L.J., Morgan, D.G., Sunter, D., Dakin, C.L., Kim, M.S*., et al.* (2001). Actions of cocaine- and amphetamine-regulated transcript (CART) peptide on regulation of appetite and hypothalamo-pituitary axes in vitro and in vivo in male rats. Brain Res *893*, 186-194.

Steiner, P., Higley, M.J., Xu, W., Czervionke, B.L., Malenka, R.C., and Sabatini, B.L. (2008). Destabilization of the postsynaptic density by PSD-95 serine 73 phosphorylation inhibits spine growth and synaptic plasticity. Neuron *60*, 788-802.

Stenvers, D.J., Scheer, F., Schrauwen, P., la Fleur, S.E., and Kalsbeek, A. (2019a). Circadian clocks and insulin resistance. Nat Rev Endocrinol *15*, 75-89.

Stenvers, D.J., Scheer, F.A.J.L., Schrauwen, P., la Fleur, S.E., and Kalsbeek, A. (2019b). Circadian clocks and insulin resistance. Nat Rev Endocrinol *15*, 75-89.

Stephan, A.H., Barres, B.A., and Stevens, B. (2012). The Complement System: An Unexpected Role in Synaptic Pruning During Development and Disease. Annual Review of Neuroscience, Vol 35 *35*, 369-389.

Streit, W.J., Walter, S.A., and Pennell, N.A. (1999). Reactive microgliosis. Prog Neurobiol *57*, 563-581.

Subhramanyam, C.S., Wang, C., Hu, Q., and Dheen, S.T. (2019). Microglia-mediated neuroinflammation in neurodegenerative diseases. Semin Cell Dev Biol.

Tan, Y.L., Yuan, Y., and Tian, L. (2020). Microglial regional heterogeneity and its role in the brain. Mol Psychiatry *25*, 351-367.

Tang, Y., and Le, W. (2016). Differential Roles of M1 and M2 Microglia in Neurodegenerative Diseases. Mol Neurobiol *53*, 1181-1194.

Taniguchi, C.M., Emanuelli, B., and Kahn, C.R. (2006). Critical nodes in signalling pathways: insights into insulin action. Nat Rev Mol Cell Bio *7*, 85-96.

Taylor, D.L., Jones, F., Kubota, E.S., and Pocock, J.M. (2005). Stimulation of microglial metabotropic glutamate receptor mGlu2 triggers tumor necrosis factor alpha-induced neurotoxicity in concert with microglial-derived Fas ligand. J Neurosci *25*, 2952-2964.

Thaler, J.P., Yi, C.X., Schur, E.A., Guyenet, S.J., Hwang, B.H., Dietrich, M.O., Zhao, X., Sarruf, D.A., Izgur, V., Maravilla, K.R*., et al.* (2012a). Obesity is associated with hypothalamic injury in rodents and humans. J Clin Invest *122*, 153-162.

Thaler, J.P., Yi, C.X., Schur, E.A., Guyenet, S.J., Hwang, B.H., Dietrich, M.O., Zhao, X.L., Sarruf, D.A., Izgur, V., Maravilla, K.R*., et al.* (2012b). Obesity is associated with hypothalamic injury in rodents and humans (vol 122, pg 153, 2012). Journal of Clinical Investigation *122*, 778-778.

Thompson, R.F., and Kim, J.J. (1996). Memory systems in the brain and localization of a memory. Proc Natl Acad Sci U S A *93*, 13438-13444.

Tikka, T., Fiebich, B.L., Goldsteins, G., Keinanen, R., and Koistinaho, J. (2001). Minocycline, a tetracycline derivative, is neuroprotective against excitotoxicity by inhibiting activation and proliferation of microglia. Journal of Neuroscience *21*, 2580-2588.

Toda, C., Santoro, A., Kim, J.D., and Diano, S. (2017). POMC Neurons: From Birth to Death. Annu Rev Physiol *79*, 209-236.

Tomita, H., Ohbayashi, M., Nakahara, K., Hasegawa, I., and Miyashita, Y. (1999). Top-down signal from prefrontal cortex in executive control of memory retrieval. Nature *401*, 699-703.

Tremblay, M.E., Stevens, B., Sierra, A., Wake, H., Bessis, A., and Nimmerjahn, A. (2011a). The role of microglia in the healthy brain. J Neurosci *31*, 16064-16069.

Tremblay, M.E., Stevens, B., Sierra, A., Wake, H., Bessis, A., and Nimmerjahn, A. (2011b). The Role of Microglia in the Healthy Brain. Journal of Neuroscience *31*, 16064-16069.

Turek, F.W., Joshu, C., Kohsaka, A., Lin, E., Ivanova, G., McDearmon, E., Laposky, A., Losee-Olson, S., Easton, A., Jensen, D.R*., et al.* (2005). Obesity and metabolic syndrome in circadian Clock mutant mice. Science *308*, 1043-1045.

Ueno, M., Fujita, Y., Tanaka, T., Nakamura, Y., Kikuta, J., Ishii, M., and Yamashita, T. (2013). Layer V cortical neurons require microglial support for survival during postnatal development. Nat Neurosci *16*, 543-551.

Urabe, H., Kojima, H., Chan, L., Terashima, T., Ogawa, N., Katagi, M., Fujino, K., Kumagai, A., Kawai, H., Asakawa, A*., et al.* (2013). Haematopoietic cells produce BDNF and regulate appetite upon migration to the hypothalamus. Nature Communications *4*.

Uylings, H.B.M., Groenewegen, H.J., and Kolb, B. (2003). Do rats have a prefrontal cortex? Behavioural Brain Research *146*, 3-17.

Valdearcos, M., Douglass, J.D., Robblee, M.M., Dorfman, M.D., Stifler, D.R., Bennett, M.L., Gerritse, I., Fasnacht, R., Barres, B.A., Thaler, J.P., *et al.* (2017). Microglial Inflammatory Signaling Orchestrates the Hypothalamic Immune Response to Dietary Excess and Mediates Obesity Susceptibility. Cell Metab *26*, 185-197 e183.

Valdearcos, M., Robblee, M.M., Benjamin, D.I., Nomura, D.K., Xu, A.W., and Koliwad, S.K. (2014a). Microglia dictate the impact of saturated fat consumption on hypothalamic inflammation and neuronal function. Cell Rep *9*, 2124-2138.

VanRyzin, J.W., Marquardt, A.E., Argue, K.J., Vecchiarelli, H.A., Ashton, S.E., Arambula, S.E., Hill, M.N., and McCarthy, M.M. (2019). Microglial Phagocytosis of Newborn Cells Is Induced by Endocannabinoids and Sculpts Sex Differences in Juvenile Rat Social Play. Neuron *102*, 435-+.

Varela, L., and Horvath, T.L. (2012). Leptin and insulin pathways in POMC and AgRP neurons that modulate energy balance and glucose homeostasis. Embo Reports *13*, 1079-1086.

Vezzani, A., and Viviani, B. (2015). Neuromodulatory properties of inflammatory cytokines and their impact on neuronal excitability. Neuropharmacology *96*, 70-82.

Viggiano, A., Monda, M., Viggiano, A., Fuccio, F., and De Luca, B. (2004). Extracellular GABA in the medial hypothalamus is increased following hypocretin-1 administration. Acta Physiol Scand *182*, 89-94.

Vijayan, V., Pradhan, P., Braud, L., Fuchs, H.R., Gueler, F., Motterlini, R., Foresti, R., and Immenschuh, S. (2019). Human and murine macrophages exhibit differential metabolic responses to lipopolysaccharide - A divergent role for glycolysis. Redox Biol *22*, 101147.

Vitaterna, M.H., King, D.P., Chang, A.M., Kornhauser, J.M., Lowrey, P.L., McDonald, J.D., Dove, W.F., Pinto, L.H., Turek, F.W., and Takahashi, J.S. (1994). Mutagenesis and mapping of a mouse gene, Clock, essential for circadian behavior. Science *264*, 719-725.

Vukovic, J., Colditz, M.J., Blackmore, D.G., Ruitenberg, M.J., and Bartlett, P.F. (2012). Microglia modulate hippocampal neural precursor activity in response to exercise and aging. J Neurosci *32*, 6435-6443.

Wake, H., Moorhouse, A.J., Jinno, S., Kohsaka, S., and Nabekura, J. (2009). Resting microglia directly monitor the functional state of synapses in vivo and determine the fate of ischemic terminals. J Neurosci *29*, 3974-3980.

Walker, F.R., Beynon, S.B., Jones, K.A., Zhao, Z., Kongsui, R., Cairns, M., and Nilsson, M. (2014). Dynamic structural remodelling of microglia in health and disease: a review of the models, the signals and the mechanisms. Brain Behav Immun *37*, 1-14.

Wang, C., Billington, C.J., Levine, A.S., and Kotz, C.M. (2000). Effect of CART in the hypothalamic paraventricular nucleus on feeding and uncoupling protein gene expression. Neuroreport *11*, 3251-3255.

Wang, L., Pavlou, S., Du, X., Bhuckory, M., Xu, H., and Chen, M. (2019). Glucose transporter 1 critically controls microglial activation through facilitating glycolysis. Mol Neurodegener *14*, 2.

Wang, Y.M., Szretter, K.J., Vermi, W., Gilfillan, S., Rossini, C., Cella, M., Barrow, A.D., Diamond, M.S., and Colonna, M. (2012). IL-34 is a tissue-restricted ligand of CSF1R required for the development of Langerhans cells and microglia. Nature Immunology *13*, 753-+.

Weinhard, L., di Bartolomei, G., Bolasco, G., Machado, P., Schieber, N.L., Neniskyte, U., Exiga, M., Vadisiute, A., Raggioli, A., Schertel, A.*, et al.* (2018). Microglia remodel synapses by presynaptic trogocytosis and spine head filopodia induction. Nat Commun *9*, 1228.

Wilber, A.A., Skelin, I., Wu, W., and McNaughton, B.L. (2017). Laminar Organization of Encoding and Memory Reactivation in the Parietal Cortex. Neuron *95*, 1406-+.

Winter, S.L., Bosnoyan-Collins, L., Pinnaduwage, D., and Andrulis, I.L. (2007). Expression of the circadian clock genes Per1 and Per2 in sporadic and familial breast tumors. Neoplasia *9*, 797-800.

Wong, E.L., Stowell, R.D., and Majewska, A.K. (2017). What the Spectrum of Microglial Functions Can Teach us About Fetal Alcohol Spectrum Disorder. Front Synaptic Neurosci *9*, 11.

Woon, P.Y., Kaisaki, P.J., Braganca, J., Bihoreau, M.T., Levy, J.C., Farrall, M., and Gauguier, D. (2007). Aryl hydrocarbon receptor nuclear translocator-like (BMAL1) is associated with susceptibility to hypertension and type 2 diabetes. P Natl Acad Sci USA *104*, 14412-14417.

Wu, L., and Reddy, A.B. (2014). Rethinking the clockwork: redox cycles and non-transcriptional control of circadian rhythms. Biochem Soc Trans *42*, 1-10.

Wu, Y., Dissing-Olesen, L., MacVicar, B.A., and Stevens, B. (2015). Microglia: Dynamic Mediators of Synapse Development and Plasticity. Trends Immunol *36*, 605-613.

Xie, Y.L., Tang, Q.M., Chen, G.J., Xie, M.R., Yu, S.L., Zhao, J.J., and Chen, L.L. (2019). New Insights Into the Circadian Rhythm and Its Related Diseases. Front Physiol *10*.

Xu, B., Goulding, E.H., Zang, K., Cepoi, D., Cone, R.D., Jones, K.R., Tecott, L.H., and Reichardt, L.F. (2003). Brain-derived neurotrophic factor regulates energy balance downstream of melanocortin-4 receptor. Nat Neurosci *6*, 736-742.

Xu, T.H., Yu, X.Z., Perlik, A.J., Tobin, W.F., Zweig, J.A., Tennant, K., Jones, T., and Zuo, Y. (2009). Rapid formation and selective stabilization of synapses for enduring motor memories. Nature *462*, 915-U108.

Yang, G., Pan, F., and Gan, W.B. (2009a). Stably maintained dendritic spines are associated with lifelong memories. Nature *462*, 920-924.

Yang, J., Kim, C.S., Tu, T.H., Kim, M.S., Goto, T., Kawada, T., Choi, M.S., Park, T., Sung, M.K., Yun, J.W.*, et al.* (2017). Quercetin Protects Obesity-Induced Hypothalamic Inflammation by Reducing Microglia-Mediated Inflammatory Responses via HO-1 Induction. Nutrients *9*.

Yang, X.M., Wood, P.A., Ansell, C.M., Quiton, D.F.T., Oh, E.Y., Du-Quiton, J., and Hrushesky, W.J.M. (2009b). The Circadian Clock Gene Per1 Suppresses Cancer Cell Proliferation and Tumor Growth at Specific Times of Day. Chronobiology International *26*, 1323-1339.

Yanguas-Casas, N., Crespo-Castrillo, A., de Ceballos, M.L., Chowen, J.A., Azcoitia, I., Arevalo, M.A., and Garcia-Segura, L.M. (2018). Sex differences in the phagocytic and migratory activity of microglia and their impairment by palmitic acid. Glia *66*, 522-537.

Yi, C.X., Serlie, M.J., Ackermans, M.T., Foppen, E., Buijs, R.M., Sauerwein, H.P., Fliers, E., and Kalsbeek, A. (2009). A major role for perifornical orexin neurons in the control of glucose metabolism in rats. Diabetes *58*, 1998-2005.

Yi, C.X., Walter, M., Gao, Y., Pitra, S., Legutko, B., Kalin, S., Layritz, C., Garcia-Caceres, C., Bielohuby, M., Bidlingmaier, M.*, et al.* (2017). TNFalpha drives mitochondrial stress in POMC neurons in obesity. Nat Commun *8*, 15143.

Yoshihara, Y., De Roo, M., and Muller, D. (2009). Dendritic spine formation and stabilization. Curr Opin Neurobiol *19*, 146-153.

Yuste, R., and Denk, W. (1995a). Dendritic Spines as Basic Functional Units of Neuronal Integration. Nature *375*, 682-684.

Zac-Varghese, S., Tan, T., and Bloom, S.R. (2010). Hormonal Interactions Between Gut and Brain. Discov Med *10*, 543-552.

Zhan, Y., Paolicelli, R.C., Sforazzini, F., Weinhard, L., Bolasco, G., Pagani, F., Vyssotski, A.L., Bifone, A., Gozzi, A., Ragozzino, D.*, et al.* (2014). Deficient neuron-microglia signaling results in impaired functional brain connectivity and social behavior. Nat Neurosci *17*, 400-406.

Zhang, J.F., Malik, A., Choi, H.B., Ko, R.W.Y., Dissing-Olesen, L., and MacVicar, B.A. (2014a). Microglial CR3 Activation Triggers Long-Term Synaptic Depression in the Hippocampus via NADPH Oxidase. Neuron *82*, 195-207.

Zhang, L.Y., Hirano, A., Hsu, P.K., Jones, C.R., Sakai, N., Okuro, M., McMahon, T., Yamazaki, M., Xu, Y., Saigoh, N.*, et al.* (2016). A PERIOD3 variant causes a circadian phenotype and is associated with a seasonal mood trait. P Natl Acad Sci USA *113*, E1536-E1544.

Zhang, R., Lahens, N.F., Ballance, H.I., Hughes, M.E., and Hogenesch, J.B. (2014b). A circadian gene expression atlas in mammals: implications for biology and medicine. Proc Natl Acad Sci U S A *111*, 16219-16224.

Zhang, X., and van den Pol, A.N. (2016). Hypothalamic arcuate nucleus tyrosine hydroxylase neurons play orexigenic role in energy homeostasis. Nat Neurosci *19*, 1341-1347.

Zhang, X., Zhang, G., Zhang, H., Karin, M., Bai, H., and Cai, D. (2008). Hypothalamic IKKbeta/NF-kappaB and ER stress link overnutrition to energy imbalance and obesity. Cell *135*, 61-73.

Zheng, B., Albrecht, U., Kaasik, K., Sage, M., Lu, W., Vaishnav, S., Li, Q., Sun, Z.S., Eichele, G., Bradley, A.*, et al.* (2001). Nonredundant roles of the mPer1 and mPer2 genes in the mammalian circadian clock. Cell *105*, 683-694.

Zhou, L., Sutton, G.M., Rochford, J.J., Semple, R.K., Lam, D.D., Oksanen, L.J., Thornton-Jones, Z.D., Clifton, P.G., Yueh, C.Y., Evans, M.L.*, et al.* (2007). Serotonin 2C receptor agonists improve type 2 diabetes via melanocortin-4 receptor signaling pathways. Cell Metab *6*, 398-405.

Zhou, Q., Tao, H.W., and Poo, M.M. (2003). Reversal and stabilization of synaptic modifications in a developing visual system. Science *300*, 1953-1957.

Zito, K., Scheuss, V., Knott, G., Hill, T., and Svoboda, K. (2009). Rapid functional maturation of nascent dendritic spines. Neuron *61*, 247-258.

Objectives of the Thesis

Objectives of the Thesis

In this thesis, firstly, we focus on the microglial core clock gene-*Bmal1*, which is closely linked with energy metabolism (Hatanaka et al., 2010; Rudic et al., 2004; Schiaffino et al., 2016; Sussman et al., 2019), redox homeostasis (Early et al., 2018b; Musiek et al., 2013a) and immune responses (Nakazato et al., 2017). Global *Bmal1* knockout mice are arrhythmic in constant darkness and show reduced locomotor activity in light/dark cycles (Bunger et al., 2000). Specific astrocytic deletion of *Bmal1* results in cognitive deficiency and metabolic imbalance in mice (Barca-Mayo et al., 2019; Barca-Mayo et al., 2017). Interestingly, age-related microglial circadian disruption sensitizes neuroinflammatory response in the hippocampus (Fonken et al., 2016). The microglial clock modulates the production of cytokines, following an immune challenge (Nakazato et al., 2017). It has been shown that microglia play an important role in memory formation and energy metabolism and microglial functions may strongly rely on its intrinsic clock.

Thus, the main aim of this thesis is to understand whether and how the *Bmal1* deletion affects microglial functions during different situations *in vivo* and *in vitro*, particularly looking at the consequences on the control of energy balance and memory formation.

In the first study, we checked whether clock genes show rhythmic expression in the microglial cells isolated from adult C57BL/6J mice at 8-time points during the 24-h light/dark-cycle by using quantitative RT-PCR. To clarify the impact of microglial *Bmal1* in systemic energy homeostasis and learning and memory processes *in vivo*, we generated microglia-specific *Bmal1* knockdown (microglia$^{Bmal1\text{-KD}}$) mice. The *Bmal1* knockdown efficiency and effect on clock machinery were evaluated on the gene level. We hypothesized that *Bmal1* deficiency will affect microglial functions under HFD conditions and during cognitive processes in mice. This effect will influence the hypothalamic POMC neuronal population and hippocampal synaptic plasticity, which finally affect energy balance and memory formation in mice.

By using this animal model, we tested the metabolic phenotype (such as body weight, daily food intake, locomotor activity, heat production, and respiratory exchange ratio) in microglia$^{Bmal1\text{-KD}}$ and Ctrl mice fed a standard chow diet or HFD in both males and females. We examined microglial immune activity (iba1-ir cell number) and phagocytosis (CD68-ir/iba1-ir, as an indication of phagocytic capacity), as well as POMC neuronal cell number in the ARC, the key brain region regulating systemic energy homeostasis, in chow or HFD-fed male and female

mice at two time-points within 24 h (ZT5 and ZT17) in mice. To identify whether microglia were able to phagocytose apoptotic cells induced by HFD consumption, we analyzed the apoptotic cell-derived DNA fragments in CD68-ir phagosomes by co-immunostaining with DAPI and iba1 in the ARC.

Using the same animal model, we also evaluated hippocampo-dependent memory formation and consolidation in microglia$^{Bmal1\text{-KD}}$ and control mice. Since the estrous cycle in female mice inevitably interferes with spatial reference memory, only males were evaluated in the cognitive study. Mice were subjected to three different Morris water maze (MWM) tests (a 4-day-training session to investigate spatial reference memory, a mild 3-day-training to evaluate long-term memory consolidation abilities, and a reversal test to verify the cognitive flexibility) and a novel object recognition test. We then assessed the number of dendritic spines in CA1 pyramidal neurons, by Golgi staining, during the memory consolidation process. Finally, we analyzed microglial immune activity (iba1-ir cell number) and phagocytosis (CD68-ir/iba1-ir, as an indication of phagocytic capacity) in the hippocampal CA1 and DG regions at two time-points within 24h (ZT5 and ZT17) in mice in both learning (MWM) and homecage groups. Since microglia also phagocytose presynaptic structures to remodel neural circuity, we checked the presence of synaptophysin1 (presynaptic marker) inside CD68-ir phagosomes in microglia.

Cellular energy metabolism and redox homeostasis also regulate microglial function (Early et al., 2018b; Gao et al., 2017b). Thus, there is a possible link among circadian clock-*Bmal1*, microglial function, cellular energy metabolism, and redox homeostasis. We hypothesized that *Bmal1* deficiency will affect the inflammatory gene expression in microglia, which could be achieved by shifting cellular energy metabolism and redox homeostasis.

In the second study, we evaluated the effect of *Bmal1* on microglial cellular metabolism and immune responses under normal and inflammatory conditions. Firstly, we checked whether inflammatory cytokines, nutrient utilization, and the antioxidative effect show daily rhythmicity in the microglial cell isolated from adult C57BL/6J mice at 8-time points during the 24-h light/dark-cycle by using quantitative RT-PCR. To further clarify the impact of microglial *Bmal1* in microglial immunometabolism *in vivo*, we used global *Bmal1* knocked out mice and studied the expression of clock genes, inflammation-related genes, and cellular metabolic-related genes in isolated microglial cells. Next, we evaluated the expression of these genes and the phagocytic capacity in microglial BV-2 cells under LPS and palmitic acid-induced inflammation.

In the third study, we investigated the role of the clock gene Rev-erbα in microglial immunometabolism. Disruption of circadian rhythmicity by the administration of the Rev-erbα agonist SR9011, reduces pro-inflammatory cytokine expression during an immune challenge by TNFα, while it increases expression of the anti-inflammatory cytokine Il10. Moreover, SR9011 decreases phagocytic activity, mitochondrial respiration, ATP production, and metabolic gene expression. We show that Rev-erbα is implicated in both metabolic homeostasis and the inflammatory responses in microglia.

In the fourth study, we investigated the effect of HFD-induced obesity on the daily rhythmicity of microglial immunometabolism in rats. We observed a time-of-day disturbance in microglial circadian and inflammatory functions in the obesogenic conditions, accompanied by changes in substrate utilization and energy production. On the other hand, evaluation of monocyte gene expression showed a small or absent effect of HFD on these peripheral myeloid cells, suggesting a cell-specific microglial inflammatory response in diet-induced obesity. An obesogenic diet affects microglial immunometabolism in a time-of-day dependent manner.

Lastly, in the fifth study, we investigated neuroinflammation, gliosis, and epigenetic changes in post-mortem brains from Alzheimer's disease patients. Two brain regions were investigated: the F2 area of the frontal cortex and the hippocampus. Overall, these data provide evidence for acetylation dysfunctions at the level of associated (epigenetic) enzymes and of histones in Alzheimer's disease's brains that may underlie transcriptional dysregulations and Alzheimer's disease-related cognitive impairments. We further point to stronger dysregulations in the F2 area of the frontal cortex than in the hippocampus at an end-stage of the disease, suggesting a differential vulnerability and/or efficiency of compensatory mechanisms.

References

Barca-Mayo, O., Boender, A.J., Armirotti, A., and De Pietri Tonelli, D. (2019). Deletion of astrocytic BMAL1 results in metabolic imbalance and shorter lifespan in mice. Glia.

Barca-Mayo, O., Pons-Espinal, M., Follert, P., Armirotti, A., Berdondini, L., and De Pietri Tonelli, D. (2017). Astrocyte deletion of Bmal1 alters daily locomotor activity and cognitive functions via GABA signalling. Nat Commun *8*, 14336.

Bunger, M.K., Wilsbacher, L.D., Moran, S.M., Clendenin, C., Radcliffe, L.A., Hogenesch, J.B., Simon, M.C., Takahashi, J.S., and Bradfield, C.A. (2000). Mop3 is an essential component of the master circadian pacemaker in mammals. Cell *103*, 1009-1017.

Early, J.O., Menon, D., Wyse, C.A., Cervantes-Silva, M.P., Zaslona, Z., Carroll, R.G., Palsson-McDermott, E.M., Angiari, S., Ryan, D.G., Corcoran, S.E.*, et al.* (2018). Circadian clock protein BMAL1 regulates IL-1beta in macrophages via NRF2. Proc Natl Acad Sci U S A *115*, E8460-E8468.

Fonken, L.K., Kitt, M.M., Gaudet, A.D., Barrientos, R.M., Watkins, L.R., and Maier, S.F. (2016). Diminished circadian rhythms in hippocampal microglia may contribute to age-related neuroinflammatory sensitization. Neurobiol Aging *47*, 102-112.

Gao, Y.Q., Vidal-Itriago, A., Kalsbeek, M.J., Layritz, C., Garcia-Caceres, C., Tom, R.Z., Eichmann, T.O., Vaz, F.M., Houtkooper, R.H., van der Wel, N.*, et al.* (2017). Lipoprotein Lipase Maintains Microglial Innate Immunity in Obesity. Cell Reports *20*, 3034-3042.

Hatanaka, F., Matsubara, C., Myung, J., Yoritaka, T., Kamimura, N., Tsutsumi, S., Kanai, A., Suzuki, Y., Sassone-Corsi, P., Aburatani, H.*, et al.* (2010). Genome-wide profiling of the core clock protein BMAL1 targets reveals a strict relationship with metabolism. Mol Cell Biol *30*, 5636-5648.

Musiek, E.S., Lim, M.M., Yang, G., Bauer, A.Q., Qi, L., Lee, Y., Roh, J.H., Ortiz-Gonzalez, X., Dearborn, J.T., Culver, J.P.*, et al.* (2013). Circadian clock proteins regulate neuronal redox homeostasis and neurodegeneration. J Clin Invest *123*, 5389-5400.

Nakazato, R., Hotta, S., Yamada, D., Kou, M., Nakamura, S., Takahata, Y., Tei, H., Numano, R., Hida, A., Shimba, S.*, et al.* (2017). The intrinsic microglial clock system regulates interleukin-6 expression. Glia *65*, 198-208.

Rudic, R.D., McNamara, P., Curtis, A.M., Boston, R.C., Panda, S., Hogenesch, J.B., and Fitzgerald, G.A. (2004). BMAL1 and CLOCK, two essential components of the circadian clock, are involved in glucose homeostasis. PLoS Biol *2*, e377.

Schiaffino, S., Blaauw, B., and Dyar, K.A. (2016). The functional significance of the skeletal muscle clock: lessons from Bmal1 knockout models. Skelet Muscle *6*, 33.

Sussman, W., Stevenson, M., Mowdawalla, C., Mota, S., Ragolia, L., and Pan, X.Y. (2019). BMAL1 controls glucose uptake through paired-homeodomain transcription factor 4 in differentiated Caco-2 cells. Am J Physiol-Cell Ph *317*, C492-C501.

Experimental Contributions

Publication 1

Microglia-specific knock-down of Bmal1 improves memory and protects mice from high fat diet-induced obesity

Xiao-Lan Wang[1,2,3], Sander Kooijman[4], Yuanqing Gao[2,3], Laura Tzeplaeff[1], Brigitte Cosquer[1,5], Irina Milanova[2,3], Samantha E.C. Wolff[3], Nikita Korpel[2,3,6], Marie-France Champy[7,8], Benoit Petit-Demoulière[7,8], Isabelle Goncalves Da Cruz[7,8], Tania Sorg-Guss[7,8], Patrick C.N. Rensen[4], Jean-Christophe Cassel[1,5], Andries Kalsbeek[2,3,6], Anne-Laurence Boutillier[1,5] *, Chun-Xia Yi[2,3.6] *

[1]Université de Strasbourg, Laboratoire de Neuroscience Cognitives et Adaptatives (LNCA), Strasbourg, France
[2]Department of Endocrinology and Metabolism, Amsterdam University Medical Centres (UMC), University of Amsterdam, Amsterdam, the Netherlands
[3]Laboratory of Endocrinology, Amsterdam University Medical Centres (UMC), University of Amsterdam, Amsterdam Gastroenterology & Metabolism, Amsterdam, the Netherlands
[4]Department of Medicine, Divison of Endocrinology, and Einthoven Laboratory for Experimental Vascular Medicine, Leiden University Medical Center, Leiden, the Netherlands
[5]CNRS UMR 7364, LNCA, Strasbourg, France
[6]Netherlands Institute for Neuroscience, an Institute of the Royal Netherlands Academy of Arts and Sciences, Amsterdam, the Netherlands
[7]PHENOMIN-ICS, Institut Clinique de la souris, CNRS, UMR7104, Illkirch, France
[8]INSERM, U964, Illkirch, France; Université de Strasbourg, France

*Equal contribution
* Co-corresponding/joint last authors

Accepted by *Molecular Psychiatry*.

Microglia-specific knock-down of Bmal1 improves memory and protects mice from high fat diet-induced obesity

Short title: **Microglial Bmal1, memory, and obesity**

Graphical Abstract

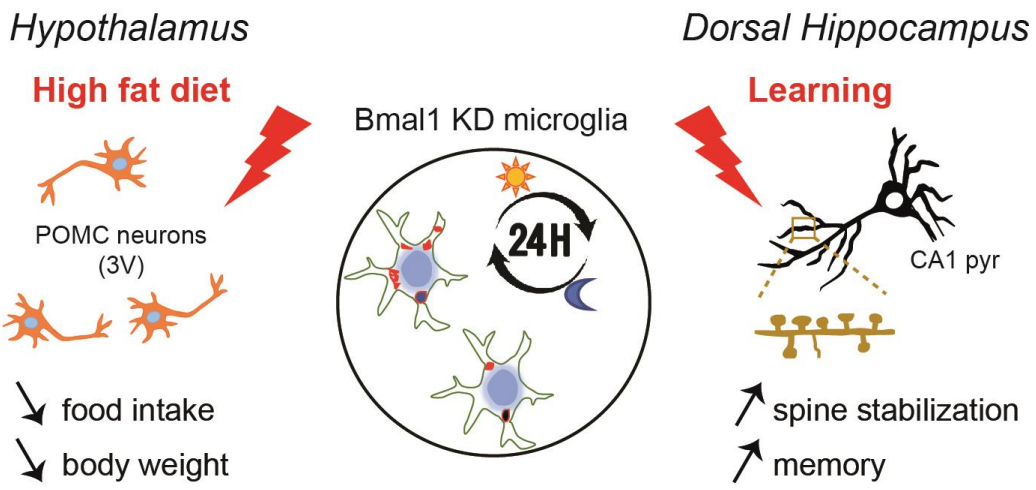

In Brief

Microglia are the brain-resident macrophages, which play a critical role in supporting neuronal function in physiological conditions. Wang et al. report that specific knock-down of the core clock gene-Bmal1 in microglia increases microglial daily phagocytosis capacity, resulting in protection from high fat diet-induced obesity and enhancement of memory performance in mice.

Abstract

Microglia play a critical role in maintaining neural function. While microglial activity follows a circadian rhythm, it is not clear how this intrinsic clock relates to their function, especially in stimulated conditions such as in the control of systemic energy homeostasis or memory formation. In this study, we found that microglia-specific knock-down of the core clock gene, *Bmal1*, resulted in increased microglial phagocytosis in mice subjected to high-fat diet (HFD)-induced metabolic stress and likewise among mice engaged in critical cognitive processes. Enhanced microglial phagocytosis was associated with significant retention of pro-opiomelanocortin (POMC)-immunoreactivity in the mediobasal hypothalamus in mice on a HFD as well as the formation of mature spines in the hippocampus during the learning process. This response ultimately protected mice from HFD-induced obesity and resulted in improved performance on memory tests. We conclude that loss of the rigorous control implemented by the intrinsic clock machinery increases the extent to which microglial phagocytosis can be triggered by neighboring neurons under metabolic stress or during memory formation. Taken together, microglial responses associated with loss of Bmal1 serve to ensure a healthier microenvironment for neighboring neurons in the setting of an adaptive response. Thus, microglial Bmal1 may be an important therapeutic target for metabolic and cognitive disorders with relevance to psychiatric disease.

Introduction

Microglia are resident brain macrophages that are responsible for elimination of apoptotic cells, cellular debris, and invading pathogens. They can regulate synaptic remodeling to optimize the microenvironment for neuronal survival and function (Colonna and Butovsky, 2017; Nimmerjahn et al., 2005). Microglial phagocytosis maintains the hypothalamic neural circuitry that controls energy homeostasis and also shapes hippocampal neuronal synapses so that they can establish mature connections (Gao et al., 2018a; Paolicelli et al., 2011a). Aberrant microglial phagocytosis is associated with obesity, neurodegenerative disorders, and psychiatric disease (Gao et al., 2017a; Zhan et al., 2014).

Microglial activity follows a circadian rhythm (Fonken et al., 2015a; Milanova et al., 2019a; Yi et al., 2017a), which is an internal timekeeping system that coordinates physiological processes and behaviors in accordance with day/night cycles (Gerstner and Yin, 2010; Man et al., 2016). In mammals, the core mechanism of the molecular clock machinery in nearly every cell type includes autoregulatory transcriptional and translational feedback loops that are

controlled by the actions of clock genes (Dudek and Meng, 2014). Molecular clocks drive circadian rhythms that modulate gene expression and cell function (Bass and Takahashi, 2010b; Rahman et al., 2015). Among the most prominent of these regulatory factors, the transcriptional activator, the Brain and Muscle Arnt-like 1 (Bmal1)/Clock complex promotes the expression of Period (*Per1*, *Per2*) and Cryptochrome (*Cry1*, *Cry2*) genes via binding interactions with their respective E-box promoter elements. The Per/Cry complex then negatively regulates its own transcription by inhibiting the activity of the Bmal1/Clock complex (Dudek and Meng, 2014; Gekakis et al., 1998). Disruption of the clock machinery has a significant impact on mammalian physiology (Barca-Mayo et al., 2017). For example, skeletal muscle-specific deficiency of the *Clock* gene results in disturbed nutrient utilization and leads to metabolic disorders (Gabriel and Zierath, 2019a; Schiaffino et al., 2016). Hippocampal-dependent cognitive performance is also controlled by the circadian clock (Hasegawa et al., 2019). However, specific functions regulated by the microglial circadian clock and its role with respect to the control of energy homeostasis and cognition have not yet been clarified.

Previous studies revealed that mice with a global knockout of the core clock gene *Bmal1,* are completely devoid of circadian rhythms in light/dark and constant dark conditions and show a variety of phenotypic abnormalities, among which age-related astrogliosis in the cortex and hippocampus, degeneration of synaptic terminals, and impaired cortical functional connectivity (Bunger et al., 2000; Musiek et al., 2013b). In cultured microglial cells, Bmal1 deficiency resulted in diminished expression of interleukin-6 (*Il6*) upon lipopolysaccharide challenging (Nakazato et al., 2017). However, this previous study did not address the impact of Bmal1 deletion on microglial phagocytic capacity. Microglial phagocytosis in the adult mouse brain is subject to region-specific differences that depend on neuronal activity (Ayata et al., 2018b). In this study, we generated mice with microglia-specific Bmal1-deficiency to explore cell-autonomous microglia-related functions, particularly regarding how the Bmal1-regulated phagocytosis is involved in stress-coping capacity by neurocircuitries in the hypothalamus and hippocampus. We also performed experiments that addressed the impact of microglial Bmal1 deletion on systemic energy homeostasis and on processes associated with learning and memory.

Materials and Methods

Animals

Two lines of transgenic mice (*Cx3cr1*^{CreER} mice (Lee et al., 2020b; Parkhurst et al., 2013), stock no. 021160 and *Bmal1*$^{lox/lox}$ mice (Storch et al., 2007), stock no. 007668) were obtained from the Jackson Laboratory (Bar Harbor, ME, USA) and crossed in this study. The *Cx3cr1*^{CreER} mice harbor a tamoxifen-inducible Cre recombinase that is fused with an enhanced yellow fluorescent protein (EYFP) attached to the chemokine (CX_3C motif) receptor 1 (*Cx3cr1*) promoter. The cellular localization of Cre was examined by the colocalization of EYFG with Iba1 immunoreactivity in our study. Almost all EYFP positive cells were Iba1 positive microglia, suggesting that the Cre is specifically expressed in microglia (Fig. S1A). To excise the loxP-flanked *Bmal1* sequences via Cre-mediated recombination, all 8-10-week-old mice were treated with tamoxifen (20 mg/ml; T5648, Sigma-Aldrich) in corn oil (S5007, Sigma-Aldrich) via intraperitoneal (i.p.) injection, once each day for 3 days at a dose of 100 µl per injection. Mice that were *Bmal1* lox-homozygous and Cre-positive (*Bmal1*$^{lox/lox}$-*Cx3cr1*^{CreER}) were used as the microglia$^{Bmal1\text{-KD}}$ model. Cre-positive, *Bmal1* wild-type mice served as littermate controls (Ctrls; *Cx3cr1*^{CreER}) (Knocking down validation and experimental groups allocation see Supplementary information).

Metabolic phenotype

After tamoxifen injection at 8-10 weeks of age, mice were fed either standard chow or a high-fat diet (HFD; Research Diets, Inc., New Brunswick, NJ, USA, cat. no. D12492). Body weight was measured weekly after tamoxifen injections. Food intake was measured daily for 5 days at ZT0 and ZT12 after 4 weeks on each diet. Energy expenditure, as well as physical activity, respiratory exchange ratio (RER), and heat production were evaluated by indirect calorimetry using the Phenomaster system (TSE Systems, Phenomaster/Labmaster, Bad Homburg, Germany) after 5 weeks on the HFD (see Supplementary information).

Cognitive phenotype

To test the learning and memory capacities, male microglia*Bmal1*-KD and Ctrl mice performed the Morris water maze (MWM) and novel object recognition tests two weeks after the tamoxifen injections. A different group of mice was used in each specific behavioral experiment as described in figure 3A-J (see Supplementary information).

Labeling and counting dendritic spines after Golgi staining

Mice were subjected to a 4-day-training in the MWM and killed 4 days after the last training. Golgi staining was performed for labeling and counting dendritic spines (see Supplementary information).

Profiling microglial phagocytic capacity and gene and protein expressions

To investigate microglial phagocytic capacity, primary microglial cells were prepared as described previously. Fluoresbrite® Polychromatic Red Microspheres (1.0 µm, 18660-5, polysciences) were used to treat the cells and the average of microspheres per cell was measured (see Supplementary information). To analyze microglial gene and protein expression, three weeks after the tamoxifen injections, mice were decapitated for extraction of brain tissue. Microglia were isolated for RT-PCR and Western blot studies (see Supplementary information).

Characterizing neurons and microglia in the hypothalamus and hippocampus.

At the end of metabolic or cognitive studies, mouse brain tissues were obtained after perfusion-fixation. Brain sections were processed for immunohistochemical or immunofluorescence staining. Bright field or fluorescent confocal images were acquired accordingly and images were analyzed using Image J or Imaris software with 3D reconstruction (Bitplane AG, Zurich, Switzerland) (Supplementary information).

Statistical analysis

Experimenters were blinded to the mouse genotype during behavioral testing and imaging analysis. Where applicable, statistical analyses were performed using two-tailed unpaired t-tests and two-way analysis of variance (ANOVA) with GraphPad Prism 8 (San Diego, CA, USA). One-way ANOVA was used to assess the effect of time on microglial gene expression in the C57BL/6J wild-type mice. The daily rhythms associated with gene expression in microglia in wild-type mice were evaluated by cosinor analysis using SigmaPlot 12.0 software (SPSS Inc., Chicago, IL, USA) (Hogenboom et al., 2019b). Data were fitted to the following regression: $y = A + B \times \cos(2\pi [x-C]/24)$ where A is the mean level, B is the amplitude, and C is the acrophase of the fitted rhythm. An overall *p* value (main *p* value, *P*m) was considered as indicating 24h-rhythmicity. The variation of data between the groups that compared is similar. All data are presented as mean ± standard error of the mean (s.e.m.) with statistical significance indicated by $P < 0.05$.

Results

Microglia-specific knock-down of Bmal1 deregulates the expression of clock-related genes

To examine the cell-specific expression of clock-related genes, we isolated microglia from brain tissue of wild-type C57BL/6J mice every 3 hrs following lights on (i.e., ZT0; Fig. 1A). We found that the expression of clock genes in mouse microglial cells follows a distinct circadian rhythm (Fig. 1B and C). In order to study the functions of Bmal1 in microglia of adult mice, we generated microglia$^{Bmal1\text{-KD}}$ mice that harbor a microglia-specific deletion of this gene. Specifically, the microglia$^{Bmal1\text{-KD}}$ strain was generated by crossing *Bmal1*$^{lox/lox}$ mice with *Cx3cr1*^{CreER} mice (Lee et al., 2020b; Parkhurst et al., 2013); *Bmal1*-sufficient *Cx3cr1*^{CreER} mice were used as controls (Ctrls; Fig. 1D). Three weeks after administration of tamoxifen, we observed marked reductions in immunoreactive Bmal1 on Western blots of microglia isolated from microglia$^{Bmal1\text{-KD}}$ mice compared with that detected in Ctrls (Fig. 1E and Fig. S1B and C). These results documented the efficient tamoxifen-mediated knock-down of microglial *Bmal1* expression in the microglia$^{Bmal1\text{-KD}}$ mouse strain. Furthermore, we found a significant reduction of *Bmal1* gene expression while both *Cry1* and *Cry2* were increased in microglia isolated from male microglia$^{Bmal1\text{-KD}}$ mice (Fig. 1F). By contrast, in female mice of this strain only expression of the D site albumin promoter binding protein gene (*Dbp*) was significantly diminished (Fig. S1D).

Fig. 1

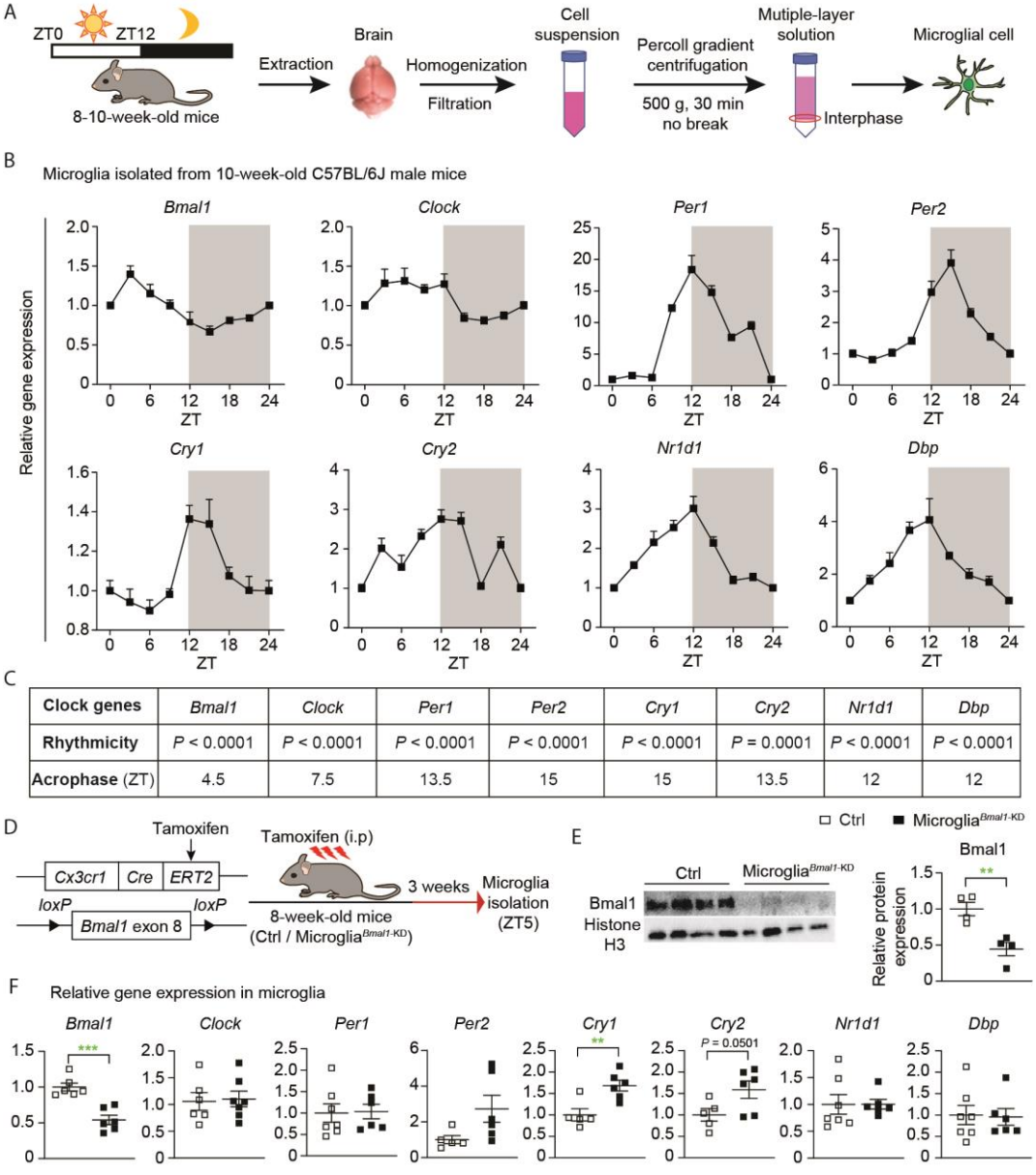

Clock genes	*Bmal1*	*Clock*	*Per1*	*Per2*	*Cry1*	*Cry2*	*Nr1d1*	*Dbp*
Rhythmicity	$P < 0.0001$	$P < 0.0001$	$P < 0.0001$	$P < 0.0001$	$P < 0.0001$	$P = 0.0001$	$P < 0.0001$	$P < 0.0001$
Acrophase (ZT)	4.5	7.5	13.5	15	15	13.5	12	12

Figure. 1 Specific knock-down of microglial *Bmal1* (microglia$^{Bmal1\text{-}KD}$) alters the expression of clock genes in adult male mice. (A) Strategy used to isolate microglia in this study. ZT0 = lights on; ZT12 = lights off. **(B)** Relative expression of clock genes in microglia isolated from brains of wild-type C57BL/6J male mice. Shown are data obtained from microglia isolated every 3 h from ZT0 through ZT21 (n = 8 mice per

group); data shown for points ZT0 and ZT24 are from the same samples. **(C)** Statistical analysis of rhythmic expression and acrophase determined for each of the clock genes; $P < 0.05$ was considered as representing significant rhythmicity. **(D)** Experimental strategy used for postnatal deletion of *Bmal1* specifically in microglia and the time course for microglial isolation. **(E)** Representative images and quantification of Western blots documenting immunoreactive Bmal1 and Histone H3 in isolated microglia (n = 4 mice per group). **(F)** Expression of clock genes in microglia isolated from the brain of Ctrl and microglia$^{Bmal1\text{-KD}}$ mice at 3 weeks after the tamoxifen injections (n = 5–7 mice per group).

Data are presented as means ± s.e.m. Green-colored * indicates a genotype effect; ** $P < 0.01$, *** $P < 0.001$.

Microglial deficiency of Bmal1 limits HFD-induced obesity

Microglial activation in the hypothalamus has been observed in association with hypercaloric diet-induced obesity, a response that was shown to be sex-dependent (Dorfman et al., 2017; Gao et al., 2017a). As such, we examined the metabolic phenotype of both male and female microglia$^{Bmal1\text{-KD}}$ and Ctrl mice provided with either a standard chow diet or with a HFD. On the standard chow diet, no differences were observed with respect to any of the metabolic parameters evaluated in comparisons between microglia$^{Bmal1\text{-KD}}$ and Ctrl, male or female mice (Fig. S2). Strikingly, we found that microglia$^{Bmal1\text{-KD}}$ mice on a HFD gained significantly less weight than did their Ctrl counterparts (Fig. 2A and B). Differential weight gain was more prominent among females than males (Fig. S3A and B). Interestingly, microglia$^{Bmal1\text{-KD}}$ male mice responded to the HFD with reduced food intake when compared to Ctrls (Fig. 2C); this response was observed mainly restricted to the dark phase in both sexes (Fig. 2D; Fig. S3C and D). Results from indirect calorimetry revealed that the mean respiratory exchange ratio (RER) increased in male Ctrls on the HFD, specifically during the dark, relative to the light phase, while no similar change was observed among microglia$^{Bmal1\text{-KD}}$ mice (Fig. S3E and F). Mean RER increased during the dark phase among female microglia$^{Bmal1\text{-KD}}$ mice relative to Ctrls (Fig. S3G and H). However, there was no genotype difference in daily physical activity and heat production in males (Fig. S3I – L) nor in females (Fig. S3M – P). Taken together, these data indicate that the microglia-specific *Bmal1* knock-down protects mice from HFD-induced obesity, mostly by lowering energy intake without affecting many other global metabolic parameters (RER, physical activity, heat production).

Fig. 2

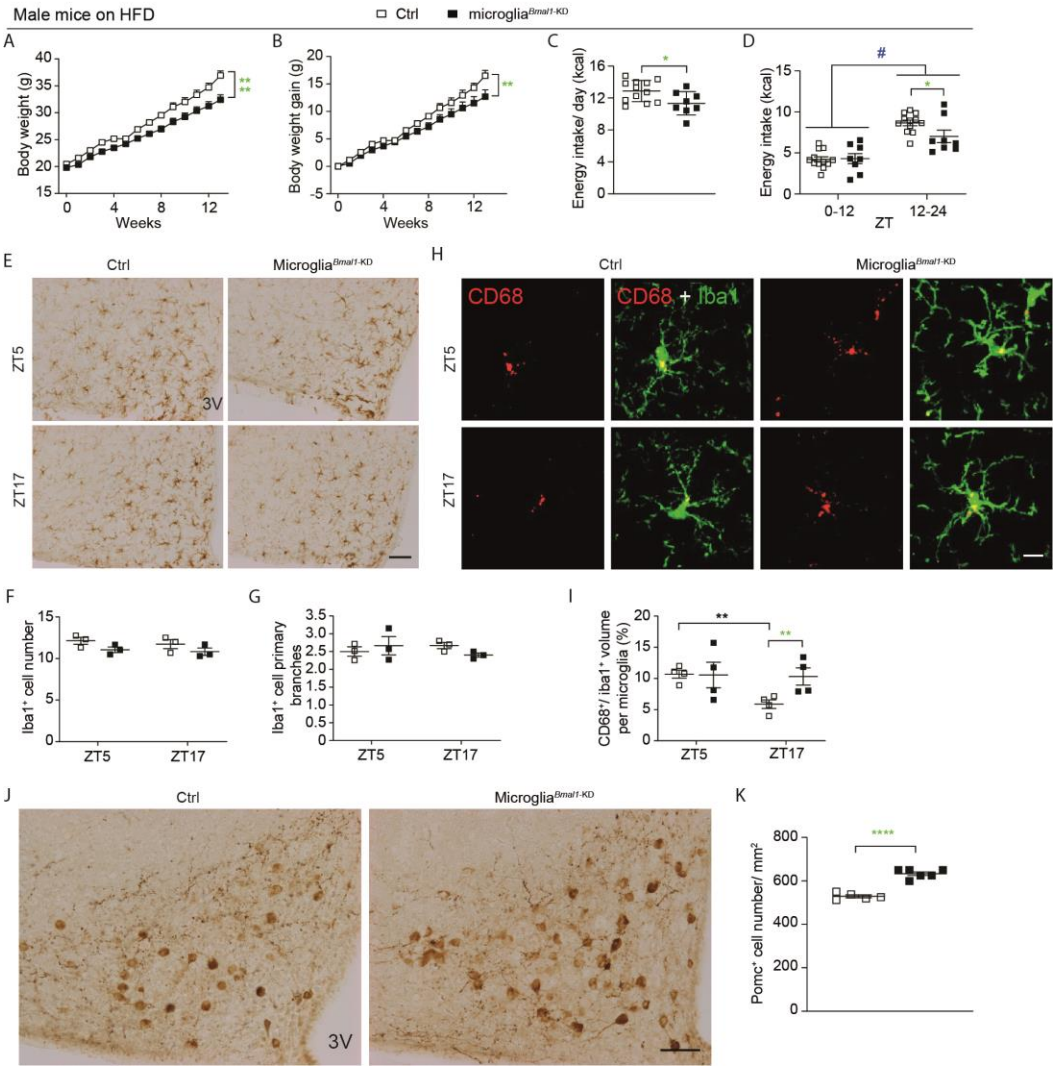

Figure. 2 Functional and cellular impact of microglial Bmal1 deletion on HFD-induced obesity in male mice. (A) Absolute body weight and (**B**) body weight gain of Ctrl and microglia$^{Bmal1\text{-KD}}$ mice fed a HFD (n = 5–7 mice per group). **(C)** Energy intake per day and (**D**) energy intake during light (ZT0–12) and dark phases (ZT12–24; n = 8–12 mice per group). **(E)** Representative images of Iba1 immunostaining in the ARC; 3V, third ventricle. Scale bar, 100 µm. **(F)** Quantification of Iba1^{+} microglial cells and (**G**) Iba1^{+} primary branches (n = 2–3 mice per group). **(H)** Confocal images of CD68 and Iba1 immunostaining in the ARC; scale bar, 10 µm. **(I)** Quantitative analysis of the volume percentage associated with CD68^{+} microglia

in the ARC (n = 4–5 mice per group; 100-125 cells were analyzed in each group). **(J)** Images of POMC^{+} neurons in the ARC; 3V, third ventricle, scale bar, 100 µm. **(K)** Analysis of POMC^{+} neurons expression (n = 5–6 mice per group).

Data are presented as means ± s.e.m. Green-colored * indicates a genotype effect. * $P < 0.05$, ** $P < 0.01$, **** $P < 0.0001$, and $^{\#}P < 0.05$ for ZT0-12 *vs*. ZT12-24.

Bmal1-deficiency results in increased microglial phagocytic capacity in response to HFD-induced metabolic challenge

The arcuate nucleus (ARC) of the hypothalamus plays a critical role in regulating systemic energy homeostasis (Morton et al., 2006). We hypothesized that disruption of the circadian rhythm secondary to Bmal1-deficiency may have an impact on systemic homeostasis via modulation of microglial phagocytic capacity. Notably, our previous results obtained from experiments using a microglial cell line (BV2 cells) showed that deletion of Bmal1 by siRNA led to increased phagocytosis of microspheres compared to control cells (Wang et al., 2020b). In the current experiment, a similarly increased phagocytosis was observed in primary microglial cells isolated from microglia$^{Bmal1\text{-KD}}$ mice (Fig. S4A and B). Subsequently, we assessed phagocytic capacity of microglia specifically in the ARC of both males and females after a 4-week trial of standard chow or HFD. Phagocytic capacity was evaluated at two specific time-points, ZT5 and ZT17, within a single 24 hr period. We evaluated several parameters associated with overall phagocytic capacity, including the number and morphology of microglia identified by their characteristic Iba1 immunoreactivity (Iba1^{+} cells), coupled with co-immunostaining with the phagosome marker, CD68. Reduced levels of primary branching have been associated with high levels of phagocytic activity (Ayata et al., 2018b). Microglial phagocytic activity can also be documented by the ratio of phagosome to soma volume (i.e., CD68^{+}/Iba1^{+} ratio). Among our findings, we detected no differences in the number of Iba1^{+} cells or the number of primary projections when comparing tissue sections from microglia$^{Bmal1\text{-KD}}$ and Ctrl, male and female mice, regardless of the dietary regimen (Fig. 2E-G, and Fig. S4C-K). Interestingly, the CD68^{+}/Iba1^{+} ratio varied in a time-dependent manner in male Ctrl mice, with a significant decrease observed at ZT17 when compared to ZT5 (Fig. 2H and I). This decrease was not detected in tissue sections from microglia$^{Bmal1\text{-KD}}$ mice, as the CD68^{+}/Iba1^{+} ratio remained high at both time points. Indeed, there was a significant increase in the CD68^{+}/Iba1^{+} ratio in microglia$^{Bmal1\text{-KD}}$ mice at ZT17 compared to results from Ctrl mice at this time point (Fig. 2H and I). Although no specific time-dependent regulation was observed in Ctrl female mice, a significantly higher CD68^{+}/Iba1^{+} ratio was detected in tissue sections from microglia$^{Bmal1\text{-KD}}$ female mice compared to Ctrls at ZT5 and to microglia$^{Bmal1\text{-KD}}$ mice at

ZT17 (Fig. S5A and B). Of note, the $CD68^+/Iba1^+$ ratio remained unchanged in all mice provided with a standard chow diet (Fig. S5E, F, I, and J). Taken together, these results suggest that the observed increase in $CD68^+$ phagosomes within the $Iba1^+$ microglia of microglia$^{Bmal1\text{-KD}}$ mice may represent a specific response to metabolic stress (e.g., the HFD). It is also critical to note that we detected no significant changes in phagosome or soma volume (Fig. S5C, D, G, H, K-N). The results obtained from microglia$^{Bmal1\text{-KD}}$ mice under HFD conditions are summarized in Table S1 and indicate that although the timing is different in male and female mice, the Bmal1-deficient microglia from both genders respond to the HFD with increased phagocytic capacity and thereby can affect more efficient clearance of the local microenvironment.

Increased microglial phagocytic capacity may prevent decrease of POMC-immunoreactive neurons

Results from a previous study revealed that consumption of a HFD resulted in increased apoptosis of hypothalamic neurons (Moraes et al., 2009). Therefore, we hypothesized that the increased phagocytic capacity observed in microglia from microglia$^{Bmal1\text{-KD}}$ mice may promote clearance of cellular debris, including DNA. To explore this issue, we performed a quantitative analysis of $CD68^+$ phagosomes within $Iba1^+$ microglial cells co-stained with 4',6-diamidino-2-phenylindole (DAPI) (Fig. S6A and B). However, we found no differences in the ratio of $CD68^+$ phagosomes that contained DNA fragments when comparing results from microglia$^{Bmal1\text{-KD}}$ and Ctrl mice of both sexes (Fig. S6C-D). Interestingly, $CD68^+$ phagosomes containing DAPI-stained DNA fragments were more prevalent in tissue sections from female mice (Fig. S6E). These results suggest that, when maintained on a HFD, female brain tissue was subject to higher levels of cellular apoptosis and/or has more effective global microglial phagocytic capacity than that in males.

The ARC includes a key population of anorexigenic POMC neurons that control food intake and body weight (Toda et al., 2017b). Defects of POMC expression cause severe obesity (Krude et al., 1998). Additionally, HFD has been shown to induce the loss of $POMC^+$ neurons (Thaler et al., 2012b; Yi et al., 2017b). Therefore, we investigated whether the disrupted microglial circadian rhythms and increased phagocytic activity would have a specific impact on $POMC^+$ neurons. We found that male microglia$^{Bmal1\text{-KD}}$ mice on a HFD had more $POMC^+$ neurons than did Ctrl mice on a HFD (Fig. 2J and K). A similar result was obtained in female mice (Fig. S7A and B). The larger number of $POMC^+$ neurons in the ARC of microglia$^{Bmal1\text{-KD}}$ mice on the HFD may contribute to diminished food intake and reduced body weight gain observed in these mice.

Microglia-specific deletion of Bmal1 results in improved long-term memory consolidation and retention

Microglia have the capacity to prune neuronal synapses, thereby establishing a mature connectivity pattern in the developing cortex and also in the adult hippocampus (Miyamoto et al., 2016a; Weinhard et al., 2018b). As such, we considered the possibility that microglia$^{Bmal1\text{-KD}}$ mice might experience different learning and memory behaviors when compared to Ctrls. We hypothesized that these differences might be most notable in experiments focusing on learning mechanisms that require synaptic rearrangements, such as memory consolidation (Squire et al., 2015). We evaluated hippocampus-dependent long-term memory formation and consolidation in microglia$^{Bmal1\text{-KD}}$ mice and Ctrls using several different protocols. It has been reported that the estrous cycle in female mice inevitably interferes with the spatial reference memory (Frick and Berger-Sweeney, 2001; ter Horst et al., 2012), thus in the hippocampus-related experiments we only evaluated male mice. First, we evaluated long-term memory using the novel object recognition (NOR) test. This test is based on the observation that rodents display a spontaneous preference for novelty and are likewise capable of recalling previously encountered objects. The mice in this study were provided with 10 min to explore two identical objects placed in the center of an open field. Recognition memory was tested one day later; specifically, mice were exposed to one familiar object (the same one as encountered on the previous day) and one novel object (Fig. 3A). Intriguingly, we found that the microglia$^{Bmal1\text{-KD}}$ mice spent more time interacting with the novel object than did the Ctrl mice. These results suggest that the microglia$^{Bmal1\text{-KD}}$ mice are capable of significantly stronger long-term retention of a familiar object (Fig. 3B). We then tested the mice in the Morris Water Maze (MWM), which is one of the most commonly used behavioral tests to test hippocampo-dependent memory. The MWM is used to evaluate different forms of spatial learning and memory in rodents, including consolidation, persistence, and reversal learning upon challenge with different protocols. For the MWM test, animals are placed in a pool filled with opaque water, and are provided with the opportunity to swim to a hidden escape platform placed in a target quadrant (TQ) which is located by relying upon outside environmental cues. After several days of acquisition training, the animals become more familiar with the task and the cues, and are thus able to locate the platform more quickly. A probe test is performed after completion of acquisition training. In this phase of testing, there is no platform in the pool; the time spent in the TQ provides the experimenter with an estimate of how effectively a given mouse can recall the original platform location. The first group of microglia$^{Bmal1\text{-KD}}$ and Ctrl mice were subjected to 4-days of acquisition training with a fixed platform location. This was followed by a probe test performed 24 hrs later which was designed as described to assess long-term retention (Fig. 3C). No

genotype-dependent differences were detected during the acquisition phase (Fig. 3D). Likewise, no differences between the mouse strains were detected with respect to measurements of latency (time required to locate the platform), swimming speed, or thigmotaxy (defined here as the time spent swimming along the border of the pool; Fig. S8A). Surprisingly, microglia$^{Bmal1\text{-KD}}$ mice revealed higher performance on the memory retention (probe) test than was observed among the Ctrl mice (Fig. 3E). These results suggest that microglia$^{Bmal1\text{-KD}}$ mice are capable of stronger long-term memory formation. The annulus crossing index, which represents the number of times the mice crossed over the platform in the TQ, was also superior in microglia$^{Bmal1\text{-KD}}$ mice compared to Ctrls (Fig. S8A). These results indicated that the microglia$^{Bmal1\text{-KD}}$ mice located the platform with a greater degree of precision.

A second group of mice was used to determine whether microglia-specific *Bmal1* knock-down would augment the memory consolidation process in mice subjected to a shorter or mild period of acquisition training. For these experiments, mice were provided with only 3 days of MWM acquisition training and were tested for memory retention at 15 days after the final training period (Fig. 3F). Under these conditions, Ctrl mice were unable to recall the correct location of the platform; this finding has been attributed to the limited extent of training associated with this protocol (Fig. 3H). However, microglia$^{Bmal1\text{-KD}}$ mice were able to locate the platform in the TQ more readily than the corresponding Ctrl mice provided with the same limited period of acquisition training (Fig. 3H). Microglia$^{Bmal1\text{-KD}}$ mice trained in this fashion also exhibited increased precision as demonstrated by the annulus crossing index (Fig. S8B). Distance, swimming speed, and thigmotaxy were not significantly different when comparing results from the two genotypes (Fig. 3G and Fig. S8B). Microglia$^{Bmal1\text{-KD}}$ mice displayed increased acquisition performance relative to Ctrl mice with respect to latencies measured at day 3 of training (Fig. S8B).

Fig. 3

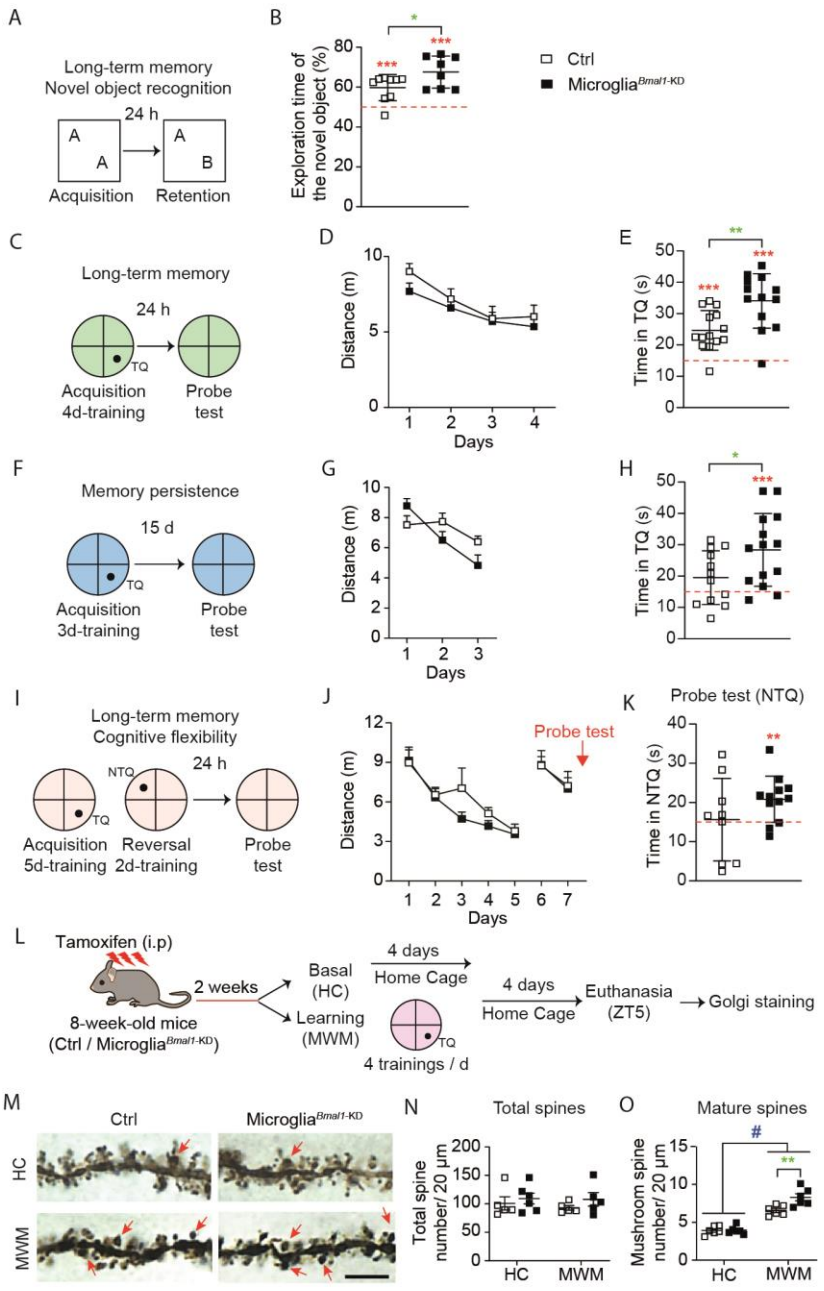

Figure. 3 Microglia$^{Bmal1\text{-}KD}$ mice exhibit improved long-term memory and more cognitive flexibility than Ctrl mice. (A) Experimental protocol and (**B**) performance in the novel object recognition (NOR) test.

Included were microglia$^{Bmal1\text{-KD}}$ (n = 8) and Ctrl (n = 9) mice. **(C)** Experimental protocol used to document long-term memory in the Morris Water Maze (MWM); TQ, Target Quadrant. **(D)** Distance required to reach the platform during each of the 4 days of acquisition training in the MWM. **(E)** Performance in the TQ during the probe test of microglia$^{Bmal1\text{-KD}}$ (n = 13) and Ctrl (n = 14) mice. **(F)** Experimental protocol used to document memory persistence. **(G)** Distance required to reach the platform during the 3 days of limited training. **(H)** Performance in the TQ during the probe test of microglia$^{Bmal1\text{-KD}}$ (n = 14) and Ctrl (n = 12) mice. **(I)** Experimental protocol used to document cognitive flexibility (reversal learning); NTQ, Novel Target Quadrant. **(J)** Distance required to reach the platform during the training. **(K)** Performance in NTQ during the probe test (9 Ctrl mice and 12 microglia$^{Bmal1\text{-KD}}$ mice). **(L)** Experimental protocol prior to Golgi staining. **(M)** Images of dendritic spines of hippocampal pyramidal neurons. Arrow, mushroom spines; scale bar, 5 µm. Quantification of (N) total spines and (O) mature spines per 20 µm segment (n = 5–6 mice per group). Total spines were evaluated in 24 segments from 4 cells per mouse; mature mushroom spines were evaluated in 48 segments from 6 cells per mouse.

Data are presented as means ± s.e.m. Green-colored * indicates a genotype effect; red-colored * indicates an effect *vs.* random (15s, red line); $^{\#}$ when home cage (HC) are compared to MWM-trained mice; $^{*}P < 0.05$, $^{**}P < 0.01$, $^{***}P < 0.001$, and $^{\#}P < 0.05$.

Microglia$^{Bmal1\text{-KD}}$ mice exhibit improved cognitive flexibility

As our initial results suggested improved memory performance as measured in several experimental conditions, we next determined whether microglia$^{Bmal1\text{-KD}}$ mice also exhibited increased perseverance or if they retained significant memory flexibility. These parameters were evaluated using a spatial reversal learning protocol. Mice were fully trained (5 days) in the MWM during which time each mouse memorized the fixed location of the platform in a TQ. The platform location was then changed to a new target quadrant (NTQ) within the same environment. Mice were then trained for an additional 2 days, and the time required to switch the new search strategy to locate the NTQ was determined. A probe test was performed 1 day later (Fig. 3I). We observed no significant differences with respect to distances traveled (Fig. 3J) or latencies associated with the platform location (Fig. S8C), regardless of its placement in the TQ or the NTQ. The microglia$^{Bmal1\text{-KD}}$ mice showed less thigmotaxy than did the Ctrl mice, a finding that may indicate reduced anxiety (Fig. S8C). We confirmed that both mouse strains displayed significant retention with respect to the TQ, with microglia$^{Bmal1\text{-KD}}$ mice exhibiting more precision during the intermediate probe trial (Fig. S8C). Importantly, in the reversal test, the microglia$^{Bmal1\text{-KD}}$ mice spent significantly more time in the NTQ than would be expected based on random events; this was not observed among the Ctrl mice (Fig. 3K). Further evaluation of specific strategies revealed that microglia$^{Bmal1\text{-KD}}$ mice had already initiated a

direct swimming approach to the NTQ during the final 3 trials carried out on day 1; likewise, their actions revealed no perseverance or persistent focus on the earlier TQ during the final 3 trials carried out on day 2. By contrast, Ctrl mice exhibited a somewhat less direct swimming strategy on day 1 and residual perseverance toward the original TQ at the final trials carried out on day 2 (Fig. S8C). As such, our findings indicate that microglia$^{Bmal1\text{-KD}}$ mice exhibit improved cognitive flexibility, as they were capable of more effective adaptation to new situations and challenges. Taken together, our results indicate that microglia-specific knockdown of *Bmal1* results in significant improvements in learning and memory processes in adult mice.

Structural plasticity, represented by the dynamic formation of dendritic spines and their stabilization over time in response to learning, is an important process associated with memory consolidation (Klein et al., 2019). As such, we performed a quantitative assessment of the different forms of dendritic spines in the CA1 pyramidal neurons of the hippocampus under basal conditions and during the consolidation processes associated with spatial memory (Fig. 3L). We used the Golgi staining method to identify dendritic spines; typical results are as shown in Fig. 3M. We detected no differences with respect to total spine numbers when comparing results from microglia$^{Bmal1\text{-KD}}$ mice to Ctrls. Specifically, we observed no differences between mice maintained in their home cages (HC; basal) and those subjected to the learning protocols (MWM; Fig. 3N). As previously observed in response to the MWM (Chatterjee et al., 2018), we detected significantly more mushroom-type spines, which are structures that are formed and stabilized by learning processes, in both genotypes at day 4 after completion of the spatial learning process (Fig. 3O). However, microglia$^{Bmal1\text{-KD}}$ mice displayed significantly larger numbers of mature spines per segment than did the Ctrl mice (Fig. 3O).

Increased microglial phagocytic capacity detected in response to learning in the hippocampal stratum radiatum of microglia$^{Bmal1\text{-KD}}$ mice

The findings from our study of microglia in the ARC suggested that their phagocytic capacity might increase in microglia$^{Bmal1\text{-KD}}$ mice in response to a functional brain challenge. As such, we next analyzed microglial number and morphology, together with the phagocytic marker, CD68, in different regions of the hippocampus in mice that underwent MWM training (MWM) and those that did not (HC). Hippocampal regions, including the stratum oriens, the stratum radiatum, and the lacunosum moleculare (CA1 region), as well as the dentate gyrus were examined at 12 h after completion of the training period; this is represented as ZT17 on the same day, during the active phase (i.e., lights off; Fig. S9 and Fig. S10). We also examined

responses at a 24 hrs after training, which is ZT5 during the day to follow, during sleeping phase, i.e., lights on; Fig. 4A and Fig. S10). Interestingly, MWM training resulted in an increase in microglial cell number and a decrease in microglial primary branches in both microglia$^{Bmal1\text{-KD}}$ and Ctrl mice compared with the mice at baseline (HC) at both ZT5 (Fig. 4B-D) and ZT17 (Fig. S9B-D). This pattern was observed in all CA1 sub-regions, but not in the dentate gyrus (Fig. S10B-I). Taken together, these results suggest that MWM training has a profound influence on microglial cells in the hippocampus. Remarkably, MWM training also induced a significant increase in CD68^{+}/Iba1^{+} volume ratio in both genotypes compared to findings from mice at baseline (HC). This response was notably higher in the microglia$^{Bmal1\text{-KD}}$ mice compared to Ctrls at ZT5 (Fig. 4E and F), but not at ZT17 (Fig. S10E and F), again suggesting that microglia may respond to spatial learning with an increase in microglial phagocytic capacity. The increased CD68^{+}/Iba1^{+} volume ratio most likely resulted from an increase in CD68 immunoreactivity that developed in response to MWM training with Iba1^{+} microglial soma volumes remaining unchanged (Fig. S10J and K). Intriguingly, these responses were not observed in either the hippocampal stratum oriens or in the lacunosum moleculare (Fig. S10L–S). These results indicate that microglial-mediated clearance activities may vary in different regions of the brain and also point to the apical dendrites of hippocampal CA1 pyramidal neurons as the main microglia targets associated with spatial learning. Together, these data indicate that MWM training promotes microglial phagocytic activity in the stratum radiatum of both Ctrl and microglia$^{Bmal1\text{-KD}}$ mice, and that this response is more pronounced in the latter strain.

Given that role of microglia in remodeling synapses involves phagocytosis of presynaptic structures, we performed experiments designed to assess levels of synaptophysin 1 within CD68^{+} microglial phagosomes. First, we found that MWM training had a global and significant impact on synaptophysin 1 levels, which were increased over baseline in both microglia$^{Bmal1\text{-KD}}$ and Ctrl mice at both ZTs (ZT5, Fig. 4G and H, and ZT17, Fig. S9G). Second, our evaluation of synaptophysin 1 content in microglia, presented as the synaptophysin 1^{+}/CD68^{+} volume ratio, revealed no differences among mice in the basal (HC) group. However, this ratio was significantly diminished in microglia from microglia$^{Bmal1\text{-KD}}$ mice compared to Ctrls at ZT5 after MWM training (Fig. 4I) while they did not differ at ZT17 (Fig. S9H). Taken together, these data indicate that while MWM training induced phagocytotic activity in microglia at ZT5, the presynaptic marker synaptophysin 1 was more prominently phagocytosed by the Ctrl than by the *Bmal1*-KD microglia at that time point.

Fig. 4

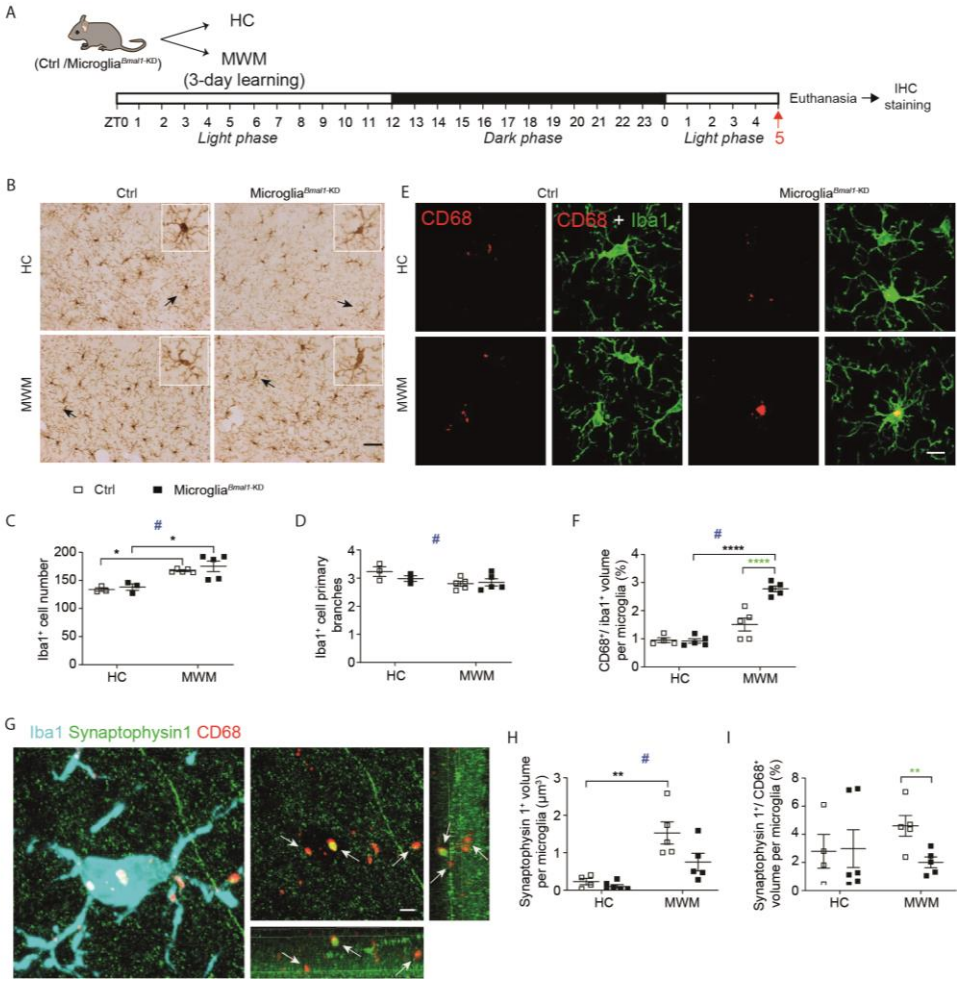

Figure. 4 Phagocytic capacity of microglia in the hippocampal stratum radiatum is increased after learning. (A) Experimental strategy. Mice underwent 3 days of training in the MWM (4 trials/ day on days 1, 2 and 3) and were sacrificed at ZT5 on day 4. **(B)** Microglial immune reactivity in hippocampal CA1 performed with Iba1 immunostaining. Scale bar, 100 µm. Arrows indicate the Iba1-positive cell shown enlarged in the box (upper right corner). Quantification of (**C**) Iba1^{+} microglial cells and (**D**) primary branches in the hippocampal CA1 regions of mice in control group (HC; n = 3 mice per group) and those subjected to MWM training (n = 4–5 mice per group). **(E)** Confocal images documenting anti-CD68 and anti-Iba1 immunostaining in the hippocampal stratum radiatum; scale bar, 10 µm. **(F)** Quantitative analysis of the volume percentage of CD68^{+} microglia identified in the hippocampal stratum radiatum

(HC, n = 4-5 mice per group; MWM, n = 5 mice per group; 100-125 cells were analyzed in each group). **(G)** Images documenting anti-Iba1, anti-synaptophysin 1, and anti-CD68 immunostaining within the hippocampal stratum radiatum. Arrows depict synaptophysin 1 and CD68 co-labeled phagosomes; scale bar, 3 µm. **(H)** Quantification of the volume represented by synaptophysin 1 in the CD68-positive phagosomes and (**I**) the ratio of synaptophysin 1^{+}/ $CD68^{+}$ volume per microglial cell in hippocampal stratum radiatum (HC, n = 4–6 mice per group; MWM, n = 5 mice per group).

Data are presented as means ± s.e.m. Green-colored * indicates a genotype effect; $^{\#}$control mice (HC) *vs*. those subjected to MWM training. $^{*}P < 0.05$, $^{**}P < 0.01$, $^{****}P < 0.0001$, and $^{\#}P < 0.05$.

Discussion

Microglia are brain macrophages that play important roles in regulating systemic energy homeostasis and cognition in rodent species. Microglial immune activity follows a circadian rhythm (Fonken et al., 2015a). As such, our study focused on the intrinsic circadian clock of microglia. Specifically, our experiments were designed to determine how cell-specific disruption of microglial circadian rhythmicity affects systemic energy homeostasis, learning, and memory processes in mice. Our findings demonstrate that microglia-specific knock-down of the clock gene *Bmal1*, promotes microglial phagocytosis in the hypothalamus in mice responding to HFD-induced metabolic stress and likewise in the hippocampus in response to learning and memory processes. As a result, mice with a microglia-specific Bmal1 deficiency exhibit decreased HFD-induced hyperphagia and body weight gain and also have an improved capacity for long-term memory consolidation and retention, while retaining cognitive flexibility.

First, we observed enhanced microglial phagocytosis in the ARC in association with a reduced loss of POMC-immunoreactivity and resistance to gain weight in response to HFD in both male and female microglia Bmal1-KD mice. Growing evidence from both human and rodent studies has revealed that HFD-induced obesity is associated with hypothalamic gliosis and microglial inflammation (Kalin et al., 2015). However, the role played by the microglial phagocytosis in this process has not been fully clarified. We recently reported that downregulation of microglial phagocytic capacity exerts a detrimental effect on the survival and function of surrounding $POMC^{+}$ neurons in the setting of a hypercaloric environment (Gao et al., 2017a). Our current data reveal that enhanced microglial phagocytic capacity may serve to prevent the reduction of $POMC^{+}$ neurons from the negative sequelae associated with a HFD. Interestingly, activation of POMC neurons results in decreased food intake and less body weight gain (Toda et al., 2017b). As such, our findings suggest that the circadian rhythm within the hypothalamic

microglia has a direct impact on its phagocytosis capacity and plays a critical role in regulating hypothalamic neural control of body weight.

Second, we observed enhanced microglial phagocytosis in the hippocampus in association with increased formation of mature dendritic spines and enhanced memory processes. In order to form long-term memory, synapses from engram cells are strengthened and new spines support additional interconnections between these cells. These two processes are believed to participate in memory storage (Hofer et al., 2009; Yang et al., 2009a). New stable dendritic spines of the mushroom-type are indeed produced in CA1 of rodents upon spatial learning in the MWM (Chatterjee et al., 2018; Klein et al., 2019). The consolidated engram may last for some time and, as circuits rewiring occurs in response to new experience and integration of newborn neurons (adult neurogenesis) (Frankland et al., 2013), the potentiated synapses may weaken over retention time leading to forgetting. Interestingly, it has recently been suggested that the synaptic elimination by microglial phagocytosis may result in normal forgetting (Wang et al., 2020a). It seems that weak synapses are tagged for removal in the adult network, a process previously demonstrated to occur during development to strengthen networks (Paolicelli et al., 2011a). Our results showing increased memory consolidation, retention, and flexibility in microglial Bmal1-KD mice are suggesting that microglial engulfing of weak synapses may be more efficient when microglial phagocytotic activity is acting “on-demand” rather than restricted by the circadian clock. Further, microglia were recently shown to have a facilitating role in synaptic circuit remodeling and maturation as they exert selective partial phagocytosis of presynaptic structures and could induce postsynaptic spine head filopodia (Weinhard et al., 2018b). Thus, our study evidencing that the presynaptic marker synaptophysin 1 is less engulfed into phagosomes of microglia$^{Bmal1\text{-KD}}$ mice than Ctrls 24h after the series of learning trials, suggests that Bmal1-KD microglia may better help in postsynaptic spine consolidation. This is emphasized by our result showing a significant increase of mushroom-type spines after learning in microglia$^{Bmal1\text{-KD}}$ mice. Yet, *Bmal1*-KD microglia may additionally better clean the environment of cellular debris and prevent inflammatory events to occur. Appropriate microglial phagocytic capacity is crucial for effective synaptic pruning and likewise for the formation of mature neural circuits.

Our results showed some sex differences in Bmal1-KD microglial clock gene expression. It is well known that the circadian system differs between the sexes and circadian clocks may be modulated by estrogen receptor signaling (Bailey and Silver, 2014; Hatcher et al., 2020; Nicolaides and Chrousos, 2020). The influence of gonadal hormones on the circadian system may also result in the differential expression of clock genes in male and female Bmal1-KD

microglia, but for now, the mechanism remains unknown. Moreover, recently it has been reported that in male rats the synaptic phagocytosis of microglia follows a circadian rhythm under physiological conditions (Choudhury et al., 2020b). Here we observed that in both genders Bmal1-KD microglia exhibit increased phagocytosis, indicated by CD68 immunoreactivity, during HFD feeding, but with different timing for males and females. This difference may be caused by the sex different clock gene expression in Bmal1-KD microglia. We further explored phagocytosis of DNA debris in hypothalamic microglia after several weeks on a HFD. As shown, no significant differences were found when comparing Bmal1-deficient microglia to those from Ctrl mice. However, we did detect more DNA fragment-containing phagosomes in microglia from females, as opposed to male mice. This finding suggests that HFD-induced neuronal loss may be sex-dependent.

However, microglial phagocytic capacity also depends on specific neuronal activity and the rate of neuronal attrition (Ayata et al., 2018b). Neural circuits involved in responses to challenges such as HFD-induced metabolic stress or learning tasks require microglial phagocytosis "on-demand". As such, suppression of the rigorous control provided by the circadian clock may have a beneficial impact on microglial function. In this study, microglia-specific knock-down of Bmal1 promoted increased microglial phagocytosis likely producing a healthier micro-environment for neighboring neurons in the hypothalamus and hippocampus. Deficiency of microglial Bmal1 ultimately protected mice from HFD-induced obesity and increased memory performance. Interestingly, the beneficial impact of this loss-of-function perfectly fits with recent findings reported for global Bmal1 knockout mice, in which both locomotor activity and insulin sensitivity were found to adapt more readily to disrupted light/dark schedules compared to the responses of these pathways in *Bmal1*-sufficient controls (Yang et al., 2019). Furthermore, in the respiratory tract, *Bmal1*-deficiency has been associated with increased phagocytic function and enhanced macrophage-mediated antibacterial immunity (Kitchen et al., 2020b). Clearly, when behavioral rhythms are disrupted it may be beneficial for optimal health that microglial activity is controlled less strictly by its internal clock.

Microglia express both Bmal1 and pro-inflammatory cytokines at comparatively high levels during the light phase (Fonken et al., 2015a). Of note, previously we showed that microglia-specific *Bmal1* deficiency reduced inflammation-related gene expression *in vivo* (Wang et al., 2020b), whereas LPS-induced IL6 up-regulation was found reduced in absence of microglial Bmal1 (Nakazato et al., 2017). Activated microglia undergo polarization toward pro-inflammatory or anti-inflammatory phenotypes (Orihuela et al., 2016). As such, our findings, including decreased inflammation (Wang et al., 2020b) and increased phagocytic

capacity, suggest that Bmal1-deficient microglia tend to become polarized toward an anti-inflammatory state. Future work will be required to identify mechanisms linking Bmal1 and microglial-mediated phagocytosis.

Microglial phagocytosis differs in distinct regions of the brain (Ayata et al., 2018b). However, in microglia$^{Bmal1\text{-KD}}$ mice, a circadian rhythm persisted as food intake, RER, locomotor activity, and heat production were not globally changed. This suggests that the microglia-specific deficiency of Bmal1 does not have a direct impact on the central pacemaker in the suprachiasmatic nucleus. We conclude that phagocytosis increases in Bmal1-deficient microglia localized specifically within the hypothalamic ARC and hippocampal stratum radiatum as an "on-demand" response to external challenges such as HFD-induced metabolic stress and learning trainings, respectively. The observed increase in phagocytosis may have a beneficial impact on microglial control of energy balance and cognition, which is reminiscent of psychiatric treatment. Together, these findings indicate that agents that target the molecular clock-Bmal1 in microglial cells might be developed as a novel means to treat both metabolic and cognitive disorders.

Acknowledgments

We thank PHENOMIN-ICS, Institut Clinique de la souris (frame program Investissements d'Avenir, ANR-10-INSB-07-PHENOMIN) (Strasbourg, France), for performing metabolic phenotype experiment in the Phenomaster system and collecting data. We would like to thank Cristina Sandu, Marie-Paule Felder-Schmittbuhl (Institute of Cellular and Integrative Neurosciences, CNRS, Université de Strasbourg, Strasbourg, France) and people from Luc Dupuis laboratory (Université de Strasbourg, INSERM, UMR-S1118, Strasbourg, France) for helping with primary microglia cultures. **Funding:** This project was supported by "NeuroTime" Erasmus Mundus program, with support from the NeuroTime Erasmus+ program of the European Commission. This project has been funded by Centre National de la Recherche Scientifique, the University of Strasbourg and ANR-18-CE16-0008 (to A.L.B), and De Nederlandse organisatie voor gezondheidsonderzoek en zorginnovatie (ZonMw 459001004 to C.X.Y). **Author contributions:** X.L.W., A.L.B., C.X.Y. designed the experiments. X.L.W. performed the experiments. S.K. contributed the C57BL/6J mice and guided experimentation. L.T. contributed to the transgenic mice's brain collection, behavior experiment, animal caring, data analysis. B.C. contributed to the transgenic mice' tamoxifen injection, brain collection, body weight monitoring, and immunohistochemistry. Y.G, I.M., S.E.C.W., N.K. contributed to the microglial isolation and tissue collection. M. F.C., B.P.D., G.D.C.I., T.S.G. performed

metabolic phenotype experiments in the Phenomaster system and collected data. A.L.B., C.X.Y supervised the work. X.L.W., A.L.B., C.X.Y. wrote the manuscript. A.K., J.C.C. edited the manuscript. All the authors discussed the results and contributed to the manuscript.

References

Ayata, P., Badimon, A., Strasburger, H.J., Duff, M.K., Montgomery, S.E., Loh, Y.H.E., Ebert, A., Pimenova, A.A., Ramirez, B.R., Chan, A.T*., et al.* (2018). Epigenetic regulation of brain region-specific microglia clearance activity. Nature Neuroscience *21*, 1049-+.

Bailey, M., and Silver, R. (2014). Sex differences in circadian timing systems: Implications for disease. Front Neuroendocrin *35*, 111-139.

Barca-Mayo, O., Pons-Espinal, M., Follert, P., Armirotti, A., Berdondini, L., and De Pietri Tonelli, D. (2017). Astrocyte deletion of Bmal1 alters daily locomotor activity and cognitive functions via GABA signalling. Nat Commun *8*, 14336.

Bass, J., and Takahashi, J.S. (2010). Circadian integration of metabolism and energetics. Science *330*, 1349-1354.

Bunger, M.K., Wilsbacher, L.D., Moran, S.M., Clendenin, C., Radcliffe, L.A., Hogenesch, J.B., Simon, M.C., Takahashi, J.S., and Bradfield, C.A. (2000). Mop3 is an essential component of the master circadian pacemaker in mammals. Cell *103*, 1009-1017.

Chatterjee, S., Cassel, R., Schneider-Anthony, A., Merienne, K., Cosquer, B., Tzeplaeff, L., Sinha, S.H., Kumar, M., Chaturbedy, P., Eswaramoorthy, M*., et al.* (2018). Reinstating plasticity and memory in a tauopathy mouse model with an acetyltransferase activator. Embo Molecular Medicine *10*.

Choudhury, M.E., Miyanishi, K., Takeda, H., Islam, A., Matsuoka, N., Kubo, M., Matsumoto, S., Kunieda, T., Nomoto, M., Yano, H*., et al.* (2020). Phagocytic elimination of synapses by microglia during sleep. Glia *68*, 44-52.

Colonna, M., and Butovsky, O. (2017). Microglia Function in the Central Nervous System During Health and Neurodegeneration. Annu Rev Immunol *35*, 441-468.

Dorfman, M.D., Krull, J.E., Douglass, J.D., Fasnacht, R., Lara-Lince, F., Meek, T.H., Shi, X., Damian, V., Nguyen, H.T., Matsen, M.E*., et al.* (2017). Sex differences in microglial CX3CR1 signalling determine obesity susceptibility in mice. Nat Commun *8*, 14556.

Dudek, M., and Meng, Q.J. (2014). Running on time: the role of circadian clocks in the musculoskeletal system. Biochem J *463*, 1-8.

Fonken, L.K., Frank, M.G., Kitt, M.M., Barrientos, R.M., Watkins, L.R., and Maier, S.F. (2015). Microglia inflammatory responses are controlled by an intrinsic circadian clock. Brain Behav Immun *45*, 171-179.

Frankland, P.W., Kohler, S., and Josselyn, S.A. (2013). Hippocampal neurogenesis and forgetting. Trends Neurosci *36*, 497-503.

Frick, K.M., and Berger-Sweeney, J. (2001). Spatial reference memory and neocortical neurochemistry vary with the estrous cycle in C57BL/6 mice. Behavioral Neuroscience *115*, 229-237.

Gabriel, B.M., and Zierath, J.R. (2019). Circadian rhythms and exercise - re-setting the clock in metabolic disease. Nat Rev Endocrinol *15*, 197-206.

Gao, Y., Vidal-Itriago, A., Kalsbeek, M.J., Layritz, C., Garcia-Caceres, C., Tom, R.Z., Eichmann, T.O., Vaz, F.M., Houtkooper, R.H., van der Wel, N.*, et al.* (2017). Lipoprotein Lipase Maintains Microglial Innate Immunity in Obesity. Cell Rep *20*, 3034-3042.

Gao, Y., Vidal-Itriago, A., Milanova, I., Korpel, N.L., Kalsbeek, M.J., Tom, R.Z., Kalsbeek, A., Hofmann, S.M., and Yi, C.-X. (2018). Deficiency of leptin receptor in myeloid cells disrupts hypothalamic metabolic circuits and causes body weight increase. Molecular Metabolism *7*, 155-160.

Gekakis, N., Staknis, D., Nguyen, H.B., Davis, F.C., Wilsbacher, L.D., King, D.P., Takahashi, J.S., and Weitz, C.J. (1998). Role of the CLOCK protein in the mammalian circadian mechanism. Science *280*, 1564-1569.

Gerstner, J.R., and Yin, J.C. (2010). Circadian rhythms and memory formation. Nat Rev Neurosci *11*, 577-588.

Hasegawa, S., Fukushima, H., Hosoda, H., Serita, T., Ishikawa, R., Rokukawa, T., Kawahara-Miki, R., Zhang, Y., Ohta, M., Okada, S.*, et al.* (2019). Hippocampal clock regulates memory retrieval via Dopamine and PKA-induced GluA1 phosphorylation. Nat Commun *10*, 5766.

Hatcher, K.M., Royston, S.E., and Mahoney, M.M. (2020). Modulation of circadian rhythms through estrogen receptor signaling. European Journal of Neuroscience *51*, 217-228.

Hofer, S.B., Mrsic-Flogel, T.D., Bonhoeffer, T., and Hubener, M. (2009). Experience leaves a lasting structural trace in cortical circuits. Nature *457*, 313-317.

Hogenboom, R., Kalsbeek, M.J., Korpel, N.L., de Goede, P., Koenen, M., Buijs, R.M., Romijn, J.A., Swaab, D.F., Kalsbeek, A., and Yi, C.X. (2019). Loss of arginine vasopressin- and vasoactive intestinal

polypeptide-containing neurons and glial cells in the suprachiasmatic nucleus of individuals with type 2 diabetes. Diabetologia *62*, 2088-2093.

Kalin, S., Heppner, F.L., Bechmann, I., Prinz, M., Tschop, M.H., and Yi, C.X. (2015). Hypothalamic innate immune reaction in obesity. Nat Rev Endocrinol *11*, 339-351.

Kitchen, G.B., Cunningham, P.S., Poolman, T.M., Iqbal, M., Maidstone, R., Baxter, M., Bagnall, J., Begley, N., Saer, B., Hussell, T.*, et al.* (2020). The clock gene Bmal1 inhibits macrophage motility, phagocytosis, and impairs defense against pneumonia. Proc Natl Acad Sci U S A *117*, 1543-1551.

Klein, M.M., Cholvin, T., Cosquer, B., Salvadori, A., Le Mero, J., Kourouma, L., Boutillier, A.L., de Vasconcelos, a.p., and Cassel, J.C. (2019). Ventral midline thalamus lesion prevents persistence of new (learning-triggered) hippocampal spines, delayed neocortical spinogenesis, and spatial memory durability. Brain Structure & Function *224*, 1659-1676.

Krude, H., Biebermann, H., Luck, W., Horn, R., Brabant, G., and Gruters, A. (1998). Severe early-onset obesity, adrenal insufficiency and red hair pigmentation caused by POMC mutations in humans. Nature Genetics *19*, 155-157.

Lee, J.Y., Hall, J.A., Kroehling, L., Wu, L., Najar, T., Nguyen, H.H., Lin, W.Y., Yeung, S.T., Silva, H.M., Li, D.Y.*, et al.* (2020). Serum Amyloid A Proteins Induce Pathogenic Th17 Cells and Promote Inflammatory Disease. Cell *180*, 79-+.

Man, K., Loudon, A., and Chawla, A. (2016). Immunity around the clock. Science *354*, 999-1003.

Milanova, I.V., Kalsbeek, M.J.T., Wang, X.L., Korpel, N.L., Stenvers, D.J., Wolff, S.E.C., de Goede, P., Heijboer, A.C., Fliers, E., la Fleur, S.E.*, et al.* (2019). Diet-Induced Obesity Disturbs Microglial Immunometabolism in a Time-of-Day Manner. Frontiers in Endocrinology *10*.

Miyamoto, A., Wake, H., Ishikawa, A.W., Eto, K., Shibata, K., Murakoshi, H., Koizumi, S., Moorhouse, A.J., Yoshimura, Y., and Nabekura, J. (2016). Microglia contact induces synapse formation in developing somatosensory cortex. Nature Communications *7*.

Moraes, J.C., Coope, A., Morari, J., Cintra, D.E., Roman, E.A., Pauli, J.R., Romanatto, T., Carvalheira, J.B., Oliveira, A.L., Saad, M.J.*, et al.* (2009). High-fat diet induces apoptosis of hypothalamic neurons. PLoS One *4*, e5045.

Morton, G.J., Cummings, D.E., Baskin, D.G., Barsh, G.S., and Schwartz, M.W. (2006). Central nervous system control of food intake and body weight. Nature *443*, 289-295.

Musiek, E.S., Lim, M.M., Yang, G.R., Bauer, A.Q., Oi, L., Lee, Y., Roh, J.H., Ortiz-Gonzalez, X., Dearborn, J.T., Culver, J.P*., et al.* (2013). Circadian clock proteins regulate neuronal redox homeostasis and neurodegeneration. Journal of Clinical Investigation *123*, 5389-5400.

Nakazato, R., Hotta, S., Yamada, D., Kou, M., Nakamura, S., Takahata, Y., Tei, H., Numano, R., Hida, A., Shimba, S*., et al.* (2017). The intrinsic microglial clock system regulates interleukin-6 expression. Glia *65*, 198-208.

Nicolaides, N.C., and Chrousos, G.P. (2020). Sex differences in circadian endocrine rhythms: Clinical implications. European Journal of Neuroscience *52*, 2575-2585.

Nimmerjahn, A., Kirchhoff, F., and Helmchen, F. (2005). Resting microglial cells are highly dynamic surveillants of brain parenchyma in vivo. Science *308*, 1314-1318.

Orihuela, R., McPherson, C.A., and Harry, G.J. (2016). Microglial M1/M2 polarization and metabolic states. Br J Pharmacol *173*, 649-665.

Paolicelli, R.C., Bolasco, G., Pagani, F., Maggi, L., Scianni, M., Panzanelli, P., Giustetto, M., Ferreira, T.A., Guiducci, E., Dumas, L*., et al.* (2011). Synaptic Pruning by Microglia Is Necessary for Normal Brain Development. Science *333*, 1456-1458.

Parkhurst, C.N., Yang, G., Ninan, I., Savas, J.N., Yates, J.R., Lafaille, J.J., Hempstead, B.L., Littman, D.R., and Gan, W.B. (2013). Microglia Promote Learning-Dependent Synapse Formation through Brain-Derived Neurotrophic Factor. Cell *155*, 1596-1609.

Rahman, S.A., Castanon-Cervantes, O., Scheer, F.A., Shea, S.A., Czeisler, C.A., Davidson, A.J., and Lockley, S.W. (2015). Endogenous circadian regulation of pro-inflammatory cytokines and chemokines in the presence of bacterial lipopolysaccharide in humans. Brain Behav Immun *47*, 4-13.

Schiaffino, S., Blaauw, B., and Dyar, K.A. (2016). The functional significance of the skeletal muscle clock: lessons from Bmal1 knockout models. Skelet Muscle *6*, 33.

Squire, L.R., Genzel, L., Wixted, J.T., and Morris, R.G. (2015). Memory Consolidation. Csh Perspect Biol *7*.

Storch, K.F., Paz, C., Signorovitch, J., Raviola, E., Pawlyk, B., Li, T., and Weitz, C.J. (2007). Intrinsic circadian clock of the mammalian retina: Importance for retinal processing of visual information. Cell *130*, 730-741.

ter Horst, J., de Kloet, E.R., Schachinger, H., and Oitzl, M.S. (2012). Relevance of Stress and Female Sex Hormones for Emotion and Cognition. Cellular and Molecular Neurobiology *32*, 725-735.

Thaler, J.P., Yi, C.X., Schur, E.A., Guyenet, S.J., Hwang, B.H., Dietrich, M.O., Zhao, X.L., Sarruf, D.A., Izgur, V., Maravilla, K.R*., et al.* (2012). Obesity is associated with hypothalamic injury in rodents and humans. Journal of Clinical Investigation *122*, 153-162.

Toda, C., Santoro, A., Kim, J.D., and Diano, S. (2017). POMC Neurons: From Birth to Death. Annual Review of Physiology, Vol 79 *79*, 209-236.

Wang, C., Yue, H., Hu, Z., Shen, Y., Ma, J., Li, J., Wang, X.D., Wang, L., Sun, B., Shi, P*., et al.* (2020a). Microglia mediate forgetting via complement-dependent synaptic elimination. Science *367*, 688-694.

Wang, X.L., Wolff, S.E.C., Korpel, N., Milanova, I., Sandu, C., Rensen, P.C.N., Kooijman, S., Cassel, J.C., Kalsbeek, A., Boutillier, A.L*., et al.* (2020b). Deficiency of the Circadian Clock Gene Bmal1 Reduces Microglial Immunometabolism. Frontiers in Immunology *11*.

Weinhard, L., di Bartolomei, G., Bolasco, G., Machado, P., Schieber, N.L., Neniskyte, U., Exiga, M., Vadisiute, A., Raggioli, A., Schertel, A*., et al.* (2018). Microglia remodel synapses by presynaptic trogocytosis and spine head filopodia induction. Nature Communications *9*.

Yang, G., Chen, L., Zhang, J., Ren, B., and FitzGerald, G.A. (2019). Bmal1 deletion in mice facilitates adaptation to disrupted light/dark conditions. JCI Insight *5*.

Yang, G., Pan, F., and Gan, W.B. (2009). Stably maintained dendritic spines are associated with lifelong memories. Nature *462*, 920-924.

Yi, C.X., Walter, M., Gao, Y., Pitra, S., Legutko, B., Kalin, S., Layritz, C., Garcia-Caceres, C., Bielohuby, M., Bidlingmaier, M*., et al.* (2017a). TNFalpha drives mitochondrial stress in POMC neurons in obesity. Nat Commun *8*, 15143.

Yi, C.X., Walter, M., Gao, Y.Q., Pitra, S., Legutko, B., Kalin, S., Layritz, C., Garcia-Caceres, C., Bielohuby, M., Bidlingmaier, M*., et al.* (2017b). TNF alpha drives mitochondrial stress in POMC neurons in obesity. Nature Communications *8*.

Zhan, Y., Paolicelli, R.C., Sforazzini, F., Weinhard, L., Bolasco, G., Pagani, F., Vyssotski, A.L., Bifone, A., Gozzi, A., Ragozzino, D*., et al.* (2014). Deficient neuron-microglia signaling results in impaired functional brain connectivity and social behavior. Nat Neurosci *17*, 400-406.

Supplemental Information

Supplemental Materials and Methods

Animals

Both microglia$^{Bmal1\text{-KD}}$ and Ctrl mice were injected with tamoxifen as noted above. Genotyping of *Bmal1*$^{lox/lox}$ and *Cx3cr1*^{CreER} was performed by polymerase chain reaction (PCR) using the following primers: *Bmal1*$^{lox/lox}$ primers, 5'– ACT GGA AGT AAC TTT ATC AAA CTG – 3' and 5'– CTG ACC AAC TTG CTA ACA ATT A – 3'; *Cx3cr1*^{CreER} primers, 5'– AAG ACT CAC GTG GAC CTG CT – 3', 5'– CGG TTA TTC AAC TTG CAC CA – 3', and 5' – AGG ATG TTG ACT TCC GAG TTG – 3'. Mice were housed in a temperature (22 ± 1°C) and humidity (55 ± 5%) controlled room under a 12 h light/dark cycle (lights on at 07:00 h, Zeitgeber Time 0 [ZT0]), with free access to food and water. Mice were fed a standard chow (Mucedola Srl, Settimo Milanese, Italy, cat. no. 4RF21). Both male and female mice were used for the metabolic phenotype study, while only male mice were used in the Morris Water Maze (MWM) and New Object Recognition (NOR) protocols. All tests are routinely used in our laboratory and sample size was decided based on our previous studies (Chatterjee et al., 2018; Gao et al., 2017b). Animals were randomly assigned to experimental groups. Experimental and animal care protocols were in compliance with the institutional guidelines (national and international laws and policies: directive 2010/63/UE, February 13, 2013, European Community). Our project has been reviewed and approved by the national and regional ethics committee, France (APAFIS#6822-2016092118336690v3 and APAFIS#9631-201801251042855 v1). For Figure 1 microglia were isolated from 10-week-old male wild-type (C57BL/6J) mice that were killed every 3 h beginning at ZT0. This study was approved by and performed according to the guidelines of the Institutional Animal Care and Use Committee of the Netherlands (Leiden, The Netherlands).

Indirect calorimetry

Mice were housed individually in TSE cages for 48 hrs; this period included a 24 hrs period for habituation and another 24 hrs for the measurement of energy expenditure. Oxygen consumption (VO_2) and carbon dioxide production (VCO_2) were measured every hour during this 24 hrs period to calculate RER using the formula RER = VCO_2/VO_2, which defines fuel preference (glucose *vs.* lipid metabolism). Heat production was calculated using the formula Heat = [3.941(VO_2) + 1.106(VCO_2)] x 1.44. Physical activity, which is a component of whole energy expenditure, was also recorded. These experiments were performed at the French

National Infrastructure for Mouse Phenogenomics (PHENOMIN) and received an ethical authorization by the French Ministry of Research, in compliance with the European Community regulation for laboratory animal care and use (Directive 2010/63/UE).

Morris Water Maze (MWM) Task

Acquisition phase Mice were placed in a circular pool (150 cm diameter) filled with opaque water at 20 ± 1°C in an experimental room that contained cues and paintings on the walls. The platform (10 cm diameter) was positioned in the southeast (SE) quadrant of the pool at 1 cm below the water surface. Mice were first subjected to a 1-day habituation trial with a visible platform; this was followed by 3, 4, or 5 days of acquisition training (4 trials/day) with a hidden platform. For each trial, the mouse was placed at the edge of the pool at a different, random starting position and provided with a maximum of 60 s to reach the submerged platform. Upon reaching the platform, the mouse was left in place for 10 s prior to initiating another round via placement at the next starting point. If a mouse failed to locate the platform within 60 s, it was gently guided to it by the experimenter and was permitted to remain in place for 10 s. A mouse would be excluded if it was floating more than 50% of the time in the pool.

Probe trial. All mice were tested for memory retention in the probe trial which was administered at 24 hrs and 15 days after the final acquisition trial as described above. For this test, the platform was removed, and all mice were released from the center of the pool. Responses were evaluated after 60 s of swimming.

Reversal phase. After 5 days of acquisition training (4 trials/day) with the platform in the SE position, mice were trained for another 2 days (4 trials/day) with the platform moved to the opposite (i.e., northwest [NW]) quadrant. During reversal training, the mouse was placed at the edge of the pool at different, random starting positions and provided with a maximum of 60 s to reach the submerged platform. Upon reaching the platform, the mouse was left in place for 10 s prior to initiating another round via placement at the next starting point. If a mouse failed to find the platform within 60 s, it was moved to its home cage by the experimenter. A probe trial as described above was performed on day 8 at 24 hrs after the final reversal training trial.

Parameters were recorded using a video-tracking system (ANY-maze, Ugo Basile, Italy). The experimenter was blinded with respect to mouse genotype. Swim path, swim speed, latency, and distance covered to reach the platform were measured during the acquisition trial. Time spent in each of the four quadrants and the number of platform crossings were recorded and

calculated for the probe trial. We addressed learning behavior during acquisition together with the different retention times with respect to the MWM test as well as cognitive flexibility during reversal training.

Novel Object Recognition (NOR) test

Mice were habituated to a 52 x 52 x 52 cm box with three different components: familiarization, acquisition, and retention phases. On day 1, mice were subjected individually to a single 10-minute familiarization session. During this time, each mouse was introduced to the empty arena and was permitted to become familiar with the apparatus. On day 2, each mouse was subjected to a single 15-minute habituation session, during which time two same objects (A1 and A2) were placed in symmetrically with respect to the center of the arena. Mice were returned to their home cages for 24 hrs, and then re-introduced to the arena where they were exposed to one familiar (A) and one new object (B) that were placed at the same locations as were the sample stimuli. Mice were provided with a 10-minute period to explore the objects. Exploration was defined as sniffing or touching the objects with the nose and/or forepaws. The arena and all objects were cleaned with 70% ethanol between each session to ensure the absence of olfactory cues. All training and testing sessions were digitally recorded (TopScan, CleverSys, Inc., Reston, VA, USA) and analyzed by the experimenter who was blinded to the mouse genotype. Behavioral experiments were performed only once with each mouse. All experimental groups were fully independent of one another.

Labeling and counting dendritic spines after Golgi staining

Mice subjected to 4-day training in the MWM were sacrificed at day 4 after the final training period. The Rapid Golgi stain kit (FD Neurotechnologies, Inc., Columbia, MD, USA) was used according to the manufacturer's instructions. One hundred μm thick coronal sections containing the hippocampal region CA1 were cut using a Vibratome (VT1000M, Leica Biosystems, Buffalo Grove, IL, USA). Integrated neuronal fragments are chosen for spine counting and spines are analyzed manually using a bright-field microscope equipped with an automated motorized stage and MorphoStrider software (Explora Nova, La Rochelle, France). Thus, morphologies of spines are dynamically identified one by one, in regard to its shape throughout the z-axis, according to the size of the spine head and length of the spine neck. For each hemisphere, three neurons are chosen in the counting window. To-be-analyzed neurons are selected under the light-transmission microscope using low magnification. A neuron has to respond to three criteria to be selected for quantification, as in Restivo et al. (2009) (Restivo et al., 2009): 1) the dendrite had to be untruncated, 2) staining and impregnation had to be

homogenous along with the entire extent of the dendrite, and 3) neurons had to be easily discernible and relatively well isolated from neighboring impregnated cells. Measurements are performed on apical and basal dendrites in each region, at least 50 µm away from the soma for the apical dendrites, and at least 30 µm away for the basal dendrites, on secondary and tertiary branches. These distances allow us to exclude dendritic segments near the soma that are essentially devoid of spines. For each neuron, 20-µm long segments are randomly selected on apical and basal dendrites within a distance of at most 100 µm from the limit of the exclusion zone. Counting is performed under a 1000 × magnification using an oil immersion objective. Spines are counted blind to the experimental conditions. For quantification of total spines, 24 dendritic segments (20 µm) were analyzed (4 cells per mouse, n = 6 mice per group). For quantification of mushroom spines, 48 dendritic segments were analyzed (6 cells per mouse, n = 6 mice per group).

Isolation of microglia from brain tissue of adult mice

Three weeks after the tamoxifen injections, mice were decapitated for extraction of brain tissue. Brain tissue was gently hand-homogenized in Roswell Park Memorial Institute (RPMI) 1640 medium (Gibco, Gaithersburg, MD, USA; cat. no. 11875093) and filtered through a 70 µm cell strainer (Corning, Inc., Corning, NY, USA; cat. no. 431751). After 5 min centrifugation at 380 x *g* at 4 °C, cells were re-suspended in 7 ml RPMI 1640 medium and mixed with 3 ml stock isotonic Percoll (SIP) solution (1 part 10X Hank's buffered saline solution [10X HBSS; Gibco, cat. no. 14185052] with 9 parts Percoll plus [Sigma-Aldrich, St. Louis, MO, USA, cat no. GE17-5445-01]). The cell suspension was layered slowly on top of 2 ml of a 70% Percoll solution (3 parts of HBSS (Gibco, cat. no. 14170112) with 7 parts SIP in a fresh 15 ml Falcon tube and centrifuged at 500 x *g* for 30 min at 18 °C, with minimal acceleration and breaking. After centrifugation, material that collected in the interphase was transferred into a fresh 15 ml Falcon tube, diluted with 8 ml HBSS, and centrifuged at 500 x *g* for 7 min. The supernatant was then discarded and isolated microglia were incubated with anti-mouse CD11b antibody-conjugated magnetic microbeads (Miltenyi Biotec, Bergisch Gladbach, Germany, cat. no. 130-093-634) for 15 min at 4°C. The $CD11b^+$ microglia were isolated using a MACS Column (Miltenyi Biotec, cat. no. 130-042-201) with an applied magnetic field. Microglial cells were collected for RNA isolation and protein extraction.

RNA isolation from isolated microglia and quantitative reverse-transcription polymerase chain reaction (qPCR)

Total RNA was isolated from freshly-isolated microglia using an RNeasy Micro Kit (QIAGEN, Hilden, Germany, cat. no. 74004) following the manufacturer's recommendations. We used 150 ng of microglial RNA to generate cDNA with a Transcriptor First Strand cDNA Synthesis Kit (Roche, Basel, Switzerland, cat. no. 04897030001) following the manufacturer's recommendations. Quantitative PCR (qPCR) was performed using a SensiFAST™ SYBR® No-ROX Kit (Roche Bioline, cat. no. BIO-98020). Data were analyzed by LC480 Conversion and LinRegPCR software with normalization to expression levels of the housekeeping gene, hypoxanthine phosphoribosyltransferase 1 (HPRT1).

Western blot analyses

Isolated microglial cells were homogenized in Laemmli buffer and sonicated twice for 10 s (ultrasonic processor, with power at 40%) followed by heating at 70°C for 10 min and then at 100°C for 5 min. Lysates were centrifuged at 14,000 x *g* for 5 min and supernatants were used for Western blot analyses. Proteins were loaded on Midi-PROTEAN TGX Stain-Free™ Precast Gels (4–20%, Bio-Rad, Hercules, CA, USA) and electrotransferred onto a nitrocellulose membrane. Primary antibodies used to probe Western blots included rabbit anti-Bmal1 (1:500 dilution, Novus Biologicals, Littleton, CA, USA, cat. no. NB100-2288) and rabbit anti-histone H3 (1:1000 dilution, Abcam, Cambridge, UK, cat. no. ab1791). Horseradish peroxidase-conjugated anti-rabbit Ig (1:5000 dilution, Jackson ImmunoResearch, West Grove, PA, USA) was used as the secondary antibody. Immunoreactive bands were detected with ECL (Clarity, Bio-Rad) using a ChemiDoc Touch system (Bio-Rad). Results were quantified using ImageLab software.

Primary microglial culture and phagocytosis assay

Primary microglial cells were prepared as described previously (Wang et al., 2020b). Briefly, brain tissues were isolated from P1-P3 microglia$^{Bmal1\text{-KD}}$ and littermate Ctrl mice, the meninges and blood vessels were removed, the parenchyma was cut into smaller pieces, and dissociated in Trypsin-EDTA solution (T4049, Sigma) at 37 °C for 8 min. Cell suspension went through 70 μm cell strainer (431751, Corning) twice and seeded in DMEM/F12 (10565018, Gibco), containing 10% FBS, 100 μg/ml penicillin-streptomycin, 5 ng/ml M-CSF (SRP3221, Sigma). Six to ten days later, the flasks were shaken (200 rpm) for 1 hr to release microglia and harvested microglia were cultured on coverslips in medium without M-CSF. Microglial cells isolated from microglia$^{Bmal1\text{-KD}}$ mice were treated with 5 μM of 4-hydroxytamoxifen (SML1666-1ML, Sigma) for 48 hrs to induce Cre-LoxP recombination and excise Bmal1, while cells isolated from Ctrl mice were treated with same volume of vehicle (DMSO). Next, microglia were synchronized with 100 nM dexamethasone (D1756, Sigma) for 2 hrs, washed with PBS for further treatment.

Fluoresbrite® Polychromatic Red Microspheres (1.0 µm, 18660-5, polysciences) were coated with 10% FBS at 37 °C for 1 hr, followed by centrifugation (12,000 rpm, 2 min) and resuspension in PBS. Coated microspheres were added to the synchronized primary microglial cells (100 microspheres per cell), and 1 hr later, cells were washed with PBS 3 times, then fixed by 4% paraformaldehyde for 5 min, followed by PBS washing. Coverslips were incubated with guinea pig anti-Iba1 (1:500 dilution, Synaptic Systems, cat. no. 234004) for 2 hrs at room temperature, followed by incubation with Alexa Fluor 488-conjugated donkey anti-guinea pig Ig (1:400 dilution, Jackson ImmunoResearch, cat. no. 706546148) for 1 hr at room temperature. Imaging was captured using a fluorescence microscope (ApoTome.2, Zeiss, Germany) with a 20x objective at 1× zoom. Microspheres per cell were analyzed manually in Image J.

Characterizing neurons and microglial cells in the hypothalamus and hippocampus

Mice were anesthetized with pentobarbital (50 mg/kg) and subjected to a 2-min transcardial perfusion with phosphate buffered saline (PBS) followed by cold 4% paraformaldehyde (PFA) for 8 min. Brains were removed and post-fixed overnight in 4% PFA and stored for an additional 48 hrs at 4^{o}C in a 30% sucrose solution for cryoprotection. Brains were cut into 30 µm thick coronal sections on a cryostat. Sections were stored in cryoprotectant solution at -20°C prior to immunostaining. For immunostaining, brain sections containing the dorsal hippocampus or mediobasal hypothalamus (MBH) were rinsed in tris-buffered saline (TBS) and incubated with primary antibodies overnight at 4°C. Primary antibodies used for immunostaining included rabbit anti-Iba1 (1:400 dilution, Synaptic Systems, Gottingen, Germany, cat. no. 234003), rat anti-CD68 (1:100 dilution, Abcam, cat. no. ab53444, guinea pig anti-synaptophysin 1 (1:400 dilution, Synaptic Systems, cat. no. 101004), and rabbit anti-POMC (1:1000 dilution, Phoenix Pharmaceuticals Inc., Burlingame, CA, USA, cat. no. H-029-30). Brain slices were then rinsed and incubated with secondary antibodies for 1 hr at room temperature. Secondary antibodies included biotinylated goat anti-rabbit Ig (Vector Laboratories, Inc., Burlingame, CA, USA, cat. no. BA-1000), biotinylated goat anti-rat Ig (Vector Laboratories, cat. no. BA-9400), Alexa Fluor 488-conjugated donkey anti-rabbit Ig (Invitrogen, Carlsbad, CA, USA, cat. no. A21206), Alexa Fluor 594-conjugated streptavidin (Jackson ImmunoResearch, cat. no. 016580084), and Alexa Fluor 647-conjugated donkey anti-guinea pig Ig (Jackson Immunoresearch, cat. no. 706605148), all diluted to 1:400. Samples were mounted with antifade mounting medium (Vector Laboratories, cat. no. H-1000) or antifade

mounting medium with 4',6-diamidino-2-phenylindole (DAPI, Vector Laboratories, cat. no. H-1200).

For immunohistochemical staining, sections were rinsed and incubated with biotinylated secondary antibody and avidin-biotin complex (ABC method, Vector Laboratories), followed by incubation in 1% diaminobenzidine with 0.01% hydrogen peroxide for 3 min. Sections were then rinsed with TBS and mounted on Superfrost Plus microscope slides (Fisher Scientific, Waltham, MA, USA). Sections dried thoroughly, followed by dehydration and delipidation via a series of ethanol washes and xylene, respectively. Imaging was performed using a brightfield microscope (Leica Biosystems, Heidelberg, Germany) with a 10x or 20x objective.

For immunofluorescence staining, fluorescent-conjugated antibodies were added as described. After several rinses, brain sections were mounted on Superfrost Plus microscope slides, covered with cover slips, and stored at 4°C. Imaging was performed using a confocal microscope (TCS-SP8, Leica Biosystems, Heidelberg, Germany). The laser power, photomultiplier gain, and offset were maintained constant for all images. For anti-Iba1 and anti-CD68 double staining with or without DAPI, 20 µm z-stack confocal images were acquired at 1 µm or 0.5 µm intervals, using a 40× /1.3 oil objective at 1× or ~4× zoom. For anti-Iba1, anti-synaptophysin 1, and anti-CD68 triple staining, 16 µm z-stack confocal images were acquired at 0.5 µm intervals, with 63× /1.4 oil objective, also at 1× or ~4× zoom.

Imaging quantification

Immunohistochemistry images were analyzed using Image J. $Iba1^+$ cells and primary projections were counted manually in a 300 µm x 300 µm frame for quantification in the fixed region of ARC. POMC-immunoreactive ($POMC^+$) cells were counted from every 5th section between Bergma -1.34 to -2.18 (Paxinos Mouse Brain Atlas) in each animal, i.e. about 8 sections/animal. MorphoStrider software (Explora Nova, La Rochelle, France) was used to analyze the surface area of ARC in each section and the $POMC^+$ cell number was counted manually in the same region. Immunofluorescent images were analyzed using Imaris 8.3 software (Bitplane AG, Zurich, Switzerland); z-stack confocal images were constructed and photographed under a 40× /1.3 or 63× /1.4 oil objective at 1× zoom. The volume of $CD68^+$ particles, $Iba1^+$ microglial cells, synaptophysin 1, and $DAPI^+CD68^+$ microglia were determined for each brain section using Imaris 8.3 and presented as the average value per mouse.

Supplemental Data

Supplementary Table 1. Summarized data obtained from both male and female mice (Bmal1-KD *versus* Ctrl).

	Isolated microglia	HFD condition						
	Gene expression	Body weight	Energy intake	RER	Physical activity	Heat production	Microglial cell number	Phagocytosis
Male	Bmal1 ↓, Cry ↑	↓	↓	None	None	None	None	↑ (at ZT17)
Female	Bmal1 ↓, Dbp ↓	↓	↓ (P=0.051)	↑	None	None	None	↑ (at ZT5)

Arrow indicates a significant genotype difference (Bmal1-KD *versus* Ctrl); None indicates no genotype difference.

Supplemental Figure. 1

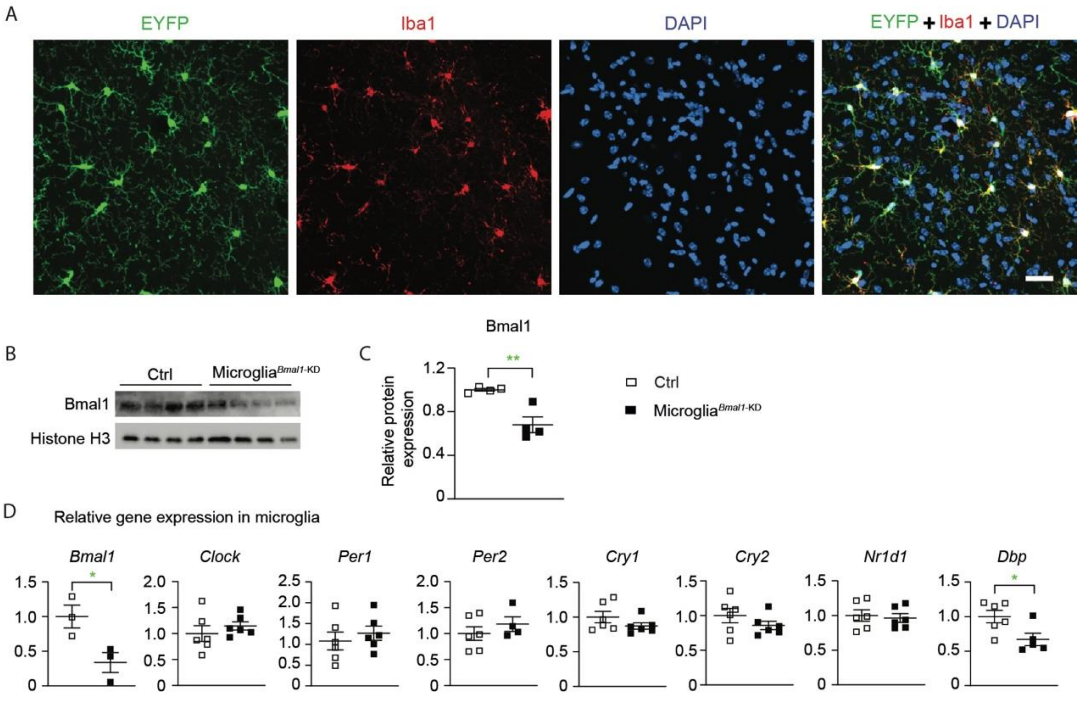

Figure. S1. Microglia specific knock-down of Bmal1 (microglia$^{Bmal1\text{-}KD}$) alters clock gene expression in adult female mice. (A) Representative confocal images of EYFP, Iba1, and DAPI

immunostaining in the hippocampus region of microglia$^{Bmal1\text{-KD}}$ or Ctrl mice used in our study; scale bar, 30 µm. **(B** and **C)** Representative images and quantification of Western blotting showing immunoreactive Bmal1 and Histone H3 in microglia (n = 4 mice per group). **(D)** Expression of *Bmal1* and other clock genes in microglia isolated from the brain of Ctrl and microglia$^{Bmal1\text{-KD}}$ female mice 3 weeks after the tamoxifen injection (n = 3-6 mice per group). Data are presented as means ± s.e.m. Green-colored asterisks * indicate a genotype effect; * $P < 0.05$, ** $P < 0.01$.

Supplemental Figure. 2

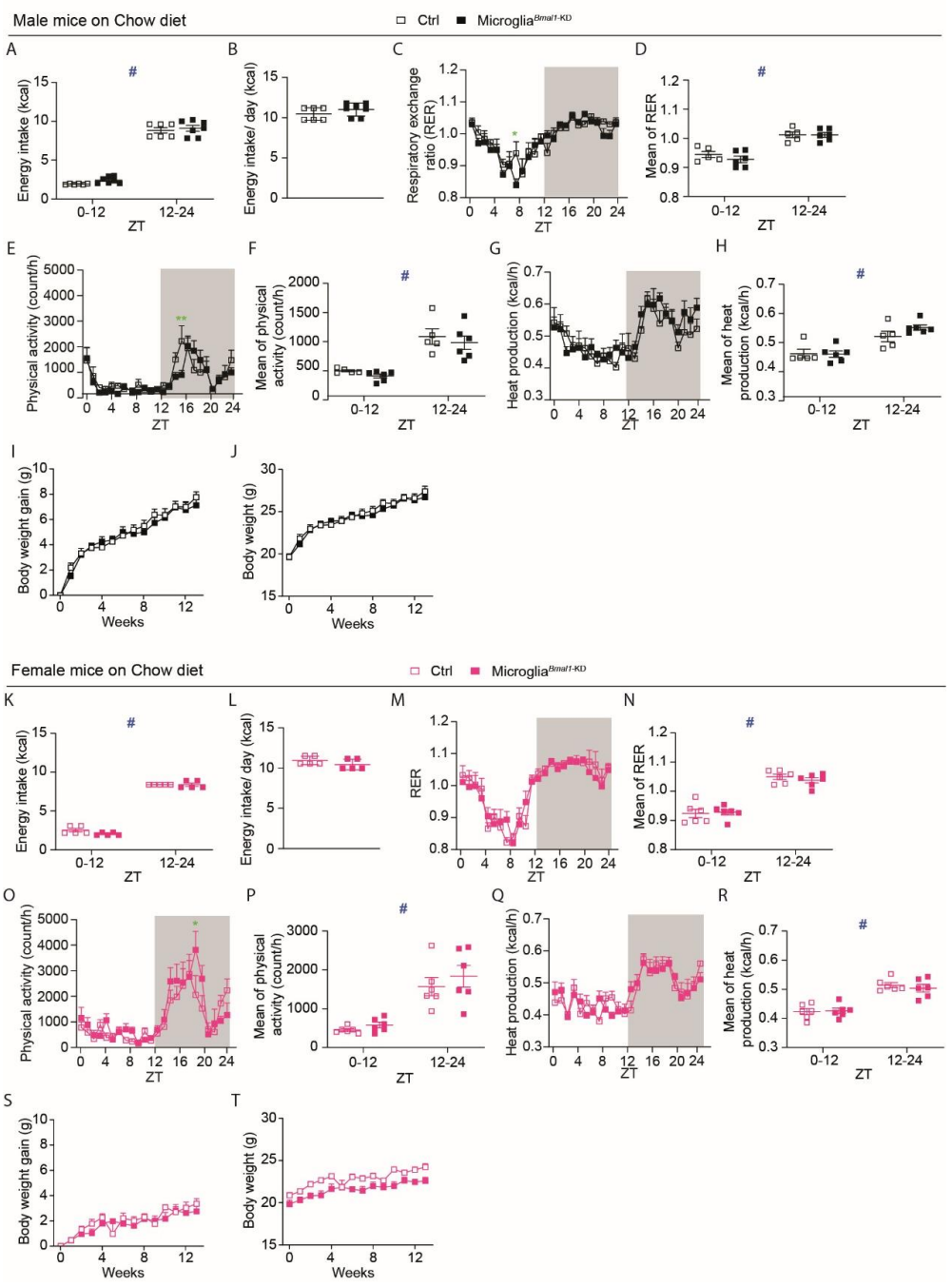

Figure. S2. Metabolic phenotype of Ctrl and microglia$^{Bmal1\text{-KD}}$ male and female mice on a standard chow diet. (A to **J)** Metabolic data from male mice. **(A** and **B)** Energy intake during light and dark phase, and per day (n = 6-7 mice per group). **(C** and **D)** RER and the mean of RER during the light phase and dark phase (n = 5-6 mice per group). **(E** and **F)** Physical activity and the mean of physical activity during the light phase and dark phase (n = 5-6 mice per group). **(G** and **H)** Heat production and the mean of heat production during the light phase and dark phase (n = 5-6 mice per group). **(I** and **J)** The body weight gain and body weight. **(K** to **T)** Metabolic data from female mice. **(K** and **L)** Energy intake during light and dark phase and per day (n = 5-6 mice per group). **(M** and **N)** RER and the mean of RER during the light phase and dark phase (n = 6 mice per group). **(O** and **P)** Physical activity and the mean of physical activity during the light phase and dark phase (n = 6 mice per group). **(Q** and **R)** Heat production and the mean of heat production during the light phase and dark phase (n = 6 mice per group). **(S** and **T)** The body weight gain and body weight. Data are presented as means ± s.e.m. Green-colored asterisks * indicate a genotype effect; **#** for ZT0-12 compared to ZT12-24. * $P < 0.05$, ** $P < 0.01$, and **#** $P < 0.05$.

Supplemental Figure. 3

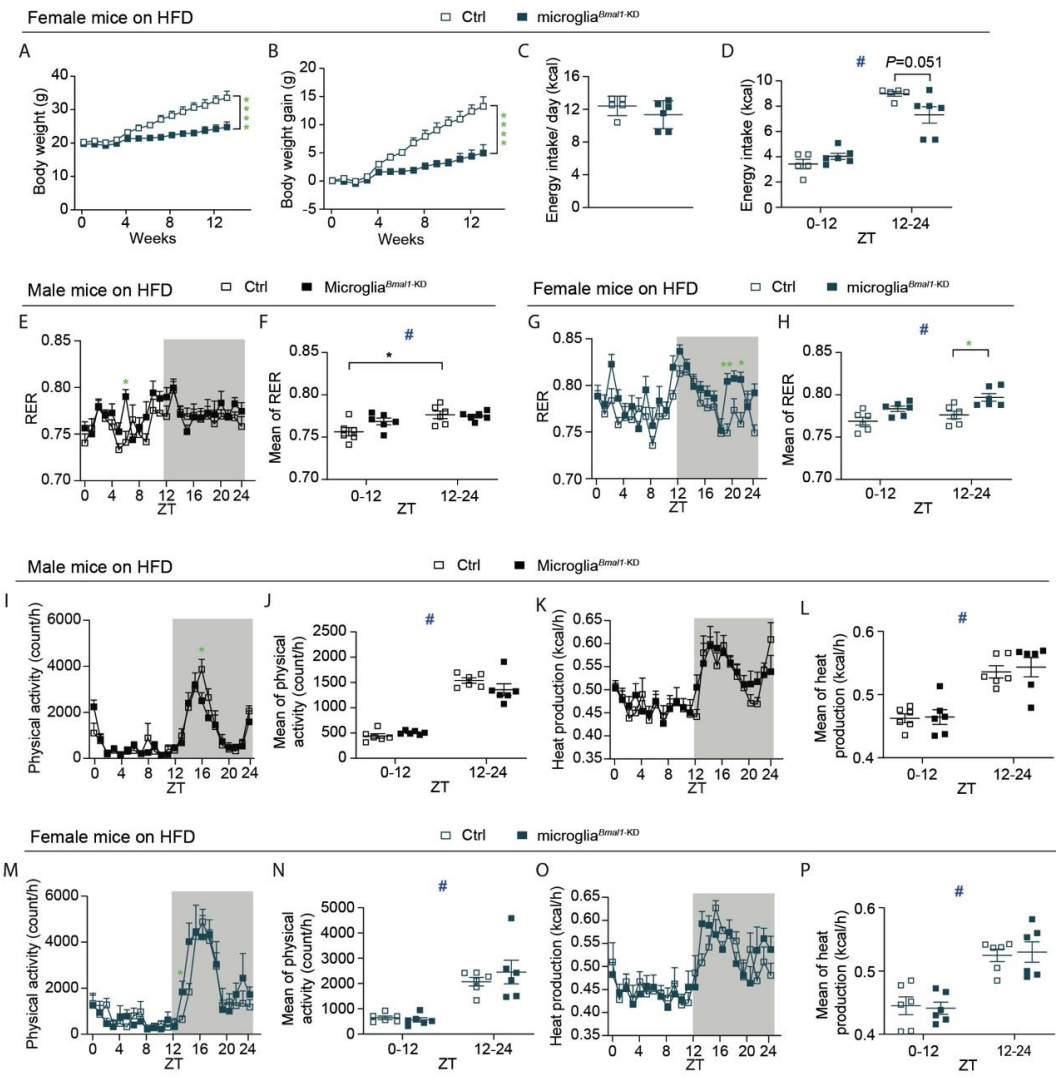

Figure. S3. Metabolic phenotype of Ctrl and microglia$^{Bmal1\text{-KD}}$ male and female mice on the HFD. (A to **J)** Metabolic parameters of female mice fed with a HFD. **(A** and **B)** Body weight and body weight gain (n = 5-6 mice per group). **(C** and **D)** Energy intake of Ctrl and microglia$^{Bmal1\text{-KD}}$ mice (n = 5-6 mice per group). **(E** and **F)** RER and the mean of RER during the light phase and dark phase of male mice fed a HFD (n = 6 mice per group). **(G** and **H)** RER and the mean of RER during the light phase and dark phase of female mice fed a HFD (n = 6 mice per group). **(I** to **L)** Metabolic data of male mice fed a HFD. **(I** and **J)** Physical activity and the mean of physical

activity during the light phase and dark phase (n = 6 mice per group). **(K** and **L)** Heat production and the mean of heat production during the light phase and dark phase (n = 6 mice per group). **(M** to **P)** Metabolic data of female mice fed a HFD. **(M** and **N)** Physical activity and the mean of physical activity during the light phase and dark phase (n = 6 mice per group). **(O** and **P)** Heat production and the mean of heat production during the light phase and dark phase (n = 6 mice per group). Data are presented as means ± s.e.m. Green-colored asterisks * indicate a genotype effect; **#** for ZT0-12 compared to ZT12-24. * $P < 0.05$, ** $P < 0.01$, **** $P < 0.0001$, and **#** $P < 0.05$.

Supplemental Figure. 4

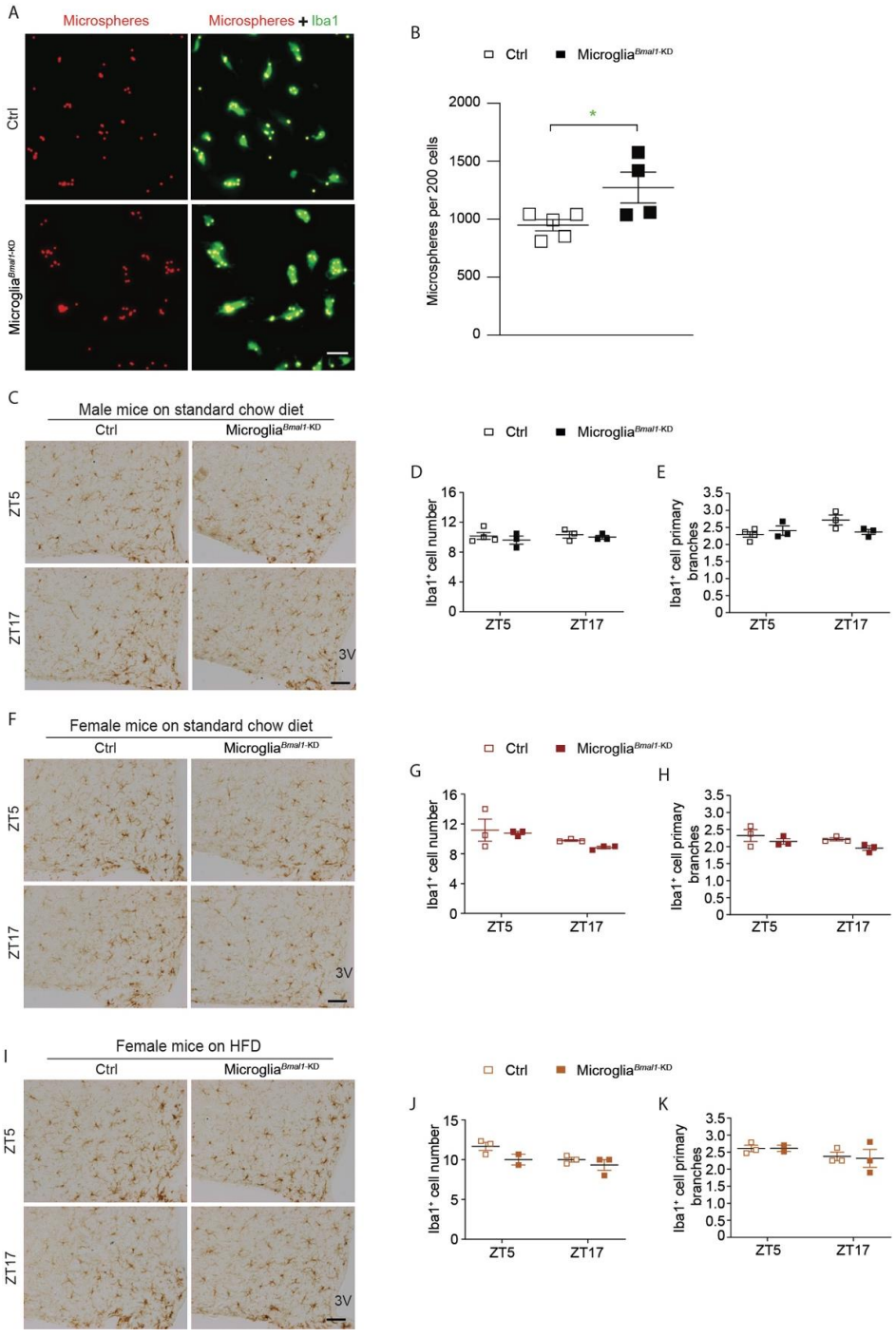

Figure. S4. Microglial phagocytic capacity as well as cell number and primary projections in Ctrl and microglia$^{Bmal1\text{-KD}}$ mice on chow diet and in response to HFD. (A) Image of microspheres in primary microglial cells in Ctrl and Bmal1-KD groups (n = 4-5 samples per group; 200 cells were counted in each sample). Scale bar, 20 µm. (**B**) Microspheres per sample (the average of microspheres per cell: 4.7 microspheres in Ctrl group; 6.4 microspheres in Bmal1-KD group). (**C**) Representative images of Iba1 immunostaining of male mice fed a standard chow diet. **(D** and **E)** Quantification of Iba^{+} microglial cell number and primary projections (n = 3 mice per group). **(F** to **H)** Representative images and quantification of Iba1^{+} microglial cell number and primary projections of female mice fed a standard chow diet (n = 3 mice per group). **(I** to **K)** Representative images and quantification of Iba1^{+} microglial cell number and primary projections of female mice fed a HFD (n = 2-3 mice per group). 3V, third ventricle. Scale bar, 100 µm. Data are presented as means ± s.e.m.

Supplemental Figure. 5

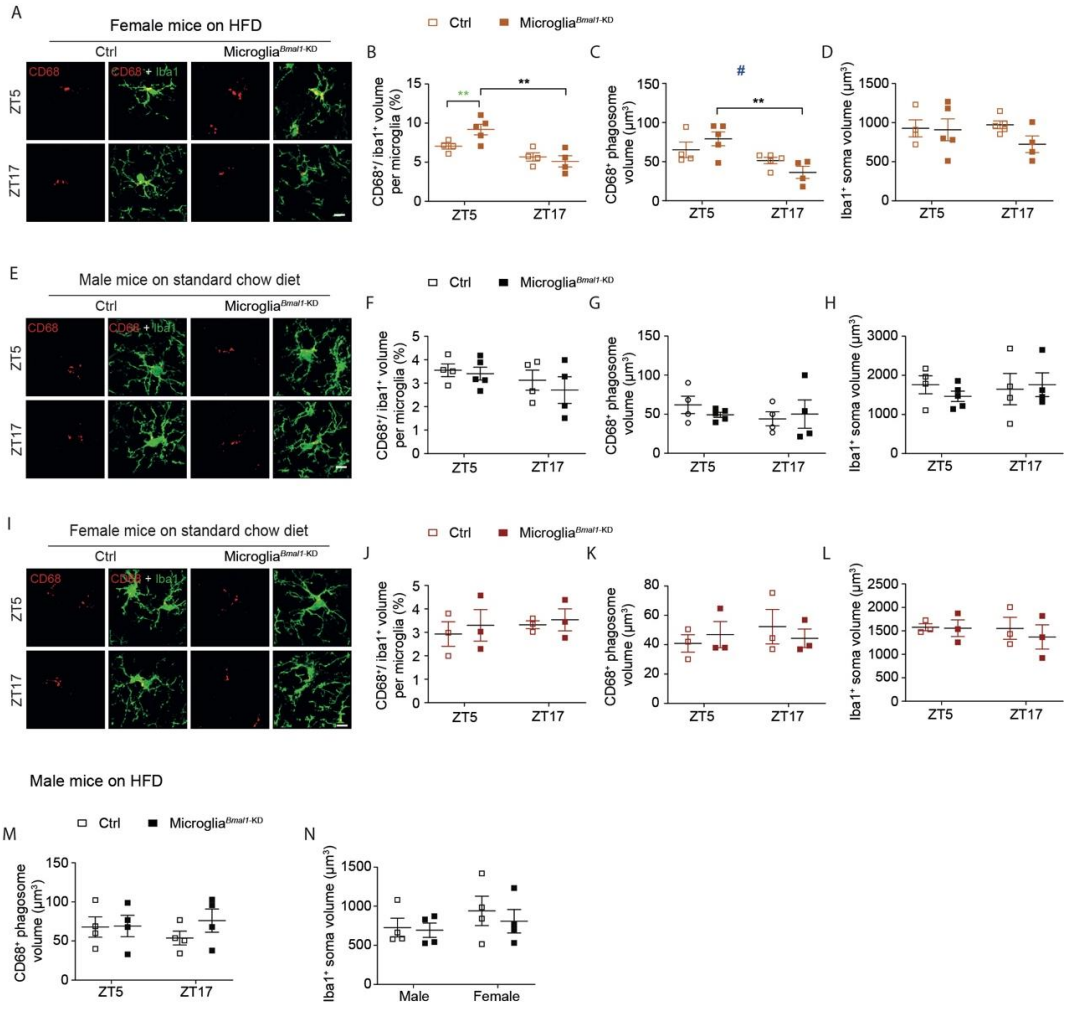

Figure. S5. Microglial CD68$^+$/ Iba1$^+$ ratio in mice on a HFD and chow diet. (A) Confocal images of CD68$^+$ and Iba1$^+$ in ARC of female mice fed a HFD (n = 4-5 mice per group). **(B** to **D)** Quantitative analyses of the percentage of CD68$^+$ volume per microglia, CD68$^+$ phagosome volume, and Iba1$^+$ soma volume in female mice fed a HFD (100-125 cells were analyzed in each group). **(E)** Confocal images of CD68$^+$ and Iba1$^+$ in ARC of male mice fed a chow diet (n = 4-5 mice per group). **(F** to **H)** Quantitative analyses of the percentage of CD68$^+$ volume per microglia, CD68$^+$ phagosome volume, and Iba1$^+$ soma volume in male mice fed a chow diet (100-125 cells were analyzed in each group). **(I)** Confocal images of CD68$^+$ and Iba1$^+$ in ARC of female mice fed a chow diet (n = 3 mice per group). **(J** to **L)** Quantitative analyses of the

percentage of CD68^{+} volume per microglia, CD68^{+} phagosome volume, and Iba1^{+} soma volume in female mice fed a chow diet (75 cells were analyzed in each group). **(M** to **N)** Quantitative analyses of CD68^{+} phagosome volume and Iba1^{+} soma volume in male mice fed a HFD (n= 4-5 mice per group). Scale bar, 10 µm. Data are presented as means ± s.e.m. Green-colored asterisks * indicate a genotype effect; **#** when ZT5 is compared to ZT17. ** $P < 0.01$.

Supplemental Figure. 6

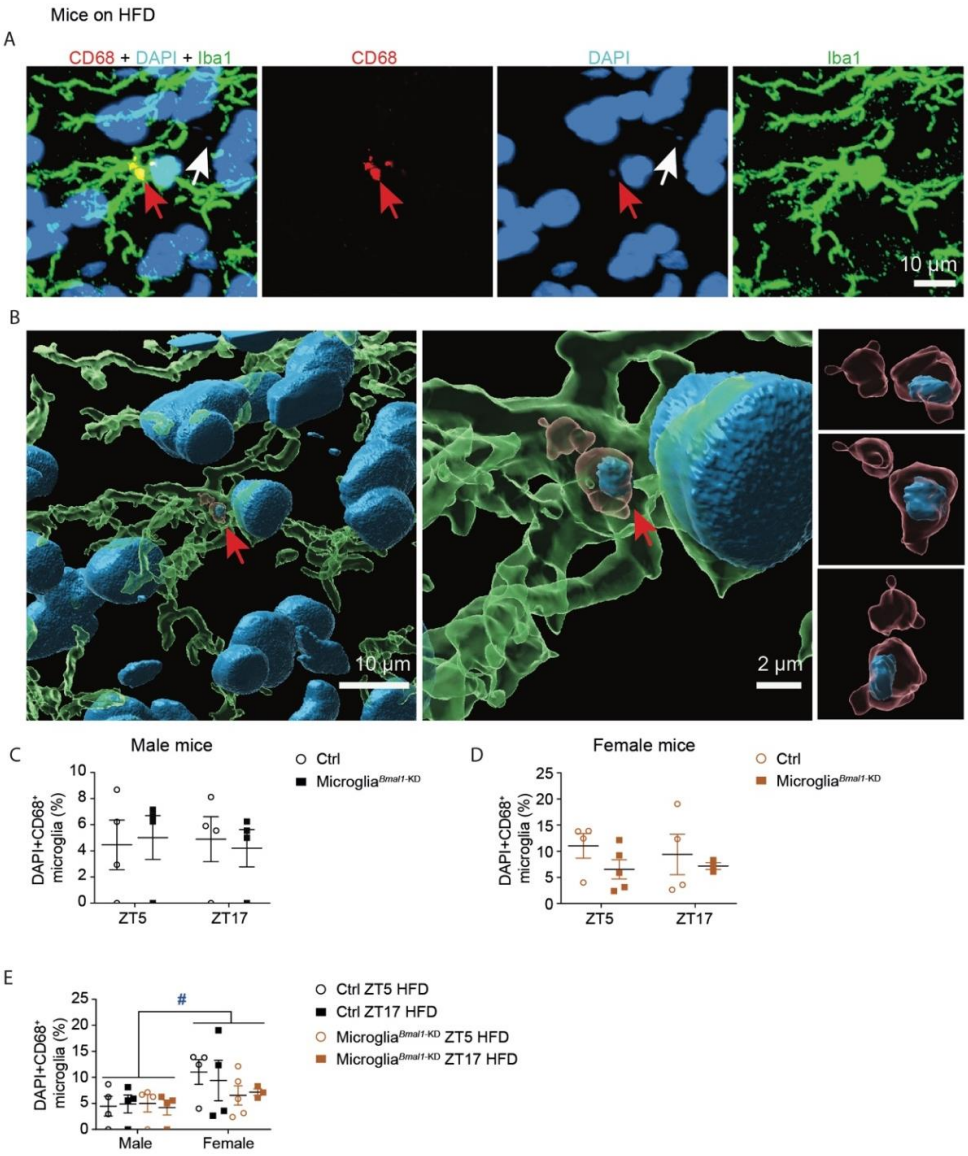

Figure. S6. CD68, DAPI, and Iba1 triple-staining in the ARC of HFD-fed male and female mice. **(A)** Confocal images of DAPI (blue), CD68 (red), and iba1 (green) triple labeling. The yellow color in the most left panel marks microglial phagosomes; the red arrow indicates the $DAPI^+$ particle inside the $CD68^+$ phagosome; the white arrow indicates the $DAPI^+$ particle outside of the $CD68^+$ phagosome. **(B)** 3D reconstruction of the confocal images in **A,** with surfacing of DAPI (solid blue), CD68 (transparent red), and iba1 (transparent green), and amplified side-scatter views**.** (**C** to **E**) Quantification of the percentage of microglia with $DAPI^+CD68^+$ phagosomes in male and female mice fed a HFD (n = 4-5 mice per group, 30-40 cells per mice). Data are presented as means + s.e.m. # $P < 0.05$.

Supplemental Figure. 7

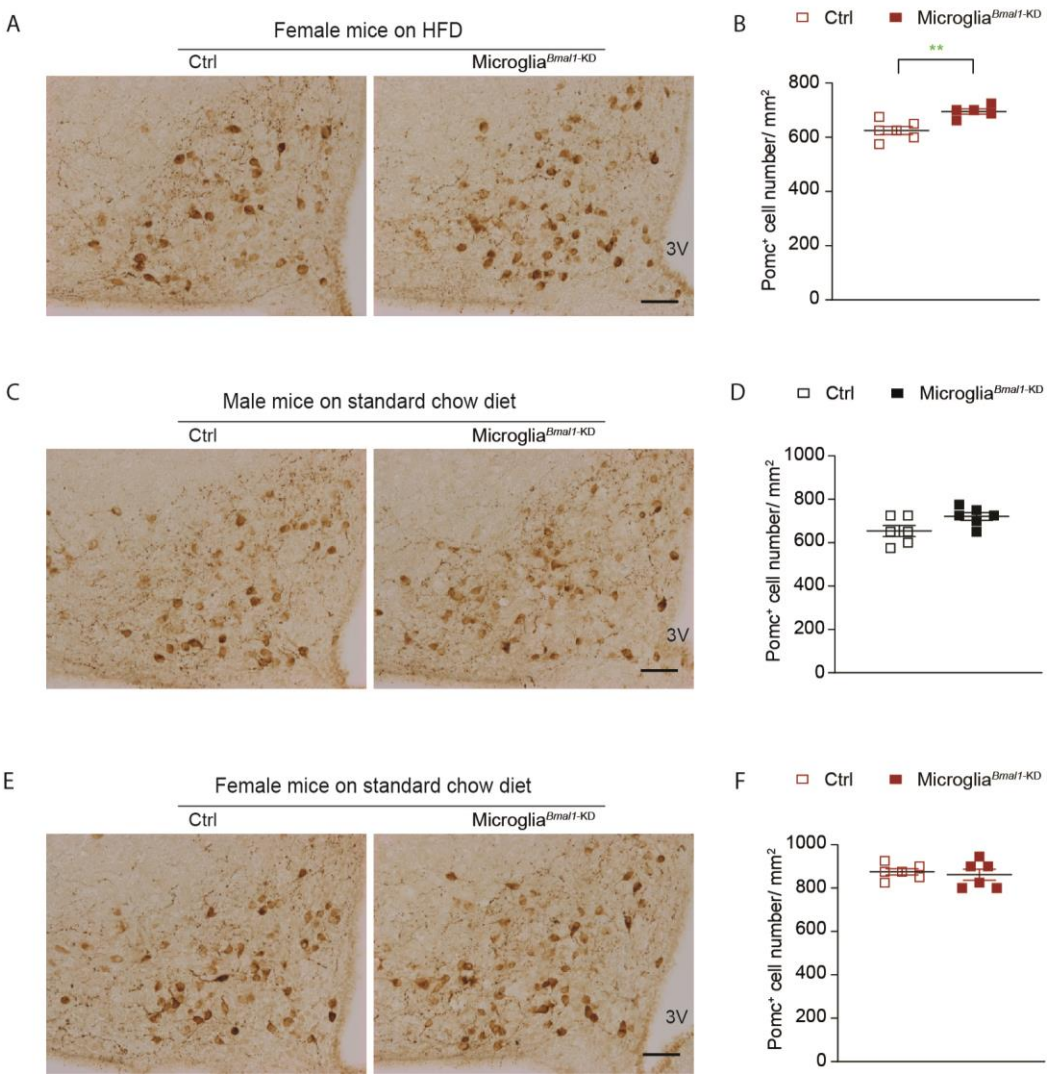

Figure. S7. POMC^{+} neurons in Ctrl and microglia$^{Bmal1\text{-}KD}$ mice, males and females, on a HFD or standard chow diet. (A and **B)** Images and quantification of POMC^{+} neuronal cell number in female mice on a HFD (n = 5-6 mice per group). **(C** and **D)** Images and quantification of POMC^{+} neurons in male mice on a chow diet (n = 6 mice per group). **(E** and **F)** Images and quantification of POMC^{+} neurons in female mice on a chow diet (n = 6 mice per group). 3V, third ventricle. Scale bar, 100 µm. Data are presented as means ± s.e.m. Green-colored asterisks * indicate a genotype effect; ** $P < 0.01$.

Supplemental Figure. 8

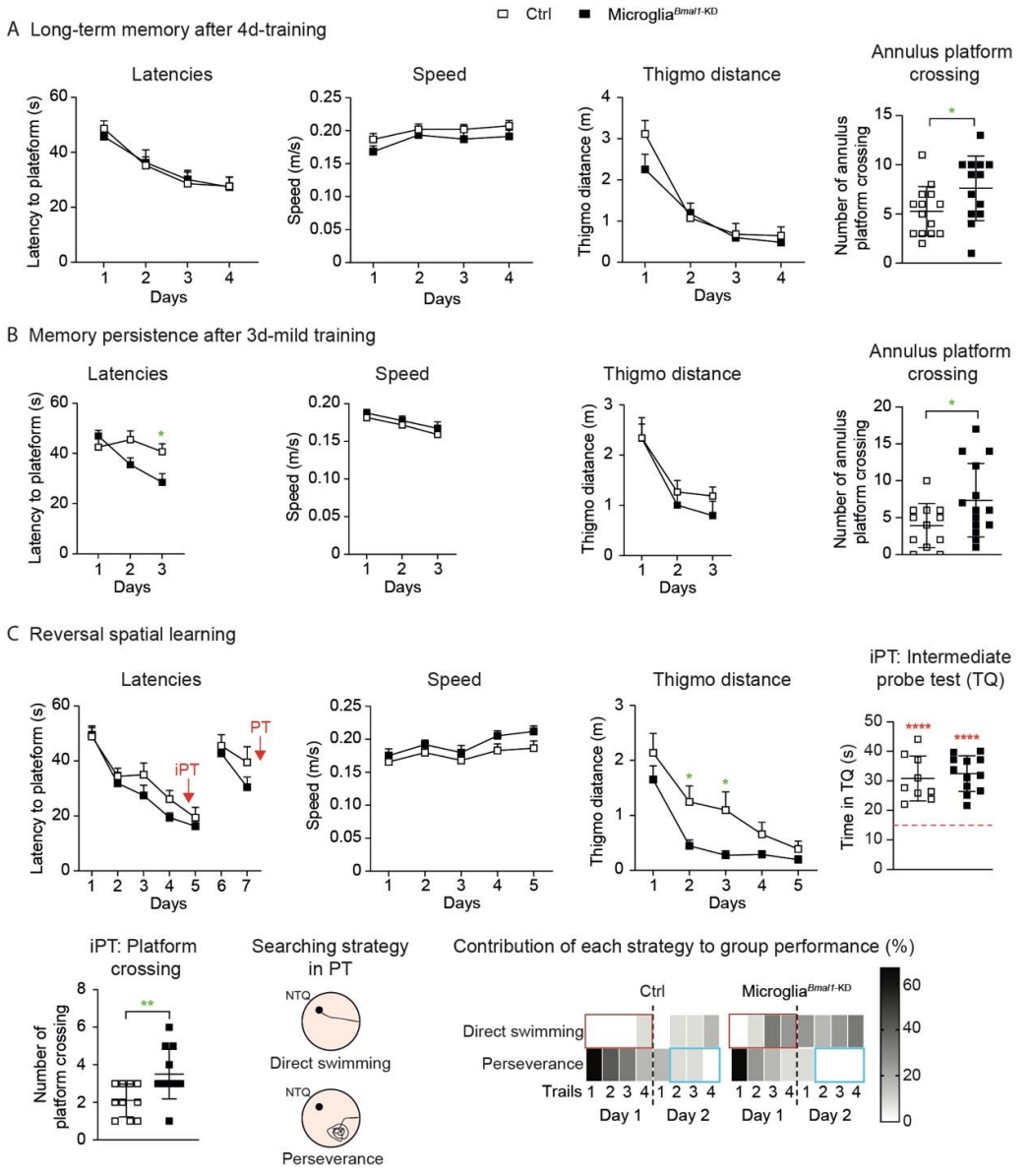

Figure. S8. Behavioral evaluation of Ctrl and microglia$^{Bmal1\text{-}KD}$ mice. (A) Parameters during 4 days MWM acquisition training and probe test (PT) (n = 13-14 mice per genotype). Related to Fig. 3C-E. **(B)** Parameters during 3 days MWM acquisition training and probe test (n = 12-14 mice per genotype). Related to Fig. 3F-H. **(C)** Parameters during 5 days of MWM acquisition

training, 2 days of reversal training, and probe tests (n = 9-12 mice per genotype). Related to Fig. 3I-K. iPT, intermediate probe test, on day 5; PT, after 24 h of the last reversal training on day 8. Data are presented as means ± s.e.m. Green-colored asterisks * indicate a genotype effect; red-colored asterisks * indicate a comparison versus random (red line). * $P < 0.05$, ** $P < 0.01$, and **** $P < 0.0001$.

Supplemental Figure. 9

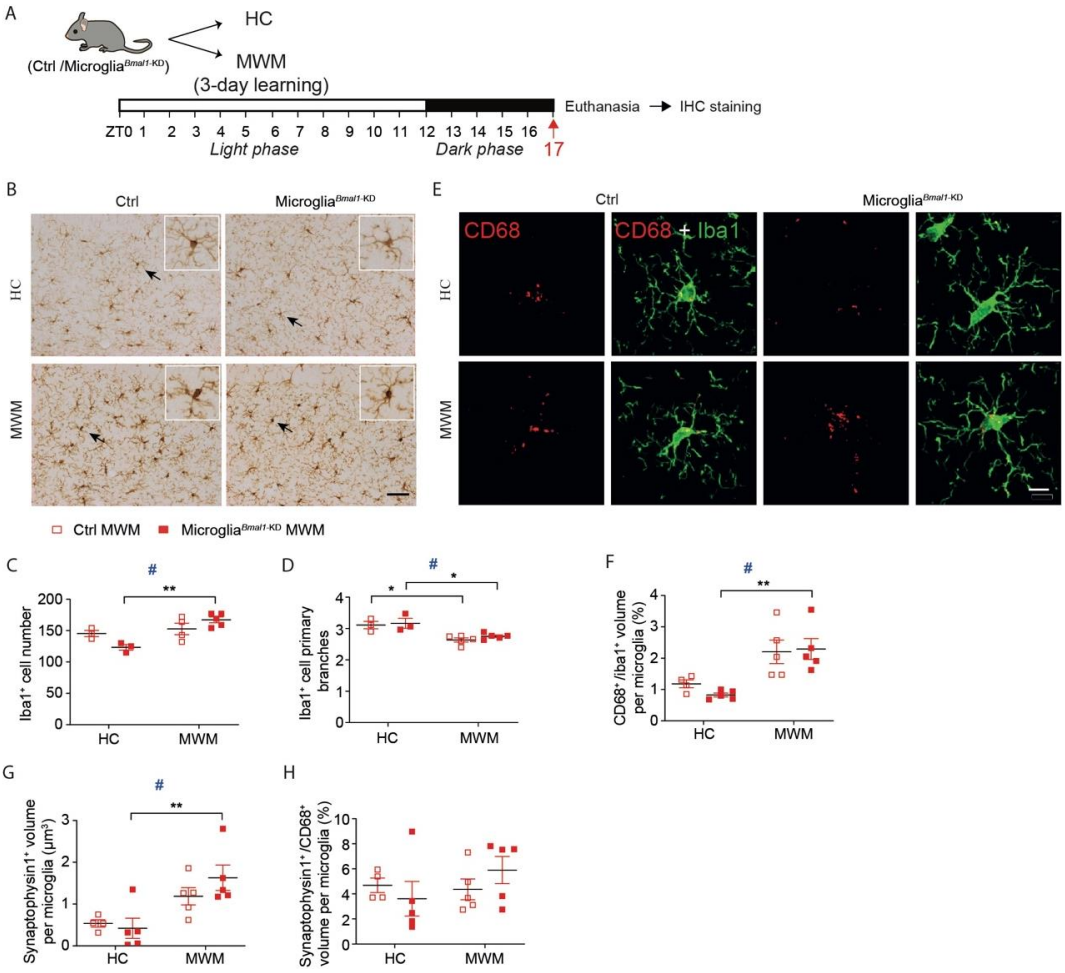

Figure. S9. Microglial phagocytic capacity in the hippocampal stratum radiatum during the dark phase after learning. (A) Experimental strategy. Mice received 3 days training in the MWM and were sacrificed at ZT17 of day 3. **(B)** Microglial immune reactivity in hippocampal CA1. Scale bar, 100 µm. **(C** and **D)** Quantification of Iba1$^+$ microglial cell number and primary

branches in home-cage (HC, n = 3 mice per group) and MWM (n = 4-5 mice per genotype) in CA1. **(E)** Confocal images of CD68 and Iba1 immunostaining in hippocampal stratum radiatum. Scale bar, 10 µm. **(F)** Quantitative analyses of the percentage of $CD68^+$ volume per microglia in hippocampal stratum radiatum (HC, n = 4-5 mice per group; MWM, n = 5 mice per group; 100-125 cells were analyzed in each group). **(G** and **H)** Quantification of the volume of $synaptophysin1^+$ in the $CD68^+$ and the ratio of $synaptophysin\ 1^+$/ $CD68^+$ volume per microglia in hippocampal stratum radiatum (HC, n = 4-6 mice per group; MWM, n = 5 mice per group). Data are presented as means ± s.e.m. **#** when HC is compared to MWM. * $P < 0.05$, ** $P < 0.01$, and **#** $P < 0.05$.

Supplemental Figure. 10

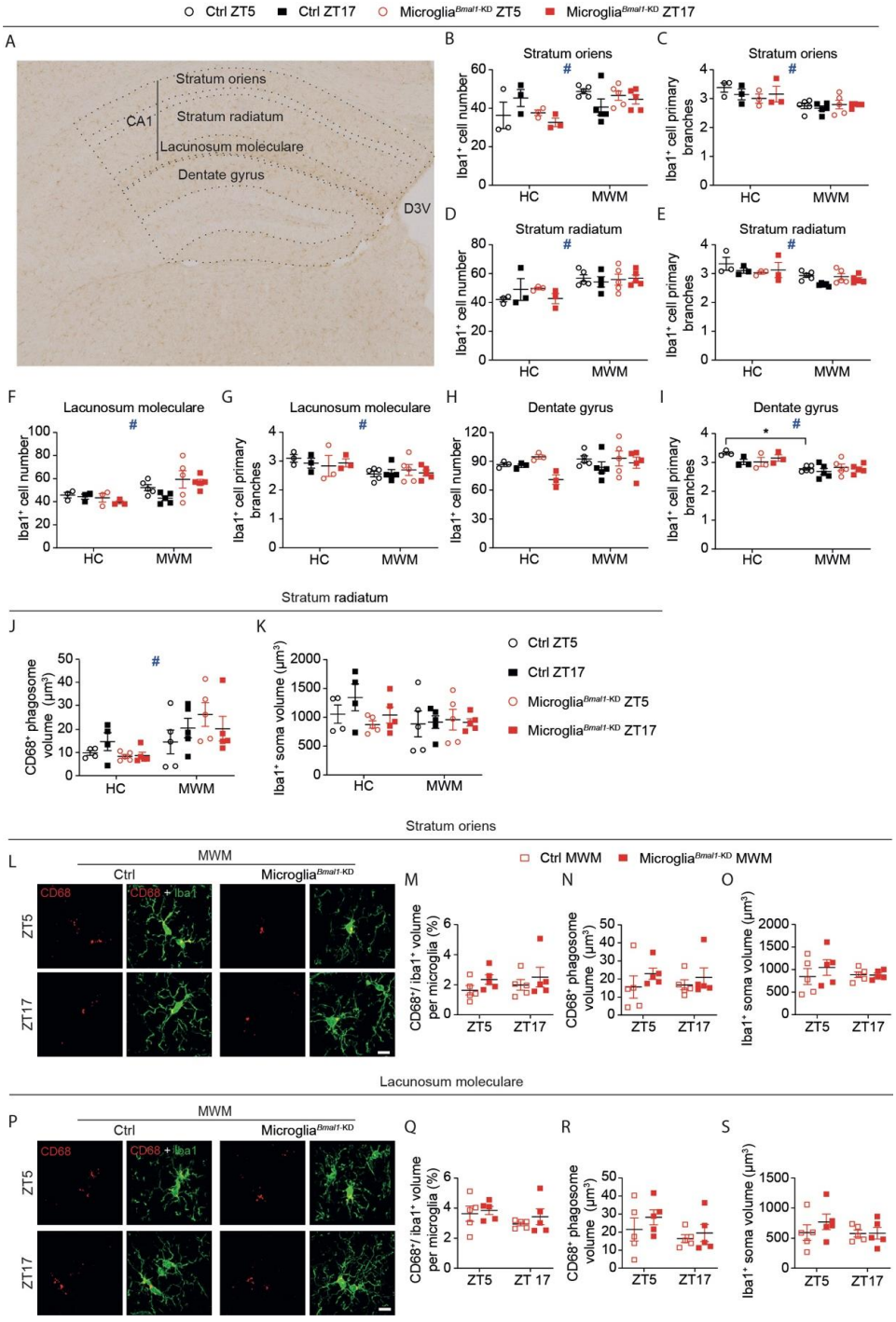

Figure. S10. Microglial Iba1 and CD68/ Iba1 immunoreactivity in different hippocampal regions of Ctrl and microglia$^{Bmal1\text{-KD}}$ mice in the HC and MWM group at ZT5 and ZT17. (A) Delineation of the area of the different hippocampal regions. D3V, dorsal third ventricle. **(B** to **I)** The microglial (Iba1^{+} cells) number and primary branches after 3 days MWM training and in the HC group in different layers of the mouse hippocampus (HC, n = 3 mice per group; MWM, n = 5 mice per group). **(J** and **K)** Quantitative analyses of the volume of CD68^{+} and Iba1^{+} in the hippocampal stratum radiatum in HC and MWM groups (HC, n = 3 mice per group; MWM, n = 5 mice per group). **(L)** Representative images of Iba1 and CD68 immunostaining in the hippocampal stratum oriens of the MWM group at ZT5 and ZT17. **(M** and **O)** Quantification of CD68 and Iba1 after 3 days of MWM training at ZT5 and ZT17 (n = 5 mice per group; 125 cells were analyzed in each group). **(P)** Representative images of Iba1 and CD68 immunostaining in the hippocampal lacunosum moleculare in the MWM group at ZT5 and ZT17. Scale bar: 10 µm. **(Q** and **S)** Quantification of CD68 and Iba1 in the hippocampal lacunosum moleculare after 3 days of MWM training at ZT5 and ZT17 (n = 5 mice per genotype; 125 cells were analyzed in each group). Scale bar, 10 µm. Data are presented as means ± s.e.m. **#** when HC is compared to MWM. * $P < 0.05$, and **#** $P < 0.05$.

References

Chatterjee, S., Cassel, R., Schneider-Anthony, A., Merienne, K., Cosquer, B., Tzeplaeff, L., Sinha, S.H., Kumar, M., Chaturbedy, P., Eswaramoorthy, M.*, et al.* (2018). Reinstating plasticity and memory in a tauopathy mouse model with an acetyltransferase activator. Embo Molecular Medicine *10*.

Gao, Y.Q., Vidal-Itriago, A., Kalsbeek, M.J., Layritz, C., Garcia-Caceres, C., Tom, R.Z., Eichmann, T.O., Vaz, F.M., Houtkooper, R.H., van der Wel, N.*, et al.* (2017). Lipoprotein Lipase Maintains Microglial Innate Immunity in Obesity. Cell Reports *20*, 3034-3042.

Restivo, L., Vetere, G., Bontempi, B., and Ammassari-Teule, M. (2009). The Formation of Recent and Remote Memory Is Associated with Time-Dependent Formation of Dendritic Spines in the Hippocampus and Anterior Cingulate Cortex. Journal of Neuroscience *29*, 8206-8214.

Wang, X.L., Wolff, S.E.C., Korpel, N., Milanova, I., Sandu, C., Rensen, P.C.N., Kooijman, S., Cassel, J.C., Kalsbeek, A., Boutillier, A.L.*, et al.* (2020). Deficiency of the Circadian Clock Gene Bmal1 Reduces Microglial Immunometabolism. Frontiers in Immunology 11.

Publication 2

Deficiency of the circadian clock gene *Bmal1* reduces microglial immunometabolism

Xiao-Lan Wang[1,2,3,*], Samantha E.C. Wolff[2,3], Nikita Korpel[2,3,4], Irina Milanova[2,3], Cristina Sandu[5], Patrick C.N. Rensen[6], Sander Kooijman[6], Jean-Christophe Cassel[1,7], Andries Kalsbeek[2,3,4], Anne-Laurence Boutillier[1,7], Chun-Xia Yi[2,3.4]

[1]Université de Strasbourg, Laboratoire de Neuroscience Cognitives et Adaptatives (LNCA), Strasbourg, France
[2]Department of Endocrinology and Metabolism, Amsterdam University Medical Center (UMC), University of Amsterdam, Amsterdam, the Netherlands
[3]Laboratory of Endocrinology, Amsterdam University Medical Center (UMC), University of Amsterdam, Amsterdam Gastroenterology & Metabolism, Amsterdam, the Netherlands
[4]Netherlands Institute for Neuroscience, an Institute of the Royal Netherlands Academy of Arts and Sciences, Amsterdam, the Netherlands
[5]Centre National de la Recherche Scientifique, Université de Strasbourg, Institut des Neurosciences Cellulaires et Intégratives, Strasbourg, France
[6]Department of Medicine, Divison of Endocrinology, and Einthoven Laboratory for Experimental Vascular Medicine, Leiden University Medical Center, Leiden, the Netherlands
[7]CNRS UMR 7364, LNCA, Strasbourg, France

Accepted by Front. Immunol. 6 Nov 2020.

Deficiency of the circadian clock gene *Bmal1* reduces microglial immunometabolism

Abstract

Microglia are brain immune cells responsible for immune surveillance. Microglial activation is, however, closely associated with neuroinflammation, neurodegeneration, and obesity. Therefore, it is critical that microglial immune response appropriately adapts to different stressors. The circadian clock controls the cellular process that involves the regulation of inflammation and energy hemostasis. Here, we observed a significant circadian variation in the expression of markers related to inflammation, nutrient utilization, and antioxidation in microglial cells isolated from mice. Furthermore, we found that the core clock gene-Brain and Muscle Arnt-like 1 (*Bmal1*) plays a role in regulating microglial immune function in mice and microglial BV-2 cells by using quantitative RT-PCR. *Bmal1* deficiency decreased gene expression of pro-inflammatory cytokines, increased gene expression of antioxidative and anti-inflammatory factors in microglia. These changes were also observed in *Bmal1* knock-down microglial BV-2 cells under lipopolysaccharide (LPS) and palmitic acid stimulations. Moreover, Bmal1 deficiency affected the expression of metabolic associated genes and metabolic processes, and increased phagocytic capacity in microglia. These findings suggest that *Bmal1* is a key regulator in microglial immune response and cellular metabolism.

Keywords: inflammation, palmitic acid, cellular metabolism, oxidative stress

Introduction

Microglia serve as the brain macrophages with immune-modulating and phagocytic capabilities. Microglial activation associated neuroinflammation has been firmly linked to the development and progression of neurodegenerative diseases, such as Alzheimer's disease, Parkinson's disease, and Huntington's disease (Hickman et al., 2018b). Severe systemic inflammation, such as sepsis, triggers microglial inflammatory activation which leads to neuronal injury and cognitive impairments in both humans (Semmler et al., 2013; Widmann and Heneka, 2014) and rodents (Semmler et al., 2007). High-fat diet-induced chronic microglial inflammation results in neuronal loss and obesity (Thaler et al., 2012c; Valdearcos et al., 2017b). Our previous study shows that microglial activation follows a circadian rhythm in rodents (Yi et al., 2017b).

Circadian rhythms are involved in the regulation and maintenance of various physiological processes, including immune responses, energy metabolism, and memory formation (Curtis et

al., 2014; Gerstner and Yin, 2010; Man et al., 2016). A growing body of literature shows that endogenous circadian clock function plays a crucial role in the control of many cellular processes that affect overall physiology (Barca-Mayo et al., 2019; Barca-Mayo et al., 2017; Bass and Takahashi, 2010b; Early et al., 2018b; Gabriel and Zierath, 2019b; Rahman et al., 2015; Stenvers et al., 2019b). For example, macrophages or microglial clock gene modulates the production of cytokines, following an immune challenge (Griffin et al., 2019; Nakazato et al., 2017; Sato et al., 2014). Besides the involvement of clock genes, it has also been shown that the immune activity is highly dependent on cellular metabolic processes (Geltink et al., 2018; Vijayan et al., 2019; Wang et al., 2019a); reduced glucose or lipid utilization inhibits microglial activation and inflammation (Gao et al., 2017b; Wang et al., 2019a). However, it is still unclear whether the intrinsic clock regulates microglial immune activity through modulation of cellular metabolism.

At the molecular level, the circadian clock machinery is based on transcriptional-translational feedback loops, which are present in almost every mammalian cell (Dudek and Meng, 2014). The transcriptional factor Bmal1 (Brain and Muscle Arnt-like 1)/Clock complex activates the expression of the period genes (*Per1*, *Per2*) and cryptochrome genes (*Cry1*, *Cry2*). Per/Cry complex suppresses its own transcription by inhibiting the activity of the Bmal1/Clock complex (Dudek and Meng, 2014; Gekakis et al., 1998). Nuclear receptor subfamily 1, group D, member 1 (Nr1d1), and RAR-related orphan receptors (Rors) fine-tune the transcription of *Bmal1*. Apart from the autoregulation, clock transcription factors also control the expression of other genes, such as the gene-D site albumin promoter binding protein (*Dbp*), by binding to their promoter (Ripperger and Schibler, 2006). In the current study, we focus on the core clock gene-*Bmal1*, which is highly expressed during the light phase in microglia in mice (Hayashi et al., 2013).

Bmal1 is closely linked with energy metabolism (Hatanaka et al., 2010; Rudic et al., 2004; Schiaffino et al., 2016; Sussman et al., 2019), redox hemostasis (Early et al., 2018b; Musiek et al., 2013a), and immune responses (Nakazato et al., 2017). Cellular energy metabolism and redox hemostasis regulate immune cell function, including those of microglia (Early et al., 2018b; Gao et al., 2017b). This suggests a possible link between circadian clock-*Bmal1* and the microglial immune response, as well as cellular energy metabolism and redox hemostasis. Here, we used the global Bmal1 knockout mice which show a complete loss of their circadian rhythms (Bunger et al., 2000). We found a significantly reduced inflammatory and metabolic associated gene expression in microglia isolated from Bmal1 knockout mice. The decrease of

inflammatory markers was also observed in *Bmal1* knocked down microglial BV-2 cells under LPS and palmitic acid stimulations.

Materials and Methods

Animals

Mice were housed in temperature (22 ± 1°C) and humidity (55 ± 5%) controlled room under a 12h/12h light/dark cycle ((lights on at 07:00 h, zeitgeber time 0 [ZT0])), with free access to food and water. B6.129-*Arntl*^{tm1Bra}/J mice (Bunger et al., 2000) (Jax stock #009100) were obtained from the Jackson Laboratory. The helix-loop-helix domain within exon 4 and all of exon 5 were replaced to create the mutation. B6.129-*Arntl*^{tm1Bra}/J mice have a C57BL/6J background. The following primers were used for genotyping: common: 5'-GCC CAC AGT CAG ATT GAA AAG-3'; wild type reverse: 5'- CCC ACA TCA GCT CAT TAA CAA-3'; mutant reverse: 5'-GCC TGA AGA ACG AGA TCA GC-3'. Mutant band: 162 bp; wild type band: 329 bp; heterozygote band: 162 bp and 329 bp. The mice containing only a mutant band were regarded as Bmal1 knockout (*Bmal1* KO). C57BL/6J mice served as control (Ctrl) (Supplementary Figure 1). *Bmal1* KO male mice were killed at ZT6 at the age of 3 months. Experimental protocol (NIN18.30.02) and animal care complied with the institutional guidelines of the Netherlands (Amsterdam, the Netherlands).

C57BL/6J male mice used for microglial isolation were sacrificed at 8-time points from ZT0 at 10 weeks old. This study was approved by and performed according to the guidelines of the Institutional Animal Care and Use Committee of the Netherlands (Leiden, the Netherlands).

Two transgenic mice lines (*Cx3cr1*^{CreER} mice, Jax mice stock no: 021160; *Bmal1*$^{lox/lox}$ mice, Jax mice stock no: 007668) were used to generate microglia-specific Bmal1 KO mice (*Bmal1* lox-homozygous and Cre-positive) and Ctrl mice (Cre-positive, but with a *Bmal1* wild-type sequence). Experimental protocols and animal care were in compliance with institutional guidelines and international laws and policies. Our project has been reviewed and approved by the national and regional ethics committee in Strasbourg (France). Experimental protocols and animal care were in compliance with the institutional guidelines (council directive 87/848, October 19, 1987, Ministère de l'agriculture et de la Forêt, Service Vétérinaire de la Santé et de la Protection Animale) and international laws (directive 2010/63/UE, February 13, 2013, European Community) and policies. Our project has been reviewed and approved by the French national and regional ethics committee (APAFIS#6822-2016092118336690v3).

Acute isolation of microglia from adult mice brain tissue

Mice were decapitated, and brains were homogenized in RPMI medium (21875-034, Gibco) with a 15 ml Dounce homogenizer on ice until the sample is fully homogeneous, without any visible tissue fragments. The final homogenate was filtered through a 70 µm cell strainer (431751, Corning). Following 5 min centrifugation at 380 g at 4°C, cell pellets were resuspended with 7 ml RPMI medium (11875093, Gibco) and mixed with 3 ml stock isotonic Percoll (SIP) solution which was made by mixing one part 10x HBSS (14185052, Gibco) in nine parts of Percoll plus (GE17-5445-01, Sigma-Aldrich). The cell suspension was then layered slowly on top of 2 ml of 70% Percoll solution which was prepared by mixing three parts of HBSS (14170112, Gibco) with seven parts SIP in a new 15 ml falcon and centrifuged at 500 g speed for 30 min at 18°C, with minimal acceleration and break rate. After centrifugation, the fuse interphases were transferred into a new 15 ml falcon with 8 ml HBSS and centrifuged at 500 g for 7 min again. The supernatant and cell debris were discarded and microglial cells were collected for RNA isolation.

RNA isolation from microglial and quantitative PCR (qPCR)

Total RNA was isolated from acutely isolated microglia using RNeasy Micro Kit (74004, QIAGEN) following the manufacturer's recommendations. We used 180 ng RNA to make cDNA with a Transcriptor First Strand cDNA Synthesis Kit (04897030001, Roche) following the manufacturer's recommendations. 4.5 ng cDNA was used to perform qPCR with SensiFAST™ SYBR® No-ROX Kit (BIO-98020, Roche Bioline). The genes *Bmal1*, *Clock*, *Cry1*, *Cry2*, *Per1*, *Per2*, *Nr1d1*, *Dbp*, *Il1b*, *Tnfa*, *Il6*, *Il10*, *Nox2*, *Gsr*, *Hmox1*, *Glut5*, *Glut1*, *Lpl*, *Gls*, and *Pcx* were evaluated. Primer sequences are presented in Supplementary Table 1. Data were analyzed by LC480 Conversion and LinRegPCR software and normalized to the housekeeping gene hypoxanthine phosphoribosyltransferase 1 (*Hprt1*).

Microglial BV-2 cell culture and transfection

Murine microglial BV-2 cells (Blasi et al., 1990) were kindly provided by Noam Zelcer (Zelcer et al., 2007) and cultured in Dulbecco's Modified Eagle's medium (DMEM, 41965-039, Gibco) supplemented with 10% fetal bovine serum (FBS, Gibco) and 100 µg/ml penicillin-streptomycin at 37°C in a humidified atmosphere containing 5% CO_2. Microglial BV-2 cells were transfected with the *Bmal1* siRNA or scrambled siRNA (Dharmacon) by using Viromer (VB-01LB-01, lipocalyx, Germany) according to the manufacturer's protocol. The medium was replaced 6 h after transfection and cells were incubated as usual. 24 h after transfection, cells were synchronized with 100 nM of dexamethasone (Sigma-Aldrich) for 2 h, then washed with PBS, and followed by exposure to lipopolysaccharide (LPS, E. coli O111:B4,

100 ng/ml, L4391, Sigma-Aldrich), palmitic acid (P0500, Sigma-Aldrich) or vehicle, and finally harvested at the appropriate time points. The time at which cells were washed with PBS was defined as 0.

Palmitic acid and bovine serum albumin (BSA) conjugation protocol

Palmitic acid was dissolved in 150 mM NaCl with robust shaking at 70°C. Fatty acid-free BSA (A8806, Sigma-Aldrich) was dissolved in 150 mM NaCl at 37°C to make a 3.2 mM BSA solution. Half of the BSA solution was mixed with the same volume of palmitic acid solution at 37°C while stirring overnight to make palmitic acid-BSA conjugated solution (5:1 molar ratio palmitic acid: BSA). Half of the BSA solution was added to the same volume of 150 mM NaCl at 37°C while stirring overnight to make a vehicle control solution. pH was adjusted to 7.4 and solutions were filtered using a 0.22 µm syringe filter.

RNA isolation from BV-2 cells

Total RNA was extracted using the High Pure RNA isolation kit (1182866500, Roche) following the manufacturer's instructions. Complementary DNA was obtained by reverse transcription of 400 ng of total mRNA using the Transcriptor First Strand cDNA Synthesis Kit (04897030001, Roche) following the manufacturer’s recommendations.

Primary microglial culture

Microglial cultures were prepared as described previously (24). Briefly, brain tissues were harvested from microglia-specific Bmal1 KO and littermate Ctrl mice at postnatal day 1 - 4 (P1-P4), the meninges and blood vessels were removed, and the parenchyma minced and triturated in DMEM/F12 (10565018, Gibco), containing 10% FBS, 100 µg/ml penicillin-streptomycin. Suspended cells were filtered (70 µm) and seeded on poly-L-lysine-coated flasks. Six to 10 days later, the flasks were shaken (200 rpm) for 1 h to specifically detach microglia. Microglial cells were treated with 5 µM of 4-hydroxytamoxifen for 48 h to induce Cre-LoxP recombination and excise *Bmal1*. Cells isolated from microglia-specific Bmal1 KO and Ctrl mice served as Bmal1 KO and Ctrl, respectively. Next, microglia were synchronized with 100 nM dexamethasone for 2 h, washed with PBS, and then treated with 100 ng/ml LPS for 1 h or 100 µM palmitic acid for 4 h, for final analysis.

Western blot analyses

Primary microglial cells were homogenized in Laemmli buffer and sonicated for 10 s twice (ultrasonic processor, power 40%) followed by heating at 70°C for 10 min and then 100°C for 5 min. Lysates were centrifuged at 14,000 *g* for 5 min, and the supernatant was used for Western blot analyses. Proteins were loaded on Midi-PROTEAN TGX Stain-Free™ Precast Gels (4–20%, Bio-Rad) and electrotransferred onto a nitrocellulose membrane. Primary antibodies used for Western blots were rabbit anti-Bmal1 (1:500, NB100-2288, Novus Biologicals) and rabbit anti-Actin (1:2000, A2066, Sigma-Aldrich), followed by horseradish peroxidase-conjugated secondary antibodies against rabbit (1:5000, Jackson ImmunoResearch). Immunoreactive bands were detected with ECL (Clarity, Bio-Rad) with a ChemiDoc Touch system (Bio-Rad).

2-NBDG glucose uptake assay

Microglial cells were plated in 96-well black plates with 3.5 x 10^4 cells/well. After synchronization, cells were cultured in glucose-free medium with LPS or palmitic acid stimulation. At the end of treatment, 2-NBDG (ab235976, Abcam), a fluorescently-labeled deoxyglucose analog, was added to a final concentration of 200 µg/ml, and fluorescent signals were recorded at 2 min, 5 min, and 10 min by microplate reader at excitation/emission wavelengths = 480/530 nm.

Free fatty acid uptake assay

Microglial cells were seeded in 96-well black plates with 3.5 x 10^4 cells/well. After synchronization, cells were treated with LPS or palmitic acid in 100 µl FBS free culture medium. At the end of treatment, 100 µl fatty acid dye (TF2-C12)-loading solution (ab176768, Abcam) was incubated with microglia for 1 h at 37°C. Fluorescent signals were detected by microplate reader at 30 min, 45 min, and 60 min at excitation/emission wavelengths = 480/530 nm.

DCFDA-cellular reactive oxygen species (ROS) detection assay

Microglial cells were plated in 96-well black plates with 3.5 x 10^4 cells/well. After synchronization, cells were stained by 25 µm DCFDA solution (ab113851, Abcam) for 25 min at 37°C. Fluorescent signals were detected immediately by microplate reader at excitation/emission wavelengths = 480/530 nm. Following the basal measurement, cells were challenged with 2% H_2O_2, and fluorescent signals were recorded up to 10 min.

Microsphere uptake assay

Microspheres (17154-10, polysciences) were coated with 10% FBS at 37°C for 1 h, followed by centrifugation (12,000 rpm, 2 min) and resuspended in PBS. Coated microspheres were added to the BV-2 cells (1000 microspheres per cell) at time 0, and 1 h later, cells were washed with PBS 3 times, then fixed by 4% paraformaldehyde for 5 min, followed by PBS washing. Mounting medium with DAPI was added for confocal imaging (Leica TCS SP5; Leica, Heidelberg, Germany). Five-µm z-stack confocal images were acquired at 0.3-µm intervals, with 40× /1.3 oil objective at 1× zoom. Images were analyzed by Imaris (Bitplane AG) to measure the total volume of microspheres in every view.

Statistical analysis

Statistical analyses were performed using two-tailed unpaired *t*-test, one-way ANOVA, and two-way ANOVA with GraphPad Prism 8 (San Diego, California, USA). Daily variation in gene expression in microglia isolated from C57BL/6J mice was evaluated by one-way ANOVA (Supplementary Table 2). The daily rhythm of genes in microglia isolated from C57BL/6J mice and BV-2 cells was assessed by cosinor analysis with SigmaPlot 14.0 software (SPSS Inc, Chicago, IL, USA). Data were fitted to the following regression: $y = A + B \cdot \cos(2\pi(x-C)/24)$; A is the mean level; B is the amplitude and C is the acrophase of the fitted rhythm (Hogenboom et al., 2019a). An overall *p* value (main *p* value, *P*m) was considered to indicate the rhythmicity in Supplementary Table 3. All data are presented as mean ± s.e.m and significance was considered at $P < 0.05$.

Results

Microglial inflammatory cytokine genes are higher expressed during the light phase

A previous rat study has demonstrated that microglial intrinsic clock genes and inflammatory cytokine genes show daily expression rhythms in the hippocampus and microglial inflammatory cytokine genes highly expressed during the light phase (Fonken et al., 2015b). It has also been shown that LPS treated rodents show increased sickness behavior or proinflammatory response during the light phase compared to the dark phase (Bellet et al., 2013; Fonken et al., 2015a). In the current mouse study, we found that in microglial cells, the gene expression of pro-inflammatory cytokines-interleukin 1 beta (*Il1b*) and interleukin 6 (*Il6*), but not tumor necrosis factor (*Tnfa*), followed a daily expression rhythm (Fig. 1A-C, and Supplementary Table 2 and 3). Both *Il1b* and *Il6* showed higher gene expression during the light phase than in the dark phase. The peak in *Tnfa* expression was also found during the light

phase (Fig. 1A-C and I). Moreover, the oxidation and inflammation-related gene NADPH oxidase 2 (*Nox2*) also showed rhythmic expression in microglia (Fig. 1D and Supplementary Table 3). Together these findings suggest that microglia may have a higher innate immune activity during the light phase in mice.

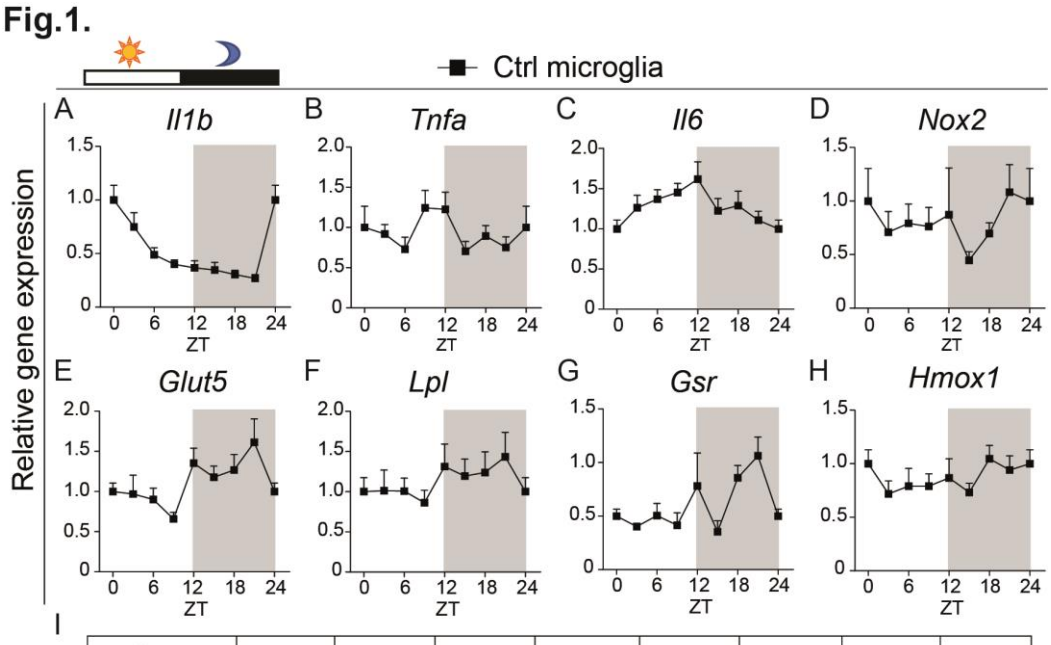

Genes	*Il1b*	*Tnfa*	*Il6*	*Nox2*	*Glut5*	*Lpl*	*Gsr*	*Hmox1*
Acrophase (ZT)	3	9	12	1.5	21	18	21	21

Figure 1

Rhythmic gene expression of inflammatory cytokines, nutrient utilization, and antioxidant anti-inflammation in microglia. (A-H) Relative expression of inflammatory genes interleukin 1 beta (*Il1b*) (A), tumor necrosis factor (*Tnfa*) (B), interleukin 6 (*Il6*) (C), and oxidation and inflammation-related gene NADPH oxidase 2 (*Nox2*) (D), and nutrient utilization genes facilitated glucose transporter member 5 (*Glut5*) (E), lipoprotein lipase (*Lpl*) (F), as well as antioxidant anti-inflammation genes glutathione reductase (*Gsr*) (G), heme oxygenase 1 (*Hmox1*) (H), were evaluated in isolated microglia from C57BL/6J male mice brain every 3 h (n = 6-8 samples per group per time point). ZT0 = lights on; ZT12 = lights off. Data of ZT0 and ZT24 were from the same samples. (I) Acrophase determined for each of the genes. Statistical significance of rhythmic expression was determined by the Cosinor analysis and one-way ANOVA. Data are presented as means ±s.e.m.

Microglial nutrient utilization and the antioxidation transcripts show daily rhythmicity

In physiological conditions, microglia are highly dynamic to clean the microenvironment and maintain neuronal survival and function (Nimmerjahn et al., 2005). The previous study showed that microglial activity is higher during the dark phase when mice are more active as compared with the light phase when mice are mainly resting (Yi et al., 2017b). Microglial activity is also highly dependent on cellular metabolism (Gao et al., 2017b). Therefore, we evaluated gene expression of facilitated glucose transporter member 5 (*Glut5*), which is highly expressed by microglia, and lipoprotein lipase (*Lpl*), which mediates lipoprotein triglyceride-derived fatty acid uptake. Both *Glut5* and *Lpl* exhibited an increased expression during the dark phase (Fig. 1E, F, and I), which suggests an increased nutrient utilization when microglia are more active. Microglial activation leads to the production of more metabolites and ROS (Ding et al., 2017; Rojo et al., 2014) that need to be eliminated to maintain proper microglial function (McLoughlin et al., 2019; Piantadosi et al., 2011; Poss and Tonegawa, 1997). Thus, we checked the gene expression of glutathione reductase (*Gsr*), a key enzyme for the production of sulfhydryl form glutathione (GSH). GSH acts as a scavenger and plays a critical role in preventing oxidative stress in cells. We also evaluated the rhythmic gene expression of heme oxygenase 1 (*Hmox1*), which has antioxidant anti-inflammation properties via the production of carbon monoxide (CO) (Piantadosi et al., 2011). We observed an increased expression of *Gsr* and *Hmox1* during the dark phase (Fig. 1G-I). The gene expression of *Glut5* and *Gsr* showed significant daily variation (Supplementary Table 2). These data indicate that the expression of nutrient utilization and the antioxidation associated genes in microglial cells follows a daily rhythm, which is in line with their activity.

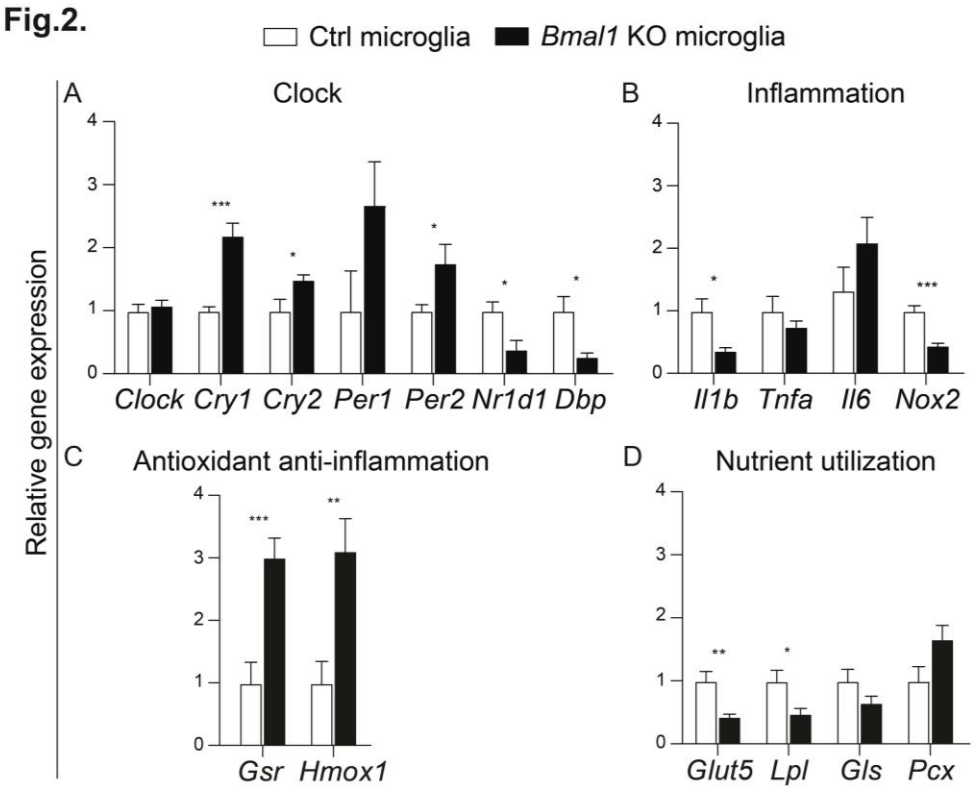

Figure 2

Bmal1 KO microglia show decreased inflammation and nutrient utilization in mice. (A-D) Relative expression of clock genes-*Clock*, cryptochrome (*Cry1*, *Cry2*), period (*Per1*, *Per2*), Nuclear receptor subfamily 1, group D, member 1 (Nr1d1), D site albumin promoter binding protein (*Dbp*) (A), inflammation-related genes *Il1b*, *Tnfa*, *Il6*, *Nox2* (B), and antioxidant anti-inflammation genes *Gsr*, *Hmox1* (C), as well as cellular metabolic-related genes *Glut5*, *Lpl*, glutaminase (*Gls*), and pyruvate carboxylase (*Pcx*) (D), were evaluated in isolated microglia from *Bmal1* KO mice and C57BL/6J mice brain at ZT6 (n = 8 samples per group). Data were analyzed with *t*-tests and are presented as means ± s.e.m. * $P < 0.05$, ** $P < 0.01$, and *** $P < 0.001$.

Bmal1 knockout microglia show decreased gene expression of inflammation and nutrient utilization

The circadian clock system is associated with the innate immune activity (Rahman et al., 2015). Therefore, we were interested in whether the *Bmal1* regulates microglial immunometabolism and evaluated the related gene expression in microglia isolated from *Bmal1* KO mice and controls in the middle of the light phase (ZT6). Expression of clock genes in *Bmal1* KO microglia

was disturbed, with a significant increase in *Cry1*, *Cry2*, and *Per2*, as well as a decrease in *Nr1d1*, and *Dbp* (Fig. 2A). *Il1b* and *Nox2* were significantly lower in *Bmal1* KO microglia, while *Tnfa* and *Il6* did not differ between both groups (Fig. 2B). Moreover, *Gsr* and *Hmox1* expression were strikingly increased (Fig. 2C). Taken together, these data suggest that *Bmal1* KO decreases inflammation and increases the anti-inflammation antioxidative effect in microglia. Furthermore, microglial *Glut5* and *Lpl* were significantly decreased in *Bmal1* KO mice (Fig. 2D). While glutaminase (*Gls*), which is involved in glutamate utilization, and pyruvate carboxylase (*Pcx*), which participates in gluconeogenesis and lipogenesis, did not differ between the two groups (Fig. 2D). These findings suggest reduced nutrient utilization in *Bmal1* KO microglia as compared to controls in physiological conditions.

Bmal1 deletion disturbs the expression of clock genes in microglial BV-2 cells

To further study the relationships among the intrinsic clock, immune activity, cellular metabolism, and antioxidative effect, specifically in microglia, we performed experiments in microglial BV-2 cells. Rhythmic expression of clock genes can be achieved in microglial BV-2 cells after synchronization with 100 nM dexamethasone for 2 h (Nakazato et al., 2017). Using this cell model we found that the inflammatory cytokines *Il1b*, *Tnfa*, interleukin 10 (*Il10*), and *Il6* showed a significant rhythmic expression after synchronization (Supplementary Figure 2 and Supplementary Table 3). To evaluate whether the intrinsic clock regulates microglial function, we knocked down *Bmal1* in BV-2 cells. First, we checked the clock gene expression every 4 h for 28 h after synchronization. We observed that *Bmal1* gene expression was significantly decreased in the *Bmal1* knock-down group (*Bmal1* siRNA) compared with the control group (scrambled siRNA) (Fig. 3A). *Bmal1* controlled genes, such as *Cry1*, *Cry2*, and *Per2*, and the *Bmal1* targeted gene *Dbp* showed a significant increase in the *Bmal1* knock-down group. While *Clock* was decreased 12 h after synchronization; *Per1* and *Nr1d1* expression did not change (Fig. 3A). The rhythmic expression of *Bmal1* was disturbed in the *Bmal1* knock-down group, but *Clock*, *Cry1*, *Per1*, *Per2*, *Nr1d1,* and *Dbp* still showed rhythmic expression (Supplementary Table 3). These results indicate that *Bmal1* deletion disturbs the core clock machinery in BV-2 cells.

Fig.3.

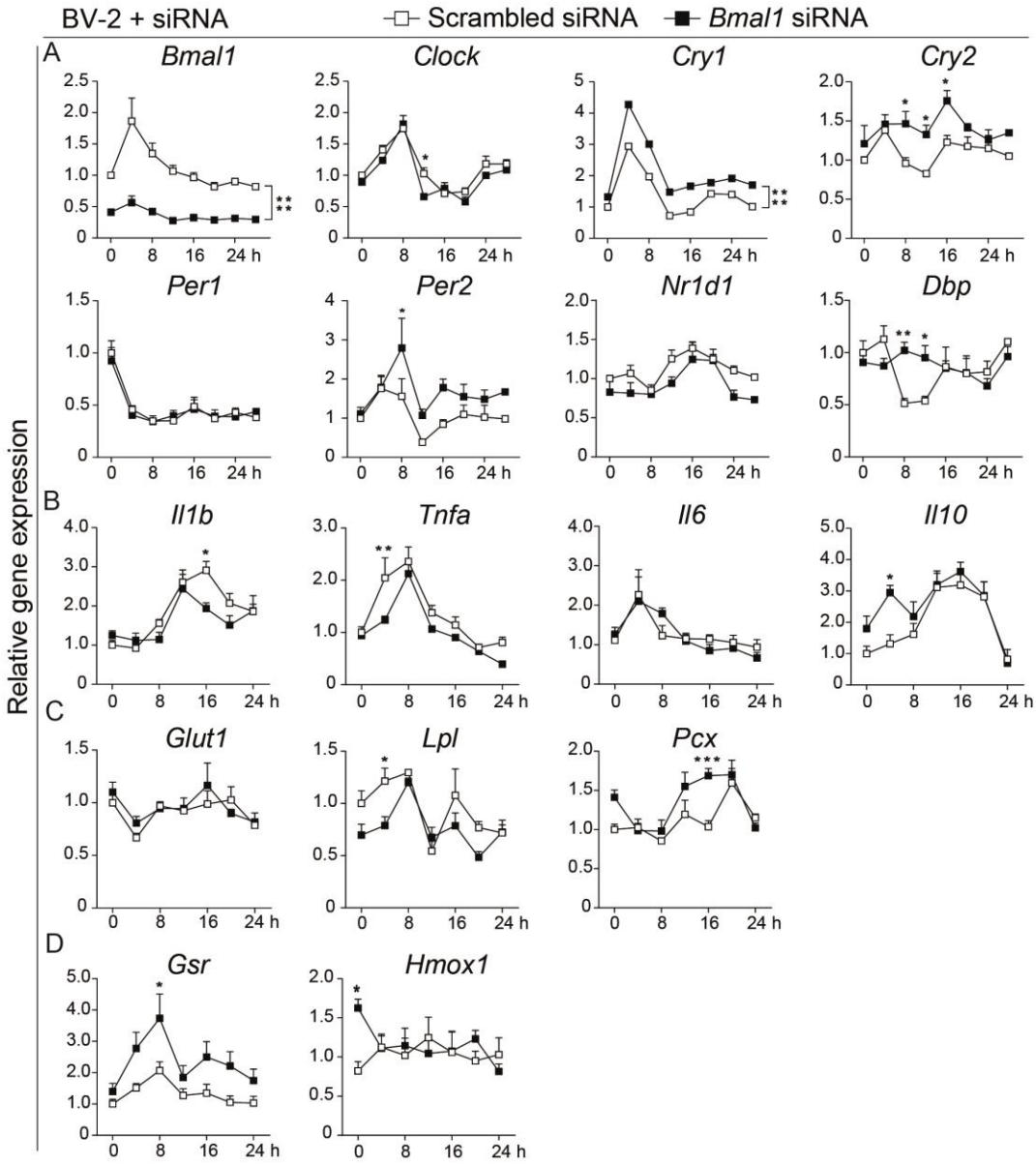

Figure 3

Bmal1 deficiency decreases inflammation and nutrient utilization of microglial BV-2 cells. (A-D) Relative gene expression in scrambled siRNA and *Bmal1* siRNA groups (n = 3-6 samples per group per time point).

Clock genes *Bmal1*, *Clock*, *Cry1*, *Cry2*, *Per1*, *Per2*, *Nr1d1*, *Dbp* (A), inflammatory cytokine genes *Il1b*, *Tnfa*, *Il6*, *Il10* (B), glucose and fatty acid metabolism genes *Glut1*, *Lpl*, *Pcx* (C), and antioxidant genes *Gsr*, *Hmox1* (D) were evaluated every 4 h for 28 h after BV-2 cells were exposed to Dex. Data were analyzed with two-way ANOVA. Statistical significance of rhythmic expression was determined by Cosinor analysis. Data are presented as means ± s.e.m. * $P < 0.05$, ** $P < 0.01$, and *** $P < 0.001$.

Bmal1 deficiency decreases the expression of inflammation and nutrient utilization associated genes in BV-2 cells

To assess whether *Bmal1* deficiency also affects immune activity in microglial BV-2 cells, we evaluated the expression of inflammatory cytokine genes and related genes. As expected, expression of the pro-inflammatory cytokines *Il1b* and *Tnfa* was decreased and expression of the anti-inflammatory cytokine *Il10* was increased in the *Bmal1* knock-down group; *Il6* was not different between the two groups (Fig. 3B). Gene expression of the glucose transporter 1 (*Glut1*), which is highly expressed in BV-2 cells, did not differ between the two groups (Fig. 3C). While *Lpl* expression was significantly reduced and *Pcx*, which plays a crucial role in gluconeogenesis and lipogenesis, was increased in the *Bmal1* knock-down group (Fig. 3C). These findings suggest reduced inflammation and nutrient utilization in the *Bmal1* knock-down group. Additionally, *Gsr* and *Hmox1* showed higher expression in the *Bmal1* knock-down group (Fig. 3D). Inflammatory cytokines showed rhythmic expression in both groups (Supplementary Table 3). All of these data suggest that in basal conditions, *Bmal1* knock-down reduces the transcription of inflammation and nutrient utilization-related genes in BV-2 cells.

Bmal1 deficient BV-2 cells show less inflammatory gene expression under LPS stimulation

To further verify the effect of *Bmal1* on the microglial immune response, we challenged the *Bmal1* knock-down and control BV-2 cells with LPS after synchronization. LPS treatment did not change the rhythmic expression of the clock genes-*Bmal1*, *Clock*, or *Per1* in either group (Supplementary Figure 3 and Supplementary Table 3). The *Bmal1* knock-down group showed significantly less pro-inflammatory *Il1b*, *Tnfa*, and *Il6* expression at 4 h and 8 h after LPS treatment, and higher anti-inflammatory *Il10* expression at 4 h than the control group (Fig. 4A). In addition to the production of inflammatory cytokines, LPS stimulation also upregulates Nox2 expression that contributes to oxidative stress (Joseph et al., 2017). But there was no genotype difference in *Nox2* expression (Fig. 4B). *Lpl*, which showed less expression in *Bmal1* deficient group in basal condition, was no difference between the *Bmal1* deficient group and

controls after LPS treatment (Fig. 4C). *Glut1*, *Gsr*, and *Hmox1* expression were similar between the two groups (Fig. 4C and D). Taken together, these data indicate that *Bmal1* knock-down alters inflammation and nutrient utilization transcripts in BV-2 cells after LPS treatment.

Fig. 4.

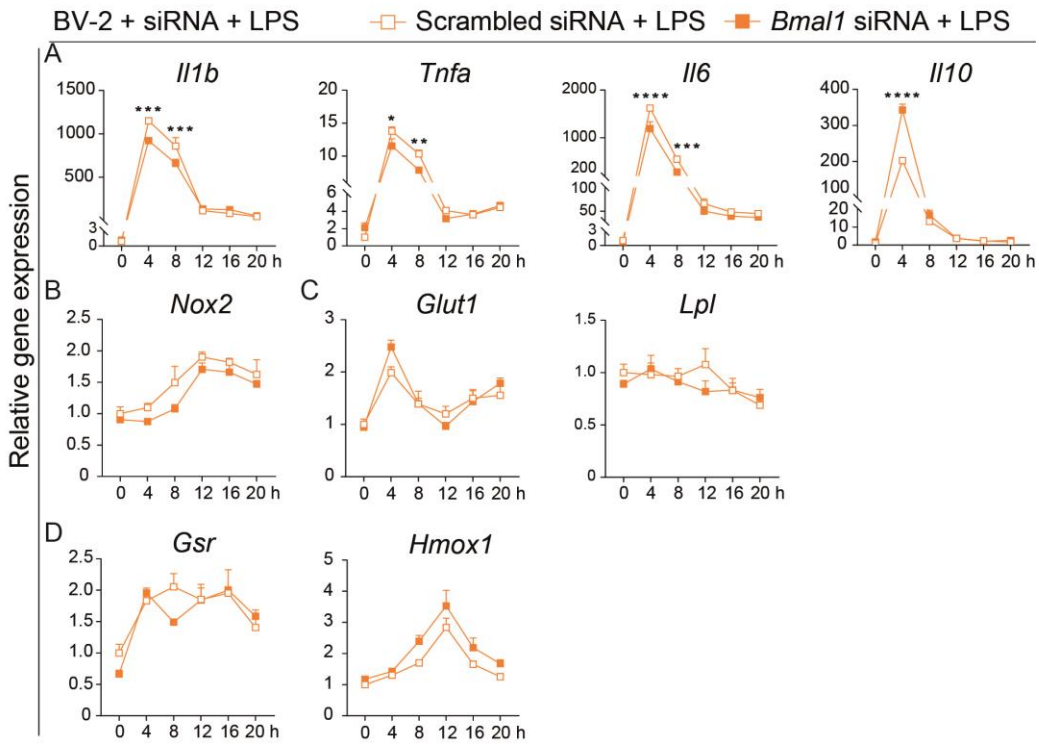

Figure 4

Bmal1 knock-down reduces the pro-inflammatory gene expression and increases the antioxidative anti-inflammatory gene expression of BV-2 cells after LPS stimulation. (A-D) Gene expression in scrambled siRNA and *Bmal1* siRNA groups every 4 h for 20 h in the presence of LPS (n = 3-6 samples per group per time point). Pro-inflammatory cytokine genes *Il1b*, *Tnfa*, *Il6* (A), anti-inflammatory cytokine gene *Il10* (A), oxidative stress gene *Nox2* (B), glucose metabolism gene *Glut1*, and lipid metabolism gene *Lpl* (C), and antioxidant anti-inflammation gene *Gsr*, *Hmox1* (D) were evaluated at 6-time points after LPS exposure. Statistical significance was determined using two-way ANOVA. Statistical significance of the rhythmic expression was determined by Cosinor analysis. Data are presented as means ±s.e.m. * $P < 0.05$, ** $P < 0.01$, and *** $P < 0.001$.

Bmal1 knock-down partially alters the expression of inflammation-related genes in palmitic acid-treated BV-2 cells

It has been shown that consumption of a high-fat diet, especially of its main ingredient the saturated fatty acids, results in hypothalamic microglial activation and inflammation (Gao et al., 2017b). It has also been demonstrated that the saturated fatty acid palmitic acid increases inflammation and oxidative stress in cultured microglial cells (Hidalgo-Lanussa et al., 2018; Yanguas-Casas et al., 2018). To test whether palmitic acid still induces inflammation after synchronization, cells were treated with two concentrations of palmitic acid (100 µM and 200 µM) for 12 h. We observed that both concentrations significantly increased *Il1b* and *Tnfa* expression; while only 100 µM palmitic acid stimulation increased *Il6* expression compared with vehicle (Supplementary Figure 4).

Since our previous study had shown that an HFD disturbs the expression of microglial clock genes and the daily rhythmicity in rats (Milanova et al., 2019b), we first studied clock genes expression in 100 µM palmitic acid-treated BV-2 cells under control and *Bmal1* knock-down conditions. Here, we observed that palmitic acid abolished the rhythmic expression of *Bmal1* and *Clock* in both groups and shifted the rhythmic expression of *Cry1*, *Cry2*, *Per2*, *Nr1d1*, and *Dbp* (Supplementary Figure 5 and Supplementary Table 3). After palmitic acid treatment, clock genes showed a significant decrease at 4 h compared with 0 h. *Bmal1* expression was still lower in the *Bmal1* knock-down group than in controls from 8 h to 24 h. *Cry1*, *Cry2*, *Per2,* and *Dbp* kept an increased expression in the *Bmal1* knock-down group at some time points. While *Clock*, *Per1*, and *Nr1d1* did not differ between the two groups (Supplementary Figure 5).

Next, we evaluated whether *Bmal1* deficiency protects microglia from palmitic acid-induced inflammation. Surprisingly, *Il1b* was significantly increased at 16 h after palmitic acid treatment in the *Bmal1* knock-down group; *Il6* decreased at a later phase (20 h, 24 h) and *Il10* was increased at 20 h in the *Bmal1* knock-down group (Fig. 5A). *Tnfa* expression did not differ between the control and *Bmal1* knock-down groups (Fig. 5A). A previous study has shown that palmitic acid treatment induces oxidative stress through Nox2 upregulation, which also plays an important role in inflammation (Ly et al., 2017). Here the gene expression of *Nox2*, *Glut1*, *Lpl*, and *Gsr* showed no differences between the two groups (Fig. 5B-D). But *Bmal1* deficiency increased *Hmox1* expression at 12 h after palmitic acid stimulation (Fig. 5D). Together, these data suggest that *Bmal1* knock-down totally disturbs the rhythmic expression of clock genes, and only partially reduces the expression of palmitic acid-induced inflammation and oxidative stress associated genes in BV-2 cells.

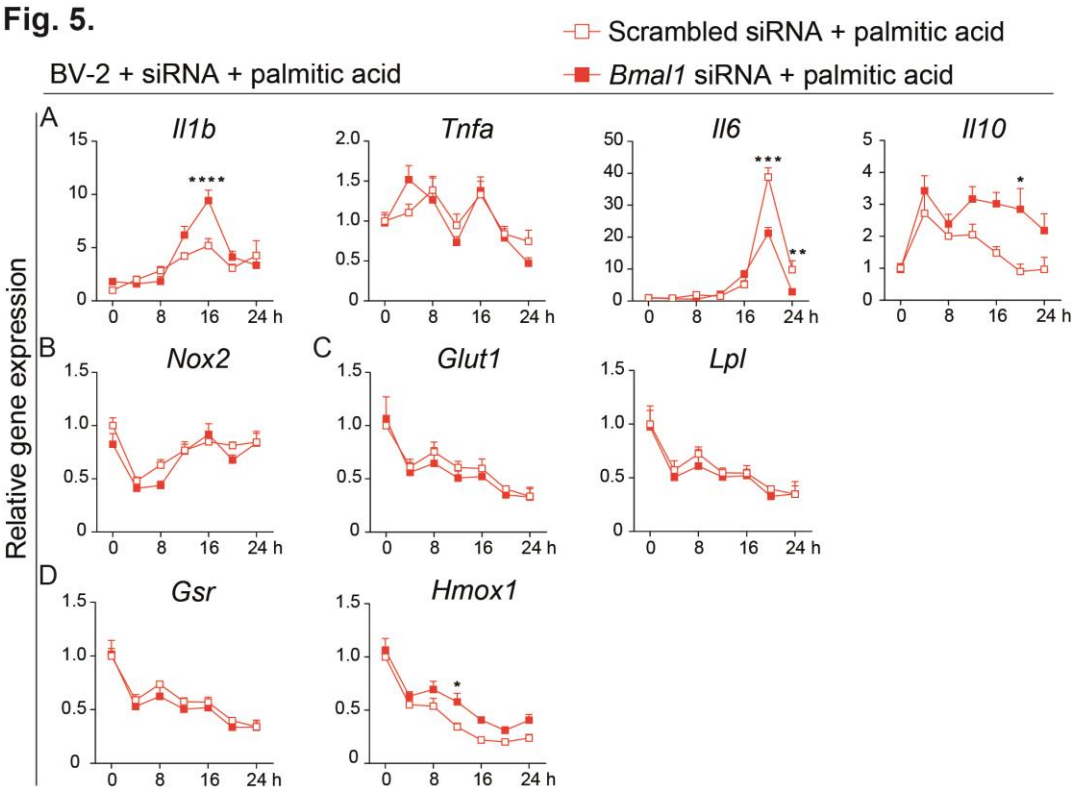

Figure 5

Bmal1 knock-down partially decreases the pro-inflammatory gene expression and increases the antioxidative anti-inflammatory gene expression in palmitic acid-treated BV-2 cells. (A-D) Gene expression in scrambled siRNA and *Bmal1* siRNA groups every 4 h for 24 h in the presence of palmitic acid (n = 3-6 samples per group per time point). Pro-inflammatory cytokine genes Il1b, Tnfa, Il6 (A), anti-inflammatory cytokine gene *Il10* (A), oxidative stress gene *Nox2* (B), glucose metabolism gene *Glut1*, and lipid metabolism gene *Lpl* (C), and antioxidant anti-inflammation gene *Gsr*, *Hmox1* (D) were evaluated at 7-time points after palmitic acid treatment. Statistical significance was determined using two-way ANOVA. Statistical significance of rhythmic expression was determined by Cosinor analysis. Data are presented as means ± s.e.m. * $P < 0.05$, ** $P < 0.01$, and *** $P < 0.001$.

Bmal1 deficiency alters metabolic processes and increases phagocytosis of microglia

To affirm the Bmal1 effects on nutrient utilization, we evaluated the dynamic process of glucose and free fatty acid uptake in primary microglial cells. Bmal1 was significantly

decreased in Bmal1 KO microglia compared with Ctrls 48 h after the 4-hydroxytamoxifen treatment (Fig. 6A). At 2 min after the treatment of 2-NBDG, we observed an increased glucose uptake in Bmal1 KO microglia compared to Ctrls in basal condition; LPS stimulation increased glucose uptake in Ctrls, however, which was not observed in Bmal1 KO microglia when compared with the basal conditions (Fig. 6B). No differences were observed when extending the incubation of 2-NBDG to 5 min and 10 min (Fig. 6B). Interestingly, Bmal1 KO microglia treated with LPS showed less free fatty acid uptake compared with their basal condition at 45min and 60 min, respectively (Fig. 6C). But there was no genotype difference in free fatty acid uptake at each time point (Fig. 6C). Moreover, we saw less cellular ROS activity in Bmal1 KO microglia than Ctrl microglia under H2O2 stimulation, while no genotype difference in basal condition (Fig. 6D). No differences were observed in glucose and free fatty acid uptake after palmitic acid stimulation (Supplementary Figure 6). Surprisingly, the phagocytic capacity was significantly increased in Bmal1 knock-down BV-2 cells (Fig. 6E-F). These data indicate that Bmal1 KO microglia shift glucose and lipid utilization, and show an increase of phagocytosis.

Fig.6.

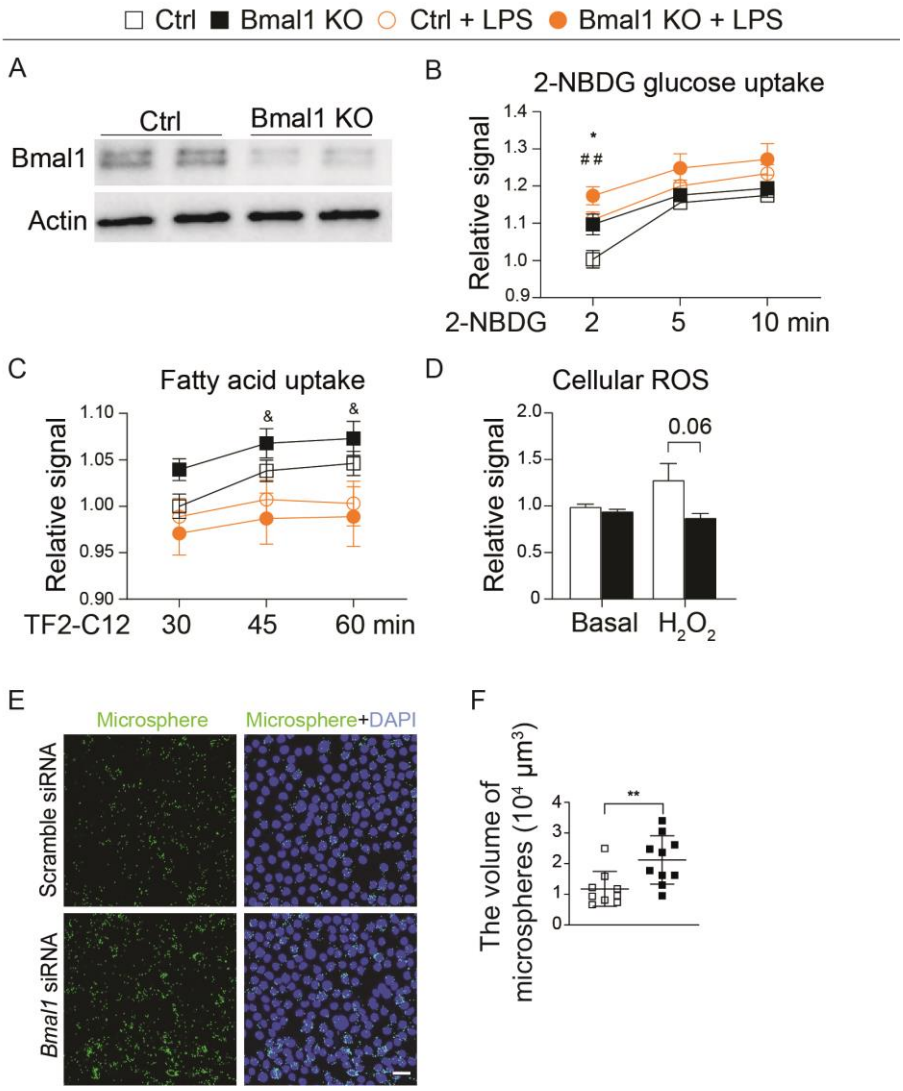

Figure 6

Knockout of Bmal1 affects energy utilization of microglial cells. (A) Bmal1 KO efficiency in microglia (n = 4 samples per group). (B-C) 2-NBDG glucose uptake (B, n = 9-10 samples per group), and free fatty acid uptake (C, n = 5 samples per group) of Ctrl and Bmal1 KO microglia under basal and LPS conditions. * Bmal1 KO *vs* Ctrl; ## Ctrl + LPS *vs* Ctrl; & Bmal1 KO + LPS *vs* Bmal1 KO. (D) Cellular ROS level in Ctrl and Bmal1 KO microglia under basal and H_2O_2 stimulation (n = 5 samples per group). (E-F) Image of

microspheres in BV-2 cells in scrambled siRNA and *Bmal1* siRNA groups after 1 h incubation (n = 9-10 samples per group). Scale bar, 30 μm. (x) The uptake of microspheres. Statistical significance was determined using two-way ANOVA and unpaired *t*-test. Data are presented as means ± s.e.m. * $P < 0.05$, & $P < 0.05$, and ## $P < 0.01$.

Discussion

Circadian rhythms are closely related to immunity and metabolism (Cedernaes et al., 2019; Man et al., 2016; Scheiermann et al., 2013). However, it was still unclear whether and if so, how the endogenous circadian clock regulates microglial immune response and metabolism. Here, we observed a significant daily rhythmic expression of inflammation, nutrient utilization, and antioxidation related genes in microglia isolated from mice. We further found that deficiency of *Bmal1* affected inflammation and nutrient utilization associated gene expression in microglial cells (Fig. 7).

Fig.7.

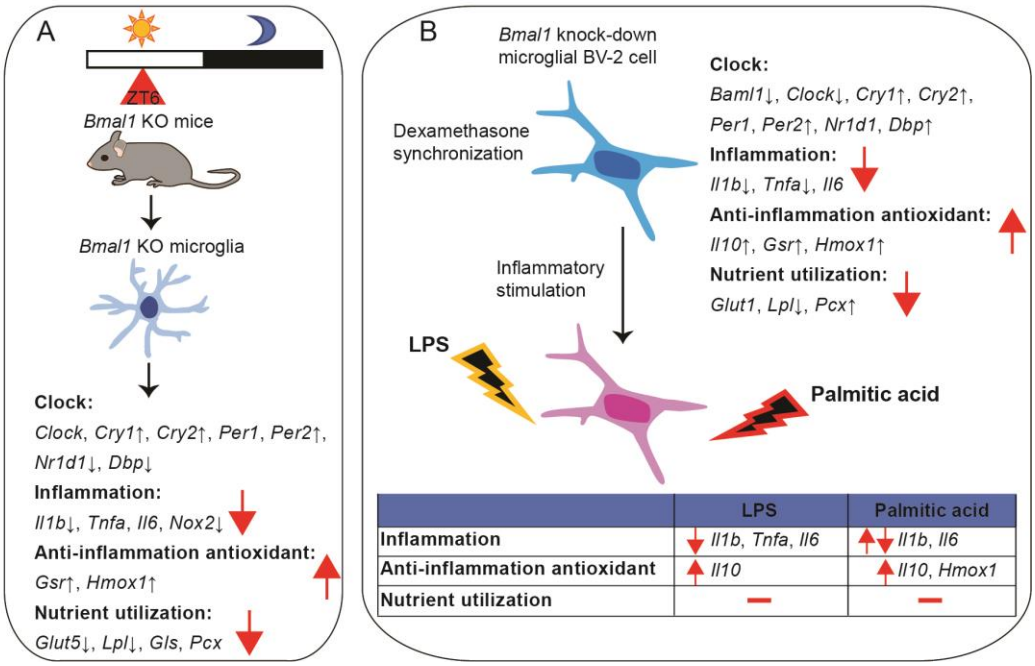

Figure 7

Gene expression summary. (A) Summary of *Bmal1* KO effects in microglia isolated from mice. (B) Summary of *Bmal1* knock-down effects in microgial BV-2 cells.

We evaluated gene expression of inflammatory cytokines in *Bmal1* knock-down microglia in both *Bmal1* KO mice and BV-2 cells. Lacking *Bmal1* decreased pro-inflammatory gene expression and increased anti-inflammatory gene expression in microglial cells. It is known that *Bmal1* expression is higher during the light phase than the dark phase (Hayashi et al., 2013), which is consistent with pro-inflammatory cytokine gene expression in microglia in mice under light/dark conditions. This may explain why *Bmal1* deficient microglia showed less inflammation. Moreover, Bmal1 as a transcription factor not only controls clock genes expression, but also regulates the expression of other genes via specific binding regulatory elements [E-box, D-box, and RORE (Ror/Rev-erb-binding element)] in their promoters (Duffield, 2003; Reppert and Weaver, 2002; Sato et al., 2004; Zhang et al., 2014b). It has been shown that Bmal1 directly regulates *Il6* transactivation in microglia; conditional Bmal1 deficiency in microglial cells attenuates the ischemic neuronal damage in mice (Nakazato et al., 2017). In macrophages, Bmal1 regulates inflammation via controlling the gene expression of *Nrf2*, which plays a critical role in the innate immune system (Early et al., 2018b). Bmal1 deficiency in bone marrow-derived macrophages leads to increased IL-1β expression and increases polymicrobial infection in mice (Deng et al., 2018; Early et al., 2018b). However, myeloid cell Bmal1 deletion protects against bacterial infection in the lung (Kitchen et al., 2020a). We noticed that in peritoneal macrophages, *Bmal1* is highly expressed during the dark phase, which is different from the daily rhythm in microglia (Deng et al., 2018). In rat monocytes, *Bmal1* does not show a clear daily rhythm in gene expression, while *Tnfa* shows a high expression during the dark phase (Milanova et al., 2019b). These data suggest that Bmal1 regulates the innate immune system, but that the rhythmicity of clock genes and inflammatory cytokines is heterogeneous among innate immune cells and depends on the specific tissue.

Furthermore, we observed that *Bmal1* deletion affected the expression level of other clock genes, especially *Cry1*, *Cry2,* and *Per2* were significantly increased in *Bmal1* KO microglia. It has been shown that overexpression of Cry1 significantly decreases inflammation in atherosclerotic mice (Yang et al., 2015), whereas the absence of Cry1 and Cry2 leads to increased pro-inflammatory cytokine expression in macrophages (Narasimamurthy et al., 2012). *Per2* negatively regulates the expression of pro-inflammatory cytokines in zebrafish (Ren et al., 2018). *Bmal1* deficiency-induced the increased gene expression of *Cry1*, *Cry2,* and *Per2* may also contribute to the reduced inflammation of *Bmal1* KO microglial cells.

Circadian clocks are fundamental physiological regulators in energy homeostasis and the immune system. Diurnal oscillations in glucose and lipid metabolism are due in part to daily changes in energy requirements (Kumar Jha et al., 2015). As the resident brain macrophages, microglia provide continually surveillant and scavenging functions in the brain (Nimmerjahn et al., 2005). Here, we found that microglial glucose and lipid utilization transcripts show clear daily rhythmicity, and both are significantly higher during the regular activity period in mice (i.e. the dark period). *Bmal1* deficiency decreased the expression of nutrient utilization related genes in microglia under basal condition and shifted the metabolic processes under LPS stimulation. Reduced substrates utilization was observed in Bmal1 KO skeletal muscle (Dyar et al., 2018; Schiaffino et al., 2016). A recent study showed that Bmal1 deletion also protects mice from insulin resistance induced by circadian disruption (Yang et al., 2019).

Prior work has demonstrated that ROS production and scavenging related genes exhibit a time-of-day specific expression under diurnal and circadian conditions (Lai et al., 2012). We found that *Bmal1* deficiency protected microglia from oxidative damage and inflammation. On the other hand, neuronal Bmal1 deletion causes oxidative damage and impaired expression of the redox defense gene (Musiek et al., 2013a), which suggests that the effect of Bmal1 on oxidative stress is different depending on the cell type involved. Moreover, microglia can polarize into a pro-inflammatory or an anti-inflammatory phenotype (Olah et al., 2011; Orihuela et al., 2016). *Bmal1* KO microglia may polarize into the anti-inflammatory state by increasing IL-10 gene expression to facilitate phagocytosis of cell debris and antagonizing the pro-inflammatory response.

Recently, it has been shown that the intrinsic circadian clocks, such as REV-ERBα, REV-ERBβ, and Bmal1, affect microglial amyloid-β clearance in the 5XFAD mouse model of Alzheimer's disease (Lee et al., 2020a). Based on our findings, future work should measure inflammatory cytokine levels in combination with mitochondrial fuel utilization in microglia lacking Bmal1. Furthermore, the immune response in microglia-specific Bmal1 knockout mice still needs to be explored. Microglia are closely related to neuroinflammation, neurodegeneration, and obesity. Thus, future work should evaluate Bmal1 knockout microglial function and neuronal changes in mice under different stressful conditions, such as LPS and high-fat diet, or in combination with neurodegenerative diseases.

In conclusion, Bmal1 is a critical regulator in microglial function. Bmal1 deficiency alters microglial inflammatory profile, including inhibiting the gene expression of pro-inflammatory cytokines and elevating the expression of antioxidative anti-inflammatory factors, as well as affects microglial nutrient utilization and phagocytosis. Our work indicates that targeting the

molecular biological clock-*Bmal1* in microglia might be a new approach to treat inflammation-related diseases in the brain.

Funding

This work was supported by the "NeuroTime" Erasmus Mundus program, University of Strasbourg, CNRS and ANR-18-CE16-0008 (to ALB).

Conflicts of interest

The authors report no competing interests.

Ethics approval

The experiments were approved by and performed according to the guidelines of the institutional Animal Care and Use Committee of the Netherlands.

Consent to participate

The authors consent to participate.

Consent to publication

The authors consent to publication.

Availability of data and material

The authors confirm that the data supporting the findings of this study are available within the article and its Supplementary Material.

Author contributions

X.L.W., S.E.C.W., N.K., I.M., S.K., performed the experiments. X.L.W. analyzed the data and wrote the manuscript. X.L.W., C.X.Y., A.L.B. designed the study. A.K., A.L.B. edited the manuscript. All authors participated in the discussion of the results, critically polished, and approved the final manuscript.

Acknowledgments

We would like to thank Marie-Paule Felder-Schmittbuhl (Institute of Cellular and Integrative Neurosciences, CNRS, Université de Strasbourg, Strasbourg, France) and people from Luc Dupuis laboratory (Université de Strasbourg, INSERM, UMR-S1118, Strasbourg, France) for helping with primary microglia cultures. This project has been funded with support from the NeuroTime Erasmus+ program of the European Commission, University of Strasbourg, CNRS. X.L.W. salary was supported by NeuroTime Erasmus+ program of the European Commission, as well as partly by ANR-18-CE16-0008 (to ALB).

References

Barca-Mayo, O., Boender, A.J., Armirotti, A., and De Pietri Tonelli, D. (2019). Deletion of astrocytic BMAL1 results in metabolic imbalance and shorter lifespan in mice. Glia.

Barca-Mayo, O., Pons-Espinal, M., Follert, P., Armirotti, A., Berdondini, L., and De Pietri Tonelli, D. (2017). Astrocyte deletion of Bmal1 alters daily locomotor activity and cognitive functions via GABA signalling. Nat Commun *8*, 14336.

Bass, J., and Takahashi, J.S. (2010). Circadian integration of metabolism and energetics. Science *330*, 1349-1354.

Bellet, M.M., Deriu, E., Liu, J.Z., Grimaldi, B., Blaschitz, C., Zeller, M., Edwards, R.A., Sahar, S., Dandekar, S., Baldi, P.*, et al.* (2013). Circadian clock regulates the host response to Salmonella. Proc Natl Acad Sci U S A *110*, 9897-9902.

Blasi, E., Barluzzi, R., Bocchini, V., Mazzolla, R., and Bistoni, F. (1990). Immortalization of murine microglial cells by a v-raf/v-myc carrying retrovirus. J Neuroimmunol *27*, 229-237.

Bunger, M.K., Wilsbacher, L.D., Moran, S.M., Clendenin, C., Radcliffe, L.A., Hogenesch, J.B., Simon, M.C., Takahashi, J.S., and Bradfield, C.A. (2000). Mop3 is an essential component of the master circadian pacemaker in mammals. Cell *103*, 1009-1017.

Cedernaes, J., Waldeck, N., and Bass, J. (2019). Neurogenetic basis for circadian regulation of metabolism by the hypothalamus. Genes Dev *33*, 1136-1158.

Curtis, A.M., Bellet, M.M., Sassone-Corsi, P., and O'Neill, L.A. (2014). Circadian clock proteins and immunity. Immunity *40*, 178-186.

Deng, W., Zhu, S., Zeng, L., Liu, J., Kang, R., Yang, M., Cao, L., Wang, H., Billiar, T.R., Jiang, J.*, et al.* (2018). The Circadian Clock Controls Immune Checkpoint Pathway in Sepsis. Cell Rep *24*, 366-378.

Ding, X.Y., Zhang, M., Gu, R.P., Xu, G.Z., and Wu, H.X. (2017). Activated microglia induce the production of reactive oxygen species and promote apoptosis of co-cultured retinal microvascular pericytes. Graef Arch Clin Exp *255*, 777-788.

Dudek, M., and Meng, Q.J. (2014). Running on time: the role of circadian clocks in the musculoskeletal system. Biochem J *463*, 1-8.

Duffield, G.E. (2003). DNA microarray analyses of circadian timing: the genomic basis of biological time. J Neuroendocrinol *15*, 991-1002.

Dyar, K.A., Hubert, M.J., Mir, A.A., Ciciliot, S., Lutter, D., Greulich, F., Quagliarini, F., Kleinert, M., Fischer, K., Eichmann, T.O.*, et al.* (2018). Transcriptional programming of lipid and amino acid metabolism by the skeletal muscle circadian clock. PLoS Biol *16*, e2005886.

Early, J.O., Menon, D., Wyse, C.A., Cervantes-Silva, M.P., Zaslona, Z., Carroll, R.G., Palsson-McDermott, E.M., Angiari, S., Ryan, D.G., Corcoran, S.E.*, et al.* (2018). Circadian clock protein BMAL1 regulates IL-1beta in macrophages via NRF2. Proc Natl Acad Sci U S A *115*, E8460-E8468.

Fonken, L.K., Frank, M.G., Kitt, M.M., Barrientos, R.M., Watkins, L.R., and Maier, S.F. (2015a). Microglia inflammatory responses are controlled by an intrinsic circadian clock. Brain Behav Immun *45*, 171-179.

Fonken, L.K., Frank, M.G., Kitt, M.M., Barrientos, R.M., Watkins, L.R., and Maier, S.F. (2015b). Microglia inflammatory responses are controlled by an intrinsic circadian clock. Brain, Behavior, and Immunity *45*, 171-179.

Gabriel, B.M., and Zierath, J.R. (2019). Circadian rhythms and exercise - re-setting the clock in metabolic disease. Nat Rev Endocrinol *15*, 197-206.

Gao, Y.Q., Vidal-Itriago, A., Kalsbeek, M.J., Layritz, C., Garcia-Caceres, C., Tom, R.Z., Eichmann, T.O., Vaz, F.M., Houtkooper, R.H., van der Wel, N.*, et al.* (2017). Lipoprotein Lipase Maintains Microglial Innate Immunity in Obesity. Cell Reports *20*, 3034-3042.

Gekakis, N., Staknis, D., Nguyen, H.B., Davis, F.C., Wilsbacher, L.D., King, D.P., Takahashi, J.S., and Weitz, C.J. (1998). Role of the CLOCK protein in the mammalian circadian mechanism. Science *280*, 1564-1569.

Geltink, R.I.K., Kyle, R.L., and Pearce, E.L. (2018). Unraveling the Complex Interplay Between T Cell Metabolism and Function. Annual Review of Immunology, Vol 36 *36*, 461-488.

Gerstner, J.R., and Yin, J.C. (2010). Circadian rhythms and memory formation. Nat Rev Neurosci *11*, 577-588.

Griffin, P., Dimitry, J.M., Sheehan, P.W., Lananna, B.V., Guo, C., Robinette, M.L., Hayes, M.E., Cedeno, M.R., Nadarajah, C.J., Ezerskiy, L.A.*, et al.* (2019). Circadian clock protein Rev-erba regulates neuroinflammation. P Natl Acad Sci USA *116*, 5102-5107.

Hatanaka, F., Matsubara, C., Myung, J., Yoritaka, T., Kamimura, N., Tsutsumi, S., Kanai, A., Suzuki, Y., Sassone-Corsi, P., Aburatani, H.*, et al.* (2010). Genome-wide profiling of the core clock protein BMAL1 targets reveals a strict relationship with metabolism. Mol Cell Biol *30*, 5636-5648.

Hayashi, Y., Koyanagi, S., Kusunose, N., Okada, R., Wu, Z., Tozaki-Saitoh, H., Ukai, K., Kohsaka, S., Inoue, K., Ohdo, S*., et al.* (2013). The intrinsic microglial molecular clock controls synaptic strength via the circadian expression of cathepsin S. Sci Rep *3*, 2744.

Hickman, S., Izzy, S., Sen, P., Morsett, L., and El Khoury, J. (2018). Microglia in neurodegeneration. Nature Neuroscience *21*, 1359-1369.

Hidalgo-Lanussa, O., Avila-Rodriguez, M., Baez-Jurado, E., Zamudio, J., Echeverria, V., Garcia-Segura, L.M., and Barreto, G.E. (2018). Tibolone Reduces Oxidative Damage and Inflammation in Microglia Stimulated with Palmitic Acid through Mechanisms Involving Estrogen Receptor Beta. Mol Neurobiol *55*, 5462-5477.

Hogenboom, R., Kalsbeek, M.J., Korpel, N.L., de Goede, P., Koenen, M., Buijs, R.M., Romijn, J.A., Swaab, D.F., Kalsbeek, A., and Yi, C.X. (2019). Loss of arginine vasopressin- and vasoactive intestinal polypeptide-containing neurons and glial cells in the suprachiasmatic nucleus of individuals with type 2 diabetes. Diabetologia.

Joseph, L.C., Kokkinaki, D., Valenti, M.C., Kim, G.J., Barca, E., Tomar, D., Hoffman, N.E., Subramanyam, P., Colecraft, H.M., Hirano, M*., et al.* (2017). Inhibition of NADPH oxidase 2 (NOX2) prevents sepsis-induced cardiomyopathy by improving calcium handling and mitochondrial function. JCI Insight *2*.

Kitchen, G.B., Cunningham, P.S., Poolman, T.M., Iqbal, M., Maidstone, R., Baxter, M., Bagnall, J., Begley, N., Saer, B., Hussell, T*., et al.* (2020). The clock gene Bmal1 inhibits macrophage motility, phagocytosis, and impairs defense against pneumonia. Proc Natl Acad Sci U S A.

Kumar Jha, P., Challet, E., and Kalsbeek, A. (2015). Circadian rhythms in glucose and lipid metabolism in nocturnal and diurnal mammals. Mol Cell Endocrinol *418 Pt 1*, 74-88.

Lai, A.G., Doherty, C.J., Mueller-Roeber, B., Kay, S.A., Schippers, J.H., and Dijkwel, P.P. (2012). CIRCADIAN CLOCK-ASSOCIATED 1 regulates ROS homeostasis and oxidative stress responses. Proc Natl Acad Sci U S A *109*, 17129-17134.

Lee, J., Kim, D.E., Griffin, P., Sheehan, P.W., Kim, D.H., Musiek, E.S., and Yoon, S.Y. (2020). Inhibition of REV-ERBs stimulates microglial amyloid-beta clearance and reduces amyloid plaque deposition in the 5XFAD mouse model of Alzheimer's disease. Aging Cell *19*.

Ly, L.D., Xu, S., Choi, S.K., Ha, C.M., Thoudam, T., Cha, S.K., Wiederkehr, A., Wollheim, C.B., Lee, I.K., and Park, K.S. (2017). Oxidative stress and calcium dysregulation by palmitate in type 2 diabetes. Exp Mol Med *49*, e291.

Man, K., Loudon, A., and Chawla, A. (2016). Immunity around the clock. Science *354*, 999-1003.

McLoughlin, M.R., Orlicky, D.J., Prigge, J.R., Krishna, P., Talago, E.A., Cavigli, I.R., Eriksson, S., Miller, C.G., Kundert, J.A., Sayin, V.I.*, et al.* (2019). TrxR1, Gsr, and oxidative stress determine hepatocellular carcinoma malignancy. Proc Natl Acad Sci U S A *116*, 11408-11417.

Milanova, I.V., Kalsbeek, M.J.T., Wang, X.L., Korpel, N.L., Stenvers, D.J., Wolff, S.E.C., de Goede, P., Heijboer, A.C., Fliers, E., la Fleur, S.E.*, et al.* (2019). Diet-Induced Obesity Disturbs Microglial Immunometabolism in a Time-of-Day Manner. Front Endocrinol (Lausanne) *10*, 424.

Musiek, E.S., Lim, M.M., Yang, G., Bauer, A.Q., Qi, L., Lee, Y., Roh, J.H., Ortiz-Gonzalez, X., Dearborn, J.T., Culver, J.P.*, et al.* (2013). Circadian clock proteins regulate neuronal redox homeostasis and neurodegeneration. J Clin Invest *123*, 5389-5400.

Nakazato, R., Hotta, S., Yamada, D., Kou, M., Nakamura, S., Takahata, Y., Tei, H., Numano, R., Hida, A., Shimba, S.*, et al.* (2017). The intrinsic microglial clock system regulates interleukin-6 expression. Glia *65*, 198-208.

Narasimamurthy, R., Hatori, M., Nayak, S.K., Liu, F., Panda, S., and Verma, I.M. (2012). Circadian clock protein cryptochrome regulates the expression of proinflammatory cytokines. Proc Natl Acad Sci U S A *109*, 12662-12667.

Nimmerjahn, A., Kirchhoff, F., and Helmchen, F. (2005). Resting microglial cells are highly dynamic surveillants of brain parenchyma in vivo. Science *308*, 1314-1318.

Olah, M., Biber, K., Vinet, J., and Boddeke, H.W. (2011). Microglia phenotype diversity. CNS Neurol Disord Drug Targets *10*, 108-118.

Orihuela, R., McPherson, C.A., and Harry, G.J. (2016). Microglial M1/M2 polarization and metabolic states. Br J Pharmacol *173*, 649-665.

Piantadosi, C.A., Withers, C.M., Bartz, R.R., MacGarvey, N.C., Fu, P., Sweeney, T.E., Welty-Wolf, K.E., and Suliman, H.B. (2011). Heme oxygenase-1 couples activation of mitochondrial biogenesis to anti-inflammatory cytokine expression. J Biol Chem *286*, 16374-16385.

Poss, K.D., and Tonegawa, S. (1997). Reduced stress defense in heme oxygenase 1-deficient cells. Proc Natl Acad Sci U S A *94*, 10925-10930.

Rahman, S.A., Castanon-Cervantes, O., Scheer, F.A., Shea, S.A., Czeisler, C.A., Davidson, A.J., and Lockley, S.W. (2015). Endogenous circadian regulation of pro-inflammatory cytokines and chemokines in the presence of bacterial lipopolysaccharide in humans. Brain Behav Immun *47*, 4-13.

Ren, D.L., Zhang, J.L., Yang, L.Q., Wang, X.B., Wang, Z.Y., Huang, D.F., Tian, C., and Hu, B. (2018). Circadian genes period1b and period2 differentially regulate inflammatory responses in zebrafish. Fish Shellfish Immun *77*, 139-146.

Reppert, S.M., and Weaver, D.R. (2002). Coordination of circadian timing in mammals. Nature *418*, 935-941.

Ripperger, J.A., and Schibler, U. (2006). Rhythmic CLOCK-BMAL1 binding to multiple E-box motifs drives circadian Dbp transcription and chromatin transitions. Nat Genet *38*, 369-374.

Rojo, A.I., McBean, G., Cindric, M., Egea, J., Lopez, M.G., Rada, P., Zarkovic, N., and Cuadrado, A. (2014). Redox control of microglial function: molecular mechanisms and functional significance. Antioxid Redox Signal *21*, 1766-1801.

Rudic, R.D., McNamara, P., Curtis, A.M., Boston, R.C., Panda, S., Hogenesch, J.B., and Fitzgerald, G.A. (2004). BMAL1 and CLOCK, two essential components of the circadian clock, are involved in glucose homeostasis. PLoS Biol *2*, e377.

Sato, S., Sakurai, T., Ogasawara, J., Takahashi, M., Izawa, T., Imaizumi, K., Taniguchi, N., Ohno, H., and Kizaki, T. (2014). A circadian clock gene, Rev-erbalpha, modulates the inflammatory function of macrophages through the negative regulation of Ccl2 expression. J Immunol *192*, 407-417.

Sato, T.K., Panda, S., Miraglia, L.J., Reyes, T.M., Rudic, R.D., McNamara, P., Naik, K.A., Fitzgerald, G.A., Kay, S.A., and Hogenesch, J.B. (2004). A functional genomics strategy reveals rora as a component of the mammalian circadian clock. Neuron *43*, 527-537.

Scheiermann, C., Kunisaki, Y., and Frenette, P.S. (2013). Circadian control of the immune system. Nat Rev Immunol *13*, 190-198.

Schiaffino, S., Blaauw, B., and Dyar, K.A. (2016). The functional significance of the skeletal muscle clock: lessons from Bmal1 knockout models. Skelet Muscle *6*, 33.

Semmler, A., Frisch, C., Debeir, T., Ramanathan, M., Okulla, T., Klockgether, T., and Heneka, M.T. (2007). Long-term cognitive impairment, neuronal loss and reduced cortical cholinergic innervation after recovery from sepsis in a rodent model. Experimental Neurology *204*, 733-740.

Semmler, A., Widmann, C.N., Okulla, T., Urbach, H., Kaiser, M., Widman, G., Mormann, F., Weide, J., Fliessbach, K., Hoeft, A.*, et al.* (2013). Persistent cognitive impairment, hippocampal atrophy and EEG changes in sepsis survivors. J Neurol Neurosur Ps *84*, 62-70.

Stenvers, D.J., Scheer, F.A.J.L., Schrauwen, P., la Fleur, S.E., and Kalsbeek, A. (2019). Circadian clocks and insulin resistance. Nat Rev Endocrinol *15*, 75-89.

Sussman, W., Stevenson, M., Mowdawalla, C., Mota, S., Ragolia, L., and Pan, X.Y. (2019). BMAL1 controls glucose uptake through paired-homeodomain transcription factor 4 in differentiated Caco-2 cells. Am J Physiol-Cell Ph *317*, C492-C501.

Thaler, J.P., Yi, C.X., Schur, E.A., Guyenet, S.J., Hwang, B.H., Dietrich, M.O., Zhao, X.L., Sarruf, D.A., Izgur, V., Maravilla, K.R.*, et al.* (2012). Obesity is associated with hypothalamic injury in rodents and humans (vol 122, pg 153, 2012). Journal of Clinical Investigation *122*, 778-778.

Valdearcos, M., Douglass, J.D., Robblee, M.M., Dorfman, M.D., Stifler, D.R., Bennett, M.L., Gerritse, I., Fasnacht, R., Barres, B.A., Thaler, J.P.*, et al.* (2017). Microglial Inflammatory Signaling Orchestrates the Hypothalamic Immune Response to Dietary Excess and Mediates Obesity Susceptibility. Cell Metabolism *26*, 185-+.

Vijayan, V., Pradhan, P., Braud, L., Fuchs, H.R., Gueler, F., Motterlini, R., Foresti, R., and Immenschuh, S. (2019). Human and murine macrophages exhibit differential metabolic responses to lipopolysaccharide - A divergent role for glycolysis. Redox Biol *22*, 101147.

Wang, L., Pavlou, S., Du, X., Bhuckory, M., Xu, H., and Chen, M. (2019). Glucose transporter 1 critically controls microglial activation through facilitating glycolysis. Mol Neurodegener *14*, 2.

Widmann, C.N., and Heneka, M.T. (2014). Long-term cerebral consequences of sepsis. Lancet Neurol *13*, 630-636.

Yang, G., Chen, L., Zhang, J., Ren, B., and FitzGerald, G.A. (2019). Bmal1 deletion in mice facilitates adaptation to disrupted light/dark conditions. JCI Insight *5*.

Yang, L., Chu, Y., Wang, L., Wang, Y., Zhao, X., He, W., Zhang, P., Yang, X., Liu, X., Tian, L.*, et al.* (2015). Overexpression of CRY1 protects against the development of atherosclerosis via the TLR/NF-kappaB pathway. Int Immunopharmacol *28*, 525-530.

Yanguas-Casas, N., Crespo-Castrillo, A., de Ceballos, M.L., Chowen, J.A., Azcoitia, I., Arevalo, M.A., and Garcia-Segura, L.M. (2018). Sex differences in the phagocytic and migratory activity of microglia and their impairment by palmitic acid. Glia *66*, 522-537.

Yi, C.X., Walter, M., Gao, Y.Q., Pitra, S., Legutko, B., Kalin, S., Layritz, C., Garcia-Caceres, C., Bielohuby, M., Bidlingmaier, M.*, et al.* (2017). TNF alpha drives mitochondrial stress in POMC neurons in obesity. Nature Communications *8*.

Zelcer, N., Khanlou, N., Clare, R., Jiang, Q., Reed-Geaghan, E.G., Landreth, G.E., Vinters, H.V., and Tontonoz, P. (2007). Attenuation of neuroinflammation and Alzheimer's disease pathology by liver x receptors. Proc Natl Acad Sci U S A *104*, 10601-10606.

Zhang, R., Lahens, N.F., Ballance, H.I., Hughes, M.E., and Hogenesch, J.B. (2014). A circadian gene expression atlas in mammals: implications for biology and medicine. Proc Natl Acad Sci U S A *111*, 16219-16224.

Supplementary Figures

Supplementary Fig. 1.

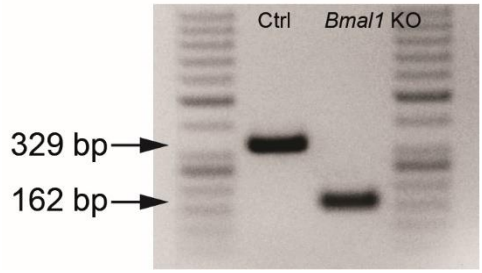

Genotyping results of Ctrl and *Bmal1* KO mice.

Supplementary Fig. 2.

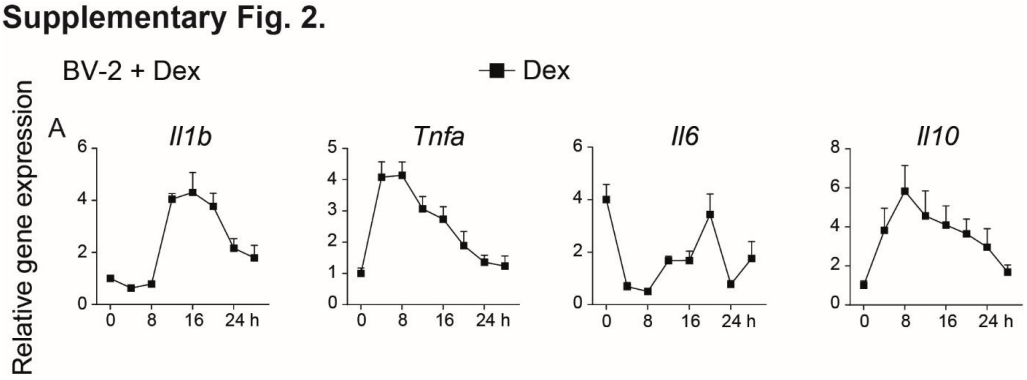

Rhythmic expression of inflammatory genes in microglial BV-2 cells after synchronization. (A) BV-2 cells were synchronized with dexamethasone (Dex, 100 nM) for 2 h, followed by RNA collection every 4 h for 28 h. Inflammatory genes-*Il1b*, *Tnfa*, *Il6*, *Il10* were evaluated by quantitative RT-PCR (n = 4-6 samples per group per time point). Statistical significance of rhythmic expression was determined by Cosinor analysis. Data are presented as means ± s.e.m.

Supplementary Fig. 3.

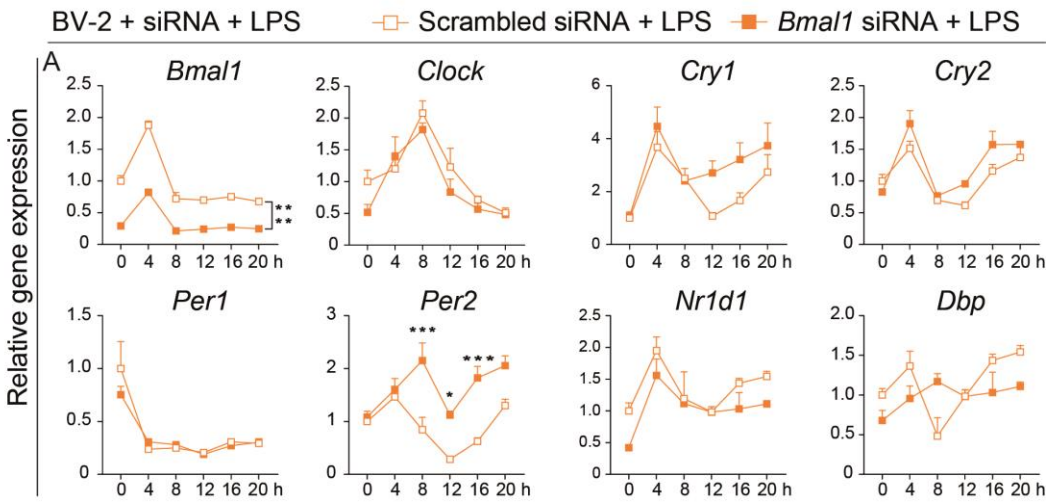

Clock gene expression in scrambled siRNA and *Bmal1* siRNA groups in BV-2 cells after LPS stimulation. (A) The expression of clock genes was evaluated every 4 h for 20 h in the presence of LPS (n = 3-6 samples per group per time point). Statistical significance was determined using two-way ANOVA. Statistical significance of the rhythmic expression was determined by Cosinor analysis. Data are presented as means ± s.e.m. * $P < 0.05$, ** $P < 0.01$, and *** $P < 0.001$.

Supplementary Fig. 4.

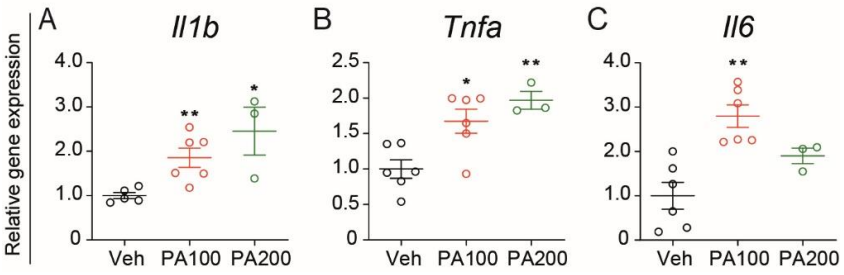

Palmitic acid treatment increases the pro-inflammatory cytokine gene expression in microglial BV-2 cells after synchronization. (A-C) Relative gene expression of pro-inflammatory cytokine genes *Il1b*, *Tnfa*, *Il6*, 12 h after palmitic acid treatment at different concentrations (PA100, palmitic acid 100 μM; PA200, palmitic acid 200 μM) (n = 3-6 samples per group). Statistical significance was determined using unpaired *t*-test. Data are presented as means ± s.e.m. Compared with Veh, * $P < 0.05$, and ** $P < 0.01$.

Supplementary Fig. 5.

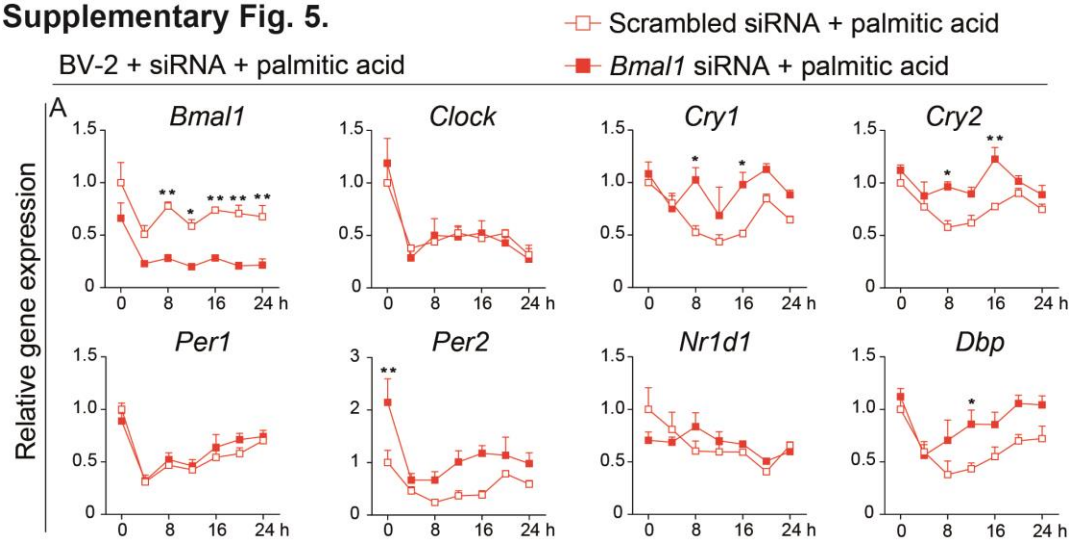

Clock gene expression in scrambled siRNA and *Bmal1* siRNA groups in palmitic acid-treated BV-2 cells. (A) The expression of clock genes was evaluated every 4 h for 24 h in the presence of palmitic acid (n = 3-6 samples per group per time point). Statistical significance was determined using two-way ANOVA. Statistical significance of rhythmic expression was determined by Cosinor analysis. Data are presented as means ± s.e.m. * $P < 0.05$, and ** $P < 0.01$.

Supplementary Fig. 6.

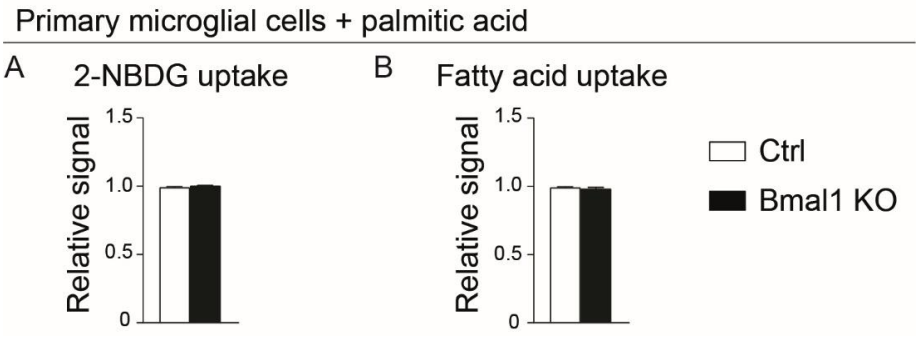

Energy utilization in Ctrl and Bmal1 KO microglial cells treated with palmitic acid. (A-B) 2-NBDG glucose uptake (A), and free fatty acid uptake (B) of Ctrl and Bmal1 KO microglia (n = 5). Statistical significance was determined using two-tailed *t*-test. Data are presented as means ± s.e.m.

Supplementary Tables

Supplementary Table 1. Primers for quantitative PCR

Genes	Accession	Forward primer 5'-3'	Reverse primer 5'-3'
Baml1	NM_007489	ACATCACAAGTACGCCTCCC	TGCTGCCTCATCGTTACTGG
Clock	NM_007715	CAGCAGTGGATATGGCTTCAGA	GACTGCGGTGTGAGATGACTT
Per1	NM_011065	TGTGCATCTGGTAAAGCACCA	TGTACCTGTAGCAAGGAGGCG
Per2	NM_011066	TCTTCCAACACTCACCCCAG	CCTCATTAGCCTTCACCTGCTT
Cry1	NM_007771	GAGGCACTTACACGTTTGGAA	GCATTCATTCGAGGTCGTTCAA
Cry2	NM_009963	TGTGTTCCCAAGGCTGTTCA	TCCCGTTCTTTCCCAAAGGG
Nr1d1	NM_145434	ACAGTGATGTTCCTGAGCCG	TTGGTGAAGCGGGAAGTCTC
Dbp	NM_016974	TGTGGGAATCTGGATGGCAA	CTAGATGTCAAGCGTGGCGAG
Il1b	NM_008361	CAGTTCTGCCATTGACCATC	TCTCACTGAAACTCAGCCGT
Il6	NM_031168	GTTCTCTGGGAAATCGTGGA	TGTACTCCAGGTAGCTATGG
Il10	NM_010548	ATGCAGGACTTTAAGGGTTACTTG	TAGACACCTTGGTCTTGGAGCTTA
Tnfa	NM_013693	TCTCATCAGTTCTATGGCCC	GGGAGTAGACAAGGTACAAC
Glut1	NM_011400	TGATGCGGGAGAAGAAGGTC	CCGTGTTGACGATACCGGAG
Glut5	NM_019741	TAGCCTGCTTAGTGCTGACG	GATGAGCCCCACAGTGAAGT
Lpl	NM_008509	CTCGCTCTCAGATGCCCTAC	AGCAGTTCTCCGATGTCCAC
Pcx	NM_008797	AGAGCTGGGTATCCGCACA	CCGCATCTACACCATTTTCCTTG
Gsr	NM_010344	CTTGCGTGAATGTTGGATGTG	GCATCCCTTTTCTGCTTGATG
Hmox1	NM_010442	ACAGAGGAACACAAAGACCAG	GTGTCTGGGATGAGCTAGTG

Nox2	NM_007807	GGGACTGGGCTGTGAATG	TGACCCAAGGAGTTTTCGAG
HPRT1	NM_013556	GCAGTACAGCCCCAAAATGG	AACAAAGTCTGGCCTGTATCCAA

Supplementary Table 2. One-way ANOVA analyses of daily variation.

Genes	*Il1b*	*Tnfa*	*Il6*	*Nox2*	*Glut5*	*Lpl*	*Gsr*	*Hmox1*
P	**P<0,0001**	0,3566	**0,0475**	0,7585	**0,0198**	0,7228	**0,0081**	0,5477

Effect of *Time* on gene expression of microglia. $P < 0.05$ (Bold) indicates a significant effect of *Time*.

Supplementary Table 3. Statistical analyses of gene rhythmicity

Genes	Pm	P_A	P_B	P_C	Genes	Pm	P_A	P_B	P_C
Related to Fig. 1									
Il1b	P<0,0001	P<0,0001	P<0,0001	0,0034	***Glut5***	0,0585	P<0,0001	0,0176	P<0,0001
Tnfa	0,333	P<0,0001	0,1397	0,0005	***Lpl***	0,3477	P<0,0001	0,1477	0,0277
Il6	0,0313	P<0,0001	0,0088	P<0,0001	***Gsr***	0,0499	P<0,0001	0,0147	P<0,0001
Nox2	0.0499	P<0,0001	0.0147	P<0,0001	***Hmox1***	0,265	P<0,0001	0,1045	0,0996
Related to supplementary Fig. 2									
Il1b	P<0,0001	P<0,0001	P<0,0001	P<0,0001	***Tnfa***	P<0,0001	P<0,0001	P<0,0001	P<0,0001
Il6	0.0021	P<0,0001	0.0005	P<0,0001	***Il10***	0.0210	P<0,0001	0.0059	P<0,0001
Related to Fig. 3 Scrambled siRNA					**Related to Fig. 3 *Bmal1* siRNA**				
Bmal1	0,0196	P<0,0001	0,0054	P<0,0001	***Bmal1***	0,062	P<0,0001	0,0194	0,0040
Clock	P<0,0001	P<0,0001	P<0,0001	P<0,0001	***Clock***	P<0,0001	P<0,0001	P<0,0001	P<0,0001

Cry1	0,0004	P<0,0001	P<0,0001	P<0,0001	***Cry1***	0,0001	P<0,0001	P<0,0001	P<0,0001
Cry2	0,1673	P<0,0001	0,0608	P<0,0001	***Cry2***	0,1737	P<0,0001	0,0628	P<0,0001
Per1	0,0135	P<0,0001	0,0036	P<0,0001	***Per1***	0,0490	P<0,0001	0,0149	0,3705
Per2	0,0539	P<0,0001	0,0165	0,0153	***Per2***	0,1701	P<0,0001	0,0612	P<0,0001
Nr1d1	0,0002	P<0,0001	P<0,0001	P<0,0001	***Nr1d1***	0,0007	P<0,0001	0,0002	P<0,0001
Dbp	0,0109	P<0,0001	0,0028	0,6877	***Dbp***	0,0056	P<0,0001	0,0014	P<0,0001
Il1b	P<0,0001	P<0,0001	P<0,0001	P<0,0001	***Il1b***	0,0174	P<0,0001	0,0050	0,0140
Tnfa	P<0,0001	P<0,0001	P<0,0001	P<0,0001	***Tnfa***	P<0,0001	P<0,0001	P<0,0001	P<0,0001
Il6	0.0719	P<0,0001	0.0227	0.0002	***Il6***	0.0127	P<0,0001	0.0033	P<0,0001
Il10	P<0,0001	P<0,0001	P<0,0001	P<0,0001	***Il10***	0,0013	P<0,0001	0,0003	P<0,0001
Glut1	0.0607	P<0,0001	0.0191	0.0034	***Glut1***	0.2667	P<0,0001	0.1081	0.0649
Lpl	0,1002	P<0,0001	0,0331	0,0003	***Lpl***	0,0005	P<0,0001	0,0001	P<0,0001
Pcx	0,0564	P<0,0001	0,0179	P<0,0001	***Pcx***	P<0,0001	P<0,0001	P<0,0001	P<0,0001
Gsr	0,0046	P<0,0001	0,0012	P<0,0001	***Gsr***	0,0731	P<0,0001	0,0240	P<0,0001
Hmox1	0,5464	P<0,0001	0,2759	0,0071	***Hmox1***	0,7167	P<0,0001	0,4178	P<0,0001
Related to supplementary Fig. 3 **Scrambled siRNA + LPS**					**Related to supplementary Fig. 3** **Bmal1 siRNA + LPS**				
Bmal1	P<0,0001	P<0,0001	P<0,0001	P<0,0001	***Bmal1***	0,0010	P<0,0001	0,0003	P<0,0001
Clock	0,0059	P<0,0001	0,0015	P<0,0001	***Clock***	0,0008	P<0,0001	0,0002	P<0,0001
Cry1	0,1838	P<0,0001	0,0686	0,1119	***Cry1***	0,9104	P<0,0001	0,6688	0,2381
Cry2	0,0093	P<0,0001	0,0025	0,4610	***Cry2***	0,5976	P<0,0001	0,3156	0,5115
Per1	0,0411	P<0,0001	0,0129	0,7308	***Per1***	0,0034	P<0,0001	0,0009	0,9361

Per2	0,0022	P<0,0001	0,0005	0,1328	***Per2***	0,5990	P<0,0001	0,3182	P<0,0001
Nr1d1	0,5111	P<0,0001	0,2536	0,2065	***Nr1d1***	0,1502	P<0,0001	0,0543	0,0001
Dbp	0,1096	P<0,0001	0,0380	0,0001	***Dbp***	0,2204	P<0,0001	0,0863	P<0,0001
Related to supplementary Fig. 5 **Scrambled siRNA + palmitic acid**					**Related to supplementary Fig. 5** **Bmal1 siRNA + palmitic acid**				
Bmal1	0,5230	P<0,0001	0,2649	P<0,0001	***Bmal1***	0,3184	P<0,0001	0,1357	0,9303
Clock	0,5315	P<0,0001	0,2708	0,0006	***Clock***	0,7186	P<0,0001	0,4255	0,6767
Cry1	0,0003	P<0,0001	P<0,0001	0,8601	***Cry1***	0,3482	P<0,0001	0,1548	P<0,0001
Cry2	0,0056	P<0,0001	0,0016	P<0,0001	***Cry2***	0,1377	P<0,0001	0,0495	0,0022
Per1	0,0007	P<0,0001	0,0002	P<0,0001	***Per1***	0,0013	P<0,0001	0,0003	P<0,0001
Per2	0,0015	P<0,0001	0,0004	0,0637	***Per2***	0,1317	P<0,0001	0,0486	0,0001
Nr1d1	0,1017	P<0,0001	0,0372	0,0554	***Nr1d1***	0,0458	P<0,0001	0,0148	P<0,0001
Dbp	0,0003	P<0,0001	P<0,0001	P<0,0001	***Dbp***	0,0099	P<0,0001	0,0027	P<0,0001

Data were fitted to the following regression: $y = A + B \cos(2\pi(x-C)/24)$; A is the mean level; B is the amplitude and C is the acrophase of the fitted rhythm. An overall *p* value (main *p* value, *P*m) was considered to indicate the rhythmicity.

Publication 3

The effect of Rev-erbα agonist SR9011 on the immune response and cell metabolism of microglia

Samantha E.C. Wolff[1,2], Xiao-Lan Wang[1], Han Jiao[2], Jia Sun[2], Andries Kalsbeek[1,3], Chun-Xia Yi[4 *], Yuanqing Gao[2 *]

1. Department of Endocrinology and Metabolism, Amsterdam University Medical Centers, University of Amsterdam, Amsterdam, Netherlands

2. Laboratory of Endocrinology, Amsterdam University Medical Centers, Amsterdam Gastroenterology & Metabolism, University of Amsterdam, Amsterdam, Netherlands

3. Key Laboratory of Cardiovascular and Cerebrovascular Medicine, School of Pharmacy, Nanjing Medical University, Nanjing, China

4. Laboratoire de Neuroscience Cognitives et Adaptatives, Université de Strasbourg, Strasbourg, France

5. Netherlands Institute for Neuroscience, Royal Netherlands Academy of Arts and Sciences, Amsterdam, Netherlands

Published in Front. Immunol. 11:550145. 25 Sep 2020. doi: 10.3389/fimmu.2020.550145

frontiers in Immunology

ORIGINAL RESEARCH
published: 25 September 2020
doi: 10.3389/fimmu.2020.550145

The Effect of Rev-erbα Agonist SR9011 on the Immune Response and Cell Metabolism of Microglia

Samantha E. C. Wolff[1,2,3], Xiao-Lan Wang[1,2,4], Han Jiao[3], Jia Sun[3], Andries Kalsbeek[1,2,5], Chun-Xia Yi[1,2,5] and Yuanqing Gao[3]**

[1] Department of Endocrinology and Metabolism, Amsterdam University Medical Centers, University of Amsterdam, Amsterdam, Netherlands, [2] Laboratory of Endocrinology, Amsterdam University Medical Centers, Amsterdam Gastroenterology & Metabolism, University of Amsterdam, Amsterdam, Netherlands, [3] Key Laboratory of Cardiovascular and Cerebrovascular Medicine, School of Pharmacy, Nanjing Medical University, Nanjing, China, [4] Laboratoire de Neuroscience Cognitives et Adaptatives, Université de Strasbourg, Strasbourg, France, [5] Netherlands Institute for Neuroscience, Royal Netherlands Academy of Arts and Sciences, Amsterdam, Netherlands

OPEN ACCESS

Edited by:
Pedro Manoel Mendes Moraes Vieira, Campinas State University, Brazil

Reviewed by:
Jennifer Lee, Beth Israel Deaconess Medical Center and Harvard Medical School, United States
Huatao Chen, Northwest A&F University, China

***Correspondence:**
Yuanqing Gao
yuanqinggao@njmu.edu.cn
Chun-Xia Yi
c.yi@amsterdamumc.nl;
c.yi@amc.uva.nl

Specialty section:
This article was submitted to Inflammation, a section of the journal Frontiers in Immunology

Received: *09 April 2020*
Accepted: *04 September 2020*
Published: *25 September 2020*

Citation:
Wolff SEC, Wang X-L, Jiao H, Sun J, Kalsbeek A, Yi C-X and Gao Y (2020) The Effect of Rev-erbα Agonist SR9011 on the Immune Response and Cell Metabolism of Microglia. Front. Immunol. 11:550145. doi: 10.3389/fimmu.2020.550145

Microglia are the immune cells of the brain. Hyperactivation of microglia contributes to the pathology of metabolic and neuroinflammatory diseases. Evidence has emerged that links the circadian clock, cellular metabolism, and immune activity in microglia. Rev-erb nuclear receptors are known for their regulatory role in both the molecular clock and cell metabolism, and have recently been found to play an important role in neuroinflammation. The Rev-erbα agonist SR9011 disrupts circadian rhythm by altering intracellular clock machinery. However, the exact role of Rev-erbα in microglial immunometabolism remains to be elucidated. In the current study, we explored whether SR9011 also had such a detrimental impact on microglial immunometabolic functions. Primary microglia were isolated from 1–3 days old Sprague-Dawley rat pups. The expression of clock genes, cytokines and metabolic genes was evaluated using RT-PCR and rhythmic expression was analyzed. Phagocytic activity was determined by the uptake capacity of fluorescent microspheres. Mitochondria function was evaluated by measuring oxygen consumption rate and extracellular acidification rate. We found that key cytokines and metabolic genes are rhythmically expressed in microglia. SR9011 disturbed rhythmic expression of clock genes in microglia. Pro-inflammatory cytokine expression was attenuated by SR9011 during an immune challenge by TNFα, while expression of the anti-inflammatory cytokine *Il10* was stimulated. Moreover, SR9011 decreased phagocytic activity, mitochondrial respiration, ATP production, and metabolic gene expression. Our study highlights the link between the intrinsic clock and immunometabolism of microglia. We show that Rev-erbα is implicated in both metabolic homeostasis and the inflammatory responses in microglia, which has important implications for the treatment of metabolic and neuroinflammatory diseases.

Keywords: clock genes, Innate immunity, microglia, immunometabolism, neuroinflammation, cytokines, phagocytosis

INTRODUCTION

The circadian brain clock orchestrates physiological and metabolic processes to prepare the body for environmental changes and to optimize energy metabolism (1). Cells in peripheral tissues, including metabolic tissues such as liver, pancreas, and kidney, also display rhythms in activity that are regulated by an intrinsic clock machinery. Since metabolic events are tightly regulated by the circadian clock, disruptions of the circadian timing system can result in metabolic dysfunctions and contribute to obesity and type 2 diabetes (2–10). Thus, the intracellular clock system is tightly involved in the control of metabolic rhythms that are essential for metabolic homeostasis.

The nuclear receptor reverse viral erythroblastosis oncogene product alpha (Rev-erbα) plays a crucial role in both the molecular clock of the circadian timing system and the regulation of metabolism. Rev-erbα stabilizes circadian rhythms by inhibiting the expression of the core clock genes brain and muscle ARNT-Like 1 (*Bmal1*) and circadian locomotor output cycles kaput (*Clock*) (11–13). The known endogenous ligand of Rev-erbα is heme, which plays an important role in mitochondrial respiration, and is required for the repressive activity of Rev-erbα/β on target genes (14–17). Additionally, nuclear receptors are sensors for dietary lipids and lipid-soluble hormones, thus rhythmic expression of Rev-erbα/β is also involved in regulating metabolic processes in a circadian manner (18, 19). Intriguingly, a recent Rev-erbα knock-out study proposed an important role for Rev-erbα in regulating neuroinflammation (20). In previous research, Rev-erbα agonists (GSK4112 and SR9011), and antagonists (SR8278) have provided us with insights about the function of Rev-erbα (21–24). For example, systemic administration of the Rev-erbα agonist SR9011 altered clock genes expression and disrupted the circadian behavior of mice leading to loss of locomotor activity during the active phase (dark phase), while vehicle administration caused no disruption (23). These results show that Rev-erb nuclear receptors have profound effects on circadian rhythm, metabolism and neuroinflammation, and possibly are eligible targets for treating metabolic diseases.

Recent research has demonstrated that a high fat, high sugar diet is associated with chronic activation of microglia, also known as microgliosis, which contributes to disturbed energy homeostasis and diet-induced obesity (DIO) (25–29). Additionally, our group recently reported that microglia activity shows a clear day/night rhythm when animals are fed a regular diet, but this rhythm is disrupted in DIO (30, 31). These findings suggest that the daily microglial rhythm is important for its normal activity and disturbance may result in metabolic diseases. However, little is known about the mechanism behind the intrinsic clock and the function of microglia. There is also a complex interplay between metabolic processes and immune responses, known as immunometabolism, in which metabolic reprogramming underlies the inflammatory state of microglia (32, 33). Therefore, considering the important role of Rev-erbα in the molecular clock machinery, neuroinflammation, and metabolism, in the current study we used the Rev-erbα agonist SR9011 to investigate the role of Rev-erbα in microglial immunometabolism.

MATERIALS AND METHODS

Primary Microglia Culture

Primary microglia cultures were prepared from brains of newborn, male Sprague Dawley rat pups (1–3 days old; Nanjing Medical University, China). After removal of the meninges, the brains were dissected and homogenized. Tissue lysates were centrifuged and suspended in Dulbecco's modified Eagle's medium (DMEM; Gibco, United States; C11885500BT) containing 1 *g*/L D-Glucose, L-Glutamine, 110 mg/L sodium pyruvate, and supplemented with 10% Fetal Bovine Serum (FBS; Gibco, United States; 10099141) and 1% Penicillin/Streptomycin (Gibco, United States; 15140122). Mixed glia cells were plated at a density of one brain per T75 flask or three brains per T175 flask, and incubated at 37°C in a humid atmosphere with 5% CO2. Culture medium was refreshed every 3 days. After the astrocyte layer reached confluency (8–14 days), the microglial cells were collected by shaking the flasks 150 rpm/min for 1 h at 37°C. Cells were seeded in 96-well plates (30k–50k cells/well) for the 3-(4,5-dimethylthiazol-2-yl)-5-(3-carboxymethoxyphenyl)-2-(4-sulfophenyl)-2H-tetrazolium (MTS) assay, 12-well plates (250k–300k cells/well) for qPCR experiments, or coverslipped in a 24-well plate (100k–150k cells/well) for phagocytosis experiments, or the Seahorse XF96 Cell Culture Microplate (Agilent, United States; 50k cells/well) for Seahorse experiments. For palmitic acid study, the palmitic – BSA solution was prepared 5:1 molar ratio palmitate: BSA in Krebs ringer buffer. All plates were coated with poly-L-lysine hydrobromide (MDBio, China). Dexamethasone (Sigma-Aldrich, United States; D4902), SR9011 (Sigma-Aldrich, United States; SML2067), DMSO (MDBio, China; D015), Fatty acids free BSA (Sigma A7030), Sodium Palmitate (Sigma-Aldrich, United States; P9767), TNFα (Peprotech, United States; 315-01A), and 0.1% BSA (Beyotime, China; ST023) were used to treat the cells during the experiments.

Cell Viability Assay

Cell viability was determined with the CellTiter 96 Aqueous assay (Promega, United States; G3582). Cells were treated with dexamethasone for 2 h, followed by a 24-h treatment with 5 μM SR9011 (or DMSO for control). Afterward, MTS solution was added followed by incubation for 3 h at 37°C, and the absorbance at 490 nm was measured on a SpectraMax M2 microplate reader (Molecular Devices).

Real-Time PCR

For gene expression analysis, total RNA was extracted from primary microglia using the RNAeasy^{TM} kit (Beyotime, China; R0026) according to the manufacturer's protocol. RNA concentration was measured with the NanoDrop Onec Spectrophotometer (Thermo Scientific, United States) and reverse transcribed into cDNA using the HiScript II qRT Supermix (Vazyme Biotech; R222-01). Gene expression levels of *Bmal1, Clock, Nr1d1 (Rev-erbα), Per2, Cry1, Il1β, Il4 Il6,*

Il10, Tnfα, Ccl2, Gm-csf, Tgfβ, CD36, CD68, Cpt1, Pdk1, Hk2, Fasn, Glut5, and *Hprt* (housekeeping gene; see **Supplementary Table 1** for primer sequences) were measured using real-time quantitative PCR on a QuantStudio 5 (Applied Biosystems Thermo Scientific), using the AceQ qPCR SYBR Green Master Mix (Vazyme Biotech; Q131-02). Gene expression levels were normalized to the housekeeping gene. Primers were designed using the Basic Local Alignment Search Tool (BLAST) from the National Center for Biotechnology Information (NCBI) and purchased from GeneRay Biotech.

Phagocytosis Assay

After treatment with SR9011 or DMSO for 12 h, microglia were incubated with 0.05% fluorescent latex microspheres (Sigma, United States; L1030-1 ml) in DMEM containing 0.25% FBS for 1 h. Subsequently, the cells were fixed with 4% paraformaldehyde for 30 min and a fluorescence staining of microglia was performed with Rabbit Anti-Iba1 (Wako, Japan; 019-19741) and the nuclei were counterstained with 4',6-diamidino-2-phenylindole (DAPI; Bioprox, France). Images were captured with an Olympus BX53F microscope equipped with an Olympus U-HGLGPS light source, and analyzed with ImageJ software (version 1.48). The relative fluorescent intensity of the beads was determined by dividing the total fluorescent intensity of the beads by the number of DAPI-stained nuclei.

Cellular Bioenergetics

Microglia were treated with 5 μM SR9011 or DMSO for 4 h prior to placement in the Seahorse XFe96 Analyzer (Agilent, United States). During the run, oxygen consumption rate (OCR), and extracellular acidification rate (ECAR) were measured and the wells were injected with modulators from the Agilent Seahorse XF Mito Stress Kit to determine parameters of mitochondrial function. After measuring basal levels of OCR and ECAR, oligomycin was injected to block ATP synthase, which decreases mitochondrial respiration. The second injection was carbonyl cyanide-4 (trifluoromethoxy) phenylhydrazone (FCCP), which disrupts the mitochondrial membrane potential and maximizes oxygen consumption. The third injection was a mixture of rotenone and antimycin A, which block complex I and III (respectively) and shut down mitochondrial respiration. Lastly, 2-deoxy-D-glucose (2-DG) was added to inhibit glycolysis, leading to a decrease in ECAR. Cellular respiration, mitochondrial respiration, cellular acidification, maximum substrate utilization, and maximum glycolytic capacity were calculated as previously described (34). ATP production was calculated from mitochondrial respiration by using a phosphate/oxygen ratio of 2.3 (35). After the measurements, cells were fixed with 4% paraformaldehyde and attached cells were quantified using a crystal violet assay by measuring absorbance at 590 nm with a SpectraMax M2 microplate reader (Molecular Devices). Data obtained from the Seahorse XF96 Analyzer was normalized to cell quantity per well.

Statistical Analyses

All results are expressed as mean ± SEM. Statistical analysis was performed using Graph-Pad PRISM (version 7.00), ImageJ software (version 1.48), and JTK_Cycle software (36). Two-way ANOVA and Bonferroni's *post hoc* test was used to assess the SR9011 effects on clock genes within 24 h after synchronization. Unpaired *t*-tests were used to evaluate the differences between DMSO and SR9011 groups in the rest of the study. ImageJ software was used for the analysis of phagocytosis assays. JTK_Cycle software (36) was used to identify rhythmic components in circadian PCR data.

RESULTS

Rhythmic Expression of Cytokines and Metabolic Genes in Microglia

The intrinsic clock machinery is present in microglia with clock genes being rhythmically expressed (30, 37). It has been well documented that cytokines and metabolic genes exhibit rhythmic expression (23, 38). To confirm whether cytokines and metabolic genes were also temporally regulated in primary microglia, we investigated the expression of three key pro-inflammatory cytokines – interleukin-1 beta (*Il1β*), interleukin-6 (*Il6*), and tumor necrosis factor-alpha (*Tnfα*), as well as three important metabolic genes – carnitine palmitoyltransferase 1 (*Cpt1*), hexokinase 2 (*Hk2*), and pyruvate dehydrogenase kinase 1 (*Pdk1*). Primary microglia were synchronized by 10 nM dexamethasone for 2 h as reported before (39) and cultured for 0, 6, 12, 18, or 24 h before being harvested. Gene expression of the cytokines and metabolic genes was determined over these time points [time post-synchronization, from now on referred to as "Time (T)" in hours] and rhythmicity was analyzed by JTK_Cycle software (**Figure 1**). *Tnfα*, *Il6*, *Pdk1*, and *Cpt1* showed a clear rhythmic expression, while *Il1β* and *Hk2* were not rhythmically expressed (**Figure 1**). The acrophase of the curves was estimated at T6, for *Il6*, *Pdk1* and *Cpt1*, and T12 for *Tnfα*. These data show that *Il6*, *Tnfα*, *Pdk1*, and *Cpt1* expression are likely orchestrated by the circadian timing system in primary microglia.

SR9011 Disrupts Clock Gene Rhythmicity in Microglia

We first determined whether SR9011 enhances Rev-erbα activity and disrupts the clock machinery in primary microglia. For this, we performed a dose-response study with 1, 5, 10, and 50 μM SR9011 (data not shown) and decided to use 5 μM for this study. To test the efficiency of SR9011, we first analyzed the effects of SR9011 on Rev-erb targets *Serpine1*, *Cyp7a1*, and *Srebf1* and found significant reductions in their expression compared to control, which confirms that SR9011 acts through Rev-erb (**Supplementary Figure 1**). When using SR9011 as a pretreatment before synchronization with dexamethasone, we found that the effect of SR9011 pretreatment did not persist after removing SR9011 from the culture (**Supplementary Figure 2** and **Supplementary Table 2**), contrary to the result from Nakazato et al. (39). Therefore, the following design was used in this study: primary rat microglia were exposed to dexamethasone for 2 h to synchronize the cells, followed by treatment with

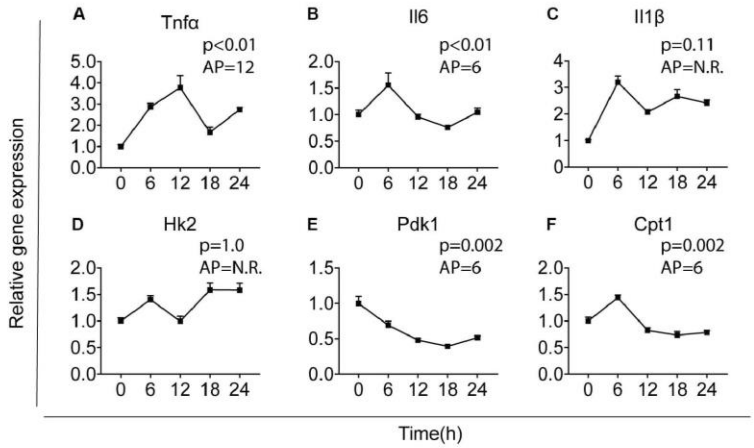

FIGURE 1 | Major cytokines and metabolic genes are rhythmically expressed in microglia. Relative gene expression of major cytokines and metabolic genes was measured in primary microglia. After synchronization by dexamethasone for 2 h, cells were cultured and harvested at the indicated post-synchronization time points (T; $n = 6$ per group, per time point). Rhythmic expression is signified by a p-value of less than 0.05 and can be found for *Tnf* **(A)**, *Il6* **(B)**, *Pdk1* **(E)**, and *Cpt1* **(F)**. The expression of *Il1* **(C)** and *Hk2* **(D)** was not rhythmic. The acrophase of the curve is not relevant (N.R.) if data does not fit a curve. Data are presented as means ± SEM and statistical significance was determined using JTK_Cycle software.

5 μm SR9011 or DMSO for 0, 6, 12, 18, or 24 h. Rhythmic expression of *Bmal1*, *Clock*, period 2 (*Per2*), cryptochrome 1 (*Cry1*), period 1 (*Per1*) and nuclear receptor subfamily 1 group d member 1 (*Nr1d1* or *Rev-erbα*) was found in primary microglia treated with DMSO, as evaluated with Two-way ANOVA (**Table 1**) and JTK_Cycle Software (**Figure 2** and **Table 2**). SR9011 exerted an inhibitory effect on *Bmal1* and *Per2* expression, as analyzed by Two way ANOVA (**Table 1**). An interactive effect of SR9011 and Time was found on *Bmal1*, *Clock*, and *Nr1d1* (=*Rev-erbα*, see **Table 1**). The impact of SR9011 at each time point was analyzed by multiple comparison (**Figures 2A–F**). Notably, SR9011 disrupted the rhythmic expression of *Bmal1* and *Clock*, and caused a shift in the acrophase of *Per2* rhythm, as analyzed by JTK_Cycle (**Table 2**). SR9011 in combination with dexamethasone had no impact on cell viability (**Figure 2G**), indicating that a decrease in gene expression could not be attributed to cell death. These results show that SR9011 disrupted the rhythm of clock gene expression, pertaining to both amplitude and phase depending on the clock gene, which means that rhythmic expression of clock gene expression became non-rhythmic after adding SR9011. SR9011 had the strongest impact on *Bmal1* and *Clock*, while the effect on *Per2* and *Cry1* was less potent. This is probably due to the direct inhibitory effect of Rev-erbα on the BMAL1 and CLOCK complex, which indirectly influences *Per2* and *Cry1* expression.

TABLE 1 | Two-way ANOVA assessment of effect of Time, SR9011, and Interaction in clock genes in primary microglia with SR9011.

Genes	Two-way ANOVA analysis		
	p-value		
	Interaction	Time	SR9011
Bmal1	**0.0195**	**<0.0001**	**0.0370**
Clock	**0.0251**	**<0.0001**	0.0659
Cry1	0.1234	**<0.0001**	0.0907
Per1	0.5030	**<0.0001**	0.3939
Per2	0.0648	**<0.0001**	**0.0489**
Nr1d1	**0.0003**	**<0.0001**	0.4462

SR9011, Time and Interaction effects were evaluated in primary microglia for clock genes after treated with DMSO or SR9011. SR9011 has significant impact on Bmal1 and Per2, and has interaction effect with time on Bmal1, Clock, and Nr1d1.

SR9011 Alters Cytokine Expression in Microglia

Cytokine secretion constitutes an essential part of microglial immune function. Rev-erbα has very recently been reported to regulate neuroinflammation (20). To evaluate the role of Rev-erbα in regulating cytokine expression, we stimulated the cells with TNFα to resemble an immune challenge and analyzed the effect of SR9011. Primary microglia were exposed to 5 μM SR9011 (or DMSO for control) for 12 h, followed by 100 ng/ml TNFα treatment (or BSA for control) for 12 h in combination with SR9011 or DMSO. TNFα significantly increased the expression of the pro-inflammatory cytokines tumor necrosis factor-alpha (*Tnfα*), interleukin-6 (*Il6*), interleukin-1 beta (*Il1β*), and C-C Motif Chemokine Ligand (*Ccl2*; **Figures 3A–E**). TNFα also significantly increased the regulatory cytokine granulocyte-macrophage colony-stimulating factor (*Gm-csf*; **Figure 3F**). In all

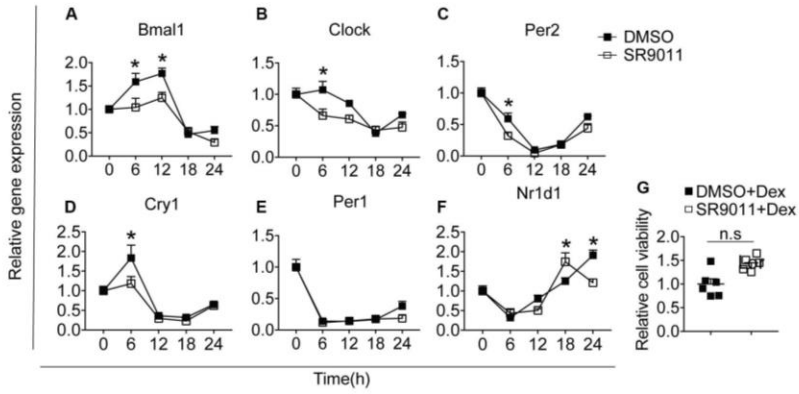

FIGURE 2 | SR9011 disrupts clock gene expression in microglia. Rhythmic and relative gene expression of clock genes in primary microglia. Cells were treated with dexamethasone for 2 h followed by SR9011 or DMSO and were harvested at the indicated time points (n = 4 per group, per time point). **(A–F)** Clock gene expression is altered by SR9011 treatment compared to DMSO (control). SR9011 disrupted the rhythmic expression of *Bmal1* and *Clock*, and caused a shift in the acrophase of *Per2* rhythm, as analyzed by JTK_Cycle. **(G)** Cell viability of primary microglia was not affected by the 24-h SR9011 treatment with dexamethasone. Data are presented as means ± SEM. $p < 0.05^*$ vs. DMSO group was determined using Two-way ANOVA followed by Bonferroni's *post hoc* test and multiple comparison.

cases, the increase in gene expression by TNFα treatment was attenuated after treatment with SR9011. Different results were found for anti-inflammatory cytokines. TNFα had no effect on the regulatory cytokine transforming growth factor-beta (*Tgf*β) expression, however, SR9011 treatment decreased *Tgf*β expression (**Figure 3G**). No changes were found in interleukin-4 (*Il4*) expression (**Figure 3H**). Interestingly, while TNFα had no effect on the expression of anti-inflammatory cytokine interleukin-10 (*Il10*), SR9011 stimulated the expression of *Il10* (**Figure 3I**). These results suggest that SR9011 attenuates the pro-inflammatory response in primary microglia in the context of an immune challenge, while stimulating the expression of the anti-inflammatory cytokine *Il10*.

SR9011 Attenuated Palmitic Acid Induced Inflammatory Response in Microglia

To further test whether SR9011 has a potential therapeutic effect for overnutrition-induced neuroinflammation, we stimulated the microglia with palmitic acid (PA) to resemble a pro-inflammatory stimulus on high-fat diet feeding. Primary microglia were exposed to 5 μM SR9011 (or DMSO for control) for 12 h, followed by 50 μM palmitic acid (or BSA for control) for 12 h in combination with SR9011 or DMSO. Palmitic acid significantly increased the expression of pro-inflammatory cytokines *Il6* and *Il1*β. which were attenuated by SR9011 (**Figures 4A,B**). Palmitic acid also significantly stimulated *Gm-csf* expression, while SR9011 had a profound inhibitory effect on *Gm-csf* expression (**Figure 4C**). *Tnf*α and *Ccl2* expression was not enhanced by palmitic acid treatment (**Figures 4D,E**), which is a slightly different outcome compared to the TNFα stimulus. In addition, palmitic acid treatment exerted impacts on the expression of core clock genes *Nr1d1* and *Per1* after 12h incubation (**Supplementary Figure 3**), which indicates palmitic acid treatment might also influence circadian rhythms. This is consistent with our previous observation that circadian rhythms of microglia are disrupted in DIO animals (30). Thus, these data suggest that SR9011 attenuates the pro-inflammatory response in primary microglia upon palmitic acid treatment, which may be beneficial for DIO-induced neuroinflammation.

SR9011 Decreases Phagocytosis in Microglia

One of the main neuroprotective functions of microglia is phagocytosis, so we evaluated the effect of SR9011 on phagocytic activity. Primary microglia were treated with 5 μM SR9011 (or DMSO) for 12 h and subsequently exposed to 0.05% fluorescent

TABLE 2 | JTK_Cycle analysis of clock genes in primary microglia with SR9011.

Gene	DMSO		SR9011	
	P-value	Acrophase	*P*-value	Acrophase
Bmal1	**0.0053**	9	0.0980	N.R.
Clock	**0.0293**	9	1	N.R.
Cry1	**<0.0001**	6	**0.0006**	6
Per1	**<0.0001**	0	**0.0293**	0
Per2	**<0.0001**	3	**<0.0001**	0
Nr1d1	**0.0364**	21	**<0.0001**	21

Clock genes rhythmicity in microglia treated with SR9011 are analyzed by JTK_Cycle software. All the clock genes were rhythmically expressed in primary microglia treated with DMSO, signified by a p-value of less than 0.05. SR9011 disrupted the rhythmic expression of Bmal1 and Clock. The acrophase of the curve is not relevant (N.R.) when data does not fit a curve.

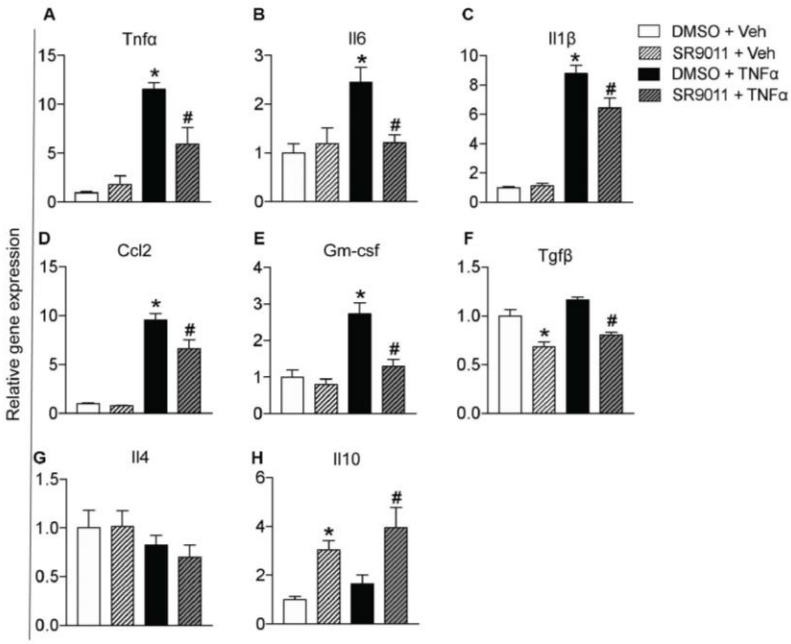

FIGURE 3 | The effect of SR9011 on cytokine expression in microglia. Relative gene expression of cytokines in primary microglia treated with SR9011 or DMSO for 12 h followed by TNFα or BSA treatment for 12 h ($n = 6$ per group). This figure shows the effect of TNFα and SR9011 on pro-inflammatory cytokine expression **(A–E)**, regulatory cytokine expression **(F)**, and anti-inflammatory cytokine expression **(G–H)**. TNFα increases the gene expression of *Tnfα*, *Il6*, *Il1β*, *Ccl2*, and *Gm-csf*. SR9011 attenuates the expression of *Tnfα*, *Il6*, *Il1β*, *Ccl2*, and *Gm-csf* compared to treatment with TNFα alone. Conversely, SR9011 increases *Il10* expression after TNFα stimulation. Data are presented as means ± SEM and statistical significance was determined using Unpaired *t*-test in all experiments. $p < 0.05^{*}$ vs DMSO + BSA and $p < 0.05^{\#}$ vs DMSO + TNFα.

beads for 1 h. A fluorescence staining was performed for IBA1 (microglia marker) and DAPI, after which the intensity of fluorescent beads per cell was determined (**Figure 5A**). The uptake of fluorescent beads was decreased in primary microglia treated with SR9011 (**Figure 5B**). Additionally, the expression of cluster of differentiation 68 (*CD68*), a phagocytic marker, was decreased in primary microglia that were starved for 6 h (0% FBS) and subsequently treated with 5 μM SR9011 for 12 h (**Figure 5C**). The purity of the cultures was tested by staining primary microglia with IBA1 and DAPI and a microglia purity of 98.81% was determined (data not shown). These results indicate that SR9011 decreases phagocytic activity, meaning that Rev-erbα plays an inhibitory role in regulating phagocytosis.

SR9011 Inhibits Mitochondrial Respiration and Metabolic Gene Expression in Microglia

Major metabolic genes are expressed in a rhythmic manner in microglia, as shown in **Figure 1**. We evaluated metabolism after disrupting the intrinsic microglial clock with SR9011. Primary microglia were treated with 5 μM SR9011 (or DMSO) for 12 h after which cellular respiration and ECAR were measured using the Seahorse XFe96 Analyzer to evaluate mitochondrial respiration and glycolysis. The raw data of OCR and ECAR are shown in **Figures 6A,B**. Cellular respiration was significantly decreased by SR9011, which was mainly attributed to less ATP-linked mitochondrial respiration, while the H^+ proton leak remained unchanged (**Figures 6C,D**). Consequently, ATP production was greatly reduced (**Figure 6E**). Furthermore, maximum substrate oxidation was decreased after SR9011 treatment (**Figure 6F**). No changes were found in cellular acidification (glycolysis) and maximum glycolytic capacity (**Figures 6G,H**). These results indicate that SR9011 decreases ATP production by inhibiting oxidative phosphorylation. This mitochondrial dysfunction is not compensated with glycolysis. Furthermore, SR9011 inhibits the expression of *Hk2*, *Pdk1*, and *Cpt1* (**Figures 6I–K**), which are key enzymes involved in substrate utilization by the citric acid cycle. Taken together, these results suggest an overall decrease in cellular metabolism caused by activation of Rev-erbα by SR9011. Thus, Rev-erbα is a potent inhibitor of cell metabolism in primary microglia.

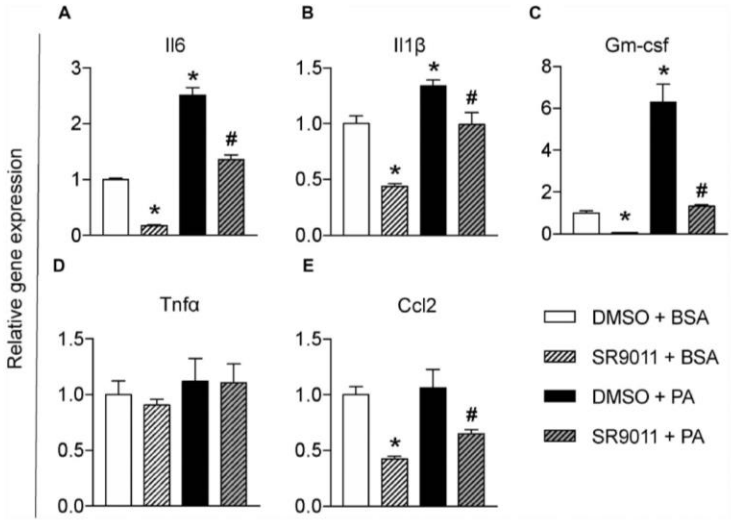

FIGURE 4 | The effect of SR9011 on palmitic acid induced inflammatory responses in microglia. Relative gene expression of cytokines in primary microglia treated with SR9011 or DMSO for 12 h followed by 50 μM palmitic acid or BSA treatment for 12 h ($n = 4$ per group). Palmitic acid treatment increases *Il6* **(A)**, *Il1β* **(B)**, and *Gm-csf* **(C)**, which are inhibited by SR9011. Palmitic acid treatment has no profound effect on the expression of *Tnfα* **(D)** and *Ccl2* **(E)**, while SR9011 decreased *Ccl2* expression with and without palmitic acid treatment **(E)**. $p < 0.05^{*}$ vs DMSO + BSA and $p < 0.05^{\#}$ vs DMSO + PA.

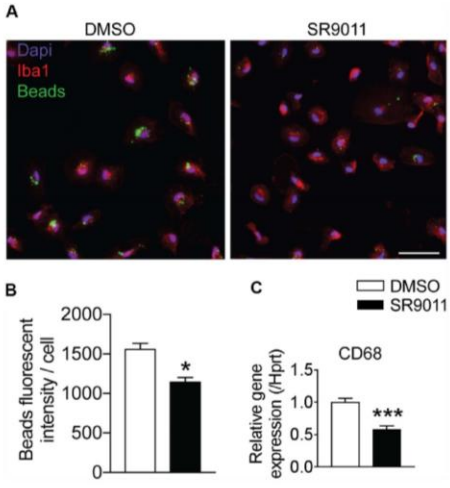

FIGURE 5 | SR9011 decreased phagocytic activity in primary microglia. **(A)** The uptake of fluorescent beads by primary microglia treated with DMSO or SR9011. **(B)** Primary microglia treated with SR9011 exhibit decreased phagocytic activity ($n = 15$). **(C)** The expression of phagocytic marker *CD68* is decreased in primary microglia treated with SR9011 for 12 h ($n = 6$). Data are presented as means ± SEM and statistical significance was determined using Unpaired *t*-test in all experiments. $p < 0.05^{*}$ and $p < 0.001^{***}$ vs. DMSO.

DISCUSSION

The aim of the current study was to determine the role of Rev-erbα in microglial immunometabolism. We show that key cytokine and metabolic genes are rhythmically expressed in primary microglia. Activation of Rev-erbα with SR9011 disrupted the intrinsic microglial clock and attenuated the phagocytosis and the pro-inflammatory response. SR9011 also decreased mitochondrial respiration and metabolic gene expression in microglia. These findings shed new light on the link between the circadian clock, cell metabolism and immune function in microglia and identify Rev-erbα as a possible important therapeutic target for treatment of neuroinflammatory diseases.

The rhythmic expression of major cytokines and metabolic genes in primary microglia observed in the current study supports our previous idea that *in vivo* the intrinsic clock is coupled with cellular metabolism (30). Such rhythmicity of cytokines may have physiological relevance *in vivo* – we reported before that microglia activity displays a day and night difference and is accompanied by a change in TNFα expression in the medial basal hypothalamus, which in turn affected the mitochondria function of nearby neurons (31). A growing body of literature reports that an obesogenic diet is associated with constant activation of microglia, leading to chronic hypothalamic inflammation, which contributes to the pathology observed (26, 27, 31, 40). We also reported that microglial circadian rhythmicity is disrupted in DIO animals (27). In this study, we found that SR9011 prevents the microglia pro-inflammatory

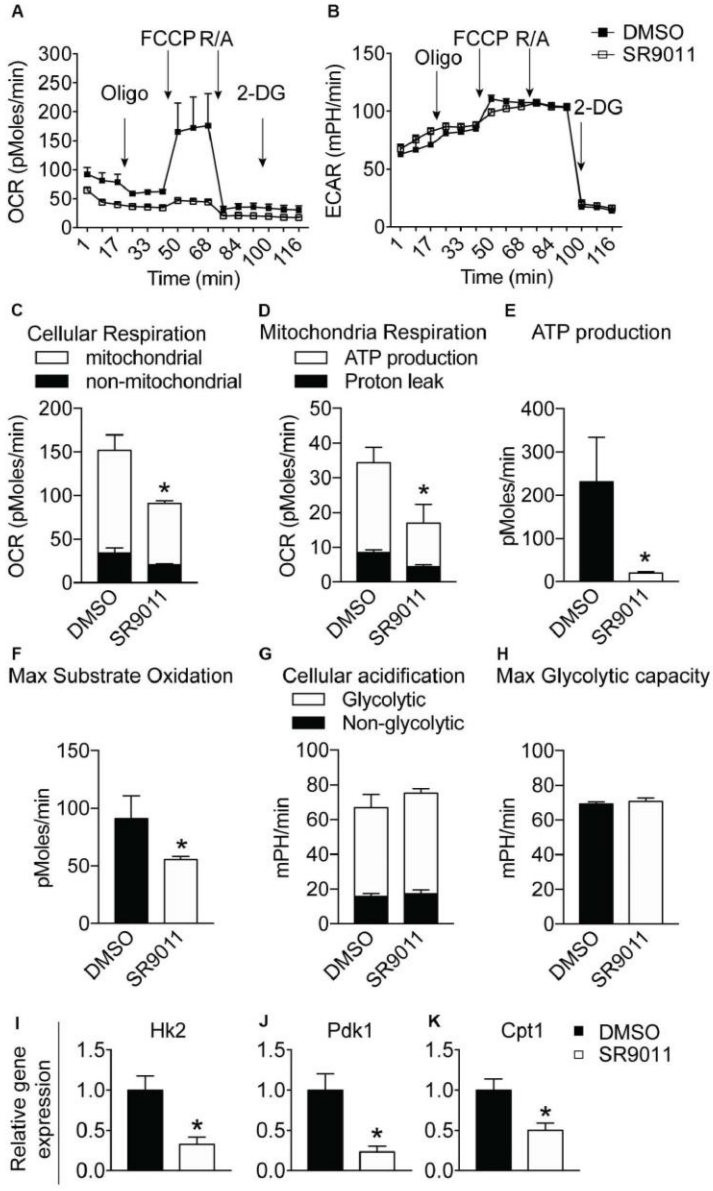

FIGURE 6 | The effect of SR9011 on cellular metabolism in primary microglia. Cellular bioenergetics and metabolic gene expression in primary microglia after SR9011 treatment ($n = 4$ per group). **(A, B)** Overview of OCR **(A)** and ECAR **(B)** of primary microglia treated with DMSO or SR9011 for 12 h. Indicated are the times on which oligomycin, FCCP, rotenone/antimycin A (R/A) and 2DG were administered. **(C–H)** SR9011 decreased cellular respiration **(C)**, which was caused by a decline in ATP-linked mitochondrial respiration **(D)**. Consequently, ATP production was significantly decreased in response to SR9011 **(E)**. SR9011 also caused a decrease in maximum substrate oxidation **(F)**. No changes were found in cellular acidification **(G)** and maximum glycolytic capacity **(H)**. **(I–K)** SR9011 decreased the expression of metabolic genes *Hk2* **(I)**, *Pdk1* **(J)**, and *Cpt1* **(K)** in primary microglia treated by dexamethasone for 2 h and SR9011 for 6 h. Data are presented as means ± SEM and statistical significance was determined using Unpaired *t*-test in all experiments. $p < 0.05$*.

responses usually observed during an inflammatory challenge and an obesogenic metabolic challenge. The mechanism behind the metabolic improvements observed in DIO mice can partially be explained by the mitigating effect of SR9011 on hyperactive microglia, thereby attenuating inflammation. This finding can have major implications for reducing microgliosis caused by obesity or neuroinflammatory diseases. A better *ex vivo* experimental setting to mimic the *in vivo* situation under a chronic high-fat diet challenge would be helpful to further elucidate these mechanisms.

The current study examined the immune function of microglia upon SR9011-associated Rev-erbα activation. Similar topics have been discussed before. In studies on knock-out mice or mice pharmacologically administered with SR9011, microglia activation and *Il6* expression was downregulated upon LPS exposure (39, 41). In another Rev-erbα deletion study, mice displayed microgliosis, increased CD68, and neuroinflammation in the hippocampus (20). Consistent with these results, we enhanced Rev-erbα activity with SR9011 and found a decreased pro-inflammatory response and phagocytosis. A recent study describes a regulatory role of Bmal1 in macrophage motility and phagocytosis (42), which may indicate a possible interplay between Rev-erb and Bmal1 in the regulation of phagocytosis in microglia – an interesting topic for future research. Additionally, SR9011 stimulated the expression of the anti-inflammatory cytokine *Il10*. This suggests Rev-erbα not only inhibits pro-inflammatory cytokines, but also promotes the anti-inflammatory response. Moreover, to more accurately mimic microglia's immune response, we used TNFα as an innate immune challenge, which is more physiologically relevant compared to lipopolysaccharide (LPS) used in the studies mentioned above. These findings suggest that the molecular clock components Bmal1 and Rev-erbα are closely related to the microglial immune response, and that Rev-erbα activity can regulate the inflammatory state in microglia under physiological and pathological conditions.

Rev-erbα nuclear receptors were reported to regulate metabolic homeostasis in cancer cells, hepatic cells and hepatoma cells (17, 18, 43). The findings of the current study show that Rev-erbα nuclear receptors regulate cell metabolism in primary microglia, the innate immune cells, as evidenced by the decrease in mitochondrial respiration and ATP production, as well as the decreased expression of rate-limiting enzymes such as *Cpt1*, *Pdk1*, and *Hk2* in response to SR9011. Our study dissected how the Rev-erbα-associated clock machinery interacts with immunometabolism in microglia. It is generally assumed that immune function is tightly linked to cell metabolism due to the metabolic demand of an inflammatory response (44). One explanation for the decline in energy metabolism is that it is a consequential phenomenon caused by less energy demand due to the attenuated pro-inflammatory response. Another possibility is a direct effect of Rev-erbα on cellular metabolism. Rev-erbα nuclear receptors, when bound to their ligand, repress the transcription of not only clock genes like *Bmal1*, but also repress metabolic genes and are involved in mitochondrial respiration (14, 15, 45, 46). The inflammatory response of microglia also involves metabolic reprogramming, which also might explain the attenuation of pro-inflammatory cytokines (32, 33). Another speculation would be that the intrinsic molecular clock orchestrates both microglial metabolism and immune response, and that it can also change the activation state of microglia. The latter would mean that SR9011-induced enhanced Rev-erbα activity is associated with disturbed microglial circadian rhythms, which consequently changed the cellular metabolism and immune response. Indeed, the *in vivo* situation might be far more complicated, because it is unknown what occurs first in the development of metabolic disorders: the disrupted circadian rhythmicity, the alterations in intracellular metabolism, the changes in immune response, or any other unknown factors. In our opinion, the disrupted circadian rhythmicity is very likely to be the driving force of the other two. In addition, the appropriate immune response of microglia is required to defend the CNS under normal conditions, so attenuated pro-inflammatory responses might not be always beneficial for the body. Further research is needed to elucidate the causal relation among the intracellular clock, cellular metabolism and immune response in microglia under physiological condition and metabolic challenges. It is interesting to note that SR9009, a REV-ERB agonist similar to SR9011, has been reported to exert Rev-erbα independent side-effects on cell proliferation and metabolism (47). Whether SR9011 has the same side-effects is currently unknown, and requires further research.

Future research should also investigate the significance of the microglial intrinsic clock *in vivo*. It is likely that the exact consequences of disturbing the microglial clock depend on the brain regions involved. Microgliosis in the hypothalamus is associated with metabolic disorders, while microglia in other brain regions will have other functions, depending on the micro-environment. On the other hand, the role of Rev-erbα should also be investigated in other immune cells and their related immune-diseases.

CONCLUSION

Our study demonstrates that disturbing circadian rhythmicity by SR9011-induced Rev-erbα activation attenuates pro-inflammatory cytokine expression and reduces cellular metabolism in microglia. In addition, expression of the anti-inflammatory cytokine *Il10* is stimulated, emphasizing the mitigating effect of Rev-erbα activation on the pro-inflammatory response. The findings of this study identify an interconnected role of Rev-erbα in the circadian rhythmicity, cell metabolism and inflammatory response of microglia and may have important implications for the employment of Rev-erbα as a potential therapeutic target for the treatment of neuroinflammatory diseases, however, further studies are required to achieve this goal.

DATA AVAILABILITY STATEMENT

The datasets presented in this study can be found in online repositories. The names of the repository/repositories and accession number(s) can be found in the article/**Supplementary Material**.

ETHICS STATEMENT

The experiments were approved by the Animal Care and Use Committee of Nanjing Medical University, and the experiments were performed according to the Guide for the Care and Use of Laboratory Animals of China.

AUTHOR CONTRIBUTIONS

SW, JS, HJ, and YG performed the experiments. C-XY and YG designed the study. SW, X-LW, and AK analyzed the data and wrote the manuscript. All authors read and approved the final manuscript.

FUNDING

This work was funded by the international student fellowship from Amsterdam Gastroenterology & Metabolism (AG&M), grants from the National Natural Science Foundation of China 81873654 and 31800971, and Jiangsu Province Science Foundation for Youths BK20180684, the Department of Cardiovascular and Cerebrovascular Medicine, Nanjing Medical University (YG Lab); and AMC fellowship, Amsterdam University Medical Center (2014; C-XY lab); and the doctoral fellowship from the 'NeuroTime" Erasmus+ Program (X-LW).

ACKNOWLEDGMENTS

We thank AG&M for granting SW the international student fellowship to conduct this valuable research at Nanjing Medical University under the supervision of YG.

SUPPLEMENTARY MATERIAL

The Supplementary Material for this article can be found online at: https://www.frontiersin.org/articles/10.3389/fimmu.2020.550145/full#supplementary-material

REFERENCES

1. Kalsbeek A, Palm IF, La Fleur SE, Scheer FAJL, Perreau-Lenz S, Ruiter M, et al. SCN outputs and the hypothalamic balance of life. *J Biol Rhythms.* (2006) 21:458–69. doi: 10.1177/0748730406293854
2. Boden G, Chen X, Polansky M. Disruption of circadian insulin secretion is associated with reduced glucose uptake in first-degree relatives of patients with type 2 diabetes. *Diabetes.* (1999) 48:2182–8. doi: 10.2337/diabetes.48.11.2182
3. Depner CM, Stothard ER, Wright KP. Metabolic consequences of sleep and circadian disorders. *Curr Diab Rep.* (2014) 14:507. doi: 10.1007/s11892-014-0507-z
4. McGinnis GR, Young ME. Circadian regulation of metabolic homeostasis: causes and consequences. *Nat Sci Sleep.* (2016) 8:163–80. doi: 10.2147/NSS.S78946
5. Turek FW, Joshu C, Kohsaka A, Lin E, Ivanova G, McDearmon E, et al. Obesity and metabolic syndrome in circadian clock mutant nice. *Science.* (2005) 308:1043–5. doi: 10.1126/science.1108750
6. Ma D, Liu T, Chang L, Rui C, Xiao Y, Li S, et al. The liver clock controls cholesterol homeostasis through trib1 protein-mediated regulation of PCSK9/Low density lipoprotein receptor (LDLR) axis. *J Biol Chem.* (2015) 290:31003–12. doi: 10.1074/jbc.M115.685982
7. Marcheva B, Ramsey KM, Buhr ED, Kobayashi Y, Su H, Ko CH, et al. Disruption of the clock components CLOCK and BMAL1 leads to hypoinsulinaemia and diabetes. *Nature.* (2010) 466:627–31. doi: 10.1038/nature09253
8. Inoue I, Shinoda Y, Ikeda M, Hayashi K, Kanazawa K, Nomura M, et al. CLOCK/BMAL1 is involved in lipid metabolism via transactivation of the peroxisome proliferator-activated receptor (PPAR) response element. *J Atheroscler Thromb.* (2005) 12:169–74. doi: 10.5551/jat.12.169
9. Sato F, Kohsaka A, Bhawal UK, Muragaki Y. Potential roles of dec and bmal1 genes in interconnecting circadian clock and energy metabolism. *Int J Mol Sci.* (2018) 19:781. doi: 10.3390/ijms19030781
10. Shimba S, Ogawa T, Hitosugi S, Ichihashi Y, Nakadaira Y, Kobayashi M, et al. Deficient of a clock gene, brain and muscle arnt-like protein-1 (BMAL1), induces dyslipidemia and ectopic fat formation. *PLoS One.* (2011) 6:e25231. doi: 10.1371/journal.pone.0025231
11. Crumbley C, Burris TP. Direct regulation of CLOCK expression by REV-ERB. *PLoS One.* (2011) 6:e17290. doi: 10.1371/journal.pone.0017290
12. Gaucher J, Montellier E, Sassone-Corsi P. Molecular cogs: interplay between circadian clock and cell cycle. *Trends Cell Biol.* (2018) 28:368–79. doi: 10.1016/j.tcb.2018.01.006
13. Preitner N, Damiola F, Lopez-Molina L, Zakany J, Duboule D, Albrecht U, et al. The orphan nuclear receptor REV-ERBα controls circadian transcription within the positive limb of the mammalian circadian oscillator. *Cell.* (2002) 110:251–60. doi: 10.1016/S0092-8674(02)00825-5
14. Padmanaban G, Venkateswar V, Rangarajan PN. Haem as a multifunctional regulator. *Trends Biochem Sci.* (1989) 14:492–6. doi: 10.1016/0968-0004(89)90182-5
15. Raghuram S, Stayrook KR, Huang P, Rogers PM, Nosie AK, McClure DB, et al. Identification of heme as the ligand for the orphan nuclear receptors REV-ERBα and REV-ERBβ. *Nat Struct Mol Biol.* (2007) 14:1207–13. doi: 10.1038/nsmb1344
16. Wu N, Yin L, Hanniman EA, Joshi S, Lazar MA. Negative feedback maintenance of heme homeostasis by its receptor, Rev-erbα. *Genes Dev.* (2009) 23:2201–9. doi: 10.1101/gad.1825809
17. Yin L, Wu N, Curtin JC, Qatanani M, Szwergold NR, Reid RA, et al. Rev-erbα, a heme sensor that coordinates metabolic and circadian pathways. *Science.* (2007) 318:1786–9. doi: 10.1126/science.1150179
18. Duez H, Staels B. Rev-erbα gives a time cue to metabolism. *FEBS Lett.* (2008) 582:19–25. doi: 10.1016/j.febslet.2007.08.032
19. Yang X, Downes M, Yu RT, Bookout AL, He W, Straume M, et al. Nuclear receptor expression links the circadian clock to metabolism. *Cell.* (2006) 126:801–10. doi: 10.1016/j.cell.2006.06.050
20. Griffin P, Dimitry JM, Sheehan PW, Lananna BV, Guo C, Robinette ML, et al. Circadian clock protein Rev-erbα regulates neuroinflammation. *Proc Natl Acad Sci USA.* (2019) 116:5102–7. doi: 10.1073/pnas.1812405116
21. Grant D, Yin L, Collins JL, Parks DJ, Orband-Miller LA, Wisely GB, et al. GSK4112, a small molecule chemical probe for the cell biology of the nuclear heme receptor rev-erbα. *ACS Chem Biol.* (2010) 5:925–32. doi: 10.1021/cb100141y
22. Chen H, Chu G, Zhao L, Yamauchi N, Shigeyoshi Y, Hashimoto S, et al. Rev-erbα regulates circadian rhythms and StAR expression in rat granulosa cells as identified by the agonist GSK4112. *Biochem Biophys Res Commun.* (2012) 420:374–9. doi: 10.1016/j.bbrc.2012.02.164
23. Solt LA, Wang Y, Banerjee S, Hughes T, Kojetin DJ, Lundasen T, et al. Regulation of circadian behaviour and metabolism by synthetic REV-ERB agonists. *Nature.* (2012) 485:62–8. doi: 10.1038/nature11030
24. Kojetin D, Wang Y, Kamenecka TM, Burris TP. Identification of SR8278, a synthetic antagonist of the nuclear heme receptor REV-ERB. *ACS Chem Biol.* (2011) 6:131–4. doi: 10.1021/cb1002575
25. Dragano NRV, Solon C, Ramalho AF, de Moura RF, Razolli DS, Christiansen E, et al. Polyunsaturated fatty acid receptors, GPR40 and GPR120, are expressed

in the hypothalamus and control energy homeostasis and inflammation. *J Neuroinflammation.* (2017) 14:91. doi: 10.1186/s12974-017-0869-7
26. Gao Y, Bielohuby M, Fleming T, Grabner GF, Foppen E, Bernhard W, et al. Dietary sugars, not lipids, drive hypothalamic inflammation. *Mol Metab.* (2017) 6:897–908. doi: 10.1016/j.molmet.2017.06.008
27. Maldonado-Ruiz R, Montalvo-Martínez L, Fuentes-Mera L, Camacho A. Microglia activation due to obesity programs metabolic failure leading to type two diabetes. *Nutr Diabetes.* (2017) 7:e254. doi: 10.1038/nutd.2017.10
28. Paolicelli RC, Angiari S. Microglia immunometabolism: from metabolic disorders to single cell metabolism. *Semin Cell Dev Biol.* (2019) 94:129–37. doi: 10.1016/j.semcdb.2019.03.012
29. Valdearcos M, Robblee MM, Benjamin DI, Nomura DK, Xu AW, Koliwad SK. Microglia dictate the impact of saturated fat consumption on hypothalamic inflammation and neuronal function. *Cell Rep.* (2014) 9:2124–38. doi: 10.1016/j.celrep.2014.11.018
30. Milanova IV, Kalsbeek MJT, Wang XL, Korpel NL, Stenvers DJ, Wolff SEC, et al. Diet-induced obesity disturbs microglial immunometabolism in a time-of-day manner. *Front Endocrinol.* (2019) 10:424. doi: 10.3389/fendo.2019.00424
31. Yi CX, Walter M, Gao Y, Pitra S, Legutko B, Kälin S, et al. TNFα drives mitochondrial stress in POMC neurons in obesity. *Nat Commun.* (2017) 8:15143. doi: 10.1038/ncomms15143
32. Orihuela R, McPherson CA, Harry GJ. Microglial M1/M2 polarization and metabolic states. *Br J Pharmacol.* (2016) 173:649–65. doi: 10.1111/bph.13139
33. Wang A, Luan HH, Medzhitov R. An evolutionary perspective on immunometabolism. *Science.* (2019) 363:eaar3932. doi: 10.1126/science.aar3932
34. Keuper M, Jastroch M, Yi CX, Fischer-Posovszky P, Wabitsch M, Tschöp MH, et al. Spare mitochondrial respiratory capacity permits human adipocytes to maintain ATP homeostasis under hypoglycemic conditions. *FASEB J.* (2014) 28:761–70. doi: 10.1096/fj.13-238725
35. Brand M. The efficiency and plasticity of mitochondrial energy transduction. *Biochem Soc Trans.* (2005) 33(Pt 5):897–904. doi: 10.1042/BST20050897
36. Hughes ME, Hogenesch JB, Kornacker K. JTK-CYCLE an efficient nonparametric algorithm for detecting rhythmic components in genome-scale data sets. *J Biol Rhythms.* (2010) 25:372–80. doi: 10.1177/0748730410379711
37. Nakazato R, Takarada T, Yamamoto T, Hotta S, Hinoi E, Yoneda Y. Selective upregulation of Per1 mRNA expression by ATP through activation of P2X7 purinergic receptors expressed in microglial cells. *J Pharmacol Sci.* (2011) 116:350–61. doi: 10.1254/jphs.11069FP
38. Logan RW, Sarkar DK. Circadian nature of immune function. *Mol Cell Endocrinol.* (2012) 349:82–90. doi: 10.1016/j.mce.2011.06.039
39. Nakazato R, Hotta S, Yamada D, Kou M, Nakamura S, Takahata Y, et al. The intrinsic microglial clock system regulates interleukin-6 expression. *Glia.* (2017) 65:198–208. doi: 10.1002/glia.23087
40. Gao Y, Ottaway N, Schriever SC, Legutko B, García-Cáceres C, de la Fuente E, et al. Hormones and diet, but not body weight, control hypothalamic microglial activity. *Glia.* (2014) 62:17–25. doi: 10.1002/glia.22580
41. Guo D, Zhu Y, Sun H, Xu X, Zhang S, Hao Z, et al. Pharmacological activation of REV-ERBα represses LPS-induced microglial activation through the NF-κB pathway. *Acta Pharmacol Sin.* (2019) 40:26–34. doi: 10.1038/s41401-018-0064-0
42. Kitchen GB, Cunningham PS, Poolman TM, Iqbal M, Maidstone R, Baxter M, et al. The clock gene Bmal1 inhibits macrophage motility, phagocytosis, and impairs defense against pneumonia. *Proc Natl Acad Sci USA.* (2020) 117:1543–51. doi: 10.1073/pnas.1915932117
43. Sulli G, Rommel A, Wang X, Kolar MJ, Puca F, Saghatelian A, et al. Pharmacological activation of REV-ERBs is lethal in cancer and oncogene-induced senescence. *Nature.* (2018) 553:351–5. doi: 10.1038/nature25170
44. Borst K, Schwabenland M, Prinz M. Microglia metabolism in health and disease. *Neurochem Int.* (2019) 130:104331. doi: 10.1016/j.neuint.2018.11.006
45. Bugge A, Feng D, Everett LJ, Briggs ER, Mullican SE, Wang F, et al. Rev-erbα and Rev-erbβ coordinately protect the circadian clock and normal metabolic function. *Genes Dev.* (2012) 26:657–67. doi: 10.1101/gad.186858.112
46. Everett LJ, Lazar MA. Nuclear receptor Rev-erbα: up, down, and all around. *Trends Endocrinol Metab.* (2014) 25:586–92. doi: 10.1016/j.tem.2014.06.011
47. Dierickx P, Emmett MJ, Jiang C, Uehara K, Liu M, Adlanmerini M, et al. SR9009 has REV-ERB–independent effects on cell proliferation and metabolism. *Proc Natl Acad Sci USA.* (2019) 16:12147–52. doi: 10.1073/pnas.1904226116

Conflict of Interest: The authors declare that the research was conducted in the absence of any commercial or financial relationships that could be construed as a potential conflict of interest.

Supplementary Material

The effect of Rev-erbα agonist SR9011 on the immune response and cell metabolism of microglia

Samantha E.C. Wolff[1,2,3], Xiao-Lan Wang[1,2,5], Han Jiao[3], Jia Sun[3], Andries Kalsbeek[1,2,4], Chun-Xia Yi[1,2,4 #], Yuanqing Gao[3 #]

Supplementary figures

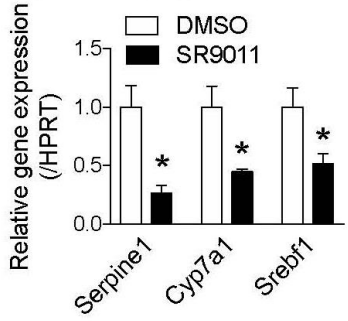

Figure S1. The effects of SR9011 on the Rev-erbα related targets. Primary microglia were treated with SR9011 or DMSO for 24 hours. The Rev-erbα responsive genes *Serpine1*, *Cyp7a1* and *Srebf1* expression is downregulated by SR9011. $p<0.05$* vs DMSO determined by unpaired t-test.

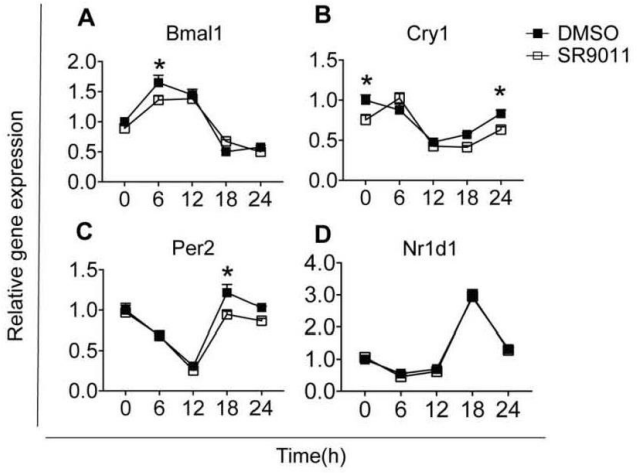

Figure S2. The effects of SR9011 do not persist in the absence of SR9011. Primary microglia were pretreated with SR9011 for 12 hours, synchronized by dexamethasone for 2 hours, and cultured for 0, 6, 12, 18 or 24 hours before being harvested. *Bmal1, Cry1, Per2* and *Nr1d1* show rhythmic expression in both DMSO and SR9011 treated groups. SR9011 does not disrupt the microglial clock genes rhythmicity when used as a pretreatment (see JTK analysis in Table S3). Data are presented as means ± SEM and statistical significance was determined using Two-Way ANOVA with Bonferroni's post-test and multiple comparison.

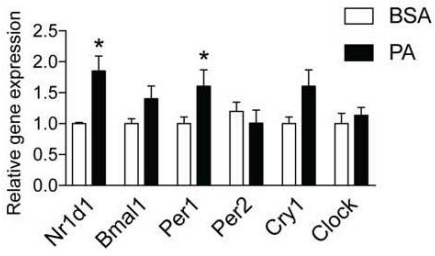

Figure S3. The effect of palmitic acid on core clock genes. Primary microglia were treated with DMSO for 12 hours followed by 50 μM palmitic acid (PA) or BSA treatment for 12 hours (n=4 per group). *Nr1d1* and *Per1* expression increased after 12h incubation with PA compared with BSA. $p<0.05$* vs BSA.

Supplementary tables

Table S1. Primer sequences of target genes.

	Genes	Forward	Reverse	Product size	RefSeq accession
Clock	*Bmal1*	CCGATGACGAACTGAAACACCT	TGCAGTGTCCGAGGAAGATAGC	215bp	NM_024362.2
	Per1	CGCACTTCGGGAGCTCAAACTTC	GTCCATGGCACAGGGCTCACC	188bp	NM_001034125.1
	Clock	CGATCACAGCCCAACTCCTT	TTGCAGCTTGAGACATCGCT	239bp	NM_001289832.1
	Nr1d1	ACAGCTGACACCACCCAGATC	CATGGGCATAGGTGAAGATTTCT	101bp	NM_001113422.1
	Per2	CACCCTGAAAAGAAAGTGCGA	CAACGCCAAGGAGCTCAAGT	148bp	NM_031678.1
	Cry1	AAGTCATCGTGCGCATTTCA	TCATCATGGTCGTCGGACAGA	196bp	NM_198750.2
Cytokines	*Il1β*	TGTGATGAAAGACGGCACAC	CTTCTTCTTTGGGTATTGTTTGG	70bp	NM_031512.2
	Il6	TTGTTGACAGCCACTGCCTTCCC	TGACAGTGCATCATCGCTGTTCA	198bp	NM_012589.2
	Il10	CGACGCTGTCATCGATTTCTC	CAGTAGATGCCGGGTGGTTC	186bp	NM_012854.2
	Tnfa	ATCGGTCCCAACAAGGAGGA	GCTTGGTGGTTTGCTACGA	137bp	NM_012675.3
	Ccl2	CCACCACTATGCAGGTCTCT	GCATTAACTGCATCTGGCTGAGA	97bp	NM_031530.1
	Gm-csf	TACAAGCAGGGTCTACGGGG	AGTCAGTTTCCGGGGTTGGA	103bp	NM_053852.1
	Tgfβ	ACCGCAACAACGCAATCTATG	CACTCAGGCGTATCAGTGGG	241bp	NM_021578.2
Metabolism	*CD36*	ACAGTTTTGGATCTTTGACGTG	CCTTGGCTAAATAACGAACTCTG	113bp	NM_031561.2
	CD68	TGTTCAGCTCCAAGCCCAAA	GCTCTGATGTCGGTCCTGTTT	196bp	NM_001031638.1
	Cpt1	AGAGCAATAGGTCCCCACTCAA	ATGAAATCACACCCACCACCA	231bp	NM_031559.2
	Pdk1	CGGCGGGGCTCGGTATG	TTCACAAGCATTTACTGACCCGAAG	230bp	NM_053826.2
	Hk2	GGTGAGCCATCGTGGTTAAG	CTTCCGGAACCGCCTAGAAA	295bp	NM_012735.2
	Glut5	TGCCCTATGTCAGCATCGTC	GGACCAAGGCCCACTTGAAT	202bp	NM_031741.1
	Fasn	CTTGGGTGCCGATTACAACC	GCCCTCCCGTACACTCACTC	185bp	NM_017332.1
	Serpine1	GGCACAATCCAACAGAGACAA	CAGTGCCGGGGTAAGAAAGA	182bp	NM_012620.1
	Cyp7a1	GGAATTGCCGTGTTGGTGAG	AGGTTCACCAGCTTTCCTTCT	72bp	NM_012942.2
	Srebf1	CTTGACCGACATCGAAGACAT	GGCATCAAATAGGCCAGGGA	74bp	NM_001276707.1
Housekeeping	*Hprt*	TTGGTCAAGCAGTACAGCCC	CTTGCCGCTGTCTTTTAGGC	227bp	NM_012583.2

Table S2.

Genes	Two-way ANOVA analysis		
	p-value		
	Interaction	Time	SR9011
Bmal1	**0.0055**	**<0.0001**	0.2253
Cry1	**0.0021**	**<0.0001**	**0.0060**
Per2	0.1216	**<0.0001**	**0.0119**
Nr1d1	0.8792	**<0.0001**	0.8006

Table S2. Two-way ANOVA assessment of effect of Time, SR9011, and Interaction in clock genes in primary microglia with SR9011 before synchronization with dexamethasone for Figure S2. SR9011, Time and Interaction effects were evaluated in primary microglia for clock genes after treatment with DMSO or SR9011. SR9011 has a significant impact on *Cry1* and *Per2*, and has an interaction effect with time on *Bmal1* and *Cry1*.

Table S3. JTK_Cycle analysis of clock genes in primary microglia pretreated with SR9011 **before synchronization with dexamethasone.**

Gene	DMSO		SR9011	
	P-value	Acrophase	P-value	Acrophase
Bmal1	<0.0001	9	0.002	12
Cry1	<0.0001	3	<0.0001	6
Per2	<0.0001	21	<0.0001	0
Nr1d1	<0.0001	21	<0.0001	21

Table S3. Primary microglia were pretreated with SR9011 for 12 hours, synchronized by dexamethasone for 2 hours, and cultured for 0, 6, 12, 18 or 24 hours before being harvested. Clock genes rhythmicity is analyzed by JTK_Cycle. SR9011 does not disrupt clock genes rhythmicity after being removed from the medium. An estimated shift in acrophase can be found for *Bmal1, Cry1,* and *Per2.*

Publication 4

Diet-Induced Obesity Disturbs Microglial Immunometabolism in a Time-of-Day Manner

Milanova IV[1,2], Kalsbeek MJT[1,2], **Wang XL**[1,2], Korpel NL[1,2], Stenvers DJ[1,2], Wolff SEC[1,2], de Goede P[1,2], Heijboer AC[2,3], Fliers E[1,2], la Fleur SE[1,2,4], Kalsbeek A[1,2,4], Yi CX[1,2].

[1] Department of Endocrinology and Metabolism, Amsterdam University Medical Center, University of Amsterdam, Amsterdam, Netherlands
[2] Laboratory of Endocrinology, Amsterdam University Medical Center, Amsterdam Gastroenterology & Metabolism, University of Amsterdam, Amsterdam, Netherlands
[3] Endocrine Laboratory, Department of Clinical Chemistry, Amsterdam University Medical Center, Amsterdam Gastroenterology & Metabolism, Vrije Universiteit Amsterdam, Amsterdam, Netherlands.
[4] Netherlands Institute for Neuroscience, Royal Netherlands Academy of Arts and Sciences, Amsterdam, Netherlands

Published in frontiers in Endocrinology (Lausanne). 2019 Jun 26;10:424.
doi: 10.3389/fendo.2019.00424.

frontiers in Endocrinology

ORIGINAL RESEARCH
published: 26 June 2019
doi: 10.3389/fendo.2019.00424

Diet-Induced Obesity Disturbs Microglial Immunometabolism in a Time-of-Day Manner

Irina V. Milanova[1,2], *Martin J. T. Kalsbeek*[1,2], *Xiao-Lan Wang*[1,2], *Nikita L. Korpel*[1,2], *Dirk Jan Stenvers*[1,2], *Samantha E. C. Wolff*[1,2], *Paul de Goede*[1,2], *Annemieke C. Heijboer*[2,3], *Eric Fliers*[1,2], *Susanne E. la Fleur*[1,2,4], *Andries Kalsbeek*[1,2,4] *and Chun-Xia Yi*[1,2*]

[1] *Department of Endocrinology and Metabolism, Amsterdam University Medical Center, University of Amsterdam, Amsterdam, Netherlands,* [2] *Laboratory of Endocrinology, Amsterdam University Medical Center, Amsterdam Gastroenterology & Metabolism, University of Amsterdam, Amsterdam, Netherlands,* [3] *Endocrine Laboratory, Department of Clinical Chemistry, Amsterdam University Medical Center, Amsterdam Gastroenterology & Metabolism, Vrije Universiteit Amsterdam, Amsterdam, Netherlands,* [4] *NetherlandsInstitute for Neuroscience, Royal Netherlands Academy of Arts and Sciences, Amsterdam, Netherlands*

Background: Disturbance of immunometabolic signaling is a key process involved in the progression of obesity. Microglia—the resident immune cells in the brain, initiate local immune responses. It is known that hypercaloric diets lead to microglial activation. Previously, we observed that hypothalamic microglial cells from mice fed high-fat diet (HFD) lose their day/night rhythm and are constantly activated. However, little is known about daily rhythmicity in microglial circadian, immune and metabolic functions, either in lean or obese conditions. Therefore, we hypothesized that HFD disturbs microglial immunometabolism in a day/night-dependent manner.

Methods: Obesity was induced in Wistar rats by feeding them HFD *ad libitum* for the duration of 8 weeks. Microglia were isolated from HFD- and chow-fed control animals at six time points during 24 h [every 4 h starting 2 h after lights on, i.e., Zeitgeber Time 2 (ZT2)]. Gene expression was evaluated using quantitative RT-PCR. JTK_Cycle software was used to estimate daily rhythmicity. Statistical analysis was performed with two-way ANOVA test.

Results: Consumption of the obesogenic diet resulted in a 40 g significantly higher body weight gain in week 8, compared to chow diet ($p < 0.0001$), associated with increased adiposity. We observed significant rhythmicity of circadian clock genes in microglia under chow conditions, which was partially lost in diet-induced obesity (DIO). Microglial immune gene expression also showed time-of-day differences, which were disrupted in HFD-fed animals. Microglia responded to the obesogenic conditions by a shift of substrate utilization with decreased glutamate and glucose metabolism in the active period of the animals, and an overall increase of lipid metabolism, as indicated by gene expression evaluation. Additionally, data on mitochondria bioenergetics and dynamics suggested an increased energy production in microglia during the inactive period on HFD. Finally, evaluation of monocyte functional gene expression showed small or absent effect of HFD on peripheral myeloid cells, suggesting a cell-specific microglial inflammatory response in DIO.

OPEN ACCESS

Edited by:
Vinicius Frias Carvalho, Oswaldo Cruz Foundation (Fiocruz), Brazil

Reviewed by:
Licio A. Velloso, Campinas State University, Brazil
Yinghua Yu, Xuzhou Medical University, China

****Correspondence:***
Chun-Xia Yi
c.yi@amsterdamumc.nl

Specialty section:
This article was submitted to Neuroendocrine Science, a section of the journal Frontiers in Endocrinology

Received: *12 April 2019*
Accepted: *12 June 2019*
Published: *26 June 2019*

Citation:
Milanova IV, Kalsbeek MJT, Wang X-L, Korpel NL, Stenvers DJ, Wolff SEC, de Goede P, Heijboer AC, Fliers E, la Fleur SE, Kalsbeek A and Yi C-X (2019) Diet-Induced Obesity Disturbs Microglial Immunometabolism in a Time-of-Day Manner. Front. Endocrinol. 10:424. doi: 10.3389/fendo.2019.00424

Conclusions: An obesogenic diet affects microglial immunometabolism in a time-of-day dependent manner. Given the central role of the brain in energy metabolism, a better knowledge of daily rhythms in microglial immunometabolism could lead to a better understanding of the pathogenesis of obesity.

Keywords: microglia, immunometabolism, neuroinflammation, diet-induced obesity, high-fat diet, daily rhythms

INTRODUCTION

Arising evidence highlights the disturbed interaction between immunity and metabolism as a key player in the pathogenesis of obesity (1–3). Immune cell function is highly dependent on metabolic adaptation of the immune cells, allowing for abrupt shifts in energy utilization, thus promoting either a resting or an activated state (4). Moreover, distinct immune cell populations show specific metabolic patterns, modulating their functional properties (4). In the brain, microglia are involved in maintaining brain homeostasis by surveying the environment, sensing invading pathogens and phagocyting dead neurons, and cellular debris, thus eliciting an innate immune response (5, 6). Microglial metabolic reprogramming is associated with polarization to pro- or anti-inflammatory state, which involves both functional and phenotypic plasticity (7, 8). It has been shown that hypercaloric environment induces a proinflammatory response in the hypothalamus via NF-kB and toll-like receptor activation, leading to disturbed energy homeostasis (9–13). This could be due to hypothalamic microglial activation as seen in rodents fed an obesogenic diet (14–17). We observed that under physiological conditions in mice, microglial cells exert their function in a strict time-of-day manner with higher activity during the dark, active phase, compared to the light, sleep phase (18). However, this day-night rhythm was abolished in animals fed an obesogenic, high-fat diet (HFD), suggesting an interaction of diet content and daily rhythms. Indeed, recent evidence suggest an involvement of circadian function in the progression of obesity (19, 20). It is well-known now that a master circadian clock in mammals generates daily rhythms in behavioral, physiological, and hormonal processes to allow adaptation to daily environmental changes, thus optimizing metabolic function to the time of day (21). However, little is known about daily rhythms in microglial function. Therefore, we performed a detailed investigation of daily rhythmicity in microglial immunometabolism in lean and obese rats. As mentioned earlier, many studies have focused on hypothalamic microglial inflammatory response due to the clear relation between the hypothalamus and energy homeostasis. Here, we chose to evaluate cortical microglial activation, to expand on available knowledge on microglial immunometabolism in obesity outside of the hypothalamus.

We induced obesity with HFD for the duration of 8 weeks in rats and evaluated the expression of key clock genes involved in maintaining circadian rhythms (**Figure 1**). Microglial cells, as many other immune cells, have a high metabolic demand (22). Therefore, we also evaluated the expression of key genes involved in microglial glucose, lipid, and glutamate metabolism. As higher activity and substrate utilization require higher energy production we also assessed the state of mitochondria bioenergetics and dynamics in response to either healthy or obesogenic diet. The immune state of the cells was studied by evaluating cytokine production and phagocytosis (**Figure 1**). Our results showed time-of-day disturbances in microglial circadian and inflammatory functions in the obesogenic conditions, accompanied with changes in substrate utilization and energy production. We compared these data to monocytes, isolated from the same animals, to evaluate the state of peripheral myeloid cells in a hypercaloric environment. We observed a small effect of HFD on monocyte function, suggesting a microglia-specific response to hypercaloric intake. These results shed further light on microglial time-of-day innate immunometabolism in health and obesity.

Abbreviations: (Abbreviations in italic represent target genes tested) *Atp5b*, ATP synthase subunit b; *Atp5g*, ATP synthase subunit g; *bactin*, Beta-actin; *Bmal1*, Brain and muscle ARNT-Like 1; *Cd36*, Cluster of differentiation 36; *Cd68*, Cluster of differentiation 68; *Clock*, Circadian locomotor output cycles kaput; *Cox4*, Cytochrome C oxidase subunit 4; *Cry1*, Cryptochrome 1; *Cry2*, Cryptochrome 2; *Dbp*, D-box binding protein; DIO, Diet-induced obesity; *Drp1*, Dynamin-related protein 1; EDTA, Ethylenediaminetetraacetic acid; FA, Fatty acid; *Fas*, Fatty acid synthesis; *Fis1*, Fission 1; *Gdh*, Glutamate dehydrogenase; *Gls*, Glutaminase; *Glut5*, Glucose transporter type 5; *Gpx1*, Glutathione peroxidase 1; HFD, High-carbohydrate-high-fat diet; *Hk2*, Hexokinase 2; *Hprt*, Hypoxanthine phosphoribosyltransferase 1; *Ikbkb*, Inhibitor of nuclear factor kappa B kinase subunit betta; *Il1b*, Interleukin 1 betta; *Lpl1*, Lipoprotein lipase 1; *Mfn2*, Mitofusin 2; *Myd88*, Myeloid differentiation primary response 88; NEFA, Non-esterified fatty acids; *Opa1*, Optic atrophy 1; *Pdk4*, Pyruvate dehydrogenase kinase 4; *Per1*, Period 1; *Per2*, Period 2; POMC, Proopiomelanocortin; *Ppard*, Peroxisome proliferator activated receptor delta; pWAT, Perirenal white adipose tissue; *Reverba*, Reverse viral erythroblastosis oncogene product alfa; RIA, Radioimmunoassay; ROS, Reactive oxygen species; SEM, Standard error of the mean; *Sirt1*, Sirtuin 1; *Tnfa*, Tumor necrosis factor alfa; ZT, Zeitgeber Time.

METHODS

Animals

Seventy-two male Wistar rats (Charles River, Germany) were group housed on a 12-h-light/12-h-dark cycle [lights on at 7:00 am; Zeitgeber time zero (ZT0)] at 22 ± 2°C with access to food and water *ad libitum*. Obesity was induced for the duration of 8 weeks, with a diet containing 60 kcal% fat and 20 kcal% carbohydrates (HFD, 5.24 kcal/g, D12492, Research Diets Inc.). Control animals were fed a standard chow diet (3.1 kcal/g, 2018, Teklad diets, Invigo). Body weight was monitored once per week, and food intake twice per week. All studies were approved by the Animal Ethics Committee of the Royal Dutch Academy of Arts and Sciences (KNAW, Amsterdam) and performed according

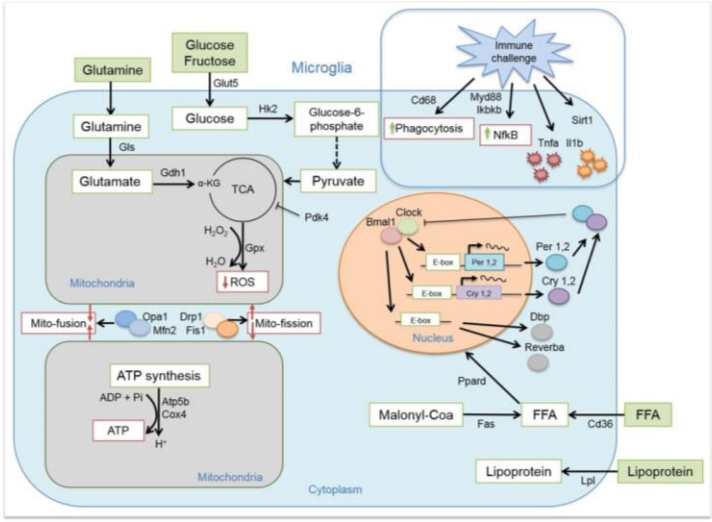

FIGURE 1 | Microglial circadian, immune, metabolic, and mitochondrial profile. Schematic representation of the pathways and/or functions tested on microglial cells from chow- and HFD-fed rats.

to the guidelines on animal experimentation of the Netherlands Institute for Neuroscience (NIN, Amsterdam).

Microglia/Monocyte Isolation and Plasma Collection

Animals were sacrificed at six time points during 24 h (every 4 h starting at ZT2) by euthanasia with 60% CO_2/40% O_2, followed by decapitation. Perirenal white adipose tissue (pWAT) was dissected for evaluation of fat mass gain, evaluating the amount of pWAT in grams weight. Microglial cells from cerebral cortex were isolated for gene expression analysis using the Percoll isopycnic isolation, as it provides a high cell number (23). Briefly, brains were mechanically homogenized with RPMI 1640 medium (Ref.: 11875-093, Gibco™) and filtered through 70 µm cell strainer (Ref.: 431751, Corning®) in a 15 mL Falcon tube. Brain homogenate was centrifuged for 5′ (380 g, 4°C). Pellets were resuspended with 7 mL RPMI medium and mixed with 100% Percoll solution [for 10 mL: 9 mL Percoll® stock (Ref.: 17-5445-01, GE Healthcare, Sigma-Aldrich®) with 1 mL 10x HBSS (Ref.: 14185-045, Gibco™)]. The cell suspension was layered slowly on 70% Percoll solution [for 10 mL: 7 mL 100% Percoll solution with 3 mL 1x HBSS (Ref.: 14175-053, Gibco™)] and centrifuged for 30′ (500 g, 18°C, break 1/0). Cell debris on the surface was discarded and fuse interphase, containing microglial cells were collected in 8 mL 1x HBSS, followed by centrifuging for 7′ (500 g, 18°C, break 9/9). Supernatant was discarded and the microglial cell pellet was used directly for RNA extraction.

During decapitation trunk blood was collected for measurement of different parameters. Briefly, blood was collected in 50 mL Falcon tubes, containing 0.5 M EDTA (ethylenediaminetetraacetic acid). Blood was filtered through a 70 µm cell strainer in a 15 mL Falcon tube and separated for monocyte isolation. For plasma collection, 2 mL blood was centrifuged for 15′ (4,000 rpm, 4°C, break 9/9). Plasma was collected in a new tube and stored at −80°C until usage. For monocyte isolation, 30 mL lysis buffer (containing 1× ACK; 155 mM NH_4Cl; 10 mM $KHCO_3$; 0.1 mM EDTA) was added to ∼3 mL blood and vortexed gently, followed by incubation at RT for 10–15′. The cell suspension was centrifuged for 5′ (200 g, RT, 9/9 break), supernatant was discarded and cells were resuspended in 2 mL PBS-FBS (PBS containing 1% FBS). The new cell suspension was again centrifuged for 5′ (200 g, RT, 9/9 break), supernatant was discarded and cells were resuspended in 0.5 mL PBS-FBS. The cell suspension was added to 4.5 mL RPMI medium and layered slowly on 5 mL Ficoll® (Ref.: 17-1440-02, GE Healthcare, Sigma-Aldrich®), followed by centrifuging for 30′ (400 g, 20°C, break 1/1). The fuse interphase, containing monocytes, was collected in 8 mL 1x HBSS, followed by centrifuging for 5′ (200 g, RT). Supernatant was discarded and the monocyte pellet was used for RNA extraction.

Real-Time PCR

For gene expression analysis, RNA from microglial cells and monocytes was extracted using the RNeasy Micro Kit (Cat No. 74004, Qiagen®) according to the manufacturer's guidelines. RNA was quantified by spectrophotometry at 260 nm (DS 11; Denovix). RNA was reverse transcribed using Transcriptor First Strand cDNA Synthesis Kit (04897030001; Roche) according to the manufacturer's guidelines. Levels of mRNA for *Tnfa, Bmal1,*

Per1, Per2, Cry1, Cry2, Dbp, Reverba, Clock, Gls, Gdh, Gpx1, Cd36, Fas, Lpl1, Opa1, Mfn2, Fis1, Drp1, Pdk4, Ppard, Ikbkb, Cd68, Il1b, Cox4, Atp5b, Atp5g, Hk2, Glut5, Myd88, Sirt1, Hprt (internal control), and *bactin* (internal control) were measured by semiquantitative real-time PCR on a LightCycler LC480 (Roche), using the SensiFAST SYBR® No-ROX Kit (BIO-98020, GC-Biotech) according to the manufacturer's guidelines. Expression levels of all genes were normalized to the geometric mean of the internal controls. Primer sequences (see **Table S1**) were designed using the Basic Local Alignment Search Tool (BLAST) from the National Center for Biotechnology Information (NCBI). Primers were purchased from Sigma-Aldrich® and validated by melt curve analysis and DNA band size and/or purity on agarose gel electrophoresis (data not shown).

Glucose, Insulin, and Non-esterified Fatty Acids (NEFA) Measurements in Plasma

Plasma glucose concentrations were measured using the Glucose GOD-PAP kit (Ref. 80009, Biolabo S.A.S.), following the manufacturer's guidelines. Absorbance of colored samples, proportional to glucose concentration, was measured at 500 nm with Varioskan® Flash spectral scanning multimode reader (Version 40053; Thermo Scientific). Insulin concentrations were measured using Rat Insulin Radioimmunoassay (RIA) Kit (RI-13K; Millipore, Merck), according to the manufacturer's guidelines. Non-esterified fatty acids (NEFA) concentration in plasma was measured using the NEFA HR(2) reagents (R1 set, Ref. 434-91795; R2 set, Ref. 436-91995; Standard, Ref. 270-77000, Wako Chemicals GmbH) following the adjusted protocol from the Mouse Metabolic Phenotyping Centers [https://www.mmpc.org/shared/document.aspx?id=196&docType=Protocol]. Within-run variations for all measurements fall in the range suggested by the manufacturers.

Statistical Analyses

All results are expressed as mean ± SEM. Statistical analyses were performed using Graph-Pad PRISM (version 7.03, GraphPad Software, Inc.) and JTK_Cycle software (24). Two-way ANOVA analysis was used for effects of *Diet*, *Time*, (ZT) and *Interaction*. Unpaired *t*-tests were used to evaluate the effect of diet for each time point, unless stated otherwise. Sidak's multiple comparison test was used to compare the effect of diet for the food intake, body weight gain, and plasma measurements data (**Figures 2A,B,D–F**). One-way ANOVA analysis was used to assess the effect of *Time* for the chow and HFD groups separately. JTK_Cycle analysis *p*-values were obtained by fitting the data on a curve with fixed 24 h period. Results were considered statistically significant when $p < 0.05$.

RESULTS

HFD Intake Induces Obesity in Rats

We observed that chronic feeding with HFD for 8 weeks induced obesogenic phenotype in adult male rats, compared to control animals on the standard chow diet. The HFD rats had a higher caloric intake (**Figure 2A**) and a 40 g higher body weight gain after 8 weeks as compared to controls (**Figure 2B**). Moreover, there was a 2-fold increase in pWAT mass in HFD-fed animals compared to controls (**Figure 2C**). These results were in line with other literature available on diet-induced obesity (DIO) in rodents (14, 25). To assess glycemic status at the time of death, we evaluated glucose and insulin concentrations in plasma over the 24 h cycle. Control animals showed the expected daily rhythm in glucose concentrations in the plasma (26). However, HFD-fed animals showed increased glucose concentrations during the light phase at ZT6 (inactive period) (**Figure 2D**). The overall high levels of glucose concentration in both conditions could be explained by our choice of euthanasia (60% CO_2/40% O_2), as it has been shown previously that CO_2 causes acidosis which stimulates enzymes of the glycolytic pathway, leading to decreased liver glycogen stores and increased plasma glucose concentrations, both in fed and fasted animals (27, 28). Insulin concentrations were significantly elevated in HFD-fed animals during the dark phase (active period) at ZT18, which could indicate an impaired insulin sensitivity, as glucose concentrations during this period were not elevated, but overall maintained during 24 h (**Figure 2E**). A similar trend of increased insulin secretion during the dark phase has also been observed in mice on a HFD (29). Evaluation of the NEFA concentrations in plasma showed a significant increase in HFD-fed animals during the light phase (ZT2-ZT10) compared to chow controls (**Figure 2F**). Together, these data indicate metabolic changes toward obesity in animals fed HFD.

HFD Disturbs Microglial Circadian Gene Expression

It has been shown previously that microglial cells express clock genes (30, 31). Diets rich in fat and/or sugar are known to alter circadian rhythms of clock gene expression in peripheral tissue (32, 33). To test whether HFD also disturbs daily microglial rhythmicity, we studied expression of genes within the transcriptional feedback loop—circadian locomotor output cycles kaput (*Clock*) and brain and muscle ARNT-Like 1 (*Bmal1*)—the so-called activators and the repressors—period and cryptochrome genes (*Per1, Per2, Cry1,* and *Cry2*). Additionally, we assessed the expression of two other clock genes—reverse viral erythroblastosis oncogene product alfa (*Reverbα*), a *Clock* and *Bmal1* repressor, and D-box binding protein (*Dbp*), a regulator of peripheral circadian input (34).

Control animals fed chow diet showed a clear rhythmic expression for all genes, except *Clock* and *Cry2* (see **Table S2**). Rhythmicity of *Bmal1, DBP,* and *Reverbα* was not influenced by HFD, although a reduced amplitude was observed for *DBP* and *Reverbα*. There was a gain of rhythm for *Clock* expression. However, *Per1, Per2,* and *Cry1* showed a loss of rhythmic expression during HFD, as evaluated with JTK_Cycle (see **Table S2**). Moreover, all genes showed a significant *Interaction* effect, as well as difference between HFD and chow-fed animals at the transition period between dark and light phase (ZT22 and/or ZT2) (**Figures 3A–H; Table 1**). These data point to a clock disturbance, which could lead to irregularity in the expression of other key microglial genes, as it is known that clock genes regulate the expression of 10–20% of all cell genes (34).

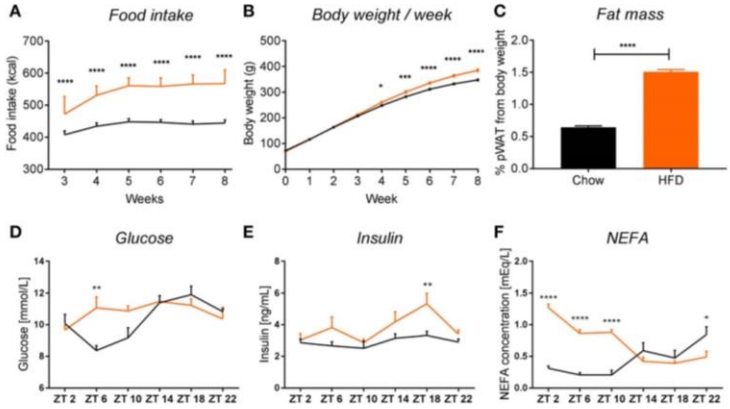

FIGURE 2 | HFD intake leads to obesity in rats. HFD (orange) leads to an increase in food intake **(A)** ($p_{int} < 0.0001$, $p_{time} < 0.0001$, $p_{diet} < 0.0001$), body weight **(B)** ($p_{int} < 0.0001$, $p_{time} < 0.0001$, $p_{diet} = 0.0003$), and fat mass gain, seen as 2-fold increase in perirenal white adipose tissue **(C)** in rats, compared to chow-fed controls (black). Plasma measurements in non-fasted HFD-fed animals show an increase in glucose at ZT6 **(D)** ($p_{int} = 0.0032$, $p_{time} = 0.0003$, $p_{diet} = 0.0874$), increased insulin at ZT18 **(E)** ($p_{int} = 0.2802$, $p_{time} = 0.0042$, $p_{diet} = 0.0006$), and significant increase in non-esterified fatty acids during the light phase **(F)** ($p_{int} < 0.0001$, $p_{time} = 0.0006$, $p_{diet} < 0.0001$). Data are presented as means ± SEM. Statistical significance was determined using Two-way ANOVA **(A,B,D–F)** or unpaired *t*-test **(C)**. Effect of diet within each time point was evaluated with Sidak's multiple comparison test **(A,B,D–F)** (*$p < 0.05$; **$p < 0.01$, ***$p < 0.001$, ****$p < 0.0001$).

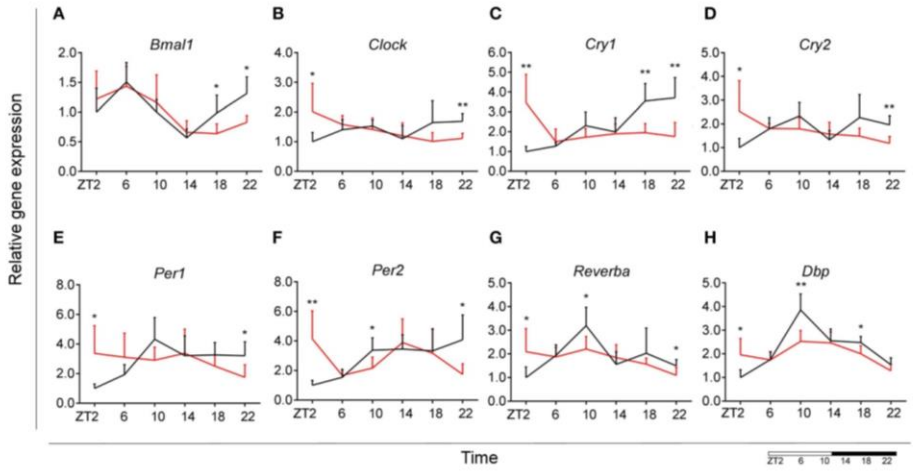

FIGURE 3 | Microglial circadian clock system in HFD-fed and control animals. Relative gene expression of circadian genes *Bmal1* **(A)**, *Clock* **(B)**, *Cry1* **(C)**, *Cry2* **(D)**, *Per1* **(E)**, *Per2* **(F)**, *Reverba* **(G),** and *Dbp* **(H)** in HFD-fed rats (red) compared to Chow-fed controls (black). Data are presented as means ± SEM. Statistical significance was determined using Two-way ANOVA effects for *Interaction*, *Diet,* and *Time* (ZT); Student *t*-test is used for diet effect within a separate time point (*$p <$ 0.05; **$p < 0.01$). Scale (bottom right) represents light (ZT0-12) and dark (ZT12-24) phase.

Microglial Time-of-Day Disturbance of Inflammatory Signaling During HFD

To evaluate the effect of HFD on daily changes in microglial activation, we assessed the relative gene expression of the main cytokines secreted by microglia—tumor necrosis factor α (*Tnfa*) and interleukin 1β (*Il1b*). We observed an increased expression of *Tnfa* at the transition between dark and light phase, as well as increased *Il1b* production at the end of the light period for animals fed HFD, pointing to an increased microglial activation in the obesogenic group, compared

TABLE 1 | Two-way ANOVA assessment of effect of *Time*, *Diet*, and *Interaction* in microglia.

Genes	Two-way ANOVA analysis		
	p-value		
	Interaction	*Time*	*Diet*
Circadian			
Bmal1	**0.0356**	**<0.0001**	0.3308
Clock	**0.0006**	0.4015	0.9599
Cry1	**<0.0001**	**0.0002**	0.1484
Cry2	**<0.0001**	0.1616	0.7026
Per1	**0.0011**	**0.0437**	0.9673
Per2	**<0.0001**	**0.0035**	0.9989
Reverba	**0.0023**	**<0.0001**	0.5351
Dbp	**<0.0001**	**<0.0001**	0.0573
Inflammatory			
Tnfa	0.1547	**0.0042**	0.1705
Il1b	**0.0085**	0.2610	0.4658
Myd88	**0.0378**	**0.0022**	**0.0140**
Ikbkb	**<0.0001**	**0.0165**	0.7572
Cd68	0.0685	**0.0226**	**0.0014**
Sirt1	**0.0004**	0.2071	0.4654
Metabolic			
Gls	**0.0138**	0.4456	0.0888
Gdh	**0.0095**	0.8306	0.8648
Gpx1	**0.0009**	0.9390	0.8424
Hk2	**0.0023**	**0.0274**	**0.0024**
Glut5	**0.0058**	0.0935	**0.0025**
Cd36	**0.0031**	**0.0004**	0.1116
Lpl	0.0554	**0.0064**	**0.0412**
Ppard	**0.0034**	0.6143	0.7868
Fas	**0.0030**	0.5214	0.6840
Mitochondrial			
Cox4	**<0.0001**	0.1598	0.8468
Atp5b	**0.0020**	**0.0257**	**0.0194**
Pdk4	0.2512	**<0.0001**	0.7817
Fis1	**0.0001**	0.3438	0.0934
Drp1	**<0.0001**	0.2189	0.6340
Mfn2	**0.0001**	0.4675	0.1899
Opa1	**0.0056**	0.9284	0.6975

Diet, Time, and Interaction effects were evaluated in microglia for circadian, inflammatory, metabolic, and mitochondrial genes. Statistical significance was determined using Two-way ANOVA effect for Interaction, Diet, and Time (ZT). Data are presented as means ± SEM. Genes are considered rhythmic when $p < 0.05$ (Bold).

to controls (**Figures 4A,B**). However, myeloid differentiation primary response 88 (*Myd88*) gene expression, an adaptor for inflammatory signaling pathways, located downstream of Il1b, showed a decrease at ZT2 in HFD-fed animals (**Figure 4C**). Therefore, we assessed the expression of inhibitor of nuclear factor kappa B kinase subunit betta (*Ikbkb*) as the protein it encodes phosphorylates the inhibitor in the inhibitor/NFkB complex, leading to activation of nuclear factor kappa-light-chain-enhancer of activated B cells NFkB—a transcriptional activator of key genes involved in cell survival, proliferation and inflammatory response. We observed an inverted daily pattern of *Ikbkb* expression between chow and HFD animals, with higher expression at the beginning of the light phase, but lower expression at the end of the dark phase for HFD-fed animals, compared to chow diet controls (**Figure 4D**). We also studied gene parameters reflecting the phagocytic capacity of microglia as this is a key function of their immune response in health, as well as different pathologies (35). We evaluated the gene expression of cluster of differentiation 68 (*Cd68*), which encodes for a microglial lysosomal protein, and is a good indicator of phagocytic activity (36). Our results showed an overall steady expression of *Cd68* during the day-night cycle for HFD-fed animals, with a loss of the time-of-day differences, as observed in control animals (**Figure 4E**). One-Way ANOVA evaluation of the effect of *Time* for each group showed a loss of significance during HFD (see **Table S3**). Recent studies have shown that Sirtuin 1 (*Sirt1*) deficiency in microglia is associated with increased Il1b production (37). We observed an inverted pattern of expression of *Sirt1* expression in animals fed HFD, compared to controls. Moreover, the significantly lower *Sirt1* expression at ZT10 coincided with an increased expression of *Il1b* at the same time point (**Figure 4F**). No significant daily rhythmicity was observed for any of the genes, apart from *Myd88* in Chow-fed animals and *Ikbkb* in HFD-fed animals (see **Table S2**). These data demonstrate that microglial innate immunity is affected in HFD-fed animals, suggesting a disruptive effect of obesogenic diets on the microglial inflammatory response.

Microglial Glutamate Metabolism Decreases During the Dark Phase During HFD

Glutamate metabolism is a key component in the biosynthesis of nucleic acids and proteins (38, 39). Microglial cells have been shown to be involved in glutamate uptake under physiological conditions, which can be directly converted to glutathione as a defense response against oxidative stress (40). This mechanism has also been observed under pathological conditions, where it has been shown that microglial cells express glutamate transporters (41). We wanted to assess the state of glutamate substrate utilization in microglial cells under control and obesogenic conditions. We observed that glutaminase (*Gls*)—a key enzyme in the glutamate pathway that converts glutamine to glutamate, showed an effect of *Time* in control animals, which was lost during HFD, with a decrease in expression during the dark phase (ZT18) (**Figure 5A**) (see **Table S3**). Similar observations were made for glutamate dehydrogenase 1 (*Gdh1*), a mitochondrial matrix enzyme that converts glutamate to α-ketoglutarate, a key intermediate in the tricarboxylic acid cycle. *Gdh1* expression showed a lower expression during the dark phase for HFD-fed animals (**Figure 5B**). Moreover, both genes show a significant *Interaction* effect between time and diet (**Table 1**). These data indicate a decrease in conversion of glutamate during the active state of the animals. Microglial activation leads to production of reactive oxygen species (ROS), therefore self-produced antioxidants could have a protective role

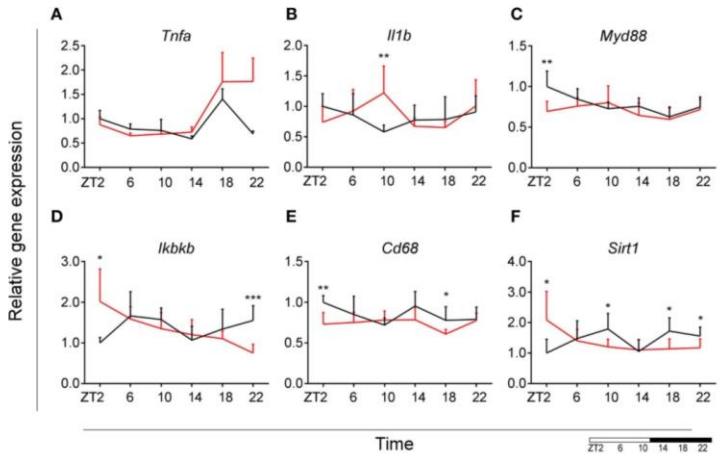

FIGURE 4 | Microglial inflammatory signaling is disturbed in DIO. Relative gene expression of innate immunity genes *Tnfa* **(A)**, *Il1b* **(B)**, *Myd88* **(C)**, *Ikbkb* **(D)** as well as phagocytic indicator gene *Cd68* **(E)** and *Sirt1* **(F)** in HFD-fed rats (red) compared to Chow-fed controls (black) evaluated at six time points, starting at ZT2. Data are presented as means ± SEM. Statistical significance was determined using Two-way ANOVA effect for *Interaction*, *Diet,* and *Time* (ZT); Student *t*-test is used for diet effect within a separate time point (*$p < 0.05$; **$p < 0.01$; ***$p < 0.001$). Scale (bottom right) represents light (ZT0-12) and dark (ZT12-24) phase.

in the cells. Expression of glutathione peroxidase 1 (*Gpx1*)—an important antioxidant enzyme, involved in reduction of organic hydroperoxides and hydrogen peroxide by glutathione, showed an inverted pattern of expression during the light phase between both groups (**Figure 5C**), suggesting a change in this protective mechanism. No significant daily rhythmicity according to JTK_Cycle analysis was observed for any of the genes under control and obesogenic conditions (see **Table S2**). Together, these data point to an overall decrease of glutamate utilization during the active period of HFD-fed animals.

Decrease of Microglial Glucose Utilization During the Dark Phase During HFD

It has been shown that glycolysis is crucial for immune cell function (42). Moreover, it has been suggested that upregulation of expression of glycolytic genes leads to M1 polarization in macrophages, known for its proinflammatory function (43). To assess the involvement of glucose metabolism in microglial immune function when rats are fed HFD, we evaluated gene expression of hexokinase 2 (*Hk2*)—the first glycolytic enzyme converting glucose to glucose-6-phosphate. We observed a decrease of *Hk2* expression during the dark phase (ZT18-22) for animals fed HFD, suggesting a decrease in glucose utilization in microglial cells (**Figure 5D**). Moreover, there was a gain of rhythm for *Hk2* in animals, fed HFD (see **Table S2**). To investigate this further, we evaluated the expression of glucose transporter type 5 (*Glut5*)—a fructose transporter, which is known to be highly specific for microglial cells (44). We observed a similar trend for *Glut5* in HFD-fed animals, with a steady decreased expression toward the end of the dark phase ZT22 (**Figure 5E**). Both genes show a significant *Interaction* effect between time and diet (**Table 1**). Together these data on glutamate and glucose metabolism, suggest that under obesogenic conditions microglial cells switch their substrate utilization to other sources during their active state.

HFD Leads to an Increase in Lipid Utilization and Sensing in Microglia During the Light Phase

Fatty acid oxidation can contribute 20% of total brain energy production (45). A recent study has shown that microglial cells determine hypothalamic inflammation in response to excess saturated fat intake through a direct and specific sensing mechanism (16). To assess microglial fatty acid (FA) metabolism in DIO, we evaluated genes involved in FA substrate utilization and sensing. Expression of cluster of differentiation 36 (*Cd36*)—a FA translocase responsible for import of FA inside the cell, showed a flattening of the time-of-day differences in animals fed HFD, compared to controls (**Figure 5F**). Evaluation of daily rhythmicity of *Cd36* gene expression confirms this observation, with a loss of rhythm under obesogenic conditions (see **Table S2**). This suggests an overall steady import of FA during the day/night cycle under HFD. Previous research from our group has shown that HFD stimulates the expression of microglial lipoprotein lipase (*Lpl*)—a triglyceride hydrolase receptor involved in receptor-mediated lipoprotein uptake, and that lack of LPL impairs microglial immune reactivity (46). Here, we show that this increase of *Lpl* expression takes place during the light phase in animals fed HFD (**Figure 5G**). These data highlight LPL as a key player in microglial immunometabolism in

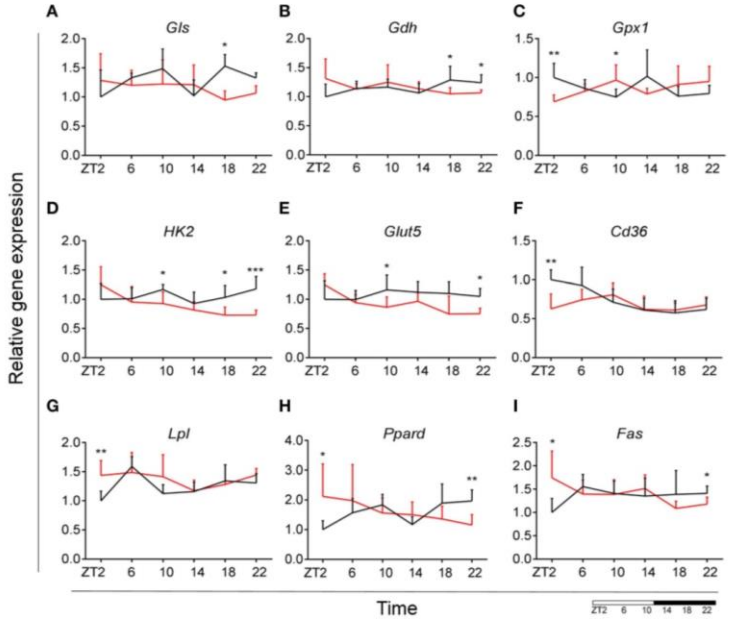

FIGURE 5 | HFD effect on glutamate, glucose and lipid microglial metabolism in rats. Relative gene expression of (top) glutamate substrate utilization genes *Gls* **(A)** and *Gdh* **(B)**, as well as antioxidant enzyme gene *Gpx1* **(C)**; (middle) glucose metabolism genes *Hk2* **(D)** and *Glut5* **(E)**, fatty acid sensing gene *Cd36* **(F)**; (bottom) fatty acid sensing genes *Lpl* **(G)** and *Ppard* **(H)**, as well as fatty acid synthesis gene *Fas* **(I)** in HFD-fed rats (red) compared to Chow-fed controls (black) evaluated at six time points, starting at ZT2. Data are presented as means ± SEM. Statistical significance was determined using Two-way ANOVA effect for *Interaction*, *Diet*, and *Time* (ZT); Student *t*-test is used for diet effect within a separate time point (*$p < 0.05$; **$p < 0.01$; ***$p < 0.001$). Scale (bottom right) represents light (ZT0-12) and dark (ZT12-24) phase.

DIO. Peroxisome proliferator-activated receptors (PPARs) have an important physiological role in lipid sensing and regulation of lipid metabolism during normal healthy conditions, as well in the development of pathologies like obesity and type two diabetes (47). PPAR delta (*Ppard*) is highly expressed by microglia and its activity increases oxidative capacity. Our results showed an inverted pattern of *Ppard* day/night expression in obesogenic animals, with highest expression during ZT2, but lowest at ZT22 (**Figure 5H**). To assess the effect of HFD-induced obesity on fatty acid synthesis we evaluated gene expression of fatty acid synthase (*Fas*)—a key enzyme catalyzing the synthesis of palmitate from malonyl coenzyme A. *Fas* expression in microglia from HFD-fed animals showed a lower expression at the end of the dark phase and higher expression at the beginning of the light phase, compared to control chow-fed animals (**Figure 5I**). These data suggest a shift of FA synthesis to the light phase in HFD-fed animals.

Taken together, these data suggest an overall increase in lipid metabolism during the light, i.e., sleep, phase of animals fed HFD. This increase could be partially explained by the higher levels of NEFA in HFD-fed rodents during the light phase (**Figure 2F**) (48, 49). Moreover, we observed a decrease in glutamate and glucose utilization as shown above. This could suggest a microglial metabolic switch to lipid substrate utilization in HFD-induced obesity.

HFD Increases Mitochondrial Bioenergetics and Dynamics Gene Expression During the Light Phase

To assess whether microglial mitochondria bioenergetics are affected by DIO, we evaluated the gene expression of cytochrome c oxidase subunit 4 (*Cox4*), encoding a terminal enzyme of the mitochondrial respiratory chain that catalyzes the reduction of oxygen to water, and ATP synthase subunit beta (*Atp5b*)—encoding a part of the enzyme, catalyzing ATP synthesis. We observed a decrease in *Cox4* and *Atp5b* expression in animals fed HFD at ZT18 (dark phase), but an increase during the beginning of the light phase (ZT2), suggesting a shift of energy production to the resting state in obese animals (**Figures 6A,B**). These data are in line with our observation on lipid metabolism; therefore, we selected another mitochondrial target, involved in FA metabolism. Pyruvate dehydrogenase kinase 4 (*Pdk4*) is an enzyme located in the mitochondrial matrix, inhibiting the pyruvate dehydrogenase complex and exerting a regulatory function on substrate utilization by suppressing

glycolysis and enhancing FA oxidation. *Pdk4* expression showed the same trend for HFD-fed animals, with an increase at ZT2 (beginning of the light phase) (**Figure 6C**). This has also been previously observed in heart tissue and soleus muscle of rats fed HFD (49). Moreover, all three genes show a daily rhythm under control conditions, which was lost in HFD-fed animals, suggesting that hypercaloric diet impairs time-of-day mitochondrial bioenergetics in microglial cells (see **Table S2**).

To test if this trend was also observed in mitochondrial dynamics, as they adjust to mitochondrial demand, we evaluated key genes involved in mitochondrial fusion—mitofusin 2 (*Mfn2*) and optic atrophy 1 (*Opa1*); as well as mitochondrial fission—fission 1 (*Fis1*) and dynamin-related protein 1 (*Drp1*). Results were supportive of changes in the bioenergetics state, with a significant increase of expression for all four genes (*Mfn2, Opa1, Fis1, Drp1*) at ZT2 for HFD-fed animals (**Figures 6D–G**). Two-way ANOVA test showed a significant *Interaction* effect for all four genes (**Table 1**).

Taken together these data suggest an increased energy production in microglia of DIO animals during the light phase, which could be explained by an increased demand to sustain the increase in lipid metabolism. Another recent study indeed showed that mitochondrial fission is elevated as a consequence of high-fat concentrated diets (50). This indicates that mitochondrial dynamics adapt to changes in the bioenergetics state in response to nutritional status.

The Effect of HFD-Induced Obesity on Blood Monocyte Immunometabolism Is Less Robust Than on Brain Microglial Cells

Following our observations in microglia, we were interested if the same effects could be seen in monocytes—peripheral myeloid cells. Originating from hematopoietic stem cells in the bone marrow, monocytes circulate in the blood and migrate to other tissue where they differentiate into tissue resident macrophages. It is known that under obesogenic conditions, circulating monocytes could infiltrate adipose tissue, leading to macrophage activation and increasing proinflammatory activity (51–53).

Our results indicated an overall loss of daily rhythmicity of circadian gene expression, with *Clock*, *Per2*, and *Dbp* showing daily rhythmicity in control animals, which was only maintained for *Per2* gene expression under obesogenic conditions (see **Table S2**). *Bmal1* and *Per1* showed a significant increase in expression at the beginning of the light phase (ZT2) in HFD-fed animals compared to control chow (**Figures 7A,C**). Gene expression of *Reverba* and *Dbp* in monocytes showed a higher expression at ZT6 in HFD-fed animals (**Figures 7E,F**). There was no difference in *Clock*, *Per2*, *Cry1* and *Cry2* gene expression between both conditions (**Figures 7B,D**) (see **Figures S1A,B**). Moreover, One-Way ANOVA analysis showed lack of *Time* effect for all circadian genes during HFD (see **Table S3**).

We did not find any difference in monocyte immune response between both groups for *Tnfa*, *Ikbkb*, *Cd68*, and *Sirt1* gene expression (see **Figures S1C–F**). However, we did observe a daily rhythm in *Tnfa* and *Cd68* in control animals, as well as gain of rhythm for *Sirt1* gene expression in HFD-fed animals (see **Table S2**). There was an increase in *Il1b* expression at ZT2 for the HFD group (**Figure 7G**). *Il1b* showed daily rhythmicity under control conditions, which was maintained under obesogenic conditions with a shift in acrophase of 6 h (see **Table S2**). Il1b-induced inflammation has been shown to be indirectly involved in insulin resistance in type 2 diabetes (54, 55). Thus, these data could indicate a reduction in insulin sensitivity. Moreover, we observed an increased expression of *Myd88* at ZT2 for HFD-fed animals (**Figure 7H**).

No differences between obese and control animals were found for representative genes of the glutamate pathway *Gls* and *Gdh* (see **Figures S1G,H**). However, there was a gain of daily rhythm for *Gls* gene expression in HFD-fed animals (see **Table S2**). We found an increase in *Gpx1* expression at ZT2 for HFD group with an overall stable day/night expression, suggesting a mechanism of constant anti-oxidant production (**Figure 7I**). This observation was supported by a loss of daily rhythmicity under obesogenic conditions (see **Table S2**). Expression of the glucose metabolic gene *Hk2* was decreased at ZT22 in HFD-fed animals, similar to what was observed in microglia (**Figure 7J**). We observed no difference in FA metabolism and sensing genes *Fas* and *Ppard* (see **Figures S1I,J**), apart from *Cd36* expression (**Figure 7K**). *Cd36* expression showed a strong daily rhythm under control conditions, which was significant also in HFD-fed animals with an acrophase shift of 6 h (see **Table S2**). The expression of the FA translocase in monocytes has also been shown to be associated with insulin resistance, supporting our observation for *Il1b* expression (56). *Lpl* evaluation showed low expression (data not shown).

We observed no difference in mitochondrial bioenergetics gene expression between both dietary groups for *Atp5b, Atp5g,* and *Cox4* (see **Figures S1K–M**). Mitochondria dynamics gene expression was affected only at ZT2 for *Opa1* and *Drp1* expression (**Figures 7L,M**), with no difference in *Mfn2* expression (see **Figure S1N**) and low expression of *Fis1* (data not shown). Interestingly, HFD led to a decrease in mitochondrial bioenergetics gene expression in monocytes at the start of the inactive period, opposite to the increase we observed in microglia under obesogenic conditions. We found no daily rhythm for any of the mitochondria genes, both under control and obesogenic conditions (see **Table S2**). One-Way ANOVA analysis showed lack of *Time* effect for all genes both during control and HFD (see **Table S3**). Two-way ANOVA analysis data is shown the in Supplementary Material (see **Table S4**).

Overall, these data suggest a small effect of the obesogenic diet on monocyte immunometabolism, suggesting that HFD specifically affects microglial immunometabolism.

DISCUSSION

It is well-known now that a hypercaloric environment is a potent inducer of microglial activation, which ultimately leads to chronic neuroinflammation (14–17). However, the daily rhythm of microglial innate immune function is poorly known,

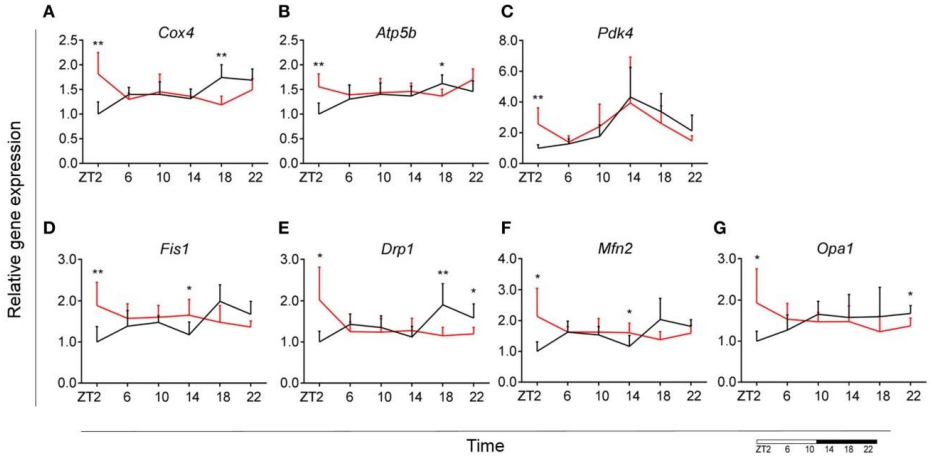

FIGURE 6 | Microglial mitochondria signaling during DIO. Relative gene expression of mitochondria bioenergetics genes *Cox4* **(A)**, *Atp5b* **(B)**, and *Pdk4* **(C)**, as well as mitochondria dynamics gene *Fis1* **(D)**, *Drp1* **(E)**, *Mfn2* **(F)**, and *Opa1* **(G)** in HFD-fed rats (red) compared to Chow-fed controls (black) evaluated at six time points, starting at ZT2. Data are presented as means ± SEM. Statistical significance was determined using Two-way ANOVA effect for *Interaction*, *Diet,* and *Time* (ZT); Student *t*-test is used for diet effect within a separate time point (*$p < 0.05$; **$p < 0.01$). Scale (bottom right) represents light (ZT0-12) and dark (ZT12-24) phase.

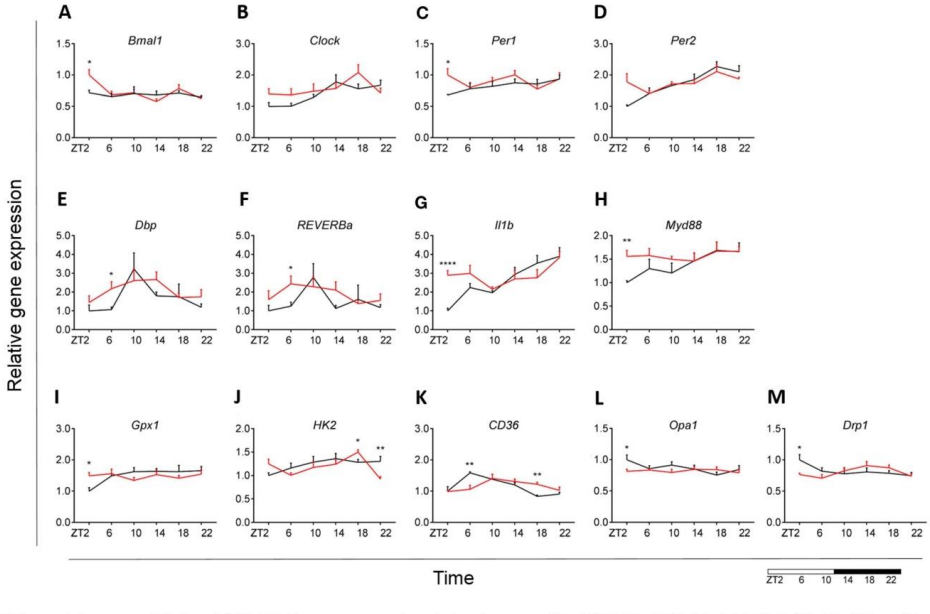

FIGURE 7 | Monocyte immunometabolism in DIO. Relative gene expression of circadian genes *Bmal1* **(A)**, *Clock* **(B)**, *Per1* **(C)**, *Per2* **(D)**, *Dbp* **(E)**, and *Reverba* **(F)**; immune genes *Il1b* **(G)** and *Myd88* **(H)**, antioxidant enzyme gene *Gpx1* **(I)**, glycolysis gene *Hk2* **(J)**, fatty acid sensing gene *Cd36* **(K)**, and mitochondria dynamic genes *Opa1* **(L)** and *Drp1* **(M)** in HFD-fed rats (red) compared to Chow-fed controls (black) evaluated at six time points, starting at ZT2. Data are presented as means ± SEM. Statistical significance was determined using Two-way ANOVA effect for *Interaction*, *Diet,* and *Time* (ZT); Student *t*-test is used for diet effect within a separate time point (*$p < 0.05$; **$p < 0.01$; ****$p < 0.0001$). Scale (bottom right) represents light (ZT0-12) and dark (ZT12-24) phase.

both in obesity and health. The purpose of this study was to evaluate the effect of an obesogenic diet on daily changes in microglial immunometabolism. Our data showed a disturbance of the microglial interaction between metabolism and immunity during DIO. We report that HFD-induced obesity leads to loss of daily rhythm of circadian genes and impaired microglial immunometabolic functions primarily at the transition period between dark and light phase (ZT22-ZT2).

To evaluate the effect of DIO on daily rhythms in microglial function and activity, we studied the microglial expression of major circadian and immune genes. Under normal conditions, microglia circadian genes were expressed in a rhythmic manner, which is disturbed by HFD, mainly due to a loss of its rhythmicity. Comparable changes have also been observed in different peripheral tissues like liver, brown adipose tissue and skeletal muscle in animals on an obesogenic diet (57–59). However, to our knowledge, we are the first to report an effect of HFD on expression rhythms of microglial clock genes. The presently reported difference in time-of-day expression of microglial cytokine genes, is in line with our previous results (18). Fonken et al. have shown previously that *Il1b* and *Tnfa* gene expression have a peak during the middle of the day, contrary to our observations (31). Possible explanation to this contradiction is the heterogeneous transcriptional identities of microglia, specific for each brain region, in this case hippocampal vs. cortical microglia (60).

Microglial cells are known to exhibit bioenergetics shifts in energy substrate, for example during aging (61). Such a shift in substrate utilization is known to have an effect on the activation status of immune cells (42, 62). We studied microglial substrate utilization, focusing on glutamate, glucose and FA metabolism and observed a difference between control and HFD-fed animals, particularly during the transition period from the dark to light phase. Key players in the glutamate pathway have been shown to be involved in macrophage immune function, *e.g.,* glutamine availability was shown to modulate macrophage phagocytic capacity, while α-ketoglutarate, generated through glutaminolysis, is crucial in eliciting an anti-inflammatory phenotype in macrophages (63, 64). We report a decrease in microglial glutamate utilization in the active period of HFD-fed animals as seen in glutamine conversion to glutamate and glutamate conversion to α-ketoglutarate. Additionally, a similar change was observed for glucose metabolism with decreased glucose utilization in the active period of HFD-fed animals. However, we observed an increase in FA sensing and synthesis at the beginning of the light period under obesogenic conditions, suggesting a shift to FA utilization during the sleep phase of the animal. It has been shown that FA treatment of BV2 cells (a microglial cell line) is a potent inducer of cytokine production via TLR4 signaling, thus leading to low-grade inflammation even in the absence of immune challenge (65). This FA metabolism increase could be a possible explanation for our previously observed constant day/night activation of hypothalamic microglia under HFD (66). Additionally, we know that immune cell activation requires higher energy production. We here show that microglial mitochondrial function in DIO is increased during the inactive period, suggesting an increase in ATP production, which could be explained by the increased FA metabolism demand. These data support the view that mitochondrial function adapts to nutritional status (50).

To investigate whether the observed effect of HFD on immunometabolism is restricted to microglial cells, we also studied monocyte immunometabolism in obesity. We report small or no effect of the hypercaloric diet on monocyte immunometabolic function, which suggests a microglia-specific functional disturbance in HFD-induced obesity. Taken together, our data suggest that microglial innate immunity is highly dependent on metabolic changes, as well as the time of day. Microglial cells are highly active cells, with a high energy demand, which is achieved by a strictly regulated cellular metabolism. A robust switch of substrate utilization is a suitable mechanism, in response to the high demands of immune defense.

The data currently presented suggest a deleterious effect of an obesogenic diet on microglial function by inducing chronic activation. It has been shown that chronic microglial activation has a negative impact on neuronal function and could play a role in obesity-associated cognitive decline (16, 67). Our data point out to the importance of microglial integrity and the negative impact of chronic exposure to a hypercaloric environment on cortical microglial function, which could ultimately lead to cognitive impairment. Previously we observed that obesity induces microglial activation in close proximity to the anorexigenic proopiomelanocortin (POMC) neurons located in the arcuate nucleus of the hypothalamus (18). Moreover, chronic HFD feeding leads to POMC neuronal loss, which would lead to further progression of obesity (66). It is possible that the current observation on cortical microglia could be translated to the hypothalamus, which would give insight in the mechanisms behind this neuronal loss.

Finally, three issues need to be addressed: firstly, we observed a clear effect of HFD on microglial immunometabolism, leading to an increase in expression of many of the presented genes around the end of the dark period, i.e., ZT22/ZT2. In order to check whether or not a higher food intake at the end of the dark period in the HFD-fed group could be responsible for these changes, we re-analyzed the food intake data from metabolic cage experiments from a separate cohort of rats fed a similar HFD (68). With respect to consumed grams, no difference in timing of food intake was found between control and obesogenic diet (see **Figure S2**). However, with respect to consumed calories, the obesogenic diet group showed a larger increase of kcal intake at the beginning and the end of the dark period, although only significant for the beginning of the dark period, suggesting that higher energy consumption (but not higher food intake) may be partially responsible for the differences in gene expression between the HFD and control group at the end of the dark period (see **Figure S2**). Secondly, we cannot distinguish between the effect of obesity and the hypercaloric diet itself. However, a hypercaloric diet can induce microglial activation in the hypothalamus after 1 day, prior to any changes in body weight, pointing to an effect of diet rather than obesity itself (69). Thirdly, the data presented only show

the transcriptional state of selected target genes, representative of the different functions investigated. Future studies should be aimed at a further understanding of activity changes in each of the represented pathways.

CONCLUSIONS

An obesogenic diet affects microglial immunometabolism in a time-of-day specific manner. The aim of this study was to increase the knowledge of microglial cell function in obesity in general and its daily rhythms in specific. To our knowledge, we are the first to point out (loss of) time-of-day differences for microglial cells during HFD. Our data are supportive of the ongoing research, focused on the interaction between immune cells and metabolism. Further studies should focus on addressing the time-of-day differences in microglial function, as more detailed knowledge of microglial immunometabolism could lead to a better understanding of the neuroinflammatory process taking place in the CNS under chronic hypercaloric environment.

DATA AVAILABILITY

All data generated or analyzed during this study are included in this published article (and its **Supplementary Information Files**).

ETHICS STATEMENT

All studies were approved by the Animal Ethics Committee of the Royal Dutch Academy of Arts and Sciences (KNAW, Amsterdam) and performed according to the guidelines on animal experimentation of the Netherlands Institute for Neuroscience (NIN, Amsterdam).

AUTHOR CONTRIBUTIONS

IM performed the animal experiments, microglia isolation, RNA extraction, cDNA synthesis, qPCR experiments, glucose and NEFA measurements in plasma, and constructed the manuscript. MK and XW helped with the animal experiments and monocyte isolation. NK performed the monocyte isolation and helped with the animal experiments. DS performed the time-of-day food intake data and helped with data analysis. SW helped with qPCR experiments. PG helped with data statistical analysis. AH supervised the measuring of the insulin plasma concentration. EF, SF, and AK provided intellectual input and drafted the manuscript. CY designed the study, supervised the experiments, interpreted the findings, and drafted the manuscript. All authors have read and approved the final manuscript.

FUNDING

This work was supported by an AMC fellowship (CY, 2014, Amsterdam University Medical Center), the Dutch Diabetes Research Foundation (CY, Diabetes Fonds, 2015.82.1826), and the ZonMW TOP grant (MK, PG, and AK, #91214047), The Netherlands.

ACKNOWLEDGMENTS

We would like to thank the Laboratory of Endocrinology, Amsterdam University Medical Center (UMC).

SUPPLEMENTARY MATERIAL

The Supplementary Material for this article can be found online at: https://www.frontiersin.org/articles/10.3389/fendo.2019.00424/full#supplementary-material

REFERENCES

1. Mathis D, Shoelson SE. Immunometabolism: an emerging frontier. *Nat Rev Immunol.* (2011) 11:81. doi: 10.1038/nri2922
2. Lee YS, Wollam J, Olefsky JM. An integrated view of immunometabolism. *Cell.* (2018) 172:22–40. doi: 10.1016/j.cell.2017.12.025
3. Hotamisligil GS. Foundations of immunometabolism and implications for metabolic health and disease. *Immunity.* (2017) 47:406–20. doi: 10.1016/j.immuni.2017.08.009
4. Norata Giuseppe D, Caligiuri G, Chavakis T, Matarese G, Netea Mihai G, Nicoletti A, et al. The cellular and molecular basis of translational immunometabolism. *Immunity.* (2015) 43:421–34. doi: 10.1016/j.immuni.2015.08.023
5. Mariani MM, Kielian T. Microglia in infectious diseases of the central nervous system. *J Neuroimmune Pharmacol.* (2009) 4:448–61. doi: 10.1007/s11481-009-9170-6
6. Yang I, Han SJ, Kaur G, Crane C, Parsa AT. The role of microglia in central nervous system immunity and glioma immunology. *J Clin Neurosci.* (2010) 17:6–10. doi: 10.1016/j.jocn.2009.05.006
7. Orihuela R, McPherson CA, Harry GJ. Microglial M1/M2 polarization and metabolic states. *Br J Pharmacol.* (2016) 173:649–65. doi: 10.1111/bph.13139
8. Butovsky O, Weiner HL. Microglial signatures and their role in health and disease. *Nat Rev Neurosci.* (2018) 19:622–35. doi: 10.1038/s41583-018-0057-5
9. De Souza CT, Araujo EP, Bordin S, Ashimine R, Zollner RL, Boschero AC, et al. Consumption of a fat-rich diet activates a proinflammatory response and induces insulin resistance in the hypothalamus. *Endocrinology.* (2005) 146:4192–9. doi: 10.1210/en.2004-1520
10. Morari J, Anhe GF, Nascimento LF, de Moura RF, Razolli D, Solon C, et al. Fractalkine (CX3CL1) is involved in the early activation of hypothalamic inflammation in experimental obesity. *Diabetes.* (2014) 63:3770–84. doi: 10.2337/db13-1495
11. Milanski M, Degasperi G, Coope A, Morari J, Denis R, Cintra DE, et al. Saturated fatty acids produce an inflammatory response predominantly through the activation of TLR4 signaling in hypothalamus: implications for the pathogenesis of obesity. *J Neurosci.* (2009) 29:359–70. doi: 10.1523/JNEUROSCI.2760-08.2009
12. Zhang X, Zhang G, Zhang H, Karin M, Bai H, Cai D. Hypothalamic IKKbeta/NF-kappaB and ER stress link overnutrition to energy imbalance and obesity. *Cell.* (2008) 135:61–73. doi: 10.1016/j.cell.2008.07.043
13. Kleinridders A, Schenten D, Konner AC, Belgardt BF, Mauer J, Okamura T, et al. MyD88 signaling in the CNS is required for development of fatty acid-induced leptin resistance and diet-induced obesity. *Cell Metab.* (2009) 10:249–59. doi: 10.1016/j.cmet.2009.08.013
14. Gao Y, Bielohuby M, Fleming T, Grabner GF, Foppen E, Bernhard W, et al. Dietary sugars, not lipids, drive hypothalamic inflammation. *Mol Metab.* (2017) 6:897–908. doi: 10.1016/j.molmet.2017.06.008

15. Gao Y, Ottaway N, Schriever SC, Legutko B, Garcia-Caceres C, de la Fuente E, et al. Hormones and diet, but not body weight, control hypothalamic microglial activity. *Glia*. (2014) 62:17–25. doi: 10.1002/glia.22580
16. Valdearcos M, Robblee MM, Benjamin DI, Nomura DK, Xu AW, Koliwad SK. Microglia dictate the impact of saturated fat consumption on hypothalamic inflammation and neuronal function. *Cell Rep*. (2014) 9:2124–38. doi: 10.1016/j.celrep.2014.11.018
17. Baufeld C, Osterloh A, Prokop S, Miller KR, Heppner FL. High-fat diet-induced brain region-specific phenotypic spectrum of CNS resident microglia. *Acta Neuropathol*. (2016) 132:361–75. doi: 10.1007/s00401-016-1595-4
18. Yi C-X, Walter M, Gao Y, Pitra S, Legutko B, Kälin S, et al. TNFα drives mitochondrial stress in POMC neurons in obesity. *Nat Commun*. (2017) 8:15143. doi: 10.1038/ncomms15143
19. Froy O. Metabolism and circadian rhythms—implications for obesity. *Endocr Rev*. (2010) 31:1–24. doi: 10.1210/er.2009-0014
20. Sun M, Feng W, Wang F, Li P, Li Z, Li M, et al. Meta-analysis on shift work and risks of specific obesity types. *Obesity Rev*. (2018) 19:28–40. doi: 10.1111/obr.12621
21. Kalsbeek A, Palm IF, La Fleur SE, Scheer FA, Perreau-Lenz S, Ruiter M, et al. SCN outputs and the hypothalamic balance of life. *J Biol Rhythms*. (2006) 21:458–69. doi: 10.1177/0748730406293854
22. Olenchock BA, Rathmell JC, Vander Heiden MG. Biochemical underpinnings of immune cell metabolic phenotypes. *Immunity*. (2017) 46:703–13. doi: 10.1016/j.immuni.2017.04.013
23. Nikodemova M, Watters JJ. Efficient isolation of live microglia with preserved phenotypes from adult mouse brain. *J Neuroinflamm*. (2012) 9:147. doi: 10.1186/1742-2094-9-147
24. Hughes ME, Hogenesch JB, Kornacker K. JTK_CYCLE: an efficient nonparametric algorithm for detecting rhythmic components in genome-scale data sets. *J Biol Rhythms*. (2010) 25:372–80. doi: 10.1177/0748730410379711
25. Bahceci M, Tuzcu A, Akkus M, Yaldiz M, Ozbay A. The effect of high-fat diet on the development of obesity and serum leptin level in rats. *Eat Weight Disord*. (1999) 4:128–32. doi: 10.1007/BF03339728
26. La Fleur SE, Kalsbeek A, Wortel J, Buijs RM. A suprachiasmatic nucleus generated rhythm in basal glucose concentrations. *J Neuroendocrinol*. (1999) 11:643–52. doi: 10.1046/j.1365-2826.1999.00373.x
27. Zardooz H, Rostamkhani F, Zaringhalam J, Faraji Shahrivar F. Plasma corticosterone, insulin and glucose changes induced by brief exposure to isoflurane, diethyl ether and CO2 in male rats. *Physiol Res*. (2010) 59:973–8.
28. Artwohl J, Brown P, Corning B, Stein S. Report of the ACLAM task force on rodent euthanasia. *J Am Assoc Lab Anim Sci*. (2006) 45:98–105.
29. Kohsaka A, Laposky AD, Ramsey KM, Estrada C, Joshu C, Kobayashi Y, et al. High-fat diet disrupts behavioral and molecular circadian rhythms in mice. *Cell Metab*. (2007) 6:414–21. doi: 10.1016/j.cmet.2007.09.006
30. Nakazato R, Takarada T, Yamamoto T, Hotta S, Hinoi E, Yoneda Y. Selective upregulation of Per1 mRNA expression by ATP through activation of P2X7 purinergic receptors expressed in microglial cells. *J Pharmacol Sci*. (2011) 116:350–61. doi: 10.1254/jphs.11069FP
31. Fonken LK, Frank MG, Kitt MM, Barrientos RM, Watkins LR, Maier SF. Microglia inflammatory responses are controlled by an intrinsic circadian clock. *Brain Behav Immun*. (2015) 45:171–9. doi: 10.1016/j.bbi.2014.11.009
32. Pendergast JS, Branecky KL, Yang W, Ellacott KLJ, Niswender KD, Yamazaki S. High-fat diet acutely affects circadian organization and eating behavior. *Eur J Neurosci*. (2013) 37:1350–6. doi: 10.1111/ejn.12133
33. Blancas-Velazquez AS, Unmehopa UA, Eggels L, Koekkoek L, Kalsbeek A, Mendoza J, et al. A free-choice high-fat high-sugar diet alters day–night Per2 gene expression in reward-related brain areas in rats. *Front Endocrinol*. (2018) 9:154. doi: 10.3389/fendo.2018.00154
34. Takahashi JS. Transcriptional architecture of the mammalian circadian clock. *Nat Rev Genet*. (2016) 18:164. doi: 10.1038/nrg.2016.150
35. Wolf SA, Boddeke HWGM, Kettenmann H. Microglia in physiology and disease. *Annu Rev Physiol*. (2017) 79:619–43. doi: 10.1146/annurev-physiol-022516-034406
36. Zotova E, Bharambe V, Cheaveau M, Morgan W, Holmes C, Harris S, et al. Inflammatory components in human Alzheimer's disease and after active amyloid-β42 immunization. *Brain*. (2013) 136:2677–96. doi: 10.1093/brain/awt210
37. Cho SH, Chen JA, Sayed F, Ward ME, Gao F, Nguyen TA, et al. SIRT1 deficiency in microglia contributes to cognitive decline in aging and neurodegeneration via epigenetic regulation of IL-1beta. *J Neurosci*. (2015) 35:807–18. doi: 10.1523/JNEUROSCI.2939-14.2015
38. Yelamanchi SD, Jayaram S, Thomas JK, Gundimeda S, Khan AA, Singhal A, et al. A pathway map of glutamate metabolism. *J Cell Commun Signal*. (2016) 10:69–75. doi: 10.1007/s12079-015-0315-5
39. Schousboe A, Scafidi S, Bak LK, Waagepetersen HS, McKenna MC. Glutamate metabolism in the brain focusing on astrocytes. *Adv Neurobiol*. (2014) 11:13–30. doi: 10.1007/978-3-319-08894-5_2
40. Persson M, Sandberg M, Hansson E, Ronnback L. Microglial glutamate uptake is coupled to glutathione synthesis and glutamate release. *Eur J Neurosci*. (2006) 24:1063–70. doi: 10.1111/j.1460-9568.2006.04974.x
41. Persson M, Ronnback L. Microglial self-defence mediated through GLT-1 and glutathione. *Amino Acids*. (2012) 42:207–19. doi: 10.1007/s00726-011-0865-7
42. O'Neill LA, Kishton RJ, Rathmell J. A guide to immunometabolism for immunologists. *Nat Rev Immunol*. (2016) 16:553–65. doi: 10.1038/nri.2016.70
43. Wang T, Liu H, Lian G, Zhang S-Y, Wang X, Jiang C. HIF1α-induced glycolysis metabolism is essential to the activation of inflammatory macrophages. *Mediators Inflamm*. (2017) 2017:9029327. doi: 10.1155/2017/9029327
44. Payne J, Maher F, Simpson I, Mattice L, Davies P. Glucose transporter Glut 5 expression in microglial cells. *Glia*. (1997) 21:327–31. doi: 10.1002/(SICI)1098-1136(199711)21:3<27::AID-GLIA7>3.0.CO;2-1
45. Ebert D, Haller RG, Walton ME. Energy contribution of octanoate to intact rat brain metabolism measured by 13C nuclear magnetic resonance spectroscopy. *J Neurosci*. (2003) 23:5928–35. doi: 10.1523/JNEUROSCI.23-13-05928.2003
46. Gao Y, Vidal-Itriago A, Kalsbeek MJ, Layritz C, Garcia-Caceres C, Tom RZ, et al. Lipoprotein lipase maintains microglial innate immunity in obesity. *Cell Rep*. (2017) 20:3034–42. doi: 10.1016/j.celrep.2017.09.008
47. Berger J, Moller DE. The mechanisms of action of PPARs. *Annu Rev Med*. (2002) 53:409–35. doi: 10.1146/annurev.med.53.082901.104018
48. Shostak A, Meyer-Kovac J, Oster H. Circadian regulation of lipid mobilization in white adipose tissues. *Diabetes*. (2013) 62:2195–203. doi: 10.2337/db12-1449
49. Stavinoha MA, RaySpellicy JW, Hart-Sailors ML, Mersmann HJ, Bray MS, Young ME. Diurnal variations in the responsiveness of cardiac and skeletal muscle to fatty acids. *Am J Physiol Endocrinol Metab*. (2004) 287:E878–E87. doi: 10.1152/ajpendo.00189.2004
50. Putti R, Sica R, Migliaccio V, Lionetti L. Diet impact on mitochondrial bioenergetics and dynamics. *Front Physiol*. (2015) 6:109. doi: 10.3389/fphys.2015.00109
51. Xu H, Barnes GT, Yang Q, Tan G, Yang D, Chou CJ, et al. Chronic inflammation in fat plays a crucial role in the development of obesity-related insulin resistance. *J Clin Investig*. (2003) 112:1821–30. doi: 10.1172/JCI200319451
52. Ghanim H, Aljada A, Hofmeyer D, Syed T, Mohanty P, Dandona P. Circulating mononuclear cells in the obese are in a proinflammatory state. *Circulation*. (2004) 110:1564–71. doi: 10.1161/01.CIR.0000142055.53122.FA
53. Krinninger P, Ensenauer R, Ehlers K, Rauh K, Stoll J, Krauss-Etschmann S, et al. Peripheral monocytes of obese women display increased chemokine receptor expression and migration capacity. *J Clin Endocrinol Metab*. (2014) 99:2500–9. doi: 10.1210/jc.2013-2611
54. Ehses JA, Lacraz G, Giroix MH, Schmidlin F, Coulaud J, Kassis N, et al. IL-1 antagonism reduces hyperglycemia and tissue inflammation in the type 2 diabetic GK rat. *Proc Natl Acad Sci USA*. (2009) 106:13998–4003. doi: 10.1073/pnas.0810087106
55. Bing C. Is interleukin-1β a culprit in macrophage-adipocyte crosstalk in obesity? *Adipocyte*. (2015) 4:149–52. doi: 10.4161/21623945.2014.979661
56. Love-Gregory L, Abumrad NA. CD36 genetics and the metabolic complications of obesity. *Curr Opin Clin Nutr Metab Care*. (2011) 14:527–34. doi: 10.1097/MCO.0b013e32834bbac9
57. Branecky KL, Niswender KD, Pendergast JS. Disruption of daily rhythms by high-fat diet is reversible. *PLoS ONE*. (2015) 10:e0137970. doi: 10.1371/journal.pone.0137970
58. de Goede P, Sen S, Oosterman JE, Foppen E, Jansen R, la Fleur SE, et al. Differential effects of diet composition and timing of feeding behavior on rat

Supplementary Materials

Table S1. Primer sequences of target genes

*Two different primers for *Gpx1* were used for monocyte and microglial cells as the primers showed tissue specificity and a single primer, suitable for both cell types was not found during optimization of the technique.

Genes	Primer sequence - Forward	Primer sequence - Reverse
Circadian		
Bmal1	CCGATGACGAACTGAAACACCT	TGCAGTGTCCGAGGAAGATAGC
Clock	CGATCACAGCCCAACTCCTT	TTGCAGCTTGAGACATCGCT
Cry1	AAGTCATCGTGCGCATTTCA	TCATCATGGTCGTCGGACAGA
Cry2	TGGATAAGCACTTGGAACGGAA	TGTACAAGTCCCACAGGCGGTA
Per1	CGCACTTCGGGAGCTCAAACTTC	GTCCATGGCACAGGGCTCACC
Per2	CACCCTGAAAAGAAAGTGCGA	CAACGCCAAGGAGCTCAAGT
Reverba	ACAGCTGACACCACCCAGATC	CATGGGCATAGGTGAAGATTTCT
Dbp	CCTTTGAACCTGATCCGGCT	TGCCTTCTTCATGATTGGCTG
Inflammatory		
Tnfa	AACACACGAGACGCTGAAGT	TCCAGTGAGTTCCGAAAGCC
Il1b	TGTGATGAAAGACGGCACAC	CTTCTTCTTTGGGTATTGTTTGG
Myd88	TCGACGCCTTCATCTGCTAC	CCATGCGACGACACCTTTTC
Ikbkb	GCAGAACTTGGCACCCAATG	GAGCCGATGCTATGTCACTCA
Cd68	TGTTCAGCTCCAAGCCCAAA	GCTCTGATGTCGGTCCTGTTT
Sirt1	TGTTTCCTGTGGGATACCTGA	TGAAGAATGGTCTTGGGTCTTT
Metabolic		
Gls	TACGACTCCAGAACAGCCCT	TTATTCCACCTGTCCTTGGGG
Gdh	CCTGCAAGGGAGGTATCCG	CCACAGCGCACTTGTATGTC
Gpx1 (microglia)*	CAAGTATGTCCGACCCGGTG	CTCACCATTCACCTCGCACT
Gpx1	CCGGGACTACACCGAAATGA	CGGGTCGGACATACTTGAGG

(monocytes) *		
Hk2	GGTGAGCCATCGTGGTTAAG	CTTCCGGAACCGCCTAGAAA
Glut5	CTTATTGCCCAGGTGTTCGG	GGCAGAAGGGCAACAGGATA
Cd36	ACAGTTTTGGATCTTTGACGTG	CCTTGGCTAAATAACGAACTCTG
Lpl	CAAAACAACCAGGCCTTCGA	AGCAATTCCCCGATGTCCA
Ppard	CTCCTGCTCACTGACAGATG	TCTCCTCCTGTGGCTGTTC
Fas	CTTGGGTGCCGATTACAACC	GCCCTCCCGTACACTCACTC
Mitochondrial		
Cox4	TGGGAGTGTTGTGAAGAGTGA	GCAGTGAAGCCGATGAAGAAC
Atp5b	CGGGTAGCTCTGACTGGTCT	AACTCAGCAATAGCACGGGA
Atp5g	GGAGATAACGGCCAATGGGAG	CACAGGCCTGATTAGACCCC
Pdk4	TGGTTTTGGTTACGGCTTGC	TGCCAGTTTCTCCTTCGACA
Fis1	GGTTGCGTGGTAAGGGATGA	CTGTAACAGTCCCCGCACAT
Drp1	ACAACAGGAGAAGAAAATGGAGTTG	CGTTGGGCGAGAAAACCTTG
Mfn2	CTCAGGAGCAGCGGGTTTATTGT	TGTCGAGGGACCAGCATGTCTAT
Opa1	AAGGCATCCACCACAGGAAG	CCTCGTGGGAATATTCGTGCT
Housekeeping		
Hprt (origin: *Mus musculus)*	GCAGTACAGCCCCAAAATGG	AACAAAGTCTGGCCTGTATCCAA
bactin	ACAACCTTCTTGCAGCTCCTC	CTGACCCATACCCACCATCAC

Table S2. Daily rhythmicity analysis

Table S2. JTK_Cycle analysis of daily rhythmicity. Diet and Time effect on daily rhythms in microglia and monocytes for circadian, inflammatory, metabolic and mitochondrial genes. Data was analyzed with JTK_Cycle software and

p-values were obtained by fitting the data on a curve with fixed 24h period. The acrophase is given for rhythmic genes (in ZT). Genes are considered rhythmic when p<0.05 (**Bold**). N/A = not applicable (gene has low or no expression); NR = not rhythmic.

Genes	**JTK_Cycle analysis for microglia**				**JTK_Cycle analysis for**			
	Chow		**HFD**		**Chow**		**HFD**	
	p-val	acroph	p-val	acroph	p-val	acroph	p-val	acroph
Circadian								
Bmal1	**0.003**	2	**<0.00**	4	0.09	NR	1	NR
Clock	1	NR	**0.002**	4	**0.001**	16	0.22	NR
Cry1	**0.003**	16	1	NR	1	NR	0.25	NR
Cry2	1	NR	0.19	NR	1	NR	1	NR
Per1	**0.001**	14	0.63	NR	1	NR	0.22	NR
Per2	**0.003**	14	0.53	NR	**0.000**	16	**0.00**	18
Reverba	**0.009**	10	**0.002**	8	0.56	NR	0.25	NR
Dbp	**<0.00**	12	**0.000**	10	**0.015**	12	0.07	NR
Inflamma								
Tnfa	1	NR	0.06	NR	**0.02**	20	0.1	NR
Il1b	0.07	NR	0.26	NR	**0.002**	16	**0.04**	22
Myd88	**0.01**	4	1	NR	0.14	NR	1	NR
Ikbkb	1	NR	**0.01**	6	1	NR	0.07	NR
Cd68	1	NR	0.88	NR	**<0.00**	12	0.37	NR
Sirt1	1	NR	0.17	NR	1	NR	**0.02**	18
Metabolic								
Gls	1	NR	0.42	NR	1	NR	**0.00**	18
Gdh	1	NR	0.39	NR	1	NR	0.44	NR
Gpx1	1	NR	1	NR	**0.04**	14	1	NR
Hk2	1	NR	**0.01**	4	0.28	NR	0.08	NR
Glut5	1	NR	0.2	NR	N/A	N/A	N/A	N/A
Cd36	**<0.00**	4	0.28	NR	**<0.00**	6	**0.00**	12
Lpl	1	NR	0.19	NR	N/A	N/A	N/A	N/A
Ppard	1	NR	1	NR	1	NR	0.63	NR
Fas	1	NR	0.25	NR	0.25	NR	0.15	NR
Mitochon								
Cox4	**0.049**	18	0.13	NR	1	NR	1	NR
Atp5b	**0.01**	16	0.56	NR	0.26	NR	0.42	NR
Atp5g	N/A	N/A	N/A	N/A	1	NR	1	NR

Pdk4	**<0.00**	14	0.53	NR	N/A	N/A	N/A	N/A
Fis1	0.07	NR	0.79	NR	N/A	N/A	N/A	N/A
Drp1	1	NR	0.56	NR	0.75	NR	0.09	NR
Mfn2	1	NR	0.71	NR	1	NR	1	NR
Opa1	0.12	NR	0.42	NR	0.53	NR	1	NR

Table S3. One-way ANOVA analysis of effect of time in separate feeding groups

Table S3. One-way ANOVA assessment of effect of *Time*. *Time* effect evaluation in separate feeding groups. Statistical significance was determined using One-way ANOVA effect *Time* (ZT). Genes are considered rhythmic when p<0.05 (**Bold**). N/A = not applicable (gene has low or no expression).

Genes	**One-way ANOVA analysis of effect of *Time* for microglia**		**One-way ANOVA analysis of effect of *Time* for monocytes**	
	Chow	**HFD**	**Chow**	**HFD**
	p-value		p-value	
Circadian				
Bmal1	**0.0001**	**0.0004**	**0.0002**	0.9491
Clock	**0.0415**	**0.0148**	**0.0019**	0.1479
Cry1	**<0.0001**	**0.0018**	0.5351	0.3658
Cry2	**0.0012**	**0.0202**	0.4521	0.6039
Per1	**<0.0001**	0.2899	0.2289	0.1508
Per2	**0.0001**	**0.0047**	**<0.0001**	0.1125
Reverba	**<0.0001**	**0.0228**	0.0702	0.3788
Dbp	**<0.0001**	**0.0004**	**0.0129**	0.2177
Inflammatory				
Tnfa	**0.0088**	**0.0387**	**0.0007**	0.0554
Il1b	0.1805	**0.0282**	**<0.0001**	0.0680
Myd88	**0.0008**	0.1974	0.0613	0.8670
Ikbkb	**0.0254**	**0.0005**	0.5558	0.0616
Cd68	**0.0312**	0.1253	**<0.0001**	0.4689
Sirt1	**0.0204**	**0.0111**	0.7105	0.0823
Metabolic				

Gls	**0.0142**	0.4831	0.5431	**0.0026**
Gdh	0.0724	0.1871	0.7926	0.2481
Gpx1	0.0600	**0.0418**	**0.0089**	0.7746
Hk2	0.2235	**0.0010**	0.1326	**0.0004**
Glut5	0.7090	**0.0007**	N/A	N/A
Cd36	**0.0003**	0.1386	**<0.0001**	**0.0272**
Lpl	**0.0001**	0.4000	N/A	N/A
Ppard	**0.0010**	0.2455	**0.0056**	0.3960
Fas	0.1286	**0.0237**	0.1446	0.2566
Mitochondrial				
Cox4	**<0.0001**	**0.0077**	0.5976	0.3726
Atp5b	**0.0018**	0.1155	0.1180	0.3308
Atp5g	N/A	N/A	0.4628	0.9706
Pdk4	**<0.0001**	0.0733	N/A	N/A
Fis1	**0.0005**	0.2790	N/A	N/A
Drp1	**0.0010**	**0.0050**	0.1263	0.0520
Mfn2	**0.0008**	0.1415	0.7031	0.6176
Opa1	0.0722	0.1677	0.1210	0.9114

Table S4. Two-way ANOVA analysis of monocytes

Table S4. Two-way ANOVA assessment of effect of *Time, Diet* and *Interaction* in monocytes. Statistical significance was determined using Two-way ANOVA effect for *Interaction*, *Diet* and *Time* (ZT). Data are presented as means ± SEM. Genes are considered rhythmic when p<0.05 (**Bold**).

Genes	**Two-way ANOVA analysis**			**Genes**	**Two-way ANOVA analysis**		
	p-value				p-value		
	Interaction	*Time*	*Diet*		*Interaction*	*Time*	*Diet*
Circadian				**Metabolic**			
Bmal1	**0.0401**	**0.0024**	0.1879	*Gls*	0.6480	**0.0044**	0.8767
Clock	0.1578	**0.0025**	0.1114	*Gdh*	0.5924	0.3948	0.3775

Cry1	0.5488	0.3290	0.6740	*Gpx1*	**0.0414**	0.0767	0.7417
Cry2	0.7040	0.3451	0.3935	*Hk2*	**0.0062**	**0.0060**	0.3444
Per1	0.1331	0.2338	0.0660	*Cd36*	**0.0012**	**<0.0001**	0.7674
Per2	**0.0226**	**<0.0001**	0.5676	*Ppard*	0.4536	**0.0024**	0.2261
Reverba	0.3139	0.0579	0.1016	*Fas*	0.9708	**0.0178**	0.1265
Dbp	0.3748	**0.0027**	0.1182				
Inflammatory				**Mitochondrial**			
Tnfa	0.5031	**<0.0001**	0.3107	*Cox4*	0.7866	0.2362	0.5052
Il1b	**0.0051**	**<0.0001**	0.1422	*Atp5b*	0.8743	**0.0261**	0.4652
Myd88	0.3699	0.0780	**0.0452**	*Atp5g*	0.8766	0.7251	0.8313
Ikbkb	0.3379	0.1678	0.2697	*Drp1*	**0.0392**	0.1454	0.5702
Cd68	0.0681	**0.0001**	0.3710	*Mfn2*	0.8240	0.4955	0.2219
Sirt1	0.2185	0.3303	0.2993	*Opa1*	0.1594	0.4131	0.1118

Figure S. Average 24h food intake

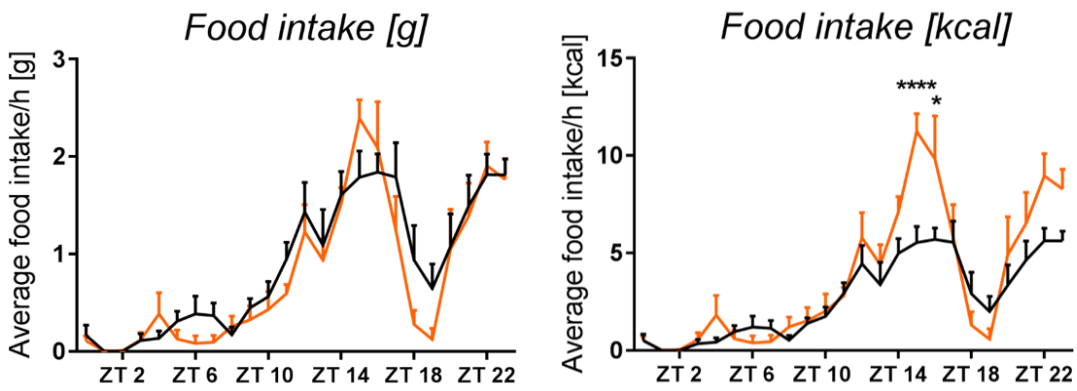

Figure S. Average time-of-day food intake per hour. Graphs represented show a re-analysis of food intake data from metabolic cages for rats fed a HFD (4.7kcal/g) or control diet (3.1 kcal/g) (Stenvers et al., 2016). Data show average food intake per hour starting at ZT0. Data are presented as food intake in gram (p_{int} = 0.7440, p_{time} <0.0001, p_{diet} = 0.1001) **(left)** and kcal (p_{int} = 0.0033, p_{time} <0.0001, p_{diet} = 0.0003) **(right)**, as 24h mean of 48h measurement for control (black) and HFD (orange) groups (n=8). Data are presented as means ± SEM. Statistical significance was determined using Two-way ANOVA effect for *Interaction*, *Time* (ZT) and *Diet*; Sidak's multiple comparison test was used to compare the effect of diet for each time point (p<0.05*; p<0.0001****).

Publication 5

Dysregulation of histone acetylation pathways in hippocampus and frontal cortex of Alzheimer's disease patients

Schueller E[1], Paiva I[1], Blanc F[2], **Wang XL**[3], Cassel JC[1], Boutillier AL[4], Bousiges O[5].

[1] Université de Strasbourg, UMR 7364 CNRS, Laboratoire de Neurosciences Cognitives et Adaptatives (LNCA), 12 Rue Goethe, Strasbourg 67000, France.
[2] Neuropsychology Unit, Neurology Service, and CNRS, ICube laboratory UMR 7357 and FMTS (Fédération de Médecine Translationnelle de Strasbourg), team IMIS/Neurocrypto, and CMRR (Memory Resources and Research Centre), and Geriatrics Day Hospital, Geriatrics Service, University Hospital of Strasbourg, Strasbourg, France.
[3] Université de Strasbourg, UMR 7364 CNRS, Laboratoire de Neurosciences Cognitives et Adaptatives (LNCA), 12 Rue Goethe, Strasbourg 67000, France; Department of Endocrinology and Metabolism, Amsterdam University Medical Center (UMC), University of Amsterdam, Amsterdam, the Netherlands.
[4] Université de Strasbourg, UMR 7364 CNRS, Laboratoire de Neurosciences Cognitives et Adaptatives (LNCA), 12 Rue Goethe, Strasbourg 67000, France. Electronic address: laurette@unistra.fr.
[5] Université de Strasbourg, UMR 7364 CNRS, Laboratoire de Neurosciences Cognitives et Adaptatives (LNCA), 12 Rue Goethe, Strasbourg 67000, France; Laboratory of Biochemistry and Molecular Biology, University Hospital of Strasbourg, Hôpital de Hautepierre, Avenue Molière, Strasbourg, France. Electronic address: bousiges@unistra.fr.

Published in Eur Neuropsychopharmacol. 2020 Feb 11.
doi: 10.1016/j.euroneuro.2020.01.015.

European Neuropsychopharmacology (2020) 33, 101–116

www.elsevier.com/locate/euroneuro

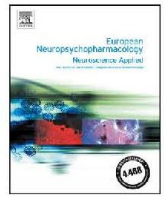

Dysregulation of histone acetylation pathways in hippocampus and frontal cortex of Alzheimer's disease patients

Estelle Schueller[a], Isabel Paiva[a], Frédéric Blanc[b], Xiao-Lan Wang[a,c], Jean-Christophe Cassel[a], Anne-Laurence Boutillier[a,*], Olivier Bousiges[a,d,*]

[a] *Université de Strasbourg, UMR 7364 CNRS, Laboratoire de Neurosciences Cognitives et Adaptatives (LNCA), 12 Rue Goethe, Strasbourg 67000, France*
[b] *Neuropsychology Unit, Neurology Service, and CNRS, ICube laboratory UMR 7357 and FMTS (Fédération de Médecine Translationnelle de Strasbourg), team IMIS/Neurocrypto, and CMRR (Memory Resources and Research Centre), and Geriatrics Day Hospital, Geriatrics Service, University Hospital of Strasbourg, Strasbourg, France*
[c] *Department of Endocrinology and Metabolism, Amsterdam University Medical Center (UMC), University of Amsterdam, Amsterdam, the Netherlands*
[d] *Laboratory of Biochemistry and Molecular Biology, University Hospital of Strasbourg, Hôpital de Hautepierre, Avenue Molière, Strasbourg, France*

Received 19 August 2019; received in revised form 18 December 2019; accepted 26 January 2020

KEYWORDS
Alzheimer's disease;
Histones (H2B and H3);
Histone acetyltransferase (CBP, PCAF);
Histone deacetylase (HDAC1, HDAC2 and HDAC3);
F2 area of frontal cortex;
Hippocampus

Abstract
Memory impairment is the main feature of Alzheimer's disease (AD). Initial impairments originate in the temporal lobe area and propagate throughout the brain in a sequential manner. Epigenetic mechanisms, especially histone acetylation, regulate plasticity and memory processes. These may be dismantled during the disease. The aim of this work was to establish changes in the acetylation-associated pathway in two key brain regions affected in AD: the hippocampus and the F2 area of frontal cortex in end-stage AD patients and age-matched controls. We found that the F2 area was more affected than the hippocampus. Indeed, CREB-Binding Protein (CBP), P300/CBP-associated protein (PCAF), Histone Deacetylase 1 (HDAC1) and HDAC2 (but not HDAC3) levels were strongly decreased in F2 area of AD compared to controls patients, whereas only HDAC1 was decreased and CBP showed a downward trend in the hippocampus. At the histone level, we detected a substantial increase in total (H3 and H2B) histone levels in the

* Corresponding authors.
E-mail addresses: laurette@unistra.fr (A.-L. Boutillier), bousiges@unistra.fr (O. Bousiges).

https://doi.org/10.1016/j.euroneuro.2020.01.015

frontal cortex, but these were decreased in nuclear extracts, pointing to a dysregulation in histone trafficking/catabolism in this brain region. Histone H3 acetylation levels were increased in cell nuclei mainly in the frontal cortex. These findings provide evidence for acetylation dysfunctions at the level of associated enzymes and of histones in AD brains, which may underlie transcriptional dysregulations and AD-related cognitive impairments. They further point to stronger dysregulations in the F2 area of the frontal cortex than in the hippocampus at an end-stage of the disease, suggesting a differential vulnerability and/or compensatory mechanisms efficiency towards epigenetic alterations.

1. Introduction

Alzheimer's disease (AD) is the most common form of dementia, mainly characterized by synaptic plasticity impairments and neurodegeneration starting from the hippocampal region and spreading to wider cortical regions. This is associated with the misfolding and aggregation of 2 proteins including the extracellular accumulation of amyloid-β peptide (Aβ) in plaques and cytoplasmic accumulation of hyper-phosphorylated tau in neurofibrillary tangles. In parallel, there are cell-signaling perturbations in the different brain structures impacted and they play an important role in the neurodegenerative processes, as well as in the memory dysfunctions observed in AD patients (Kozlov et al., 2017). Notably, AD brains present deregulated gene transcription, which may alter cognitive processes such as long-term memory formation (Alberini and Kandel, 2014). Importantly, transcriptional regulation of gene expression relies on a state of "chromatin competence", itself dependent on epigenetic regulations (Kouzarides, 2007).

Epigenetic mechanisms are involved in memory and long-term synaptic plasticity (for recent review Campbell and Wood, 2019), and it is thought that epigenetic dysregulations could also underlie the aberrant gene expression associated with the loss of synaptic plasticity and memory in Alzheimer's disease (Guan et al., 2009; Graff et al., 2012; Gjoneska et al., 2015; Chatterjee et al., 2018; De Jager et al., 2018). Among these mechanisms, histone modifications and more particularly histone acetylations are key players in memory processes but also in regulating the neuroprotection/neurodegeneration balance (for review, Graff and Mansuy, 2008, 2009; Stilling and Fischer, 2011; Graff and Tsai, 2013; Schneider et al., 2013; Benito et al., 2015; Chatterjee et al., 2018). Histone acetylations are regulated by two types of enzymes: histone acetyltransferases (HATs) and histone deacetylases (HDACs). HATs are responsible for histone acetylation on lysine residues, thereby opening chromatin conformation and favoring transcription factor and co-activator recruitment necessary for transcriptional activation. *A contrario* HDACs remove acetylation from the histones, thereby conferring a more closed chromatin conformation and transcriptional inactivation. It has been shown that some HATs, such as CREB-binding protein (CBP) (Alarcon et al., 2004; Korzus et al., 2004; Wood et al., 2005; Chen et al., 2010; Valor et al., 2011; Barrett et al., 2011; Bousiges et al., 2010), p300 (Oliveira et al., 2007), or p300/CBP-associated factor (PCAF) (Maurice et al., 2008), are associated with long-term memory mechanisms. Moreover, memory processes also rely on HDACs, such as HDAC2, the first HDAC for which a role in memory formation and synaptic plasticity was clearly demonstrated (Guan et al., 2009; Graff et al., 2012; Nott et al., 2008). HDAC1 was further shown to be important for fear memory extinction (Bahari-Javan et al., 2012) as well as HDAC3, which is a critical negative regulator of long-term memory formation (McQuown et al., 2011; Alaghband et al., 2017; Kwapis et al., 2017).

The fate of HAT and HDAC enzymes during the course of AD has been investigated in humans with contrasting results. Reduction of expression of CBP and its homolog p300 have been reported in postmortem prefrontal cortex of individuals with AD compared to age-matched controls (Bartolotti et al., 2016), whereas an increase in phospho-p300 has been observed in hippocampal area CA1 of human brains (Aubry et al., 2015). Graff and colleagues showed an increase of HDAC2 and no variation for HDAC1 in the hippocampus of AD patients, effects that were also observed in mouse models of neurodegeneration (Graff et al., 2012; Bie et al., 2014). By contrast, other studies showed a strong decrease of HDAC1 and HDAC2 in the cortex of AD patients (Mastroeni et al., 2011; Anderson et al., 2015). A recent in vivo study led with a new PET imaging agent capable of marking Class I HDACs ([^{11}C]Martinostat) suggests an overall loss of HDAC class I enzymes in posterior cingulate, precuneus, and inferior parietal cortices of AD patients (Pascoal et al., 2018). Moreover, comparable patterns between controls and MCI patients were observed suggesting that the decrease of class I HDAC enzymes appears at the demented stage. However, such study cannot document which subtype is predominantly affected. Lastly, the sirtuins, another class of HDACs, have also been shown to be altered during the clinical course of the pathology and may play a role in the cognitive symptoms of AD (for review Cacabelos et al., 2019).

Concerning acetylation changes in AD, the literature is also divergent, with the additional observation that post-translational modifications of histones are sensitive to post-mortem delays (Barrachina et al., 2012; Jarnasz et al., 2019). In humans, Rao and colleagues (Rao et al., 2012) did not detect H3Ac changes in the frontal cortex of AD patients compared to controls, whereas Zhang and colleagues highlighted H3Ac decrease in AD patient's temporal lobe (Zhang et al., 2012). Interestingly, comparison of old and AD subjects revealed a genomic redistribution of H4K16ac, as assessed by ChIP-sequencing, in the lateral temporal lobe of AD subjects, with more losses than gains (Nativio et al., 2018). Some other studies described an acetylated H3 increase of bulk chromatin in inferior temporal gyrus and middle temporal gyrus (Narayan et al., 2015) or in occipital cortex of AD patients (Lithner et al., 2013) of

post-mortem AD brain compared to those of age-matched control patients. In rodent models, many studies led on epigenetic changes measurements have reported different results, e.g.: acetylation decrease (Bie et al., 2014; Benito et al., 2015; Chatterjee et al., 2018), acetylation increase (Lithner et al., 2013; Wu et al., 2013; Marques et al., 2012), or no change (Francis et al., 2009; Cadena-del-Castillo et al., 2014).

Thus, there is a conflicting literature on establishing how the histone acetylation pathway is altered during AD in human brains. A potent explanation could be that most studies investigated specific proteins of interest in a specific brain region in different cohorts of AD patients. Herein, we have undertaken a more comprehensive study, evaluating a panel of acetylation-modifying enzymes (CBP, PCAF, HDAC1, 2 and 3), as well as different histone acetylation motifs, in two AD-key regions obtained from the same patients, the F2 area of frontal cortex (F2) and the hippocampus from *post-mortem* pathological AD brains compared to healthy brains. We show that AD patients presented a dramatic decrease of several enzymes, i.e. CBP, PCAF, HDAC1, and HDAC2 in the F2 area of the frontal cortex, while changes were more moderate in their hippocampus. Histone acetylation levels changes were more complex to analyze as a global increase of the total level of H3 and H2B histones was measured in whole tissues of frontal cortex. Further assessments specifically performed in nuclear extracts revealed that the total histone levels were in fact significantly lowered in the frontal cortex of AD patients and the net nuclear histone H3 acetylation levels were then increased, with no change in H2B acetylation. No overall change of total histone was observed in the hippocampus, but acetylation levels were also altered. These results show that epigenetic enzymes, total histone, and acetylated histone levels are dramatically altered in the end-stage AD brains. This may account for dysregulated gene expression programs. Our data also emphasize that the frontal cortex, a region that is affected at later stage than the hippocampus within the course of the disease, shows more pronounced epigenetic dysregulations than in the hippocampus. This may account for early decreased plasticity in this structure and decrease in associated functions.

2. Experimental procedures

2.1. Human brain tissue

We have obtained control and AD post-mortem tissues from NeuroCEB (a French national organization dedicated to provide brain samples, either normal or pathological; identification number: "Neuro-CEB BB-0033-00011"). The samples were obtained from brains collected in a Brain Donation Program of the Brain Bank "Neuro-CEB" run by a consortium of Patients Associations: CSC (cerebellar ataxias), Fondation ARSEP (research on multiple sclerosis), France Parkinson, Fondation Vaincre Alzheimer. The consents were signed by the patients themselves or their next of kin in their name, in accordance with the French Bioethical Laws. The Brain Bank Neuro-CEB has been declared at the Ministry of Higher Education and Research and has received approval to distribute samples (agreement AC-2013-1887). All brains were examined by neuropathologists and classified based on neuropathological abnormalities, or lack thereof in neurologically normal controls. Cases were classified using Braak staging (I-VI) (Braak and Braak, 1995). All AD patients studied in this article were at a terminal stage (stage VI), while the controls were at stage 0-I (Table 1). Hippocampal and frontal cortex samples frozen at −80 °C were used for biochemical research, samples from hippocampal and frontal cortex sectioned to obtain 10 μm thick sections, mounted on slides and frozen with isopentane cooled in liquid nitrogen were used for histological studies. As described in Table 1, we analyzed 8 blocks from AD patients and 5 blocks from control patients for frontal cortex; and 6 blocks from AD patients and 5 blocks from control patients for hippocampus. For histological studies $n = 3$ AD and $n = 2$ controls patients were obtained for frontal cortex. Table 1 describes also in detail the available clinicopathological information for all the cases and controls (gender, age, frozen hemisphere, postmortem delay, profession, neuropathological diagnosis and potential associated pathology). The post-mortem delays for controls were 12.3 ± 7.0 h versus 22.1 ± 11.4 h for AD (non-significant difference, $p = 0.113$) and the age at death was of 76.4 ± 7.5 years for controls versus 80.4 ± 4.7 years for AD (non-significant difference, $p = 0.171$).

All the patients (controls and AD) were controlled for different Alzheimer hallmarks, such as phospho-Tau (Ser396, Thr231, Thr212/ Ser214, Ser404) and amyloid β by both western blot and immunohistochemistry analysis. AD patients also showed, as expected at this age, a significant loss of NeuN in parallel with increased GFAP labeling (Fig. 1).

2.2. Protein preparation and western blot analyses

Total protein preparation. Tissues were lysed and homogenized in Laemmli buffer. After 10 min at 70 °C, samples were sonicated two times for 10 s (Ultrasonic Processor, power 40%), boiled 5 min and centrifuged (14 000 g, 5 min). The supernatant was frozen at −20 °C.

Nuclear protein extractions were adapted from Dignam et al. (1983) (). The samples were suspended in five packed pellet volumes of buffer A (0.32 M sucrose, 1 mM $MgCl_2$, 0.25% Triton). Samples were lysed by 10 strokes with a dounce homogenizer (tight pestle). The homogenate was centrifuged for 10 min at 1000 g to pellet nuclei. The pellets were kept and washed with buffer B (buffer A without triton). The homogenates were again centrifuged for 10 min at 1000 g to remove residual cytoplasmic material. The nuclear pellets were then collected in buffer C (TRIS 10 mM and EDTA 13 mM pH7.4) supplemented with protease inhibitor cocktail and sodium butyrate (1 mM). They were then centrifuged, the soluble nuclear fractions were homogenized in Laemmli buffer and samples were sonicated two times for 10 s (Ultrasonic Processor, power 40%), boiled 5 min and centrifuged (14 000 g, 5 min). The supernatant was frozen at −20 °C. The synaptic protein Neurogranin is detectable in total but not in nuclear extracts confirming the quality of nuclear extraction (Fig. 1).

Table 1 Patients characteristics.

Anonimity No	Sex	Age	Frozen hemisphere	Brain weight (g)	Post Mortem delay	Profession	Neuropathological diagnosis	Associated pathology	Frozen samples at −80 °C		Histological sections
	Alzheimeir's disease (Braak stage V-VI)								Hippocampus	Frontal cortex	Frontal cortex
7853	F	86	R	1180	30 h	nd	Alz Braak stage: VI; Thal stage: V	-	Ok	Ok	No
8629	M	81	R	1230	17 h30	nd	Alz Braak stage: VI; Thal stage: V	-	Ok	Ok	Ok
7654	M	78	R	1250	8 h30	Draughtsman	Alz Braak stage: VI; Thal stage: II	-	Ok	Ok	Ok
6563	M	82	R	1238	25 h	nd	Alz Braak stage: VI; Thal stage: V	-	Ok	Ok	No
7689	M	72	R	1458	44 h	Engineer	Alz Braak stage: VI; Thal stage: V	-	Ok	Ok	No
6742	M	76	L	1215	10 h	nd	Alz Braak stage: VI; Thal stage: V	Electrode stimulation carrier	No	Ok	Ok
7106	M	83	L	1070	21 h	nd	Alz Braak stage: VI; Thal stage: IV		No	Ok	No
7857	F	85	L	1195	21 h	Librarian	Alz Braak stage: VI; Thal stage: V	Dementia with Lewy body	Ok	Ok	No
	Controls (Braak stage 0-I)										
4078	M	73	R	508 (right hemisphere)	10 h	nd	Control	-	Ok	Ok	No
8866	M	84	R	1355	15 h30	nd	Control	-	Ok	Ok	No
5991	M	66	R	1500	7 h	Rail agent	Control	Vasculopathy	Ok	Ok	No
3356	F	86	R	1226	nd	nd	Control	Cerebrovascular accident	Ok	Ok	No
8251	M	79	R	1273	nd	nd	Control	Mild atrophy and discrete spongiosis	Ok	Ok	No
6203	M	78	L	1280	23 h	nd	Control	Dramatic amyloid angiopathy	No	No	Ok
3549	M	69	L	1254	6 h	Engineer	Control	Epileptic	No	No	Ok

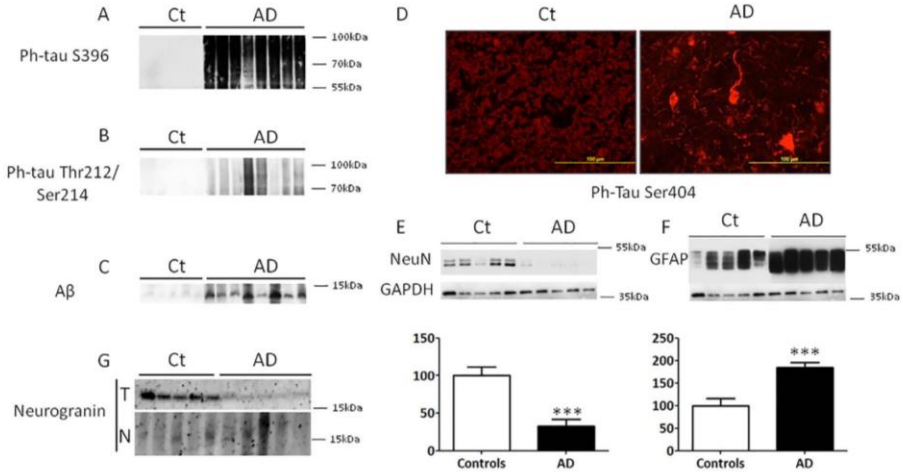

Fig. 1 Characteristic hallmarks of Alzheimer's disease (AD) in frontal cortex of controls ($n = 5$) and AD patients ($n = 8$). Samples were tested with three different types of Tau phosphorylation antibodies, two by western blot: S396, Thr212/Ser214 (A, B) and one in immunohistochemistry: Ser404 (D). The presence of Aβ peptides was also evaluated (C). For characteristic hallmarks of AD, all the patients are represented. The results show that only the AD patients displayed the pathological markers. Other markers of neurodegeneration (NeuN) (E) or gliosis (GFAP) (F) were also studied in the F2 area of the frontal cortex. Blots are shown in quintuplicate. Quantified results are represented as fold induction of the protein of interest, the result obtained in the controls being arbitrarily set at 100%. Student's t-test: $^{***}p<0.001$. (G) To control our nuclear protein-extraction we analyzed the neurogranin (which is a postsynaptic protein) by western blot. Protein amount loaded in the gels and exposition time (1 min exposition) of the membranes to the chemidoc touch were similar between total extraction and nuclear extraction (frontal cortex). Neurogranin was not detectable in nuclear extraction and in total protein extraction from AD patients. AD: Alzheimer's disease patients, Ct: control patients.

Western blot analyses. Protein concentration was measured using the RC-DC Protein Assay (Bio-Rad). Western blots were performed as described previously (Bousiges et al., 2013) with polyclonal antibodies against CBP (sc-369 or sc-7300), HDAC1 (sc-81598), neurogranin (sc-50401) (Santa Cruz Biotechnology), HDAC2 (05-814), phospho-Tau S396 (05-885), acetyl-histone H2B (H2B tetra-Ac, 07-373), acetyl-histone H3 (06-599) (Upstate Biotechnology, New York, NY, USA), phospho-Tau Thr2012/Ser214 (AT100, MN1060), phospho-Tau S404 (44-758 G) (Thermo Fisher Scientific, France), GAPDH (ab22555), acetyl-histone H3 K27 (ab4729), histone H3 (ab24834) (Abcam, Cambridge, UK), PCAF (C14G9) (Cell Signaling Technology Europe, Leiden, The Netherlands), histone H2B (H2-2A8) (Euromedex, Strasbourg, France). Secondary antibodies were a horseradish peroxidase-conjugated whole-goat anti-rabbit IgG (111-035-003), or a horseradish peroxidase-conjugated whole-goat anti-mouse IgG (115-035-003) (Jackson Immunoresearch, Suffolk, UK). Western blots have been performed using 2 different technologies: Precast Criterion Gels, wet transfer to nitrocellulose followed by ECL, and film exposure and autoradiography for the studies in the Frontal Cortex (except for HDAC3 blots). Other blots in the hippocampus (and including HDAC3 in the frontal cortex) were performed using Precast Criterion Tgx stain-free gels® (#5678095, Bio-Rad), and after proteins transfer on nitrocellulose membrane with Trans Blot® Turbo™ transfer system (Bio-Rad) the proteins were revealed with Clarity ECL (170-5061, Bio-Rad) and exposed in Chemidoc Touch® (Bio-Rad). When blots have been revealed by autoradiography, proteins of interest (enzymes, total histones and modified histones) have been normalized on beta Actin levels present in each corresponding sample. When the blots have been revealed with the ChemiDoc Touch, results were quantified using Image Lab® software: bands of interest were normalized relative to the total amount of protein detected on the nitrocellulose after transfer for each sample.

Immunohistochemistry. Frontal cortex sections were sent ready for immunohistochemistry use (10 μm thickness sample fixed on a slide) by the French national brain bank neuroCEB. The tissue sections were fixed by paraformaldehyde 4% for 5 min and then were permeabilized in 1XPBS/2% Triton for 15 min. Nonspecific labeling was blocked by 1XPBS/0.1% Triton/5% horse serum for 30 min, and sections were then incubated overnight with Phospho-Tau (Ser404) antibody (Thermo-Fischer reference: 44-758 G). After three washes, they were incubated with Alexa Fluo 594 donkey anti-rabbit (1 h at room temperature) followed by 3 washes with 1xPBS/0.1%Triton X-100. After two PBS washes, the sections were mounted with Mowiol.

2.3. Statistical analysis

Statistical analyses were performed using Student's t-test (PRISM version 5; GraphPad, San Diego, CA, USA). Data are

expressed as the mean ± SEM. Differences at $p < 0.05$ were considered significant. In cases of variance inequality, a Welch's *t*-test was performed. In addition, when the test for normal distribution (Shapiro-Wilk test) was not respected, we used the non-parametric Mann-Whitney test.

2.4. Power analysis

Due to the small number of patients in the study, we determined for each result a post hoc or retrospective power analysis. This analysis takes into account the *N* and the standard deviation for each group and gives a minimum expected difference between the group means according to the power chosen. It is generally considered that the power must be at least 0.80 to be satisfactory. For this purpose, each analysis was taken over with a statistical software (GraphPad - StatMate 2.00) to determine if, for each of them, the power was sufficient. When the power analysis exceeded 80%, we left the result as statistically significant. Conversely, when the power analysis showed that the difference observed between the two groups was less than 0.80, we considered the difference as corresponding to a tendency (despite statistically significant with the *t*-test). For these analyses, there is a need to get larger samples in order to conclude.

3. Results

3.1. Creb-binding-protein (CBP) levels are strongly decreased in frontal cortex of AD brain

Post-mortem human brain samples were obtained from control ($n = 5$) and AD patients ($n = 8$ for frontal cortex and $n = 6$ for hippocampus), on which we controlled the specific hallmarks of AD. All AD samples from the frontal cortex showed hyper-phosphorylation of several Tau epitopes, increased amounts of amyloid β peptides, neuronal loss (NeuN), and increased neuroinflammation (GFAP) (Fig. 1, see materials and methods).

CBP acetyltransferase levels were evaluated by western blot analyses in *post-mortem* brain extracts from AD and aged-matched controls. Interestingly, CBP was dramatically decreased in AD patients F2 area (73% lower compared to controls, Welch's *t*-test $p < 0.05$, Fig. 2(A)); it only tended to decrease in the hippocampus (61% lower in AD patients compared to controls, Fig. 2(B)). PCAF, another acetyltransferase involved in memory processes (Maurice et al., 2008), tends to decrease in frontal cortex of AD patients, (25% decrease in AD patients compared to controls, $p < 0.05$, but analysis power <80%, Fig. 2(A)). In the hippocampus, no significant differences were observed for PCAF levels (Fig. 2(B)).

3.2. HDAC1 and HDAC2 are decreased in frontal cortex while only HDAC1 is decreased in hippocampal region of AD patients

The Class I family of HDACs plays a significant role in learning and memory processes (Guan et al., 2009; Nott et al., 2008; McQuown et al., 2011; Shu et al., 2018) as well as in extinction processes (Bahari-Javan et al., 2012); thus, the levels of HDAC1, 2 and 3 were investigated. We found that HDAC1 levels tended to decrease in frontal cortex and were decreased in hippocampus samples of AD patients (45% lower compared to controls, $p<0.05$ but analysis power < 80% for frontal cortex; 72% lower compared to controls, $p<0.05$, for hippocampus, Fig. 3(B)). We also found a strong reduction of HDAC2 in AD patients F2 area compared to the controls (more than 85%, Mann-Whitney test $p<0.01$, Fig. 3(A)), but HDAC2 levels were unchanged in the hippocampus samples (Fig. 3(B)). HDAC3 was not affected in the AD samples, neither in the frontal cortex nor in the hippocampus (Fig. 3(A) and (B)).

3.3. Total histone levels are increased in whole tissue extracts but decreased in nuclear extracts of AD patient's frontal cortex

Analyses of the AD frontal cortex F2 area surprisingly revealed that total H3 and H2B histone levels were both increased when measured in total protein extracts, but significantly only for H3tot (H3tot, 51% higher, $p<0.0001$, H2Btot, 46% higher, $p<0.05$ but power analyses <80%, Fig. 4(A) and (B)). Then, whereas the bulk acetylation levels of H3 (H3K9K14, H3Ac) and of H2B (tetra-acetylation, H2BAc) were significantly increased in AD tissues, the ratio of H3Ac/H3tot and H2BAc/H2Btot were not significantly different in the F2 area of AD compared to controls (Fig. 4(C)). By contrast, in the hippocampus, total histone levels were similar between AD patients and controls (Fig. 4(D) and (E)), and the acetylation status of H3 and H2B showed opposite regulation. The H3Ac/H3tot ratio was significantly decreased in AD patients (60% lower compared to the controls, Welch's *t*-test $p<0.05$, Fig. 4(F)) whereas the H2BAc/H2Btot ratio tended to increase in pathological samples (71% higher compared to the controls, $p<0.05$ but analysis power <80%, Fig. 4(F)).

Taking into consideration that histones are produced and degraded in the cytoplasm, we investigated if their levels in the nucleus were comparable to that found in whole cells. For this, we prepared nuclear protein extracts from frontal cortex and hippocampal region of AD and control cases. To validate the nuclear extraction, we analyzed the presence of the post-synaptic protein neurogranin by Western blot in the total and nuclear protein-extracts. We confirmed the absence of this cytoplasmic protein in the nuclear protein-extracts, neurogranin being only found in the total protein-extracts (of the control patients) (Fig. 1(H) for frontal cortex, data not shown for hippocampus).

Interestingly, in the frontal cortex, nuclear-extracted total histone levels presented a different regulation as compared to whole tissue extracts: total H3 histone levels tended to decrease in AD patients compared to controls (H3tot, 12% lower compared to controls, $p<0.05$ but analysis power <80%, Fig. 5(A) and (B)) and H2B histone levels showed also a decrease tendency (H2Btot, 16% lower compared to controls, $p = 0.06$, Fig. 5(A) and (B)). As the net nuclear levels of H3 acetylation were unchanged, then the H3ac/H3total ratio was significantly increased (14% higher, Mann-Whitney test $p<0.01$, Fig. 5(C)). The H2BAc/H2Btot

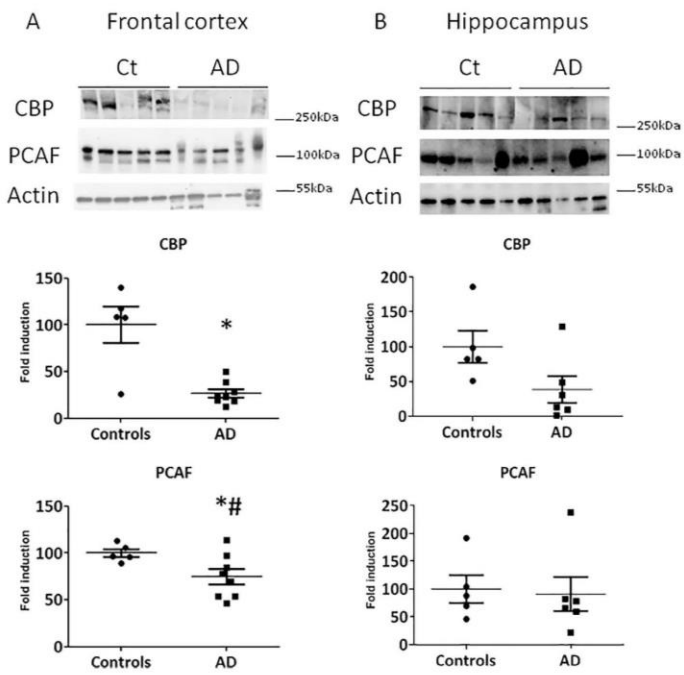

Fig. 2 Decrease of CBP levels in AD patients. (A) HAT (CBP and PCAF) protein expression assessed by western blot and normalized on beta Actin in frontal cortex of controls ($n = 5$) and AD patients ($n = 8$). (B) HAT (CBP and PCAF) protein expression assessed by western blot and normalized on total proteins in hippocampus of controls ($n = 5$) and AD patients ($n = 6$). Blots are shown in quintuplicate. Quantified results are represented as fold induction of the enzyme, the result obtained in the controls being arbitrarily set at 100%. Student's t-test: $^{*}p<0.05$; # the power analysis is less than 80%, which means that larger samples would be required to get conclusive data. AD: Alzheimer's disease patients, Ct: control patients.

ratio in the nuclear extracts remained unchanged in both regions as also observed in whole tissue extracts.

In the hippocampal region, nuclear-extracted total H3 or H2B histone levels remained unchanged. However, we noticed that H3 acetylation levels were very heterogeneous between nuclear extracts from the different AD patients and that the H3Ac/H3total ratio was increase, although not significantly (100% upper compared to controls, $p = 0.07$) (Fig. 5(D)). Globally, acetylation of histones seemed much less impacted when nuclear extracts were analyzed compared to whole tissue samples (Fig. 6).

4. Discussion

Epigenetic studies in the human brain of AD patients are poorly documented and/or have generated conflicting results, but the clear identification of specific epigenetic dysregulations could help defining new therapeutic targets. Notably, identifying by which alterations and how different brain regions are affected are important aspects to design new therapeutic strategies. In this study, we assessed a series of acetylation modifying enzymes and histone levels in two brain regions of the same patients: the F2 area of the frontal cortex, and the hippocampus. We provide evidence of differential dysregulations in each brain region. A major result is that the frontal cortex displayed the main epigenetic impairments (epigenetic enzyme levels) compared to the hippocampus in end-stage AD patients. Additionally, the frontal cortex also displayed dysregulations of total histone levels that were not observed in the hippocampus (Fig. 6). Lastly, we found that the net levels of acetylated-histones H3 measured in nuclear extracts were increased mainly in frontal cortex.

4.1. Epigenetic impairments are more severe in the frontal cortex than in the hippocampus of AD patients

AD brains exhibit significant atrophy, predominantly in the temporal and parietal lobes, with deposition of senile plaques and neurofibrillary degeneration initially in the entorhinal cortex and the hippocampus, which spread out to associative regions of the neocortex with disease progression (Braak and Braak, 1995). Thus, in end-stage brains, one could expect stronger dysregulations in regions that are primarily affected. Herein, when assessing hippocampal and frontal areas from the same patients, we showed that most of the epigenetic enzymes, i.e. CBP, PCAF,

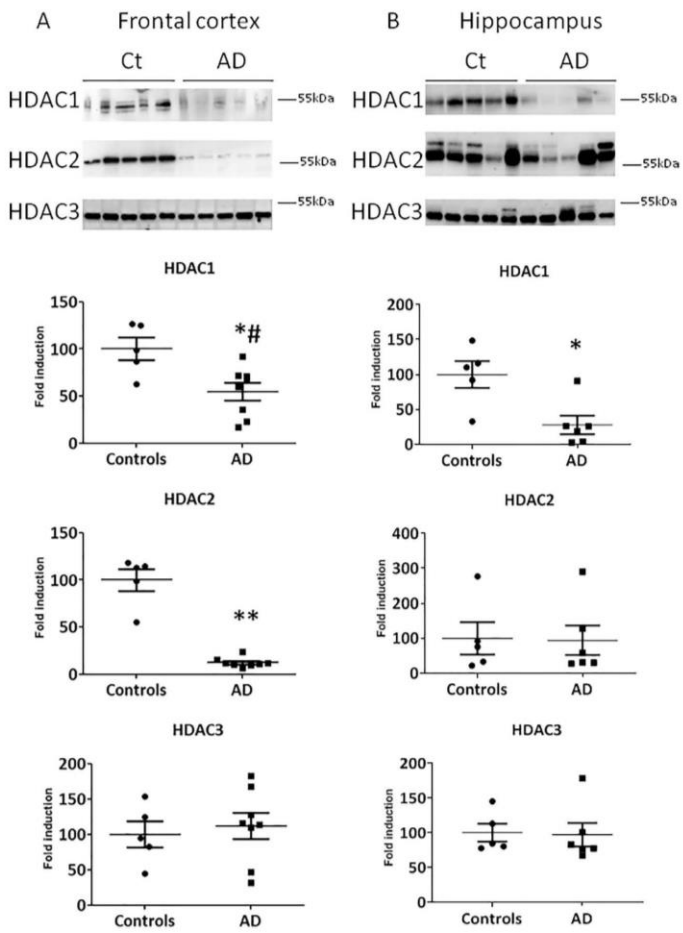

Fig. 3 Decrease of HDAC1 and HDAC2 in frontal cortex and HDAC1 decrease in hippocampus of AD patients. (A) HDAC (HDAC1, HDAC2 and HDAC3) protein expression assessed by western blot and normalized on beta Actin in frontal cortex of controls ($n = 5$) and AD patients ($n = 8$). (B) HDAC (HDAC1, HDAC2 and HDAC3) protein expression assessed by western blot and normalized on total proteins in hippocampus of controls ($n = 5$) and AD patients ($n = 6$). Blots are shown in quintuplicate. Quantified results are represented as fold induction of the enzyme, the result obtained in the controls being arbitrarily set at 100%. Student's t-test: $^{**}p<0.01$, $^{*}p<0.05$; # the power analysis is less than 80%, which means that larger samples would be required to get conclusive data. AD: Alzheimer's disease patients, Ct: control patients.

HDAC1 and HDAC2 levels were significantly decreased in the frontal area of AD patients compared to controls, when only HDAC1 levels were significantly affected and CBP showed a trend to decrease in their hippocampal area. Regarding histone levels, we found an increase in their total amounts only in the frontal cortex. These results suggest that neurons from the frontal cortex area are more vulnerable to epigenetic changes and/or that (remaining) hippocampal neurons are able to better compensate epigenetic dysregulations than neurons from the frontal cortex area. These dramatic changes observed in the frontal cortex are likely associated to the severe loss in neuronal plasticity and synaptic functions. Such epigenetic damage in the frontal cortex may impair functions requiring hippocampo-cortical interactions such as systemic consolidation for long term memory formation, an early symptom of AD (Braak and Braak, 1995).

4.2. CBP loss in brain structures involved in memory processes in AD patients

An interesting finding is that CBP levels were strongly decreased in the F2 area of the frontal cortex and showed a strong downward trend in the hippocampus of AD patients. This confirms previous observations that CBP and

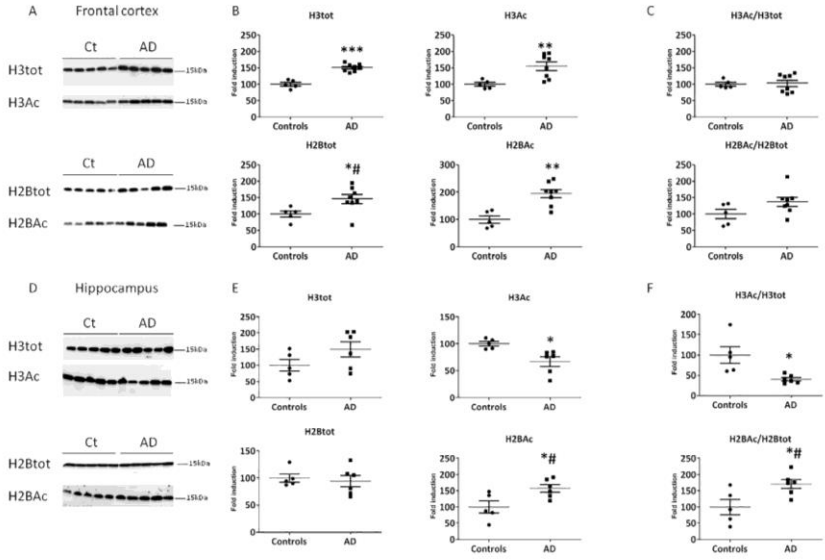

Fig. 4 Increase of total (H3 and H2B) histone levels in whole tissue extracts from AD patients F2 cortical area. Acetylated (Ac) and Total (Tot) histone levels were measured by western blot analyses and normalized on beta Actin for histone H3 and H2B in (A,B) frontal cortex of controls ($n = 5$) and AD ($n = 8$) patients and normalized on total proteins in hippocampus (D,E) of controls ($n = 5$) and AD patients ($n = 6$). Lysine acetylation measured here are H3K9K14 and H2BK5K12K15K20. Western blots are represented in quintuplicates. Quantified results are represented as fold induction of the total or acetylated histone or (C,F) the Ac/Tot ratio for each histone, the result obtained in the controls being arbitrarily set at 100%. Student's *t*-test: ***$p<0.001$, **$p<0.01$; *$p<0.05$; # the power analysis is less than 80%, which means more samples would be required to get conclusive data. AD: Alzheimer's disease patients, Ct: control patients.

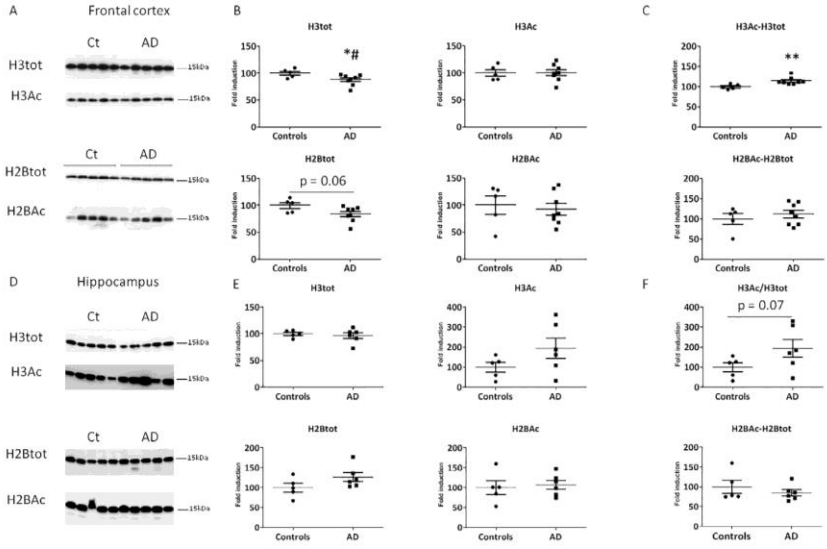

Fig. 5 Total and acetylated histone levels in nuclear protein extracts from AD patients brain. Acetylated (Ac) and Total (Tot) histone levels were measured by western blot analyses and normalized on beta Actin for histone H3 and H2B in frontal cortex (A) of controls ($n = 5$) and AD ($n = 8$) patients and normalized on total proteins in hippocampus (D) of controls ($n = 5$) and AD patients ($n = 6$). Lysine acetylation measured here are H3K9K14 and H2BK5K12K15K20. Western blots are represented in quintuplicates. Quantified results (B, C for frontal cortex and E, F for hippocampus) are represented as fold induction of the total histone or the Ac/Tot ratio for each histone, the result obtained in the controls being arbitrarily set at 100%. Student's *t*-test: **$p<0.01$; *$p<0.05$; # the power analysis is less than 80%, which means that larger samples would be required to get conclusive data. AD: Alzheimer's disease patients, Ct: control patients.

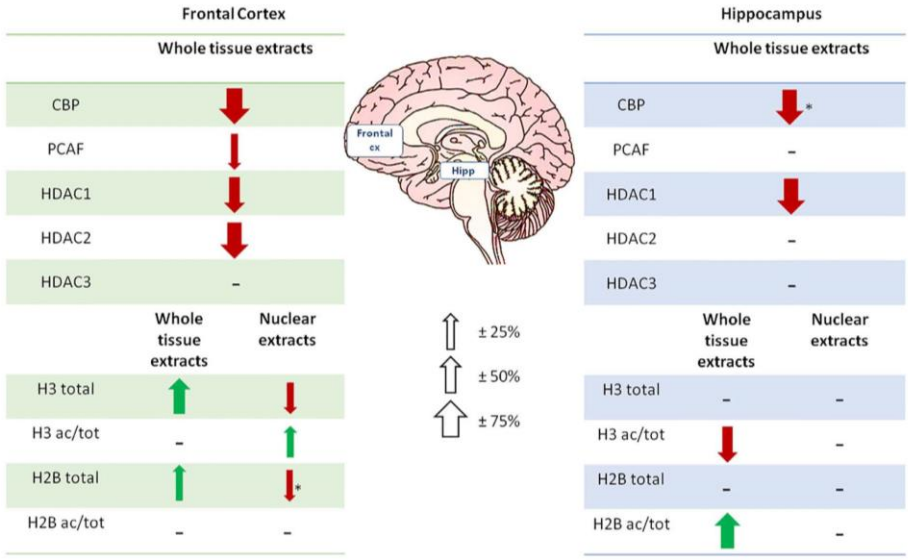

Fig. 6 Schematization of the data. The figure shows the results obtained during total tissue extraction and nuclear extraction of hippocampal and frontal cortex structures for enzymes regulating histone acetylation (CBP, PCAF, HDAC1, HDAC2, HDAC3) as well as for total and acetylated histone modifications. The increases and decreases are represented by green arrows pointing upwards and red arrows pointing downwards, respectively. The level of variation is represented by the thickness of the arrow: a thick arrow represents a large variation while a thin arrow represents a small variation. $^{*}p = 0.06$ for H2Btot in the nuclear frontal cortex and $p = 0.075$ for CBP hipp, not significant but suggests a trend.

its homolog p300 expression present a significant reduction in the prefrontal cortex of AD patients (Bartolotti et al., 2016), and extent this result to the hippocampus. Taking into consideration the role of CBP in cognitive processes (Alarcon et al., 2004; Korzus et al., 2004; Wood et al., 2005; Chen et al., 2010; Valor et al., 2011; Barrett et al., 2011; Bousiges et al., 2010), this dramatic CBP decrease may play a role in the clinical AD symptoms. Along this line, our group has shown recently that CBP levels were decreased in the dorsal hippocampus of 12-month-old mice presenting a tauopathy (THY-Tau22 mice) and displaying memory and plasticity dysfunctions (Chatterjee et al., 2018). Similarly, the amyloid pathway appears to be involved in the CBP decline, as an early CBP downregulation in the hippocampus of APPswe/PS1ΔE9 mice was associated with their memory loss (Bartolotti et al., 2016; Ettcheto et al., 2017). CBP is known to play a role in neuronal survival, both during development and in the adult brain (Del Blanco et al., 2019; Lipinski et al., 2019). In neurons, CBP protein loss (Rouaux et al., 2003) or inactivation of its enzymatic activity (Saha and Pahan, 2006) has been associated with neurodegenerative conditions. Interestingly, the bromodomain of CBP promotes cell survival by blocking Aβ42 mediated neurodegeneration in the retinal neurons of a transgenic fruit fly model with a phenotype resembling Alzheimer's like neuropathology (Cutler et al., 2015). Thus, it is likely that CBP loss observed in the AD human brain might potentiate Aβ and/or Tau-mediated neurodegeneration. In addition, it has been shown that Aβ induces post-translational degradation of CBP (Song et al., 2015), an event which could underlie CBP loss in AD brains. Thus, we suggest that CBP loss in AD patients is functionally important and might be a potential target for therapeutic interventions. This hypothesis is supported by the study of Caccamo and colleagues, who showed that CBP gene transfer in the brain of an animal model of AD restored CREB function and improved learning and memory (Caccamo et al., 2010). Furthermore, we recently showed that deficient memory formation and plasticity processes could be fully restored in tauopathic mice (THY-Tau22 mice) after a treatment with a CBP/p300 HAT activator molecule (Chatterjee et al., 2018), thereby emphasizing the importance of CBP in such processes and demonstrating the feasibility of a pharmacological approach targeting this enzyme at symptomatic stages in mice. Lastly, as CBP is a circadian clock regulator via the formation of complex with CLOCK (Gustafson and Partch, 2015), severe CBP loss could also contribute to the circadian rhythms disturbances observed in AD patients (Leng et al., 2019). Notably, Aβ-mediated CBP degradation in AD mice was shown in the context of circadian rhythm disruption (Song et al., 2015).

We also observed a 25% decrease of PCAF levels in frontal cortex, but these levels were less impacted than those of CBP; PCAF levels were not changed in the hippocampus. CBP is specifically targeted by caspases and calpains at the onset of neuronal apoptosis, and CBP was identified as a caspase-6 substrate whereas PCAF was not (Rouaux et al., 2003). Caspase 6 activation is an early event in AD (LeBlanc, 2013) which may preferentially trigger CBP degradation (over PCAF) in the AD patients' samples.

4.3. Class I HDACs alterations in AD patients

In AD compared to control brains, we found that HDAC1 was strongly decreased in both structures, whereas HDAC2 levels were only found decreased in the frontal cortex, and HDAC3 levels remained unchanged. In the frontal cortex of AD patients, our findings are in agreement with those of Anderson et al. (2015) who reported a decrease in both HDAC1 and 2. The decrease of HDAC2 was further confirmed in this structure by Mastroeni et al. (2011). Other studies reported increased levels of these HDACs in AD brains (Graff et al., 2012; Mahady et al., 2018). However, the study led by Graff et al. focused on the hippocampus of Braak stage I-II AD patients (Graff et al., 2012). Mahady and colleagues assessed HDAC levels in the frontal cortex of patients with no, mild, moderate or severe AD status. They found an increase of HDAC1 and HDAC3 levels in mild and moderate AD, while the level of both HDACs strongly decreased in severe AD patient's brains (Mahady et al., 2018). Apparently conflicting, these studies actually focused on different regions of the brain independently and for different Braak stages. Thus, our study led at the end stage of the disease in the frontal cortex and hippocampal region of the same AD patients reconcile most of the literature by showing that indeed, a differential effect is observed in these regions: some epigenetic alterations can be measured in the frontal area while these regulations seem relatively preserved in the hippocampus at the same stage.

HDAC1 levels were severely impaired in both structures evaluated. This contrast with the fact that HDAC1 levels are found increased in the prefrontal cortex of schizophrenia compared with control subjects (Sharma et al., 2008; Jakovcevski et al., 2013) and suggests that HDAC1 decrease is a correlate of neurodegenerative conditions. Notably, Aβ toxicity may account for HDAC1 degradation as it was shown to target HDAC1 SUMOylation, which has a neuroprotective role (Tao et al., 2017). HDAC1 plays a prominent role in DNA repair in postmitotic neurons (Dobbin et al., 2013) through interactions with FUS (Wang et al., 2013) and the strong decrease of HDAC1 may be relevant to excessive neuronal DNA damage observed in AD patients (Brasnjevic et al., 2008). Lastly, HDAC1 also has a role in memory extinction processes (Bahari-Javan et al., 2012).

HDAC2, which is clearly involved in memory formation and synaptic plasticity (Guan et al., 2009; Graff et al., 2012; Nott et al., 2008), is strongly decreased in frontal cortex but seems less impacted in the hippocampal region in our study. As described in Graff et al. (2012), HDAC2 is upregulated in the hippocampus at early stages of AD and this was suggested to participate to AD-induced synaptic loss (Yamakawa et al., 2017). The c-Abl tyrosine kinase phosphorylation - a kinase otherwise reported to be increased in the hippocampal CA1 area of AD patients - prevents HDAC2 proteasomal degradation, thereby increasing its stabilization (Gonzalez-Zuniga et al., 2014). Thus, HDAC2 levels may be stabilized in the hippocampus at an early stage and stay somewhat elevated in the hippocampus of end-stage patients, when compared to HDAC1 levels for example. Such regulation may not occur in the frontal area. Further studies will be needed in order to determine whether these alterations are a result of the pathological progression or if they are associated with cell protective mechanisms.

HDAC3 levels were surprisingly not affected in AD brains. As observed for HDAC2, they may also have been increased at earlier stages of the disease as found in rodent AD models (Zhu et al., 2017; Janczura et al., 2018). HDAC3 is also involved in memory processes with participation of memory formation and extinction (McQuown et al., 2011; Alaghband et al., 2017).

Thus, at late stage of the disease, specific HDAC isoforms - such as HDAC1 - seem to be preferentially targeted for degradation, but their degree of alteration is region-specific and some compensatory mechanisms may take place. However, it is becoming clearer that HDAC levels are changing upon the pathological course of the disease, some of them being induced at early stages of AD. Most studies, however, agree that there is a significant decrease at later stages of the pathology for the majority of HDACs. This is also emphasized by recent in vivo PET studies showing an overall loss of class I HDAC activities in different cortices of AD patients (Pascoal et al., 2018), and our result point to HDAC1 as one of the mainly altered HDAC isoform. These observations call for caution in the use of HDAC inhibitors as therapeutics in late stage (symptomatic) AD patients, especially when used as systemic treatment (Narayan and Dragunow, 2010).-12pt

4.4. Different histones subcellular distribution in AD patient's brain

We found that the total level of both H3 and H2B histones was increased in the F2 area of the frontal cortex cells of AD patients. Narayan and colleagues previously showed a global histone (H3tot and H4tot) increase in inferior and middle temporal gyrus of AD patients (Narayan et al., 2015). In our study, after nuclear extraction, the levels of total histones were no longer increased in AD patients compared to controls (Fig. 5(A)), suggesting that the increased histone levels were associated with the cytoplasmic fraction (Fig. 5(C)) and pointing to a dysregulation in histone trafficking/catabolism in this brain region. Interestingly, Narayan and colleagues also showed an increase of H3 and H4 histones in the cytoplasm of inferior and middle temporal gyri of AD patients. They hypothesized that this increase could be a consequence of compromised degradation pathways during the disease, more particularly due to the ubiquitin-proteasome system impairment that potentially leads to the accumulation of non-degraded histones (Narayan et al., 2015). However, we cannot exclude that increased histone levels might be nuclear and that the nuclear envelop may show greater leakage in AD patients than in controls after long *post-mortem* delays. An old study showed that dinucleosomes and polymeric nucleosome structures were increased in isolated nuclei of neuronal fractions obtained from AD *post-mortem* brain tissues compared to a predominantly mononucleosome load in neurologically normal controls (Lewis et al., 1981). This study suggested that mononucleosomes are structurally more susceptible to internal degradation and, therefore, are rapidly digested into smaller entities in control brain. In the AD brain, the reduced clearance of these mononucleosome structures

may lead to the aberrant accumulation of polymeric nucleosomes as a consequence of reduced/compromised protein degradation pathways. Furthermore, anti-histones antibodies were found increased in serum of AD patients and a significant correlation was found between anti-histone serum titers and degree of dementia in the AD group, suggesting a global increase of histones in AD. Anti-histone antibodies increase can be due to the alteration of cell membrane fluidity and integrity, which facilitates the leakage of the histones to the serum (Mecocci et al., 1993). This histone leakage is known to be toxic to the surrounding cells and interestingly, it was found that histones bind with high affinity and specificity to the secreted amyloid protein precursor (sAPP) decreasing the histone cytotoxicity (Potempska et al., 1993; Currie et al., 1997).

However, H3tot may be decreased in the nucleus of frontal cortex as we found when analyzing nuclear extracts. Lithner and colleagues also reported a total histone decrease in Tg2576 mice (Lithner et al., 2013) and suggested that it could reflect a disruption of nucleosome turnover, which could affect nucleosome occupancy of chromatin and influence gene transcription (Deal et al., 2010; Wang et al., 2011). Altogether, these modifications of total histones in AD, whether nuclear or cytoplasmic, could have a strong impact on the 3D chromatin structure, gene transcription and pathology progression. Thus, future treatments should focus on a way to improve the turnover of histones in order to ensure their replacement and thus maintain the physiological transcriptional activity.

In conclusion, we report a strong disruption of some HAT / HDAC enzymes in brain of AD patients, particularly of the CBP HAT and the class I HDAC1. This is likely to modify the brain histone acetylation homeostasis at rest, but also the ability of the brain to respond to learning. However, histone acetylation was shown to be highly variable upon the post-mortem delays (Barrachina et al., 2012; Jarmasz et al., 2019). Interestingly, Jarmasz et al. (2019) showed that after death, histone acetylation loss occurred primarily in the nuclei of large neurons, while immunoreactivity in glial cell nuclei was relatively unchanged and increased H3 acetylation levels were observed in the F2 frontal area of AD patients (Fig. 5(C)) may be associated with glial cells. This also emphasizes the difficulty of interpreting studies obtained in whole (aged) tissues with some post-mortem delays.

To summarize, we showed a decrease of epigenetic enzymes (HDAC1, CBP) occurring concomitantly in two key structures of AD patients, the hippocampus and the frontal cortex. In these patients, the frontal cortex seemed more vulnerable as it was more severely altered than the hippocampus: PCAF and HDAC2 levels were further decreased, as was the total amount of nuclear histones. These changes may thus occur early in the pathology and drive neuronal plasticity and synaptic loss at very early stages of the disease. Moreover, these modifications may vary during the progression of the pathology (Mahady et al., 2018) in a structure-dependent manner. Our observations suggest that neuropsychological tests assessing complex cognitive functions relying on hippocampo-cortical interactions (such as long-term memory formation) could be routinely run in the aging population for more efficient diagnosis of AD.

Role of the funding source

This work was supported by the CNRS (UMR7364), the University of Strasbourg, ANR (ANR-12-MALZ-0002-01), France Alzheimer (AAP SM 2017 #1664), and the Alsace Alzheimer 67 association. IPdC is supported by France Alzheimer.

Contributors

OB and ALB designed the study. OB supervised the study. ES, OB and XLW performed the experiments. OB, IPdC and ALB analyzed and interpreted the data. OB, IPdC, JCC, FB and ALB wrote the manuscript.

Conflict of interest

All other authors declare that they have no conflicts of interest.

Acknowledgments

We would like to thank Joelle Son, Mireilla Peterson, Sarah Humbert-Levy and Kelly Louis (student interns) for their assistance in some experiments. We are grateful to *NeuroCEB* for their collaboration and for providing the brain samples. A consortium of the following patient's associations - ARSLA, CSC, Fondation ARSEP, Fondation Vaincre Alzheimer, France DFT, France Parkinson - is supporting the NeuroCEB brainbank. The NeuroCEB Neuropathology network includes: Franck Letournel (CHU Angers), Marie-Laure Martin-Négrier (CHU Bordeaux), Maxime Faisant (CHU Caen), Catherine Godfraind (CHU Clermont-Ferrand), Claude-Alain Maurage (CHU Lille), Vincent Deramecourt (CHU Lille), David Meyronnet (CHU Lyon), Nathalie Streichenberger (CHU Lyon), André Maues de Paula (CHU Marseille), Valérie Rigau (CHU Montpellier), Fanny Vandenbos-Burel (Nice), Charles Duyckaerts (CHU PS Paris), Danielle Seilhean (CHU PS, Paris), Susana Boluda (CHU PS, Paris), Isabelle Plu (CHU PS, Paris), Serge Milin (CHU Poitiers), Dan Christian Chiforeanu (CHU Rennes), Annie Laquerrière (CHU Rouen), Dr Béatrice Lannes (CHU Strasbourg). The laboratory is supported by CNRS, the University of Strasbourg, ANR-12-MALZ-0002-01 (ATACTAD), ANR-16-CE92-0031 (EPIFUS), France Alzheimer (AAP SM 2017 #1664) and Alsace Alzheimer 67. We also thank *FORNASEP* and the *Fondation Plan Alzheimer*, which financed Olivier Bousiges' salary for 2.5 years.

References

Alaghband, Y., Kwapis, J.L., Lopez, A.J., White, A.O., Aimiuwu, O.V., Al-Kachak, A., Bodinayake, K.K., Oparaugo, N.C., Dang, R., Astarabadi, M., Matheos, D.P., Wood, M.A., 2017. Distinct roles for the deacetylase domain of HDAC3 in the hippocampus and medial prefrontal cortex in the formation and extinction of memory. Neurobiol. Learn. Mem. 145, 94-104.

Alarcon, J.M., Malleret, G., Touzani, K., Vronskaya, S., Ishii, S., Kandel, E.R., Barco, A., 2004. Chromatin acetylation, memory, and LTP are impaired in CBP+/- mice: a model for the cognitive deficit in Rubinstein-Taybi syndrome and its amelioration. Neuron 42, 947-959.

Alberini, C.M., Kandel, E.R., 2014. The regulation of transcription in memory consolidation. Cold Spring Harb. Perspect. Biol. 7, a021741.

Anderson, K.W., Mast, N., Pikuleva, I.A., Turko, I.V., 2015. Histone H3 Ser57 and Thr58 phosphorylation in the brain of 5XFAD mice. FEBS Open Bio. 5, 550-556.

Aubry, S., Shin, W., Crary, J.F., Lefort, R., Qureshi, Y.H., Lefebvre, C., Califano, A., Shelanski, M.L., 2015. Assembly and interrogation of Alzheimer's disease genetic networks reveal novel regulators of progression. PLoS One 10, e0120352.

Bahari-Javan, S., Maddalena, A., Kerimoglu, C., Wittnam, J., Held, T., Bahr, M., Burkhardt, S., Delalle, I., Kugler, S., Fischer, A., Sananbenesi, F., 2012. HDAC1 regulates fear extinction in mice. J. Neurosci. 32, 5062-5073.

Barrachina, M., Moreno, J., Villar-Menendez, I., Juves, S., Ferrer, I., 2012. Histone tail acetylation in brain occurs in an unpredictable fashion after death. Cell Tissue Bank. 13, 597-606.

Barrett, R.M., Malvaez, M., Kramar, E., Matheos, D.P., Arrizon, A., Cabrera, S.M., Lynch, G., Greene, R.W., Wood, M.A., 2011. Hippocampal focal knockout of CBP affects specific histone modifications, long-term potentiation, and long-term memory. Neuropsychopharmacology 36, 1545-1556.

Bartolotti, N., Segura, L., Lazarov, O., 2016. Diminished CRE-induced plasticity is linked to memory deficits in familial Alzheimer's disease mice. J. Alzheimers Dis. 50, 477-489.

Brasnjevic, I., Hof, P.R., Steinbusch, H.W., Schmitz, C., 2008. Accumulation of nuclear DNA damage or neuron loss: molecular basis for a new approach to understanding selective neuronal vulnerability in neurodegenerative diseases. DNA Repair 7, 1087-1097.

Benito, E., Urbanke, H., Ramachandran, B., Barth, J., Halder, R., Awasthi, A., Jain, G., Capece, V., Burkhardt, S., Navarro-Sala, M., Nagarajan, S., Schutz, A.L., Johnsen, S.A., Bonn, S., Luhrmann, R., Dean, C., Fischer, A., 2015. HDAC inhibitor-dependent transcriptome and memory reinstatement in cognitive decline models. J. Clin. Invest. 125, 3572-3584.

Bie, B., Wu, J., Yang, H., Xu, J.J., Brown, D.L., Naguib, M., 2014. Epigenetic suppression of neuroligin 1 underlies amyloid-induced memory deficiency. Nat. Neurosci. 17, 223-231.

Bousiges, O., Neidl, R., Majchrzak, M., Muller, M.A., Barbelivien, A., Pereira de Vasconcelos, A., Schneider, A., Loeffler, J.P., Cassel, J.C., Boutillier, A.L., 2013. Detection of histone acetylation levels in the dorsal hippocampus reveals early tagging on specific residues of H2B and H4 histones in response to learning. PLoS One 8, e57816.

Bousiges, O., Vasconcelos, A.P., Neidl, R., Cosquer, B., Herbeaux, K., Panteleeva, I., Loeffler, J.P., Cassel, J.C., Boutillier, A.L., 2010. Spatial memory consolidation is associated with induction of several lysine-acetyltransferase (Histone acetyltransferase) expression levels and H2B/H4 acetylation-dependent transcriptional events in the rat hippocampus. Neuropsychopharmacology 35, 2521-2537.

Braak, H., Braak, E., 1995. Staging of Alzheimer's disease-related neurofibrillary changes. Neurobiol. Aging 16, 271-278.

Cacabelos, R., Carril, J.C., Cacabelos, N., Kazantsev, A.G., Vostrov, A.V., Corzo, L., Cacabelos, P., Goldgaber, D., 2019. Sirtuins in Alzheimer's disease: SIRT2-Related genophenotypes and implications for pharmacoepigenetics. Int. J. Mol. Sci. Mar. 12, 20-25.

Caccamo, A., Maldonado, M.A., Bokov, A.F., Majumder, S., Oddo, S., 2010. CBP gene transfer increases BDNF levels and ameliorates learning and memory deficits in a mouse model of Alzheimer's disease. Proc. Natl. Acad. Sci. U.S.A. 107, 22687-22692.

Cadena-del-Castillo, C., Valdes-Quezada, C., Carmona-Aldana, F., Arias, C., Bermudez-Rattoni, F., Recillas-Targa, F., 2014. Age-dependent increment of hydroxymethylation in the brain cortex in the triple-transgenic mouse model of Alzheimer's disease. J. Alzheimers Dis. 41, 845-854.

Campbell, R.R., Wood, M.A., 2019. How the epigenome integrates information and reshapes the synapse. Nat. Rev. Neurosci. 20, 133-147.

Chatterjee, S., Cassel, R., Schneider-Anthony, A., Merienne, K., Cosquer, B., Tzeplaeff, L., Halder Sinha, S., Kumar, M., Chaturbedy, P., Eswaramoorthy, M., Le Gras, S., Keime, C., Bousiges, O., Dutar, P., Petsophonsakul, P., Rampon, C., Cassel, J.C., Buee, L., Blum, D., Kundu, T.K., Boutillier, A.L., 2018. Reinstating plasticity and memory in a tauopathy mouse model with an acetyltransferase activator. EMBO Mol. Med. 10, pii: e8587.

Chen, G., Zou, X., Watanabe, H., van Deursen, J.M., Shen, J., 2010. CREB binding protein is required for both short-term and long-term memory formation. J. Neurosci. 30, 13066-13077.

Currie, J.R., Chen-Hwang, M.C., Denman, R., Smedman, M., Potempska, A., Ramakrishna, N., Rubenstein, R., Wisniewski, H.M., Miller, D.L., 1997. Reduction of histone cytotoxicity by the Alzheimer beta-amyloid peptide precursor. Biochim. Biophys. Acta 1355, 248-258.

Cutler, T., Sarkar, A., Moran, M., Steffensmeier, A., Puli, O.R., Mancini, G., Tare, M., Gogia, N., Singh, A., 2015. Drosophila eye model to study neuroprotective role of CREB binding protein (CBP) in Alzheimer's disease. PLoS One 10, e0137691.

De Jager, P.L., Yang, H.S., Bennett, D.A., 2018. Deconstructing and targeting the genomic architecture of human neurodegeneration. Nat. Neurosci. 21, 1310-1317.

Deal, R.B., Henikoff, J.G., Henikoff, S., 2010. Genome-wide kinetics of nucleosome turnover determined by metabolic labeling of histones. Science 328, 1161-1164.

Del Blanco, B., Guiretti, D., Tomasoni, R., Lopez-Cascales, M.T., Munoz-Viana, R., Lipinski, M., Scandaglia, M., Coca, Y., Olivares, R., Valor, L.M., Herrera, E., Barco, A., 2019. CBP and SRF co-regulate dendritic growth and synaptic maturation. Cell Death Differ. 11, 2208-2222.

Dignam, J.D., Lebovitz, R.M., Roeder, R.G., 1983. Accurate transcription initiation by RNA polymerase II in a soluble extract from isolated mammalian nuclei. Nucleic Acids Res. 11, 1475-1489.

Dobbin, M.M., Madabhushi, R., Pan, L., Chen, Y., Kim, D., Gao, J., Ahanonu, B., Pao, P.C., Qiu, Y., Zhao, Y., Tsai, L.H., 2013. SIRT1 collaborates with ATM and HDAC1 to maintain genomic stability in neurons. Nat. Neurosci. 16, 1008-1015.

Ettcheto, M., Abad, S., Petrov, D., Pedrós, I., Busquets, O., Sánchez-López, E., Casadesús, G., Beas-Zarate, C., Carro, E., Auladell, C., Olloquequi, J., Pallàs, M., Folch, J., Camins, A., 2017. Early preclinical changes in hippocampal CREB-Binding protein expression in a mouse model of familial Alzheimer's disease. Mol. Neurobiol. 55, 4885-4895.

Francis, Y.I., Fa, M., Ashraf, H., Zhang, H., Staniszewski, A., Latchman, D.S., Arancio, O., 2009. Dysregulation of histone acetylation in the APP/PS1 mouse model of Alzheimer's disease. J. Alzheimers Dis. 18, 131-139.

Gjoneska, E., Pfenning, A.R., Mathys, H., Quon, G., Kundaje, A., Tsai, L.H., Kellis, M., 2015. Conserved epigenomic signals in mice and humans reveal immune basis of Alzheimer's disease. Nature 518, 365-369.

Gonzalez-Zuniga, M., Contreras, P.S., Estrada, L.D., Chamorro, D., Villagra, A., Zanlungo, S., Seto, E., Alvarez, A.R., 2014. c-Abl stabilizes HDAC2 levels by tyrosine phosphorylation repressing neuronal gene expression in Alzheimer's disease. Mol. Cell 56, 163-173.

Graff, J., Mansuy, I.M., 2008. Epigenetic codes in cognition and behaviour. Behav. Brain Res. 192, 70-87.
Graff, J., Mansuy, I.M., 2009. Epigenetic dysregulation in cognitive disorders. Eur. J. Neurosci. 30, 1-8.
Graff, J., Rei, D., Guan, J.S., Wang, W.Y., Seo, J., Hennig, K.M., Nieland, T.J., Fass, D.M., Kao, P.F., Kahn, M., Su, S.C., Samiei, A., Joseph, N., Haggarty, S.J., Delalle, I., Tsai, L.H., 2012. An epigenetic blockade of cognitive functions in the neurodegenerating brain. Nature 483, 222-226.
Graff, J., Tsai, L.H., 2013. Histone acetylation: molecular mnemonics on the chromatin. Nat. Rev. Neurosci. 14, 97-111.
Guan, J.S., Haggarty, S.J., Giacometti, E., Dannenberg, J.H., Joseph, N., Gao, J., Nieland, T.J., Zhou, Y., Wang, X., Mazitschek, R., Bradner, J.E., DePinho, R.A., Jaenisch, R., Tsai, L.H., 2009. HDAC2 negatively regulates memory formation and synaptic plasticity. Nature 459, 55-60.
Gustafson, C.L., Partch, C.L., 2015. Emerging models for the molecular basis of mammalian circadian timing. Biochemistry 54, 134-149.
Jakovcevski, M., Bharadwaj, R., Straubhaar, J., Gao, G., Gavin, D.P., Jakovcevski, I., Mitchell, A.C., Akbarian, S, 2013. Prefrontal cortical dysfunction after overexpression of histone deacetylase 1. Biol. Psychiatry 74 (9), 696-705. doi:10.1016/j.biopsych.2013.03.020.
Janczura, K.J., Volmar, C.H., Sartor, G.C., Rao, S.J., Ricciardi, N.R., Lambert, G., Brothers, S.P., Wahlestedt, C., 2018. Inhibition of HDAC3 reverses Alzheimer's disease-related pathologies in vitro and in the 3xTg-AD mouse model. Proc. Natl. Acad. Sci. U.S.A. 20, 11148-11157.
Jarmasz, J.S., Stirton, H., Davie, J.R., Del Bigio, M.R., 2019. DNA methylation and histone post-translational modification stability in post-mortem brain tissue. Clin. Epigenetics 11, 5.
Korzus, E., Rosenfeld, M.G., Mayford, M., 2004. CBP histone acetyltransferase activity is a critical component of memory consolidation. Neuron 42, 961-972.
Kouzarides, T., 2007. Chromatin modifications and their function. Cell 128, 693-705.
Kozlov, S., Afonin, A., Evsyukov, I., Bondarenko, A., 2017. Alzheimer's disease: as it was in the beginning. Rev. Neurosci. 28, 825-843.
Kwapis, J.L., Alaghband, Y., Lopez, A.J., White, A.O., Campbell, R.R., Dang, R.T., Rhee, D., Tran, A.V., Carl, A.E., Matheos, D.P., Wood, M.A., 2017. Context and auditory fear are differentially regulated by HDAC3 activity in the lateral and basal subnuclei of the amygdala. Neuropsychopharmacology 42, 1284-1294.
LeBlanc, A.C., 2013. Caspase-6 as a novel early target in the treatment of Alzheimer's disease. Eur. J. Neurosci. 37, 2005-2018.
Leng, Y., Musiek, E.S., Hu, K., Cappuccio, F.P., Yaffe, K., 2019. Association between circadian rhythms and neurodegenerative diseases. Lancet Neurol. 18, 307-318.
Lewis, P.N., Lukiw, W.J., De Boni, U., McLachlan, D.R., 1981. Changes in chromatin structure associated with Alzheimer's disease. J. Neurochem. 37, 1193-1202.
Lipinski, M., Del Blanco, B., Barco, A., 2019. CBP/p300 in brain development and plasticity: disentangling the KAT's cradle. Curr. Opin. Neurobiol. 59, 1-8.
Lithner, C.U., Lacor, P.N., Zhao, W.Q., Mustafiz, T., Klein, W.L., Sweatt, J.D., Hernandez, C.M., 2013. Disruption of neocortical histone H3 homeostasis by soluble Abeta: implications for Alzheimer's disease. Neurobiol. Aging 34, 2081-2090.
Mahady, L., Nadeem, M., Malek-Ahmadi, M., Chen, K., Perez, S.E., Mufson, E.J., 2018. Frontal cortex epigenetic dysregulation during the progression of Alzheimer's disease. J. Alzheimers Dis. 62, 115-131.
Marques, S.C., Lemos, R., Ferreiro, E., Martins, M., de Mendonca, A., Santana, I., Outeiro, T.F., Pereira, C.M., 2012. Epigenetic regulation of BACE1 in Alzheimer's disease patients and in transgenic mice. Neuroscience 220, 256-266.
Mastroeni, D., Grover, A., Delvaux, E., Whiteside, C., Coleman, P.D., Rogers, J., 2011. Epigenetic mechanisms in Alzheimer's disease. Neurobiol. Aging 32, 1161-1180.
Maurice, T., Duclot, F., Meunier, J., Naert, G., Givalois, L., Meffre, J., Celerier, A., Jacquet, C., Copois, V., Mechti, N., Ozato, K., Gongora, C., 2008. Altered memory capacities and response to stress in p300/CBP-associated factor (PCAF) histone acetylase knockout mice. Neuropsychopharmacology 33, 1584-1602.
McQuown, S.C., Barrett, R.M., Matheos, D.P., Post, R.J., Rogge, G.A., Alenghat, T., Mullican, S.E., Jones, S., Rusche, J.R., Lazar, M.A., Wood, M.A., 2011. HDAC3 is a critical negative regulator of long-term memory formation. J. Neurosci. 31, 764-774.
Mecocci, P., Ekman, R., Parnetti, L., Senin, U., 1993. Antihistone and anti-dsDNA autoantibodies in Alzheimer's disease and vascular dementia. Biol. Psychiatry 34, 380-385.
Narayan, P., Dragunow, M., 2010. Pharmacology of epigenetics in brain disorders. Br. J. Pharmacol 159, 285-303.
Narayan, P.J., Lill, C., Faull, R., Curtis, M.A., Dragunow, M., 2015. Increased acetyl and total histone levels in post-mortem Alzheimer's disease brain. Neurobiol. Dis. 74, 281-294.
Nativio, R., Donahue, G., Berson, A., Lan, Y., Amlie-Wolf, A., Tuzer, F., Toledo, J.B., Gosai, S.J., Gregory, B.D., Torres, C., Trojanowski, J.Q., Wang, L.S., Johnson, F.B., Bonini, N.M., Berger, S.L., 2018. Dysregulation of the epigenetic landscape of normal aging in Alzheimer's disease. Nat. Neurosci. 21, 497-505.
Nott, A., Watson, P.M., Robinson, J.D., Crepaldi, L., Riccio, A., 2008. S-Nitrosylation of histone deacetylase 2 induces chromatin remodelling in neurons. Nature 455, 411-415.
Oliveira, A.M., Wood, M.A., McDonough, C.B., Abel, T., 2007. Transgenic mice expressing an inhibitory truncated form of p300 exhibit long-term memory deficits. Learn. Mem. 14, 564-572.
Pascoal, T.A., Chamoun, M., Shin, M., Benedet, A.L., Mathotaarachchi, S., Kang, M.S., Therriault, J., Savard, M., Thomas, E., Massarweh, G., Soucy, J.P., Gauthier, S., Rosa-Neto, P., 2018. Imaging epigenetics in the human brain with the novel [^{11}C]MARTINOSTAT PET in preclinical AD, MCI, AD, and frontotemporal dementia individuals. Alzheimer's Dement. 14, 9-10.
Potempska, A., Ramakrishna, N., Wisniewski, H.M., Miller, D.L., 1993. Interaction between the beta-amyloid peptide precursor and histones. Arch. Biochem. Biophys. 304, 448-453.
Rao, J.S., Keleshian, V.L., Klein, S., Rapoport, S.I., 2012. Epigenetic modifications in frontal cortex from Alzheimer's disease and bipolar disorder patients. Transl. Psychiatry 2, e132.
Rouaux, C., Jokic, N., Mbebi, C., Boutillier, S., Loeffler, J.P., Boutillier, A.L., 2003. Critical loss of CBP/p300 histone acetylase activity by caspase-6 during neurodegeneration. EMBO J. 22, 6537-6549.
Saha, R.N., Pahan, K., 2006. HATs and HDACs in neurodegeneration: a tale of disconcerted acetylation homeostasis. Cell Death Differ. 13, 539-550.
Schneider, A., Chatterjee, S., Bousiges, O., Selvi, B.R., Swaminathan, A., Cassel, R., Blanc, F., Kundu, T.K., Boutillier, A.L., 2013. Acetyltransferases (HATs) as targets for neurological therapeutics. Neurotherapeutics 10, 568-588.
Sharma, R.P., Grayson, D.R., Gavin, D.P, 2008. Histone deactylase 1 expression is increased in the prefrontal cortex of schizophrenia subjects: analysis of the National Brain Databank microarray collection. Schizophr. Res. 98 (1-3), 111-117.
Shu, G., Kramar, E.A., Lopez, A.J., Huynh, G., Wood, M.A., Kwapis, J.L., 2018. Deleting HDAC3 rescues long-term memory impairments induced by disruption of the neuron-specific chromatin remodeling subunit BAF53b. Learn. Mem. 25, 109-114.

General Discussion and Perspectives

General Discussion and Perspectives

Overview

In this thesis we focussed on the question whether *Bmal1* affects microglial functions during different situations, and what is the final effect of microglial *Bmal1* deficiency on memory formation and energy homeostasis in mice. In addition, we investigated the impact of SR9011, an agonist of Rev-erbα, and a high-fat diet (HFD) on the microglial immunometabolic functions. Finally, we evaluated gliosis and epigenetic changes in the frontal cortex and hippocampus of post-mortem brains from Alzheimer's disease patients. In *Publication* 1, we found that in mice *Bmal1* deficiency robustly enhances the microglial phagocytic capacity under HFD conditions and during cognitive processes. This enhancement was associated with a reduced loss of POMC neurons in the hypothalamus when mice were fed a HFD, and also related to the formation of more mature spines in the hippocampus during the learning process. As a result, mice with microglia lacking *Bmal1* not only exhibited decreased HFD-induced hyperphagia and body weight gain, but also showed improved long-term memory consolidation and retention. In *Publication* 2, we observed that *Bmal1* deficiency in microglial BV-2 cells decreases gene expression of pro-inflammatory cytokines, increases gene expression of anti-oxidative and anti-inflammatory factors, and increases phagocytic capacity in microglia. These changes protect the microglial BV-2 cells from LPS and palmitic acid-induced inflammation. Moreover, the lack of *Bmal1* facilitated microglial BV-2 cells to adjust their nutrient utilization to increased energy demand. In *Publication* 3, we found that disruption of circadian rhythmicity by the administration of the Rev-erbα agonist SR9011, reduced pro-inflammatory cytokine expression in primary microglial cells during an immune challenge by TNFα, while it increased expression of the anti-inflammatory cytokine IL10. Moreover, SR9011 decreased phagocytic activity, mitochondrial respiration, ATP production, and metabolic gene expression. In *Publication* 4, we observed a disturbance in the daily rhythm of microglial circadian and inflammatory gene expression during obesogenic conditions, accompanied by changes in substrate utilization and energy production. The obesogenic diet affected microglial immunometabolism in a time-of-day dependent manner. Lastly, in *Publication* 5, we found gliosis and acetylation dysfunctions in AD brains that may underlie the AD-related cognitive impairments. Our results further pointed to stronger dysregulations in the F2 area of the frontal cortex than in the hippocampus at an end-stage of the disease.

1. The role of *Bmal1* in the microglial clock machinery

Bmal1 is a key clock gene and plays an important role in the core clock machinery that is based on a number of autoregulatory transcriptional/translational feedback loops. The Bmal1/Clock complex promotes gene expression of the *Per1*, *Per2*, *Cry1*, *Cry2*, *Nr1d1*, and *Dbp* genes. The Per/Cry complex negatively regulates its own transcription by inhibiting the activity of the Bmal1/Clock complex and Nr1d1 suppresses the expression of *Bmal1* (Dudek and Meng, 2014). However, it was still unknown whether these clock genes also follow a daily rhythm in microglial cells, and how *Bmal1* affects the microglial clock machinery.

In this study, we observed that the expression of the clock genes *Bmal1*, *Clock, Per1*, *Per2*, *Cry1*, *Cry2*, *Nr1d1*, and *Dbp* follow a daily rhythm in isolated microglia from C57BL/6J mice; peak expression of *Bmal1* was found during the light phase. *Bmal1* knock-out from microglia, such as in microglial BV-2 cells, in global Bmal1-KO mice, or specifically in microglia, resulted in a significantly increased expression of the *Bmal1* negatively controlled genes -*Cry1*, *Cry2*, and *Per2*. Experiments in microglial BV-2 cells also showed that the rhythmic expression of *Bmal1* was disturbed in the *Bmal1* knock-down group, but *Clock*, *Cry1*, *Per1*, *Per2*, *Nr1d1*, and *Dbp* still showed rhythmic expression. These results indicate that the deletion of *Bmal1* disturbs the core clock machinery in microglia, as previously also shown in astrocytes (Barca-Mayo et al., 2017). These findings suggest that lacking *Bmal1* in microglia may lead to a profound influence on microglial metabolism and functions.

2. The role of *Bmal1* in microglial metabolism

In a previous study we showed that microglia are more active during the dark phase when mice are awake as compared with the light phase when mice are mainly resting (Yi et al., 2017b). Microglial activity highly depends on cellular metabolism (Gao et al., 2017b). Moreover, microglial activation leads to the production of more metabolites and reactive oxygen species (ROS) (Ding et al., 2017; Rojo et al., 2014), which need to be eliminated to maintain proper microglia functioning (McLoughlin et al., 2019; Piantadosi et al., 2011; Poss and Tonegawa, 1997). In *Publication* 2, we observed that the nutrient utilization and the anti-oxidative effects follow a daily rhythm in microglial cells, with a peak during the dark phase, in line with microglial activity. Bmal1 serves as a transcription factor and belongs to the bHLH family. Except for regulation of the clock machinery, Bmal1 controls 10%-43% of other genes expressed in cells or tissues, via binding to specific regulatory elements in their promoters (Duffield, 2003; Reppert and Weaver, 2002; Sato et al., 2004; Zhang et al., 2014b). We found that in normal conditions, there is a decreased nutrient utilization in isolated microglia from global *Bmal1* KO mice. Specific muscle Bmal1 knockout mice also show reduced

glucose uptake in normal physiological conditions (Schiaffino et al., 2016). During the immune response, there is a high energy demand in immune cells (Geltink et al., 2018; Wang et al., 2019b). We also observed an increased glucose uptake after LPS administration, which was more significant in *Bmal1* deficient microglial BV-2 cells. It could be that the clock gene-transcriptional regulators cooperate with other factors to control the expression of target metabolic genes. For example, Rev-erbα regulates metabolic genes by recruiting the histone deacetylase 3 co-repressor to specific sites in the liver (Zhang et al., 2015). Bmal1 and Cry1/2 regulate anaerobic glycolysis and mitochondrial respiration via interaction with hypoxia-inducible factor 1α in skeletal muscle (Peek et al., 2017). Cry proteins also suppress signaling downstream of the glucagon receptor, thereby leading to a time-of-day-specific effect of glucagon on gluconeogenesis (Zhang et al., 2010). Similarly, Nr1d1 interacts with HNF6 to regulate lipid metabolism in adult mouse liver (Zhang et al., 2016b). Moreover, we found that *Bmal1* deficiency increases anti-oxidant gene expression in microglia in physiological conditions in mice and protects microglial BV-2 cells from LPS and palmitic acid-induced oxidative stress. Yet, neuronal Bmal1 deletion causes oxidative damage and impaired expression of the redox defense genes; Bmal1 deficient macrophages show an increased ROS accumulation, suggesting that the effect of Bmal1 on oxidative stress is different in different kind of cells (Early et al., 2018a; Musiek et al., 2013a).

Taken together, these findings suggest that Bmal1 plays an important role in microglial metabolism, and may have a profound influence on microglial functions.

3. The role of *Bmal1* in microglial functions in different situations

Microglia are highly motile resident immune cells and provide a surveillance and scavenging function in the CNS (Davalos et al., 2005). The main functions of microglia are related to immune response and phagocytosis, which play an important role in maintaining optimal brain function. Upon stimulation, microglia polarize into a pro-inflammatory (M1) or an anti-inflammatory (M2) phenotype, leading to neurotoxic and neuroprotective effects, respectively (Subhramanyam et al., 2019b).

a) Immune response

In *Publication* 2, we found that microglial inflammatory cytokine genes show higher expression during the light phase in wild-type mice in normal physiological conditions. This effect was also shown in a rat study (Fonken et al., 2015a). Moreover, it has been shown that LPS-treated rodents show increased sickness behavior and proinflammatory response during the light

phase as compared to the dark phase (Bellet et al., 2013; Fonken et al., 2015a). These findings suggest that microglia have a higher innate immune activity during the light phase, which is consistent with microglial *Bmal1* expression in mice under light/dark conditions. Thus, we evaluated gene expression of inflammatory cytokines in *Bmal1* knockout microglia isolated from global *Bmal1* KO mice, after *Bmal1* knockdown in microglial BV-2 cells, and from microglia$^{Bmal1\text{-KD}}$ mice in normal conditions. Lacking *Bmal1* decreased pro-inflammatory gene expression and increased anti-inflammatory gene expression in microglial cells, both *in vivo* and *in vitro*. These changes protect microglial BV-2 cells from LPS and palmitic acid-induced inflammation.

It has been shown that Bmal1 directly regulates *Il6* transactivation in microglia (Nakazato et al., 2017), while in macrophages, Bmal1 regulates inflammation via regulating the gene expression of *Nrf2* (Ma, 2013). *Bmal1* deletion from myeloid cells protects against bacterial infection in the lung (Kitchen et al., 2020a). These data suggest that Bmal1 regulates the innate immune system. Furthermore, we observed that *Cry1*, *Cry2*, and *Per2* are significantly increased in *Bmal1* KO microglia, which may contribute to the reduced inflammation. It has been observed that overexpression of Cry1 significantly decreases inflammation in atherosclerotic mice (Yang et al., 2015), whereas the absence of Cry1 and Cry2 leads to increased pro-inflammatory cytokine expression in macrophages (Narasimamurthy et al., 2012). *Per2* negatively regulates the expression of pro-inflammatory cytokines in zebrafish (Ren et al., 2018). Deletion of Rev-erbα causes increased expression of pro-inflammatory genes in microglia, whereas its pharmacological agonist inhibits LPS-stimulated inflammation (Gibbs et al., 2012; Griffin et al., 2019). Another mechanism for circadian gating of inflammation could be that Bmal1 recruits the glucocorticoid receptor to promoters of inflammatory genes (Gibbs et al., 2014). We observed a higher glucose uptake after LPS administration in *Bmal1* deficient microglial BV-2 cell as compared to control cells, which may also contribute to its anti-inflammatory phenotype. These findings suggest that *Bmal1* is one of the key regulators in microglial immunometabolism. Microglial *Bmal1* deletion might be a new strategy to treat inflammation in the brain.

b) Phagocytic capacity

Moreover, we found that the deletion of *Bmal1* increases the phagocytic capacity of microglial BV-2 cells. Microglia play an important role in the maintenance of a healthy microenvironment in the brain by phagocytosis. Thus, we further evaluated in mice the effect of lacking *Bmal1* on microglial phagocytic capacity in the hypothalamus after receiving a HFD and in the

hippocampus after learning. We found that *Bmal1* deficiency robustly enhances microglial phagocytic capacity under HFD conditions and during cognitive processes in mice. A recent study showed a circadian variation of microglial phagocytosis in rats, with phagocytosis of more synapses at the onset of the light phase than at the onset of the dark phase (Choudhury et al., 2020a). The deletion of *Bmal1* also increased phagocytic function in macrophages (Kitchen et al., 2020b).

Microglial phagocytic capacity depends on specific neuronal activity and the rate of neuronal attrition (Ayata et al., 2018a). When mice need to cope with HFD-induced metabolic stress or with learning tasks, neural circuits involved in these challenges require on-demand microglial phagocytosis (Ayata et al., 2018a). Therefore, suppressing the rigorous control of the circadian clock may exert a beneficial impact on microglial function. Knocking down *Bmal1* increases the flexibility of microglia and maintains a healthier microenvironment for the surrounding neurons in both the hypothalamus and hippocampus. Moreover, we noticed that *Bmal1* deficiency reduces microglial inflammation, which was also reported in a previous study (Nakazato et al., 2017), supporting that *Bmal1* deficiency shifts microglia to an anti-inflammatory state with increased phagocytic capacity.

Microglia are responsible for the elimination of apoptotic cells and cellular debris, as well as for regulation of synaptic remodeling to optimize the microenvironment for neuronal survival and functioning (Ayata et al., 2018a; Colonna and Butovsky, 2017; Nimmerjahn et al., 2005; Paolicelli et al., 2011b). HFD leads to hypothalamic POMC neuronal loss. By further exploring the phagosome content in hypothalamic microglia after HFD feeding, we observed more phagosomes containing DNA fragments in female than male microglia. This finding suggests that HFD leads to more neuronal loss in female mice than male mice. Microglia phagocytose presynaptic structures to remodel neural circuitries. By evaluating the phagosome content in hippocampal microglia, we found that learning increases the phagocytosis of presynapses, although *Bmal1* deficient microglia still phagocytose more cellular debris than presynapses during learning processes. All these findings suggest that *Bmal1* deficient microglia phagocytose more cellular debris than Bmal1-intact microglia during metabolic stress and synaptic plasticity processes.

4. The role of microglial *Bmal1* in the learning and memory process

Microglia not only engulf presynapses, but also help postsynaptic formation during synaptic remodeling (Wang et al., 2020a). The ablation of microglia reduces the formation of mature

synapses (Miyamoto et al., 2016b; Parkhurst et al., 2013). Deficient synaptic pruning results in impaired functional brain connectivity and deficits in social behavior (Filipello et al., 2018). Thus, we evaluated hippocampo-dependent memory formation and consolidation in microglia$^{Bmal1\text{-KD}}$ mice and WT control mice. We found that microglia$^{Bmal1\text{-KD}}$ mice show better performance in three different MWM tasks (a 4-day-training session to investigate long-term memory (24 h), a mild 3-day-training to evaluate long-term memory consolidation (15 days), and a reversal test to verify the cognitive flexibility (24 h)) and the novel object recognition test. We observed that microglia$^{Bmal1\text{-KD}}$ mice have more mature spines on CA1 pyramidal neurons during the memory consolidation process. Knocking down *Bmal1* may facilitate microglia to adjust their activity state according to the demand, in that way providing a healthier microenvironment and increased memory performance in mice. It is also known that the microglial clock-controlled gene *Cats* regulates synaptic strength and locomotor activity in mice (Hayashi et al., 2013). In addition, a recent finding in global Bmal1 knockout mice showed that locomotor activity and insulin sensitivity of those knockout mice adapt more readily to a disrupted light/dark schedules (Yang et al., 2019). However, increased synaptic elimination could also lead to impaired cognition, such as Alzheimer's disease (AD) (Merlini et al., 2019; Rajendran and Paolicelli, 2018), and schizophrenia (Sekar et al., 2016; Wang et al., 2019c). Therefore, establishing appropriate microglial phagocytic capacity is crucial for synaptic pruning and the formation of mature neural circuits.

5. The role of microglial *Bmal1* in metabolic regulation

Microglial Bmal1 deficient mice showed a reduced loss of POMC neurons after feeding a HFD. As a result, mice with microglia lacking *Bmal1* exhibit less HFD-induced hyperphagia and body weight gain. Growing evidence has shown that HFD-induced obesity is associated with hypothalamic gliosis and microglia inflammation in both humans and rodents (Andre et al., 2017; De Souza et al., 2005; Kalin et al., 2015; Valdearcos et al., 2017a). We recently reported that in a hypercaloric environment, optimal microglial phagocytic capacity is essential to maintain a healthy microenvironment for surrounding neuronal survival and functioning (Gao et al., 2017a). When mice need to cope with HFD-induced metabolic stress, neural circuits involved in these challenges require on-demand microglial phagocytosis (Ayata et al., 2018a). Therefore, manipulating microglial phagocytosis could be an effective way to treat HFD-induced metabolic diseases.

6. The role of Rev-erbα in microglial immunometabolism

Rev-erbα is a circadian clock gene, which can fine-tune *Bmal1* gene expression and also regulate circadian rhythms, metabolic homeostasis, and inflammation (Delezie and Challet, 2011; Forman et al., 1994; Ko and Takahashi, 2006; Lo et al., 2016). For instance, the deletion of the *Rev-erbα* gene leads to diet-induced obesity and alters glucose and lipid metabolism, which makes mice more prone to become diabetic (Delezie et al., 2012). Administration of the Rev-erbα agonist SR9011 disrupted circadian rhythms, and attenuated phagocytosis and the pro-inflammatory response of microglia. SR9011 also decreased microglial mitochondrial respiration and metabolic gene expression. It has been reported that Rev-erbα deletion leads to microgliosis, increased phagocytosis, and neuroinflammation in the hippocampus. Consistent with these results, we activated Rev-erbα and found a decreased pro-inflammatory response and phagocytosis. Besides, SR9011 stimulated the expression of the anti-inflammatory cytokine IL10. It is known that Rev-erbα regulates metabolic homeostasis in cancer cells. In *Publication* 3 we show that Rev-erbα controls cell metabolism in microglia resulting in a decrease in mitochondrial respiration and ATP production, as well as decreased expression of rate-limiting enzymes such as Cpt1, Pdk1, and Hk2 in response to SR9011. This study pointed out how the Rev-erbα-associated clock machinery interacts with immunometabolism in microglia. The decline in energy metabolism may be a consequential phenomenon caused by less energy demand due to the attenuated pro-inflammatory response or a direct effect of Rev-erbα on cellular metabolism.

7. The effect of diet-induced obesity on the microglial immunometabolism

Under physiological conditions, microglial cells exert their function in a strict time-of-day dependent manner with higher activity during the dark and active phase, compared to the light and sleep phase in rodents. But, this daily rhythm is abolished in animals fed a HFD, suggesting an interaction of diet content and daily rhythms in microglia. Recent evidence showed the involvement of the circadian timing system in the progression of obesity. We found that the daily rhythm of microglial immune gene expression was disrupted in HFD-induced obese rats. Microglia responded to the obesogenic conditions by a shift of substrate utilization with decreased glutamate and glucose metabolism in the active period of the animals, and an overall increase of lipid metabolism, as indicated by gene expression evaluation. The glutamate pathway is involved in macrophage immune function, *e.g.*, glutamine availability was shown to modulate macrophage phagocytic capacity, while α-ketoglutarate, generated through glutaminolysis, is crucial in eliciting an anti-inflammatory phenotype in macrophages. The increase in fatty acid sensing and synthesis at the beginning of the light period under obesogenic conditions, suggests more lipid utilization in microglia

during the sleep phase in obese rats. It has been shown that fatty acid treatment of BV-2 cells results in a potent induction of cytokine production via TLR4 signaling, thus leading to low-grade inflammation even in the absence of an immune challenge. This increased lipid metabolism could be an explanation for the constant activation of hypothalamic microglia under HFD. Additionally, immune cell activation requires higher energy production. Results from mitochondria bioenergetics and dynamics suggested an increased energy production in microglia during the inactive period during HFD conditions, suggesting an increase in ATP production, which could be explained by the increased lipid metabolism demand.

8. The role of neuroinflammation and dysregulation of histone acetylation in Alzheimer's disease

Microglia are the brain's resident macrophages with immune-modulating and phagocytic capabilities. Brain cell-type-specific enhancer-promoter interactome maps reveal an extended microglial gene network in Alzheimer's disease (Nott et al., 2019). Microglia play an important role in the regulation of synaptic plasticity and its activation-induced neuroinflammation contributes to memory impairment in Alzheimer's disease. Microglial activation follows Aβ deposition but precedes tau pathology and cognitive decline (Felsky et al., 2019). Moreover, histone acetylation is a key player in memory processes and in regulating the neuroprotection/neurodegeneration balance. Epigenetic enzymes such as the histone acetyltransferases (HATs), CREB-binding protein (CBP), P300, and p300/CBP-associated factor, as well as histone deacetylases (HDACs), such as HDAC1 and HDAC2, are also associated with long-term memory mechanisms. We found increased gliosis and reduced CBP and HDAC1 expression in the frontal cortex and hippocampus in post-mortem brains from Alzheimer's disease patients. CBP is a circadian clock regulator via the formation of a complex with Clock (Gustafson and Partch, 2015), thus severe CBP loss could also contribute to the circadian rhythm disturbances observed in AD patients (Leng et al., 2019). Notably, Aβ-mediated CBP degradation in AD mice was shown in the context of circadian rhythm disruption (Song et al., 2015). The total and acetylated histone levels are dysregulated in the frontal cortex of Alzheimer's disease patients. Our results further indicate that the frontal cortex is more vulnerable, as it was more severely altered than the hippocampus at an end-stage of the disease, suggesting a differential vulnerability and/or efficiency of compensatory mechanisms. The dramatic changes observed in the frontal cortex are likely associated with the severe loss in neuronal plasticity and synaptic functions.

Perspectives

1. Further validation of Bmal1 for microglial functions

Our data show that *Bmal1* has a profound influence on microglial immune response and phagocytosis. *Bmal1* deficiency leads to reduced expression of pro-inflammatory genes, increased expression of anti-inflammatory genes, and improved phagocytic capacity of microglia in both *in vivo* and *in vitro* experiments. These effects eventually protect mice from HFD-induced obesity and increase memory performance. However, it is still unclear how Bmal1 regulates the microglial immune response in mice. Chip-sequencing analysis will be needed to identify the DNA that interacts with Bmal1 in microglia under inflammation, such as LPS-treated mice. We also will need to perform RNA-sequencing to define the mechanism that induces phagocytosis in microglia lacking *Bmal1* and isolated from specific brain regions. For example, we will isolate microglia from the hippocampus of Ctrl and microglia$^{Bmal1\text{-KD}}$ mice with or without MWM training at a specific time point (total 4 groups). We also will isolate microglia from the hypothalamus of Ctrl and microglia$^{Bmal1\text{-KD}}$ mice, both males and females, with a chow or HFD fed at a specific time point (total 8 groups).

Moreover, *Bmal1* knockdown also affected cellular metabolism related to microglial functions. More *in vitro* experiments will need to be done in *Bmal1* deficient microglia, measuring inflammatory cytokine levels in combination with mitochondrial fuel utilization, to further understand the mechanisms involved.

2. Determine the mechanism of cross-talk between microglia and neurons in microglia$^{Bmal1\text{-KD}}$ and SR9011 treated mouse model

In the current thesis, we showed that *Bmal1* deficiency enhances the microglial phagocytic capacity, which may be associated with reduced neuronal loss in the hypothalamus when mice are fed a HFD, and formation of more mature spines in the hippocampus during the learning process. Thereby, microglial *Bmal1* deficiency protects mice from HFD-induced obesity and increases memory performance. On the other hand, disturbance of the microglial molecular clock with SR9011 attenuated the phagocytosis and the pro-inflammatory response of microglia. However, the mechanism linking microglia clock disturbance and postsynaptic spine maturation and formation of neuronal circuits is still unknown, both with regard to *Bmal1* deficiency and SR9011 treatment. We will isolate neurons from the hippocampal CA1 region to perform RNA-sequencing or extract synaptic proteins (Aono et al., 2017) to localize interesting molecular changes in both animal models.

Microglial functioning affects the survival of surrounding neurons by determining the functioning, neuronal cell number, and specific units (such as pre- or post-synapse) in the different brain regions (Tan et al., 2019). For example, in the striatum, the spine density of striatal medium spiny neurons is checked, which are involved in regulating motor activity, mood, and reward (Ayata et al., 2018a). Therefore, specific phenotype changes should be evaluated according to the neuronal morphology changes in a specific brain region in microglial *Bmal1* knockout mice.

3. Further examination of the cognitive performance in microglia$^{Bmal1\text{-KD}}$ and SR9011 treated mouse model under different conditions

Microglia are involved in neuroinflammation, neurodegeneration, neuropsychiatry, and diet-induced obesity. Studies have shown that the long-term intake of high-fat high-sugar diets impairs cognition dependent on the hippocampus and surrounding cortex in both rodents and humans, which may be mediated by oxidative stress, neuroinflammation, as well as decreased levels of neurotrophic factors (Morris et al., 2015). Age and age-related neurodegenerative diseases lead to neuroinflammation and neuronal structural changes, such as loss of dendritic spines, a decreased number of axons, an increase in axons with segmental demyelination, and a significant loss of synapses and neurons (Hickman et al., 2018b; Norden and Godbout, 2013; Pannese, 2011; Sveinbjornsdottir, 2016). Thus, future work should evaluate microglial function and cognition in *Bmal1* knockout and SR9011 treated mice under different conditions, such as challenges with HFD, systemic inflammation, aging, and aging-related neurodegenerative diseases, i.e. Alzheimer's disease (AD), Parkinson's disease (PD), and Multiple sclerosis (MS).

References

Andre, C., Guzman-Quevedo, O., Rey, C., Remus-Borel, J., Clark, S., Castellanos-Jankiewicz, A., Ladeveze, E., Leste-Lasserre, T., Nadjar, A., Abrous, D.N.*, et al.* (2017). Inhibiting Microglia Expansion Prevents Diet-Induced Hypothalamic and Peripheral Inflammation. Diabetes *66*, 908-919.

Aono, H., Choudhury, M.E., Higaki, H., Miyanishi, K., Kigami, Y., Fujita, K., Akiyama, J., Takahashi, H., Yano, H., Kubo, M.*, et al.* (2017). Microglia may compensate for dopaminergic neuron loss in experimental Parkinsonism through selective elimination of glutamatergic synapses from the subthalamic nucleus. Glia *65*, 1833-1847.

Ayata, P., Badimon, A., Strasburger, H.J., Duff, M.K., Montgomery, S.E., Loh, Y.E., Ebert, A., Pimenova, A.A., Ramirez, B.R., Chan, A.T.*, et al.* (2018). Epigenetic regulation of brain region-specific microglia clearance activity. Nat Neurosci *21*, 1049-1060.

Barca-Mayo, O., Pons-Espinal, M., Follert, P., Armirotti, A., Berdondini, L., and De Pietri Tonelli, D. (2017). Astrocyte deletion of Bmal1 alters daily locomotor activity and cognitive functions via GABA signalling. Nat Commun *8*, 14336.

Bellet, M.M., Deriu, E., Liu, J.Z., Grimaldi, B., Blaschitz, C., Zeller, M., Edwards, R.A., Sahar, S., Dandekar, S., Baldi, P.*, et al.* (2013). Circadian clock regulates the host response to Salmonella. Proc Natl Acad Sci U S A *110*, 9897-9902.

Choudhury, M.E., Miyanishi, K., Takeda, H., Islam, A., Matsuoka, N., Kubo, M., Matsumoto, S., Kunieda, T., Nomoto, M., Yano, H.*, et al.* (2020). Phagocytic elimination of synapses by microglia during sleep. Glia *68*, 44-59.

Colonna, M., and Butovsky, O. (2017). Microglia Function in the Central Nervous System During Health and Neurodegeneration. Annu Rev Immunol *35*, 441-468.

Davalos, D., Grutzendler, J., Yang, G., Kim, J.V., Zuo, Y., Jung, S., Littman, D.R., Dustin, M.L., and Gan, W.B. (2005). ATP mediates rapid microglial response to local brain injury in vivo. Nat Neurosci *8*, 752-758.

De Souza, C.T., Araujo, E.P., Bordin, S., Ashimine, R., Zollner, R.L., Boschero, A.C., Saad, M.J., and Velloso, L.A. (2005). Consumption of a fat-rich diet activates a proinflammatory response and induces insulin resistance in the hypothalamus. Endocrinology *146*, 4192-4199.

Delezie, J., and Challet, E. (2011). Interactions between metabolism and circadian clocks: reciprocal disturbances. Year in Diabetes and Obesity *1243*, 30-46.

Delezie, J., Dumont, S., Dardente, H., Oudart, H., Grechez-Cassiau, A., Klosen, P., Teboul, M., Delaunay, F., Pevet, P., and Challet, E. (2012). The nuclear receptor REV-ERB alpha is required for the daily balance of carbohydrate and lipid metabolism. Faseb Journal *26*, 3321-3335.

Ding, X.Y., Zhang, M., Gu, R.P., Xu, G.Z., and Wu, H.X. (2017). Activated microglia induce the production of reactive oxygen species and promote apoptosis of co-cultured retinal microvascular pericytes. Graef Arch Clin Exp *255*, 777-788.

Dudek, M., and Meng, Q.J. (2014). Running on time: the role of circadian clocks in the musculoskeletal system. Biochem J *463*, 1-8.

Duffield, G.E. (2003). DNA microarray analyses of circadian timing: the genomic basis of biological time. J Neuroendocrinol *15*, 991-1002.

Early, J.O., Menon, D., Wyse, C.A., Cervantes-Silva, M.P., Zaslona, Z., Carroll, R.G., Palsson-McDermott, E.M., Angiari, S., Ryan, D.G., Corcoran, S.E.*, et al.* (2018). Circadian clock protein BMAL1 regulates IL-1 beta in macrophages via NRF2. P Natl Acad Sci USA *115*, E8460-E8468.

Felsky, D., Roostaei, T., Nho, K., Risacher, S.L., Bradshaw, E.M., Petyuk, V., Schneider, J.A., Saykin, A., Bennett, D.A., and De Jager, P.L. (2019). Neuropathological correlates and genetic architecture of microglial activation in elderly human brain. Nature Communications *10*.

Filipello, F., Morini, R., Corradini, I., Zerbi, V., Canzi, A., Michalski, B., Erreni, M., Markicevic, M., Starvaggi-Cucuzza, C., Otero, K.*, et al.* (2018). The Microglial Innate Immune Receptor TREM2 Is Required for Synapse Elimination and Normal Brain Connectivity. Immunity *48*, 979-+.

Fonken, L.K., Frank, M.G., Kitt, M.M., Barrientos, R.M., Watkins, L.R., and Maier, S.F. (2015). Microglia inflammatory responses are controlled by an intrinsic circadian clock. Brain Behav Immun *45*, 171-179.

Forman, B.M., Chen, J., Blumberg, B., Kliewer, S.A., Henshaw, R., Ong, E.S., and Evans, R.M. (1994). Cross-Talk among Ror-Alpha-1 and the Rev-Erb Family of Orphan Nuclear Receptors. Mol Endocrinol *8*, 1253-1261.

Gao, Y., Vidal-Itriago, A., Kalsbeek, M.J., Layritz, C., Garcia-Caceres, C., Tom, R.Z., Eichmann, T.O., Vaz, F.M., Houtkooper, R.H., van der Wel, N.*, et al.* (2017a). Lipoprotein Lipase Maintains Microglial Innate Immunity in Obesity. Cell Rep *20*, 3034-3042.

Gao, Y.Q., Vidal-Itriago, A., Kalsbeek, M.J., Layritz, C., Garcia-Caceres, C., Tom, R.Z., Eichmann, T.O., Vaz, F.M., Houtkooper, R.H., van der Wel, N.*, et al.* (2017b). Lipoprotein Lipase Maintains Microglial Innate Immunity in Obesity. Cell Reports *20*, 3034-3042.

Geltink, R.I.K., Kyle, R.L., and Pearce, E.L. (2018). Unraveling the Complex Interplay Between T Cell Metabolism and Function. Annual Review of Immunology, Vol 36 *36*, 461-488.

Gibbs, J., Ince, L., Matthews, L., Mei, J., Bell, T., Yang, N., Saer, B., Begley, N., Poolman, T., Pariollaud, M.*, et al.* (2014). An epithelial circadian clock controls pulmonary inflammation and glucocorticoid action. Nat Med *20*, 919-926.

Gibbs, J.E., Blaikley, J., Beesley, S., Matthews, L., Simpson, K.D., Boyce, S.H., Farrow, S.N., Else, K.J., Singh, D., Ray, D.W.*, et al.* (2012). The nuclear receptor REV-ERB alpha mediates circadian regulation of innate immunity through selective regulation of inflammatory cytokines. P Natl Acad Sci USA *109*, 582-587.

Griffin, P., Dimitry, J.M., Sheehan, P.W., Lananna, B.V., Guo, C., Robinette, M.L., Hayes, M.E., Cedeno, M.R., Nadarajah, C.J., Ezerskiy, L.A.*, et al.* (2019). Circadian clock protein Rev-erba regulates neuroinflammation. P Natl Acad Sci USA *116*, 5102-5107.

Hayashi, Y., Koyanagi, S., Kusunose, N., Okada, R., Wu, Z., Tozaki-Saitoh, H., Ukai, K., Kohsaka, S., Inoue, K., Ohdo, S.*, et al.* (2013). The intrinsic microglial molecular clock controls synaptic strength via the circadian expression of cathepsin S. Sci Rep *3*, 2744.

Hickman, S., Izzy, S., Sen, P., Morsett, L., and El Khoury, J. (2018). Microglia in neurodegeneration. Nature Neuroscience *21*, 1359-1369.

Kalin, S., Heppner, F.L., Bechmann, I., Prinz, M., Tschop, M.H., and Yi, C.X. (2015). Hypothalamic innate immune reaction in obesity. Nat Rev Endocrinol *11*, 339-351.

Kitchen, G.B., Cunningham, P.S., Poolman, T.M., Iqbal, M., Maidstone, R., Baxter, M., Bagnall, J., Begley, N., Saer, B., Hussell, T.*, et al.* (2020a). The clock gene Bmal1 inhibits macrophage motility, phagocytosis, and impairs defense against pneumonia. Proc Natl Acad Sci U S A.

Kitchen, G.B., Cunningham, P.S., Poolman, T.M., Iqbal, M., Maidstone, R., Baxter, M., Bagnall, J., Begley, N., Saer, B., Hussell, T.*, et al.* (2020b). The clock gene Bmal1 inhibits macrophage motility, phagocytosis, and impairs defense against pneumonia. Proc Natl Acad Sci U S A *117*, 1543-1551.

Ko, C.H., and Takahashi, J.S. (2006). Molecular components of the mammalian circadian clock. Hum Mol Genet *15 Spec No 2*, R271-277.

Lo, B.C., Gold, M.J., Hughes, M.R., Antignano, F., Valdez, Y., Zaph, C., Harder, K.W., and McNagny, K.M. (2016). The orphan nuclear receptor ROR alpha and group 3 innate lymphoid cells drive fibrosis in a mouse model of Crohn's disease. Sci Immunol *1*.

Ma, Q. (2013). Role of nrf2 in oxidative stress and toxicity. Annu Rev Pharmacol Toxicol *53*, 401-426.

McLoughlin, M.R., Orlicky, D.J., Prigge, J.R., Krishna, P., Talago, E.A., Cavigli, I.R., Eriksson, S., Miller, C.G., Kundert, J.A., Sayin, V.I.*, et al.* (2019). TrxR1, Gsr, and oxidative stress determine hepatocellular carcinoma malignancy. Proc Natl Acad Sci U S A *116*, 11408-11417.

Merlini, M., Rafalski, V.A., Rios Coronado, P.E., Gill, T.M., Ellisman, M., Muthukumar, G., Subramanian, K.S., Ryu, J.K., Syme, C.A., Davalos, D.*, et al.* (2019). Fibrinogen Induces Microglia-Mediated Spine Elimination and Cognitive Impairment in an Alzheimer's Disease Model. Neuron.

Miyamoto, A., Wake, H., Ishikawa, A.W., Eto, K., Shibata, K., Murakoshi, H., Koizumi, S., Moorhouse, A.J., Yoshimura, Y., and Nabekura, J. (2016). Microglia contact induces synapse formation in developing somatosensory cortex. Nat Commun *7*, 12540.

Morris, M.J., Beilharz, J.E., Maniam, J., Reichelt, A.C., and Westbrook, R.F. (2015). Why is obesity such a problem in the 21st century? The intersection of palatable food, cues and reward pathways, stress, and cognition. Neurosci Biobehav R *58*, 36-45.

Musiek, E.S., Lim, M.M., Yang, G., Bauer, A.Q., Qi, L., Lee, Y., Roh, J.H., Ortiz-Gonzalez, X., Dearborn, J.T., Culver, J.P.*, et al.* (2013). Circadian clock proteins regulate neuronal redox homeostasis and neurodegeneration. J Clin Invest *123*, 5389-5400.

Nakazato, R., Hotta, S., Yamada, D., Kou, M., Nakamura, S., Takahata, Y., Tei, H., Numano, R., Hida, A., Shimba, S.*, et al.* (2017). The intrinsic microglial clock system regulates interleukin-6 expression. Glia *65*, 198-208.

Narasimamurthy, R., Hatori, M., Nayak, S.K., Liu, F., Panda, S., and Verma, I.M. (2012). Circadian clock protein cryptochrome regulates the expression of proinflammatory cytokines. Proc Natl Acad Sci U S A *109*, 12662-12667.

Nimmerjahn, A., Kirchhoff, F., and Helmchen, F. (2005). Resting microglial cells are highly dynamic surveillants of brain parenchyma in vivo. Science *308*, 1314-1318.

Norden, D.M., and Godbout, J.P. (2013). Review: Microglia of the aged brain: primed to be activated and resistant to regulation. Neuropath Appl Neuro *39*, 19-34.

Nott, A., Holtman, I.R., Coufal, N.G., Schlachetzki, J.C.M., Yu, M., Hu, R., Han, C.Z., Pena, M., Xiao, J.Y., Wu, Y.*, et al.* (2019). Brain cell type-specific enhancer-promoter interactome maps and disease-risk association. Science *366*, 1134-+.

Pannese, E. (2011). Morphological changes in nerve cells during normal aging. Brain Structure & Function *216*, 85-89.

Paolicelli, R.C., Bolasco, G., Pagani, F., Maggi, L., Scianni, M., Panzanelli, P., Giustetto, M., Ferreira, T.A., Guiducci, E., Dumas, L.*, et al.* (2011). Synaptic pruning by microglia is necessary for normal brain development. Science *333*, 1456-1458.

Parkhurst, C.N., Yang, G., Ninan, I., Savas, J.N., Yates, J.R., Lafaille, J.J., Hempstead, B.L., Littman, D.R., and Gan, W.B. (2013). Microglia Promote Learning-Dependent Synapse Formation through Brain-Derived Neurotrophic Factor. Cell *155*, 1596-1609.

Peek, C.B., Levine, D.C., Cedernaes, J., Taguchi, A., Kobayashi, Y., Tsai, S.J., Bonar, N.A., McNulty, M.R., Ramsey, K.M., and Bass, J. (2017). Circadian Clock Interaction with HIF1 alpha Mediates Oxygenic Metabolism and Anaerobic Glycolysis in Skeletal Muscle. Cell Metabolism *25*, 86-92.

Piantadosi, C.A., Withers, C.M., Bartz, R.R., MacGarvey, N.C., Fu, P., Sweeney, T.E., Welty-Wolf, K.E., and Suliman, H.B. (2011). Heme oxygenase-1 couples activation of mitochondrial biogenesis to anti-inflammatory cytokine expression. J Biol Chem *286*, 16374-16385.

Poss, K.D., and Tonegawa, S. (1997). Reduced stress defense in heme oxygenase 1-deficient cells. Proc Natl Acad Sci U S A *94*, 10925-10930.

Rajendran, L., and Paolicelli, R.C. (2018). Microglia-Mediated Synapse Loss in Alzheimer's Disease. Journal of Neuroscience *38*, 2911-2919.

Ren, D.L., Zhang, J.L., Yang, L.Q., Wang, X.B., Wang, Z.Y., Huang, D.F., Tian, C., and Hu, B. (2018). Circadian genes period1b and period2 differentially regulate inflammatory responses in zebrafish. Fish Shellfish Immun *77*, 139-146.

Reppert, S.M., and Weaver, D.R. (2002). Coordination of circadian timing in mammals. Nature *418*, 935-941.

Rojo, A.I., McBean, G., Cindric, M., Egea, J., Lopez, M.G., Rada, P., Zarkovic, N., and Cuadrado, A. (2014). Redox control of microglial function: molecular mechanisms and functional significance. Antioxid Redox Signal *21*, 1766-1801.

Sato, T.K., Panda, S., Miraglia, L.J., Reyes, T.M., Rudic, R.D., McNamara, P., Naik, K.A., Fitzgerald, G.A., Kay, S.A., and Hogenesch, J.B. (2004). A functional genomics strategy reveals rora as a component of the mammalian circadian clock. Neuron *43*, 527-537.

Schiaffino, S., Blaauw, B., and Dyar, K.A. (2016). The functional significance of the skeletal muscle clock: lessons from Bmal1 knockout models. Skelet Muscle *6*, 33.

Sekar, A., Bialas, A.R., de Rivera, H., Davis, A., Hammond, T.R., Kamitaki, N., Tooley, K., Presumey, J., Baum, M., Van Doren, V.*, et al.* (2016). Schizophrenia risk from complex variation of complement component 4. Nature *530*, 177-+.

Subhramanyam, C.S., Wang, C., Hu, Q.D., and Dheen, S.T. (2019). Microglia-mediated neuroinflammation in neurodegenerative diseases. Seminars in Cell & Developmental Biology *94*, 112-120.

Sveinbjornsdottir, S. (2016). The clinical symptoms of Parkinson's disease. J Neurochem *139 Suppl 1*, 318-324.

Tan, Y.L., Yuan, Y., and Tian, L. (2019). Microglial regional heterogeneity and its role in the brain. Mol Psychiatry.

Valdearcos, M., Douglass, J.D., Robblee, M.M., Dorfman, M.D., Stifler, D.R., Bennett, M.L., Gerritse, I., Fasnacht, R., Barres, B.A., Thaler, J.P.*, et al.* (2017). Microglial Inflammatory Signaling Orchestrates the Hypothalamic Immune Response to Dietary Excess and Mediates Obesity Susceptibility. Cell Metab *26*, 185-197 e183.

Wang, C., Yue, H., Hu, Z., Shen, Y., Ma, J., Li, J., Wang, X.D., Wang, L., Sun, B., Shi, P.*, et al.* (2020). Microglia mediate forgetting via complement-dependent synaptic elimination. Science *367*, 688-694.

Wang, L.X., Pavlou, S., Du, X., Bhuckory, M., Xu, H.P., and Chen, M. (2019a). Glucose transporter 1 critically controls microglial activation through facilitating glycolysis. Mol Neurodegener *14*.

Wang, M.Y., Zhang, L., and Gage, F.H. (2019b). Microglia, complement and schizophrenia. Nature Neuroscience *22*, 333-334.

Yang, G., Chen, L., Zhang, J., Ren, B., and FitzGerald, G.A. (2019). Bmal1 deletion in mice facilitates adaptation to disrupted light/dark conditions. JCI Insight *5*.

Yang, L., Chu, Y., Wang, L., Wang, Y., Zhao, X., He, W., Zhang, P., Yang, X., Liu, X., Tian, L.*, et al.* (2015). Overexpression of CRY1 protects against the development of atherosclerosis via the TLR/NF-kappaB pathway. Int Immunopharmacol *28*, 525-530.

Yi, C.X., Walter, M., Gao, Y.Q., Pitra, S., Legutko, B., Kalin, S., Layritz, C., Garcia-Caceres, C., Bielohuby, M., Bidlingmaier, M.*, et al.* (2017). TNF alpha drives mitochondrial stress in POMC neurons in obesity. Nature Communications *8*.

Zhang, E.E., Liu, Y., Dentin, R., Pongsawakul, P.Y., Liu, A.C., Hirota, T., Nusinow, D.A., Sun, X., Landais, S., Kodama, Y.*, et al.* (2010). Cryptochrome mediates circadian regulation of cAMP signaling and hepatic gluconeogenesis. Nat Med *16*, 1152-1156.

Zhang, R., Lahens, N.F., Ballance, H.I., Hughes, M.E., and Hogenesch, J.B. (2014). A circadian gene expression atlas in mammals: implications for biology and medicine. Proc Natl Acad Sci U S A *111*, 16219-16224.

Zhang, Y.X., Fang, B., Damle, M., Guan, D.Y., Li, Z.H., Kim, Y.H., Gannon, M., and Lazar, M.A. (2016). HNF6 and Rev-erb alpha integrate hepatic lipid metabolism by overlapping and distinct transcriptional mechanisms. Gene Dev *30*, 1636-1644.

Zhang, Y.X., Fang, B., Emmett, M.J., Damle, M., Sun, Z., Feng, D., Armour, S.M., Remsberg, J.R., Jager, J., Soccio, R.E.*, et al.* (2015). Discrete functions of nuclear receptor Rev-erb alpha couple metabolism to the clock. Science *348*, 1488-1492.

Summary

Summary

Microglia are the brain's resident macrophages with immune-modulating and phagocytic capabilities. Microglia phagocytose apoptotic cells, cellular debris, unwanted synapses, and pathogens, as well as release inflammatory cytokines and neurotrophic factors to optimize the surrounding microenvironment and shape the neural circuits. Disruption of microglial function results in deficits in cognition and energy balance, which are mainly controlled by the hippocampus and hypothalamus, respectively. Moreover, the microglial immune activity and phagocytic capacity follow a circadian variation. The endogenous circadian clock function plays a crucial role in the control of cellular metabolism that subsequently affects overall physiological functions.

In this thesis we aimed to understand whether the microglial core clock gene *Bmal1* is involved in the control of energy balance and memory formation in mice, and how the *Bmal1* gene affects microglial functions during different situations.

We found that clock genes show rhythmic expression in microglial cells isolated from adult C57BL/6J mice over the 24-h light/dark cycle. To clarify the impact of microglial *Bmal1* in systemic energy homeostasis and learning and memory processes *in vivo*, we generated microglia-specific *Bmal1* knockdown (microglia$^{Bmal1\text{-KD}}$) mice. We observed that *Bmal1* deficiency robustly enhances the microglial phagocytic capacity under HFD conditions and during cognitive processes in these mice. This enhancement was associated with reduced POMC neuronal loss in the hypothalamus when mice are fed a HFD, and was also related to the formation of more mature spines in the hippocampus during the learning process. As a result, mice with microglia lacking *Bmal1* not only exhibit decreased HFD-induced hyperphagia and body weight gain, but also show improved long-term memory consolidation and retention.

We also observed that inflammatory cytokines, nutrient utilization, and the anti-oxidative effect show daily rhythmicity over the 24h light/dark cycle in the microglial cells isolated from adult C57BL/6J mice. To evaluate the effect of *Bmal1* on microglial cellular metabolism and immune response under normal and inflammatory conditions, we used global *Bmal1* knock-out mice and BV-2 cells with a Bmal1 knockdown to study the expression of clock genes, inflammation-related genes, and cellular metabolic-related genes. We observed that *Bmal1* deficiency decreases gene expression of pro-inflammatory cytokines, and increases gene

expression of anti-oxidative and anti-inflammatory factors in microglia. These changes protect the microglial BV-2 cells from LPS and palmitic acid-induced inflammation. Moreover, the lack of *Bmal1* facilitates microglial BV-2 cells to adjust nutrient utilization according to the increased energy demand.

Samenvatting

Microglia zijn de residente macrofagen van de hersenen met immuunmodulerende en fagocytische mogelijkheden. Microglia fagocyteren apoptotische cellen, cellulair afval, ongewenste synapsen en pathogenen, en produceren inflammatoire cytokines en neurotrofe factoren om de condities in de omringende micro-omgeving te optimaliseren en neurale circuits op de juiste manier te vormen. Verstoring van de microgliale functie resulteert in een verslechterde cognitie en verstoorde energiebalans, twee processen die voornamelijk bestuurd worden door respectievelijk de hippocampus en de hypothalamus. Bovendien vertonen de microgliale immuunactiviteit en fagocytische capaciteit een circadiane variatie. De endogene circadiane klokfunctie speelt een cruciale rol bij de controle van het cellulaire metabolisme dat vervolgens het geheel aan fysiologische functies beïnvloedt.

Doel van dit proefschrift was om te onderzoeken of het klokgen *Bmal1* in microglia betrokken is bij de controle van de energiebalans en geheugenvorming bij muizen, en hoe *Bmal1* de microgliale immuun functies in verschillende situaties beïnvloedt.

We ontdekten dat ook klokgenen geïsoleerd uit volwassen C57BL/6J-muizen een ritmische expressie vertonen gedurende de 24-uurs dag/nacht cyclus. Om de *in vivo* impact van microgliale *Bmal1* op de systemische energiehomeostase en leer- en geheugenprocessen te verduidelijken, hebben we microglia-specifieke *Bmal1*-knockdown (microglia$^{Bmal1\text{-KD}}$) muizen gegenereerd. We vonden dat in deze muizen de afwezigheid van *Bmal1* de microgliale fagocytische capaciteit sterk verbeterde onder zowel hoog-vet dieet condities als ook tijdens cognitieve processen. Deze verbetering ging gepaard met minder verlies van POMC-neuronen in de hypothalamus wanneer muizen een hoog-vet dieet kregen, en de vorming van meer volwassen synapsen in de hippocampus tijdens het leerproces. Dientengevolge vertonen muizen met microglia zonder het *Bmal1* gen, niet alleen een verminderde hyperfagie en toename van het lichaamsgewicht door een hoog-vet dieet, maar ook een verbeterde geheugenconsolidatie en retentie op lange termijn.

We hebben ook aangetoond dat inflammatoire cytokines, nutriëntengebruik en het anti-oxidatieve effect een dagelijkse 24-uurs ritmiek vertonen in de microgliale cellen die waren geïsoleerd uit volwassen C57BL/6J-muizen. Om het effect van *Bmal1* op het cellulaire metabolisme en de immuunrespons van microglia te onderzoeken, onder normale en inflammatoire omstandigheden, hebben we gebruik gemaakt van globale *Bmal1* knock-out muizen en BV-2-cellen met een *Bmal1* knockdown om hierin de expressie van klokgenen,

ontstekingsgerelateerde genen en genen betrokken bij het cellulaire metabolisme te bestuderen. We vonden dat *Bmal1*-deficiëntie de genexpressie van pro-inflammatoire cytokines verminderde en de genexpressie van anti-oxidatieve en ontstekingsremmende factoren in microglia verhoogde. Deze veranderingen beschermen de microgliale BV-2-cellen tegen LPS en palmitinezuur veroorzaakte ontstekingen. Bovendien verbeterde het ontbreken van *Bmal1* de mogelijkheid van microgliale BV-2-cellen om het gebruik van voedingsstoffen aan te passen aan de toegenomen energiebehoefte.

Résumé

General framwork (In French)

Cadre général

Le cerveau agit comme centre de contrôle dans tout le corps et régule précisément les fonctions biologiques via des cellules particulières dans la région cérébrale spécifique. Par exemple, les neurones pyramidaux hippocampiques participent à la régulation du processus d'apprentissage et de mémoire et les neurones hypothalamiques anorexigènes proopiomélanocortine (POMC) jouent un rôle clé dans le contrôle de l'homéostasie énergétique. La transmission du signal dans les circuits neuronaux est une caractéristique essentielle du fonctionnement du cerveau. Les axones neuronaux transmettent des signaux à d'autres neurones via des jonctions spécialisées appelées synapses. Le neurone et la synapse sont le fondement structurel des fonctions cérébrales, mais leur formation est affectée par les comportements complexes et les changements dans leur micro-environnement. Par exemple, l'activité d'apprentissage induit une modification synaptique, qui est un mécanisme principal pour la formation de la mémoire (Caroni et al., 2014a; Wu et al., 2015) et les rongeurs et les humains obèses induits par l'alimentation à haute teneur en graisses (HFD) montrent une diminution nombre de neurones POMC (Thaler et al., 2012c). Cependant, les neurones ne sont pas les seules cellules à piloter les fonctions cérébrales et nos connaissances sur le rôle d'autres types de cellules, parmi lesquelles les cellules gliales telles que les astrocytes et la microglie, dans ces réglementations, augmentent rapidement.

Le maintien d'un micro-environnement optimal et de circuits neuronaux repose sur la microglie, les cellules immunitaires innées extrêmement dynamiques et sensibles du cerveau, même à l'état de repos. Par exemple, les microglies étendent et rétractent continuellement leurs processus pour scanner le parenchyme cérébral, interagir avec les épines dendritiques et détecter l'activité neuronale; une activité neuronale accrue déclenchera un mouvement accru des processus microgliaux (Dissing-Olesen et al., 2014; Nimmerjahn et al., 2005). En tant que cellule immunitaire principale dans le cerveau, la microglie non seulement les cellules apoptotiques phagocyteuses, les débris cellulaires, les synapses indésirables et les agents pathogènes, mais elles libèrent également des cytokines inflammatoires (telles que IL-1β, IL-6, TNFa et IL-10) et des facteurs neurotrophiques (tels que BDNF, IGF-1 et TGF-β) pour affecter la population neuronale et les connexions. Ainsi, la microglie fournit des fonctions de

surveillance et de nettoyage pour optimiser le micro-environnement environnant et façonner les circuits neuronaux.

La phagocytose microgliale des synapses joue un rôle actif dans la maturation des synapses (Paolicelli et al., 2011; Schafer et al., 2012) et la perturbation de ce processus entraîne des déficits de connectivité synaptique (Mallya et al., 2019; Schafer et al. , 2013; Schafer et Stevens, 2013). Récemment, des preuves montrent que la microglie joue également un rôle important dans la formation synaptique et la neurogenèse au cours du développement du SNC (Miyamoto et al., 2016; Weinhard et al., 2018). Nous avons signalé que l'activation microgliale est impliquée dans la perte induite par HFD des neurones hypothalamiques anorexigènes POMC (Gao et al., 2017a). La phagocytose microgliale aberrante est associée à l'obésité, ainsi qu'aux maladies neurodégénératives et psychiatriques (Gao et al., 2017a; Zhan et al., 2014). De plus, l'activité microgliale suit une variation circadienne, qui est plus élevée pendant la phase quotidienne active et d'alimentation chez le rat maigre (Yi et al., 2017a). De plus, la réponse immunitaire microgliale au lipopolysaccharide (LPS) dépend du temps (Fonken et al., 2015b). De plus, la microglie phagocytose a plus de synapses au début de la phase claire que le début de la phase sombre, ce qui correspond à l'expression des protéines synaptiques dans le cortex préfrontal (Choudhury et al., 2020).

Dans la première étude présentée dans ce manuscrit de thèse, nous avons étudié l'hypothèse selon laquelle la machinerie horlogère intrinsèque pourrait jouer un rôle important dans la régulation des fonctions microgliales, et enfin affecter la plasticité synaptique de l'hippocampe pendant les processus d'apprentissage et de mémoire et l'homéostasie énergétique contrôlée par l'hypothalamus .

Le système de chronométrage circadien est un système de chronométrage interne, qui joue un rôle crucial dans le contrôle des processus cellulaires, et affecte ensuite les fonctions physiologiques globales (Bass et Takahashi, 2010b; Early et al., 2018b; Gabriel et Zierath, 2019a). Par exemple, une déficience du gène de l'horloge musculaire squelettique perturbe l'utilisation des nutriments et entraîne des troubles métaboliques (Gabriel et Zierath, 2019b; Schiaffino et al., 2016; Stenvers et al., 2019a). Les gènes d'horloge dans les macrophages et les microglies modulent la production de cytokines, suite à un défi immunitaire (Griffin et al., 2019; Nakazato et al., 2017; Sato et al., 2014). Il est connu que l'activité immunitaire dépend fortement des processus métaboliques cellulaires (Geltink et al., 2018; Vijayan et al., 2019; Wang et al., 2019a); une utilisation réduite du glucose ou des lipides inhibe l'activation microgliale et l'inflammation (Gao et al., 2017b; Wang et al., 2019a).

Dans la deuxième étude présentée dans ce manuscrit de thèse, nous avons étudié l'hypothèse selon laquelle l'horloge intrinsèque pourrait réguler la fonction immunitaire microgliale par la modulation du métabolisme cellulaire.

Dans la troisième étude, réalisée dans l'équipe d'Amsterdam, nous avons étudié le rôle du gène d'horloge Rev-erbα dans l'immunométabolisme microglial. La perturbation de la rythmicité circadienne par l'administration de l'agoniste Rev-erbα SR9011, réduit l'expression des cytokines pro-inflammatoires lors d'une provocation immunitaire par le TNFα, tandis qu'elle augmente l'expression de la cytokine anti-inflammatoire Il10. De plus, SR9011 diminue l'activité phagocytaire, la respiration mitochondriale, la production d'ATP et l'expression des gènes métaboliques. Cette étude met en évidence le lien entre l'horloge intrinsèque et l'immunométabolisme de la microglie. Nous montrons que Rev-erbα est impliqué à la fois dans l'homéostasie métabolique et dans les réponses inflammatoires de la microglie.

La quatrième étude, réalisée dans l'équipe d'Amsterdam, étudie l'effet de l'obésité induite par HFD sur la rythmicité quotidienne de l'immunométabolisme microglial chez le rat. Nous avons observé une perturbation de l'heure de la journée dans les fonctions circadiennes et inflammatoires microgliales dans les conditions obésogènes, accompagnée de changements dans l'utilisation du substrat et la production d'énergie. D'autre part, l'évaluation de l'expression du gène des monocytes a montré un effet faible ou absent de l'HFD sur ces cellules myéloïdes périphériques, suggérant une réponse inflammatoire microgliale spécifique aux cellules dans l'obésité induite par l'alimentation. Un régime obésogène affecte l'immunométabolisme microglial de manière dépendante de l'heure. Compte tenu du rôle central du cerveau dans le métabolisme énergétique, une meilleure connaissance des rythmes quotidiens de l'immunométabolisme microglial pourrait conduire à une meilleure compréhension de la pathogenèse de l'obésité.

Enfin, dans la cinquième étude, réalisée dans l'équipe de Strasbourg, nous avons étudié la neuroinflammation, la gliose et les changements épigénétiques dans le cerveau post mortem des patients atteints de la maladie d'Alzheimer. Deux régions cérébrales ont été étudiées: la zone F2 du cortex frontal et l'hippocampe. Dans l'ensemble, ces données fournissent des preuves de dysfonctionnements de l'acétylation au niveau des enzymes (épigénétiques) associées et des histones dans le cerveau de la maladie d'Alzheimer qui peuvent être à l'origine de troubles de la transcription et de troubles cognitifs liés à la maladie d'Alzheimer. Nous signalons en outre des dérégulations plus fortes dans la zone F2 du cortex frontal que dans l'hippocampe à un stade terminal de la maladie, suggérant une vulnérabilité et / ou une efficacité différentielle des mécanismes compensatoires.

General objectives (In French)

Objectifs généraux

Dans cette thèse, tout d'abord, nous nous concentrons sur le gène de l'horloge du noyau microglial-Bmal1, qui est étroitement lié au métabolisme énergétique (Hatanaka et al., 2010; Rudic et al., 2004; Schiaffino et al., 2016; Sussman et al. , 2019), l'homéostasie redox (Early et al., 2018b; Musiek et al., 2013) et les réponses immunitaires (Nakazato et al., 2017). Les souris knockout Bmal1 globales sont arythmiques dans l'obscurité constante et présentent une activité locomotrice réduite dans les cycles lumière / obscurité (Bunger et al., 2000b). La suppression astrocytaire spécifique de Bmal1 entraîne une déficience cognitive et un déséquilibre métabolique chez la souris (Barca-Mayo et al., 2019; Barca-Mayo et al., 2017). Fait intéressant, la perturbation circadienne microgliale liée à l'âge sensibilise la réponse neuroinflammatoire dans l'hippocampe (Fonken et al., 2016). L'horloge microgliale module la production de cytokines, suite à un défi immunitaire (Nakazato et al., 2017). Il a été démontré que la microglie joue un rôle important dans la formation de la mémoire et le métabolisme énergétique et les fonctions microgliales peuvent fortement s'appuyer sur son horloge intrinsèque.

Ainsi, l'objectif principal de cette thèse est de comprendre si et comment la délétion Bmal1 affecte les fonctions microgliales au cours de différentes situations in vivo et in vitro, en examinant notamment les conséquences sur le contrôle de l'équilibre énergétique et la formation de la mémoire.

Premièrement, nous avons vérifié si les gènes d'horloge montrent une expression rythmique dans les cellules microgliales isolées de souris C57BL / 6J adultes à 8 moments dans le cycle clair / sombre de 24 heures en utilisant la RT-PCR quantitative. Pour clarifier l'impact de Bmal1 microglial dans l'homéostasie de l'énergie systémique et les processus d'apprentissage et de mémoire in vivo, nous avons généré des souris knockdown Bmal1 spécifiques à la microglie (microgliaBmal1-KD). L'efficacité de knockdown de Bmal1 et l'effet sur la machinerie d'horloge ont été évalués au niveau du gène. Nous avons émis l'hypothèse que la carence en Bmal1 affectera les fonctions microgliales dans les conditions HFD et pendant les processus cognitifs chez la souris. Cet effet influencera la population neuronale hypothalamique de POMC et la plasticité synaptique hippocampique, qui affectent finalement l'équilibre énergétique et la formation de la mémoire chez la souris.

En utilisant ce modèle animal, nous avons testé le phénotype métabolique (comme le poids corporel, l'apport alimentaire quotidien, l'activité locomotrice, la production de chaleur et le rapport d'échange respiratoire) chez des souris microgliaBmal1-KD et Ctrl nourries avec un régime standard de chow ou HFD chez les mâles et les femelles. Nous avons examiné l'activité immunitaire microgliale (nombre de cellules iba1-ir) et la phagocytose (CD68-ir / iba1-ir, comme indication de la capacité phagocytaire), ainsi que le nombre de cellules neuronales POMC dans l'ARC, la région cérébrale clé qui régule l'homéostasie de l'énergie systémique , chez des souris mâles et femelles nourries au chow ou HFD à deux moments dans les 24 heures (ZT5 et ZT17) chez la souris. Pour identifier si les microglies étaient capables de phagocyter les cellules apoptotiques induites par la consommation de HFD, nous avons analysé les fragments d'ADN dérivés des cellules apoptotiques dans les phagosomes CD68-ir par co-immunocoloration avec DAPI et iba1 dans l'ARC.

En utilisant le même modèle animal, nous avons également évalué la formation et la consolidation de la mémoire dépendante de l'hippocampe chez des souris microgliaBmal1-KD et témoins. Étant donné que le cycle œstral chez les souris femelles interfère inévitablement avec la mémoire de référence spatiale, seuls les mâles ont été évalués dans l'étude cognitive. Les souris ont été soumises à trois tests différents du labyrinthe aquatique de Morris (MWM) (une session de formation de 4 jours pour étudier la mémoire de référence spatiale, une formation de 3 jours pour évaluer les capacités de consolidation de la mémoire à long terme et un test d'inversion pour vérifier la flexibilité cognitive) et un nouveau test de reconnaissance d'objets. Nous avons ensuite évalué le nombre d'épines dendritiques dans les neurones pyramidaux CA1, par coloration de Golgi, au cours du processus de consolidation de la mémoire. Enfin, nous avons analysé l'activité immunitaire microgliale (nombre de cellules iba1-ir) et la phagocytose (CD68-ir / iba1-ir, comme une indication de la capacité phagocytaire) dans les régions hippocampiques CA1 et DG à deux moments dans 24h (ZT5 et ZT17) chez la souris dans les groupes d'apprentissage (MWM) et de home-cage. Étant donné que la microglie phagocytent également les structures présynaptiques pour remodeler la circuité neurale, nous avons vérifié la présence de synaptophysine1 (marqueur présynaptique) à l'intérieur des phagosomes CD68-ir dans la microglie.

Le métabolisme de l'énergie cellulaire et l'homéostasie redox régulent également la fonction microgliale (Early et al., 2018b; Gao et al., 2017b). Ainsi, il existe un lien possible entre l'horloge circadienne-Bmal1, la fonction microgliale, le métabolisme énergétique cellulaire et l'homéostasie redox. Nous avons émis l'hypothèse que la carence en Bmal1 affectera

l'expression des gènes inflammatoires dans la microglie, ce qui pourrait être obtenu en modifiant le métabolisme énergétique cellulaire et l'homéostasie redox.

Pour évaluer l'effet de Bmal1 sur le métabolisme cellulaire microglial et les réponses immunitaires dans des conditions normales et inflammatoires, nous avons d'abord vérifié si les cytokines inflammatoires, l'utilisation des nutriments et l'effet antioxydant montrent une rythmicité quotidienne dans la cellule microgliale isolée de souris C57BL / 6J adultes à 8-points de temps au cours du cycle lumière / obscurité de 24 h en utilisant la RT-PCR quantitative. Pour clarifier davantage l'impact du Bmal1 microglial dans l'immunométabolisme microglial in vivo, nous avons utilisé des souris knock-out Bmal1 globales et étudié l'expression des gènes d'horloge, des gènes liés à l'inflammation et des gènes liés au métabolisme cellulaire dans les cellules microgliales isolées. Ensuite, nous avons évalué l'expression de ces gènes et la capacité phagocytaire dans les cellules microgliales BV-2 sous LPS et inflammation induite par l'acide palmitique.

Rev-erbα, un récepteur nucléaire a des effets profonds sur l'horloge moléculaire, le métabolisme et joue également un rôle important dans la neuroinflammation. SR9011, un agoniste de Rev-erbα perturbe le rythme circadien en modifiant la machinerie de l'horloge intracellulaire. Nous avons émis l'hypothèse que SR9011 avait un impact néfaste sur les fonctions immunométaboliques microgliales. Pour évaluer l'effet de SR9011 sur l'immunométabolisme microglial, nous avons vérifié la réponse immunitaire, l'activité phagocytaire et la fonction des mitochondries sur la microglie primaire qui ont été isolées chez des rat rat Sprague-Dawley âgés de 1 à 3 jours.

La perturbation de l'immunométabolisme est un processus clé impliqué dans la progression de l'obésité. HFD conduit à l'activation microgliale. Cependant, la façon dont l'HFD affecte la rythmicité quotidienne de la fonction circadienne, immunitaire et métabolique microgliale est encore inconnue. Par conséquent, nous avons émis l'hypothèse que HFD perturbe l'immunométabolisme microglial de manière dépendante jour / nuit chez les rats obèses. L'obésité a été induite chez les rats Wistar en les nourrissant HFD ad libitum pendant une durée de 8 semaines. Des microglies ont été isolées à partir d'animaux témoins HFD et nourris à la bouffe à six points dans le temps pendant 24 h [toutes les 4 h à partir de 2 h après allumage]. L'horloge circadienne, les fonctions inflammatoires, l'utilisation du substrat et la production d'énergie ont été évaluées par RT-PCR quantitative.

La microglie joue un rôle important dans la régulation de la plasticité synaptique et sa neuroinflammation induite par l'activation contribue aux troubles de la mémoire dans la

maladie d'Alzheimer. Les acétylations d'histones sont également des acteurs clés dans les processus de mémoire et dans la régulation de l'équilibre neuroprotection / neurodégénérescence. Enfin, nous avons étudié la gliose et les changements épigénétiques dans le cerveau post mortem des patients atteints de la maladie d'Alzheimer. Deux régions cérébrales ont été étudiées: la zone F2 du cortex frontal et l'hippocampe.

General discussion and perspective (In French)

Discussion générale et perspective

Aperçu

Cette thèse porte sur la question de savoir si Bmal1 régule les fonctions microgliales dans différentes situations, et l'effet final de la carence microgliale Bmal1 sur la formation de la mémoire et l'homéostasie énergétique chez la souris. Cette thèse vise également à comprendre l'impact de SR9011, un agoniste de Rev-erbα et HFD sur les fonctions immunométaboliques microgliales. Enfin, nous avons évalué la gliose et les changements épigénétiques dans le cortex frontal et l'hippocampe de cerveaux post-mortem de patients atteints de la maladie d'Alzheimer. Dans la publication 1, nous avons constaté que la carence en Bmal1 améliore de manière robuste la capacité phagocytaire microgliale sous HFD et pendant les processus cognitifs chez la souris. Cette amélioration est associée à une perte neuronale de POMC réduite dans l'hypothalamus lorsque les souris sont nourries avec un HFD, et concerne également la formation de la colonne vertébrale plus mature dans l'hippocampe pendant le processus d'apprentissage. En conséquence, non seulement les souris microgliales dépourvues de Bmal1 présentent une hyperphagie et une prise de poids corporelles induites par l'HFD, mais elles présentent également une consolidation et une rétention améliorées de la mémoire à long terme. Dans la publication 2, nous avons observé que la carence en Bmal1 diminue l'expression des gènes des cytokines pro-inflammatoires, augmente l'expression des gènes des facteurs antioxydants et anti-inflammatoires et augmente la capacité phagocytaire dans la microglie. Ces changements protègent les cellules microgliales BV-2 du LPS et de l'inflammation induite par l'acide palmitique. De plus, le manque de Bmal1 facilite les cellules microgliales BV-2 pour ajuster l'utilisation des nutriments en fonction de l'augmentation de la demande d'énergie. Dans la publication 3, nous avons constaté que la perturbation de la rythmicité circadienne par l'administration de SR9011, réduit l'expression des cytokines pro-inflammatoires lors d'une provocation immunitaire par le TNFα, alors qu'elle augmente l'expression de la cytokine anti-inflammatoire Il10. De plus, SR9011 diminue l'activité phagocytaire, la respiration mitochondriale, la production d'ATP et l'expression des gènes

métaboliques. Dans la publication 4, nous avons observé une perturbation du rythme quotidien des fonctions circadiennes et inflammatoires microgliales dans les conditions obésogènes, accompagnée de changements dans l'utilisation du substrat et la production d'énergie. Un régime obésogène affecte l'immunométabolisme microglial de manière dépendante de l'heure. Enfin, dans la publication 5, nous avons trouvé des dysfonctionnements de la gliose et de l'acétylation dans le cerveau de la MA qui peuvent être à l'origine des troubles cognitifs liés à la MA. Nous signalons en outre des dysrégulations plus fortes dans la zone F2 du cortex frontal que dans l'hippocampe à un stade terminal de la maladie.

1. Le rôle de Bmal1 dans les machines d'horloge microgliale

Bmal1 est un gène d'horloge clé et joue un rôle important dans le mécanisme d'horloge de base qui repose sur des boucles de rétroaction transcriptionnelles / traductionnelles autorégulatrices. Le complexe Bmal1 / Clock favorise l'expression des gènes de Per1, Per2, Cry1, Cry2, Nr1d1 et Dbp. Le complexe Per / Cry régule négativement sa propre transcription en inhibant l'activité du complexe Bmal1 / Clock. Nr1d1 supprime l'expression de Bmal1 (Dudek et Meng, 2014). Cependant, on ne savait pas encore si et comment ces gènes d'horloge suivent un rythme quotidien dans les cellules microgliales et l'effet Bmal1 dans la machinerie d'horloge microgliale.

Dans cette étude, nous avons observé que l'expression des gènes d'horloge-Bmal1, Clock, Per1, Per2, Cry1, Cry2, Nr1d1 et Dbp suit un rythme quotidien dans la microglie isolée des souris C57BL / 6J; l'expression maximale de Bmal1 est pendant la phase légère. Le knock-out de Bmal1 à partir de la microglie, comme les cellules BV-2 microgliales, les souris globales ou la microglie spécifique chez la souris, se traduit par une expression significativement accrue des gènes Bmal1 contrôlés négativement - Cry1, Cry2 et Per2. Les expériences sur les cellules microgliales BV-2 ont également montré que l'expression rythmique de Bmal1 est perturbée dans le groupe knockdown de Bmal1, mais Clock, Cry1, Per1, Per2, Nr1d1 et Dbp montrent toujours une expression rythmique. Ces résultats indiquent que la suppression de Bmal1 perturbe le mécanisme de l'horloge centrale de la microglie, qui est également approuvée chez les astrocytes chez la souris (Barca-Mayo et al., 2017). Ces résultats suggèrent que l'absence de Bmal1 dans la microglie peut entraîner une profonde influence sur le métabolisme et les fonctions microgliales.

2. Le rôle de Bmal1 dans le métabolisme microglial

Notre étude précédente a montré que les microglies sont plus actives pendant la phase sombre lorsque les souris sont plus actives par rapport à la phase claire lorsque les souris se reposent principalement (Yi et al., 2017b). L'activité microgliale dépend fortement du métabolisme cellulaire (Gao et al., 2017b). De plus, l'activation microgliale conduit à la production de plus de métabolites et réactifs espèces d'oxygène (ROS) (Ding et al., 2017; Rojo et al., 2014), qui doivent être éliminées pour maintenir le bon fonctionnement de la microglie (McLoughlin et al., 2019; Piantadosi et al., 2011; Poss et Tonegawa, 1997). Dans la publication 2, nous avons observé que l'utilisation des nutriments et les effets antioxydants dans les cellules microgliales suivent un rythme quotidien chez la souris, qui est augmenté pendant la phase sombre et en ligne avec l'activité microgliale. Bmal1 sert de facteur de transcription et appartient à la famille bHLH. À l'exception de l'autorégulation de la machinerie d'horloge, Bmal1 contrôle 10% à 43% des autres gènes exprimés dans les cellules ou les tissus, via la liaison à des éléments régulateurs spécifiques dans leurs promoteurs (Duffield, 2003; Reppert et Weaver, 2002; Sato et al., 2004; Zhang et al., 2014b). Nous avons constaté que dans des conditions normales, il y a une diminution de l'utilisation des nutriments dans les microglies isolées de souris Bmal1 KO globales. Des souris knock-out spécifiques de muscle Bmal1 montrent également une absorption réduite de glucose dans des conditions physiologiques normales (Schiaffino et al., 2016). Pendant la réponse immunitaire, il y a une forte demande d'énergie dans les cellules immunitaires (Geltink et al., 2018; Wang et al., 2019b). Nous avons également observé une augmentation de l'absorption du glucose après l'administration de LPS, qui était plus importante dans les cellules microgliales BV-2 déficientes en Bmal1. Il pourrait s'agir des gènes d'horloge - les régulateurs transcriptionnels coopèrent avec d'autres facteurs pour contrôler l'expression des gènes métaboliques cibles. Par exemple, Rev-erbα régule les gènes métaboliques en recrutant le co-répresseur de l'histone désacétylase 3 sur des sites spécifiques du foie (Zhang et al., 2015). Bmal1 et Cry1 / 2 régulent la glycolyse anaérobie et la respiration mitochondriale via l'interaction avec le facteur inductible par l'hypoxie 1α dans le muscle squelettique (Peek et al., 2017). Les protéines Cry suppriment également la signalisation en aval du récepteur du glucagon, conduisant ainsi à un effet spécifique du moment du jour sur la gluconéogenèse (Zhang et al., 2010). De même, Nr1d1 interagit avec HNF6 pour réguler le métabolisme lipidique dans le foie de souris adulte (Zhang et al., 2016b). De plus, nous avons constaté que la carence en Bmal1 augmente l'expression des gènes d'antioxydant dans la microglie dans des conditions physiologiques chez la souris et protège les cellules microgliales BV-2 du LPS et du stress oxydatif induit par l'acide palmitique. Pourtant, la suppression neuronale de Bmal1 provoque des dommages oxydatifs et une altération de l'expression du gène de défense redox; Les macrophages déficients en Bmal1

montrent une accumulation accrue de ROS, suggérant que l'effet de Bmal1 sur le stress oxydatif est différent dans différents types de cellules (Early et al., 2018a; Musiek et al., 2013).

Pris ensemble, ces résultats suggèrent que Bmal1 joue un rôle important dans le métabolisme microglial, qui peut avoir une profonde influence sur les fonctions microgliales.

3. Le rôle de Bmal1 dans les fonctions microgliales dans différentes situations

Les microglies sont des cellules immunitaires résidentes très mobiles et assurent une fonction de surveillance et de nettoyage dans le SNC (Davalos et al., 2005). Les principales fonctions de la microglie sont liées à la réponse immunitaire et à la phagocytose, qui jouent un rôle important dans le maintien d'une fonction cérébrale optimale. Lors de la stimulation, la microglie se polarise en un phénotype pro-inflammatoire (M1) ou anti-inflammatoire (M2), conduisant respectivement à des effets neurotoxiques et neuroprotecteurs (Subhramanyam et al., 2019b).

a) Réponse immunitaire

Dans cette étude, nous avons constaté que les gènes de cytokines inflammatoires microgliales montrent une expression plus élevée pendant la phase légère chez des souris de type sauvage dans des conditions physiologiques normales. Cet effet a également été approuvé dans une étude chez le rat (Fonken et al., 2015b). De plus, il a été démontré que les rongeurs traités au LPS présentent un comportement de maladie ou une réponse pro-inflammatoire accrue pendant la phase claire par rapport à la phase sombre (Bellet et al., 2013; Fonken et al., 2015b). Ces résultats suggèrent que les microglies ont une activité immunitaire innée plus élevée pendant la phase légère, ce qui est cohérent avec l'expression microgliale de Bmal1 chez les souris dans des conditions claires / sombres. Ainsi, nous avons évalué l'expression génique de cytokines inflammatoires dans des microglies knockout Bmal1 isolées de souris globales Bmal1 KO, de cellules BV-2 microgliales Bmal1 Knockdown et de souris microgliaBmal1-KD dans des conditions normales. L'absence de Bmal1 diminue l'expression des gènes pro-inflammatoires et augmente l'expression des gènes anti-inflammatoires dans les cellules microgliales, à la fois in vivo et in vitro. Ces changements protègent les cellules microgliales BV-2 des lipopolysaccharides et des inflammations induites par l'acide palmitique.

Il a montré que Bmal1 régule directement la transactivation de Il6 dans la microglie (Nakazato et al., 2017), tandis que dans les macrophages, Bmal1 régule l'inflammation en régulant l'expression des gènes de Nrf2 (Ma, 2013). La suppression de la cellule myéloïde Bmal1 protège contre l'infection bactérienne dans le poumon (Kitchen et al., 2020a). Ces données

suggèrent que Bmal1 régule la système immunitaire inné. De plus, nous avons observé que Cry1, Cry2 et Per2 sont significativement augmentés dans la microglie Bmal1 KO, ce qui peut contribuer à réduire l'inflammation. Il a été observé que la surexpression de Cry1 diminue considérablement l'inflammation chez les souris athérosclérotiques (Yang et al., 2015), tandis que l'absence de Cry1 et Cry2 conduit à une expression accrue des cytokines pro-inflammatoires dans les macrophages (Narasimamurthy et al., 2012). Per2 régule négativement l'expression des cytokines pro-inflammatoires chez le poisson zèbre (Ren et al., 2018). La suppression de Rev-erbα provoque une expression accrue des gènes pro-inflammatoires dans la microglie, tandis que son agoniste pharmacologique inhibe l'inflammation stimulée par le LPS (Gibbs et al., 2012; Griffin et al., 2019). Un autre mécanisme de déclenchement circadien de l'inflammation pourrait être que Bmal1 recrute le récepteur des glucocorticoïdes aux promoteurs des gènes inflammatoires (Gibbs et al., 2014). Nous avons observé une absorption de glucose plus élevée après l'administration de LPS dans les cellules microgliales BV-2 déficientes en Bmal1 que dans les Ctrls, ce qui peut également contribuer à son phénotype anti-inflammatoire. Ces résultats suggèrent que Bmal1 est l'un des principaux régulateurs de l'immunométabolisme microglial. La suppression microgliale de Bmal1 pourrait être une nouvelle stratégie pour traiter l'inflammation dans le cerveau.

b) Capacité phagocytaire

De plus, nous avons constaté que la suppression de Bmal1 augmente la capacité phagocytaire des cellules microgliales BV-2. La microglie joue un rôle important dans le maintien du microenvironnement dans le cerveau par phagocytose. Ainsi, nous avons en outre évalué l'effet du manque de Bmal1 sur la capacité phagocytaire microgliale dans l'hypothalamus après avoir reçu HFD et dans l'hippocampe après avoir appris chez la souris, respectivement. Nous avons constaté que la carence en Bmal1 améliore fortement la capacité phagocytaire microgliale sous HFD et pendant les processus cognitifs chez la souris. Une étude récente a montré une variation circadienne de la phagocytose microgliale chez le rat, avec une phagocytose de plus de synapses au début de la phase claire que le début de la phase sombre (Choudhury et al., 2020). La suppression de Bmal1 augmente également la fonction phagocytaire dans les macrophages (Kitchen et al., 2020b).

La capacité phagocytaire microgliale dépend de l'activité neuronale spécifique et du taux d'attrition neuronale (Ayata et al., 2018a). Lorsque les souris doivent faire face au stress métabolique induit par l'HFD ou à des tâches d'apprentissage, les circuits neuronaux impliqués dans ces défis nécessitent une phagocytose microgliale à la demande (Ayata et al., 2018a). Par conséquent, la suppression du contrôle rigoureux des horloges circadiennes peut avoir un

impact bénéfique sur la fonction microgliale. La suppression de Bmal1 augmente la flexibilité de la microglie et maintient un microenvironnement plus sain dans l'hypothalamus et l'hippocampe pour les neurones voisins. De plus, nous avons remarqué que la carence en Bmal1 réduit l'inflammation microgliale, ce qui avait également été signalé dans l'étude précédente (Nakazato et al., 2017), soutenant que la carence en Bmal1 déplace la microglie vers un état anti-inflammatoire avec une capacité phagocytaire accrue.

La microglie est responsable de l'élimination des cellules apoptotiques et des débris cellulaires, ainsi que de la régulation du remodelage synaptique pour optimiser le microenvironnement pour la survie et le fonctionnement neuronaux (Ayata et al., 2018a; Colonna et Butovsky, 2017; Nimmerjahn et al., 2005; Paolicelli et al., 2011). HFD conduit à une perte neuronale hypothalamique POMC. En explorant davantage la teneur en phagosomes dans la microglie hypothalamique après l'alimentation HFD, nous avons observé plus de phagosomes contenant des fragments d'ADN dans la microglie femelle que chez les mâles. Cette découverte suggère que HFD conduit à plus de perte neuronale chez les souris femelles que chez les mâles. Microglia phagocytose structures présynaptiques pour remodeler la circuité neuronale. En évaluant la teneur en phagosomes dans la microglie hippocampique, nous avons constaté que l'apprentissage augmente la phagocytose des présynapses. Mais la microglie déficiente en Bmal1 phagocytose plus de débris cellulaires que de présynapses au cours des processus d'apprentissage. Tous les résultats suggèrent que la microglie déficiente en Bmal1 phagocytose plus de débris cellulaires que les Ctrls pendant le stress métabolique et les processus de plasticité synaptique.

4. Le rôle du microglial Bmal1 dans le processus d'apprentissage et de mémoire

La microglie engloutit non seulement les présynapses mais aide également à la formation postsynaptique lors du remodelage synaptique (Wang et al., 2020). L'ablation de la microglie réduit la formation synaptique mature (Miyamoto et al., 2016; Parkhurst et al., 2013). Une taille synaptique déficiente entraîne une altération de la connectivité cérébrale fonctionnelle et des déficits de comportement social (Filipello et al., 2018). Ainsi, nous avons évalué la formation et la consolidation de la mémoire dépendante de l'hippocampe chez des souris et des Ctrls microgliaBmal1-KD. Nous avons constaté que les souris microgliaBmal1-KD ont de meilleures performances dans trois tâches MWM différentes (une session de formation de 4 jours pour étudier la mémoire à long terme (24 h), unégère formation de 3 jours pour évaluer la consolidation de la mémoire à long terme (15 jours), et un test d'inversion pour vérifier la flexibilité cognitive (24 h)) et le nouveau test de reconnaissance d'objet. Nous avons observé

que les souris microgliaBmal1-KD ont des épines plus matures dans les neurones pyramidaux CA1 pendant le processus de consolidation de la mémoire. Faire tomber Bmal1 peut faciliter la microglie pour ajuster son état en fonction de la demande, ce qui fournit un microenvironnement plus sain et augmente les performances de la mémoire chez la souris. Il est également connu que les gènes-chats contrôlés par l'horloge microgliale régulent la force synaptique et l'activité locomotrice chez la souris (Hayashi et al., 2013). Une découverte récente chez des souris knockout Bmal1 mondiales a montré que l'activité locomotrice et la sensibilité à l'insuline de ces souris knockout s'adaptent plus facilement à un horaire clair / sombre perturbé (Yang et al., 2019). Cependant, une élimination synaptique accrue pourrait entraîner une altération de la cognition, comme la maladie d'Alzheimer (MA) (Merlini et al., 2019; Rajendran et Paolicelli, 2018) et la schizophrénie (Sekar et al., 2016; Wang et al., 2019c) . Par conséquent, l'établissement d'une capacité phagocytaire microgliale appropriée est crucial pour l'élagage synaptique et la formation de circuits neuronaux matures.

5. Le rôle du Bmal1 microglial dans la régulation métabolique

Les souris microgliales déficientes en Bmal1 ont montré moins de perte neuronale de POMC après avoir nourri un HFD. En conséquence, les souris atteintes de Bmal1 microgliales manquent d'hyperphagie induite par HFD et de gain de poids corporel. Des preuves de plus en plus nombreuses ont montré que l'obésité induite par l'HFD est associée à la gliose hypothalamique et à l'inflammation de la microglie chez l'homme et les rongeurs (Andre et al., 2017; De Souza et al., 2005; Kalin et al., 2015; Valdearcos et al., 2017). Nous avons récemment signalé que dans un environnement hypercalorique, une capacité phagocytaire microgliale optimale est essentielle pour maintenir un microenvironnement sain pour la survie et le fonctionnement neuronaux environnants (Gao et al., 2017a). Lorsque les souris doivent faire face au stress métabolique induit par l'HFD, les circuits neuronaux impliqués dans ces défis nécessitent une phagocytose microgliale à la demande (Ayata et al., 2018a). Par conséquent, la manipulation de la phagocytose microgliale pourrait être un moyen efficace de traiter les maladies métaboliques induites par l'HFD.

6. Le rôle de Rev-erbα dans l'immunométabolisme microglial

Rev-erbα est une horloge circadienne, qui peut affiner l'expression du gène Bmal1 et également réguler les rythmes circadiens, l'homéostasie métabolique et l'inflammation (Delezie et Challet, 2011; Forman et al., 1994; Ko et Takahashi, 2006; Lo et al. ., 2016). Par exemple, la suppression du Rev-erbα entraîne une obésité induite par le régime alimentaire et

altère le métabolisme du glucose et des lipides, ce qui facilite le diabète des souris (Delezie et al., 2012). L'agoniste de Rev-erbα SR9011 a perturbé le rythme circadien, atténué la phagocytose et la réponse pro-inflammatoire de la microglie. SR9011 a également diminué la respiration mitochondriale microgliale et l'expression des gènes métaboliques. Il a été rapporté que la suppression de Rev-erbα entraîne une microgliosie, une augmentation de la phagocytose et une neuroinflammation dans l'hippocampe. Conformément à ces résultats, nous avons activé Rev-erbα et trouvé une diminution de la réponse pro-inflammatoire et de la phagocytose. De plus, SR9011 a stimulé l'expression de la cytokine anti-inflammatoire Il10. On sait que Rev-erbα régule l'homéostasie métabolique dans les cellules cancéreuses. L'étude actuelle montre que Rev-erbα contrôle le métabolisme cellulaire dans la microglie avec une diminution de la respiration mitochondriale et de la production d'ATP, ainsi que la diminution de l'expression des enzymes limitant le débit telles que Cpt1, Pdk1 et Hk2 en réponse à SR9011. Notre étude a montré comment la machinerie d'horloge associée à Rev-erbα interagit avec l'immunométabolisme dans la microglie. La baisse du métabolisme énergétique peut être un phénomène consécutif causé par une demande d'énergie moindre en raison de la réponse pro-inflammatoire atténuée ou d'un effet direct de Rev-erbα sur le métabolisme cellulaire.

7. L'effet de l'obésité induite par l'alimentation sur l'immunométabolisme microglial

Dans des conditions physiologiques, les cellules microgliales exercent leur fonction de manière stricte au cours de la journée avec une activité plus élevée pendant la phase sombre et active, par rapport à la phase légère de sommeil chez les rongeurs. Mais, ce rythme quotidien est aboli chez les animaux nourris avec un HFD, suggérant une interaction du contenu de l'alimentation et des rythmes quotidiens dans la microglie. Des preuves récentes ont montré l'implication de la fonction circadienne dans la progression de l'obésité. Nous avons constaté que le rythme quotidien de l'expression des gènes immunitaires microgliaux était perturbé chez les rats obèses induits par HFD. La microglie a répondu aux conditions obésogènes par un changement d'utilisation du substrat avec une diminution du métabolisme du glutamate et du glucose pendant la période active des animaux, et une augmentation globale du métabolisme lipidique, comme indiqué par l'évaluation de l'expression des gènes. La voie du glutamate est impliquée dans la fonction immunitaire des macrophages, par exemple, la disponibilité de la glutamine modulait la capacité phagocytaire des macrophages, tandis que l'α-cétoglutarate, généré par la glutaminolyse, est crucial pour obtenir un phénotype anti-inflammatoire dans les macrophages. Bien qu'une augmentation de la détection et de la synthèse des acides gras au début de la période de lumière dans des conditions obésogènes, suggère une utilisation

accrue des lipides dans la microglie pendant la phase de sommeil chez les rats obèses. Il a été démontré que le traitement aux acides gras des cellules BV2 est un puissant inducteur de la production de cytokines via la signalisation TLR4, conduisant ainsi à une inflammation de bas grade même en l'absence de provocation immunitaire. Cette augmentation du métabolisme lipidique pourrait être une explication de l'activation constante de la microglie hypothalamique sous HFD. De plus, l'activation des cellules immunitaires nécessite une production d'énergie plus élevée. Les résultats de la bioénergétique et de la dynamique des mitochondries suggèrent une augmentation de la production d'énergie dans la microglie pendant la période d'inactivité sur HFD, suggérant une augmentation de la production d'ATP, qui pourrait s'expliquer par l'augmentation de la demande du métabolisme lipidique.

8. Le rôle de la neuroinflammation et de la dérégulation de l'acétylation des histones dans la maladie d'Alzheimer

Les microglies sont les macrophages résidents du cerveau dotés de capacités immunomodulatrices et phagocytaires. Les cartes d'interactome activateur-promoteur spécifiques au type de cellule cérébrale révèlent un réseau de gènes microgliaux étendu dans la maladie d'Alzheimer (Nott et al., 2019). La microglie joue un rôle important dans la régulation de la plasticité synaptique et sa neuroinflammation induite par activation contribue aux troubles de la mémoire dans la maladie d'Alzheimer. L'activation microgliale suit le dépôt d'Aβ mais précède la pathologie tau et le déclin cognitif (Felsky et al., 2019). De plus, les acétylations d'histones sont des acteurs clés dans les processus de mémoire et dans la régulation de l'équilibre neuroprotection / neurodégénérescence. Les enzymes épigénétiques-histone acétyltransférases (THA), telles que la protéine de liaison au CREB (CBP), le facteur P300 et p300 / CBP, ainsi que les histone désacétylases (HDAC), telles que HDAC1 et HDAC2, sont également associées aux mécanismes de mémoire à long terme. Nous avons trouvé la gliose et réduit le CBP et le HDAC1 dans le cortex frontal et l'hippocampe dans le cerveau post-mortem de patients atteints de la maladie d'Alzheimer. Le CBP est un régulateur d'horloge circadien via la formation du complexe avec Clock (Gustafson et Partch, 2015), ainsi une perte sévère de CBP pourrait également contribuer aux perturbations du rythme circadien observées chez les patients atteints de MA (Leng et al., 2019). Notamment, la dégradation du CBP médiée par Aβ chez les souris AD a été montrée dans le contexte de la perturbation du rythme circadien. Les niveaux d'histones totales et acétylées sont dérégulés dans le cortex frontal du patient atteint de la maladie d'Alzheimer. Nous soulignons en outre que le cortex frontal semblait plus vulnérable car il était plus sévèrement altéré que l'hippocampe à un stade terminal de la maladie, suggérant une vulnérabilité et / ou une efficacité différentielle

des mécanismes compensatoires. Ces changements spectaculaires observés dans le cortex frontal sont probablement associés à la perte sévère de plasticité neuronale et de fonctions synaptiques.

Points de vue

1. Validation supplémentaire de Bmal1 pour les fonctions microgliales

Nos données montrent que Bmal1 a une influence profonde sur la réponse immunitaire microgliale et la phagocytose. La carence en Bmal1 conduit à une expression réduite des gènes pro-inflammatoires, à une expression accrue des gènes anti-inflammatoires et à une amélioration de la capacité phagocytaire de la microglie dans les expériences in vivo et in vitro. Ces effets protègent finalement les souris contre l'obésité induite par HFD et augmentent les performances de la mémoire. Cependant, on ne sait toujours pas comment le Bmal1 régule la réponse immunitaire microgliale chez la souris. L'analyse de séquençage des puces est nécessaire pour identifier l'ADN qui interagit avec Bmal1 dans la microglie sous inflammation, comme les souris traitées au LPS. Nous devons également effectuer un séquençage d'ARN pour définir le mécanisme entre l'absence de Bmal1 et la phagocytose de microglies isolées de régions cérébrales spécifiques. Par exemple, nous aurons isolé des microglies de l'hippocampe avec ou sans souris Ctrl entraînées par MWM et des souris microgliaBmal1-KD à un moment précis (4 groupes au total). Nous pouvons également avoir des microglies isolées de l'hypothalamus avec ou sans souris Ctrl nourries par HFD et microgliaBmal1-KD à un moment précis chez les mâles et les femelles (8 groupes au total).

De plus, le knockdown de Bmal1 affecte également le métabolisme cellulaire lié aux fonctions microgliales. Les autres expériences in vitro en mesurant les niveaux de cytokines inflammatoires en combinaison avec l'utilisation du carburant mitochondrial dans la microglie déficiente en Bmal1 doivent être effectuées.

2. Détermination supplémentaire du mécanisme entre la microglie et la diaphonie neuronale dans le modèle de souris traité avec microgliaBmal1-KD et SR9011

Ici, nous montrons que la carence en Bmal1 améliore la capacité phagocytaire microgliale, qui peut être associée à une perte neuronale réduite dans l'hypothalamus lorsque les souris reçoivent un HFD, et concerne également la formation de la colonne vertébrale plus mature dans l'hippocampe pendant le processus d'apprentissage chez la souris microgliaBmal1-KD. La carence microgliale Bmal1 protège les souris de l'obésité induite par HFD et augmente les

performances de la mémoire. De plus, SR9011 a atténué la phagocytose et la réponse pro-inflammatoire de la microglie. Cependant, le mécanisme entre la microglie déficiente en Bmal1 et la formation de la colonne vertébrale postsynaptique mature est encore inconnu. Il n'est pas clair si et comment le SR9011 peut affecter les circuits neuronaux. Nous pouvons isoler des neurones de l'hippocampe CA1 pour effectuer un séquençage d'ARN ou extraire des protéines synaptiques (Aono et al., 2017) pour analyser les molécules intéressées dans les deux modèles animaux.

Étant donné que les fonctions microgliales affectent la survie et le fonctionnement neuronaux environnants, le nombre de cellules neuronales ou des unités spécifiques (telles que la pré- ou post-synapse) peuvent être déterminés dans les différentes régions du cerveau (Tan et al., 2019). Par exemple, la densité de la colonne vertébrale dans les neurones épineux moyens striataux peut être vérifiée, ce qui est impliqué dans la régulation de l'activité motrice, de l'humeur et de la récompense (Ayata et al., 2018a). En outre, le phénotype spécifique doit être évalué en fonction des changements de morphologie neuronale dans une région cérébrale spécifique chez les souris microgliales Bmal1 knockout.

3. Examen plus approfondi des performances cognitives dans les modèles de souris traités avec microgliaBmal1-KD et SR9011 dans différentes conditions

La microglie est impliquée dans la neuroinflammation, la neurodégénérescence, la neuropsychiatrie et l'obésité induite par l'alimentation. Des études ont montré que la consommation à long terme de régimes riches en graisses et en sucre altère l'hippocampe et la cognition cortex-dépendante environnante chez les rongeurs et les humains, qui peuvent être médiateurs par le stress oxydatif, la neuroinflammation, ainsi que par une diminution des niveaux de facteurs neurotrophiques (Morris et al., 2015). L'âge et les maladies neurodégénératives liées à l'âge entraînent une neuroinflammation et des changements structurels neuronaux, tels que la perte d'épines dendritiques, une diminution du nombre d'axones, une augmentation des axones avec démyélinisation segmentaire et une perte importante de synapses et de neurones (Hickman et al., 2018b; Norden et Godbout, 2013; Pannese, 2011; Sveinbjornsdottir, 2016). Ainsi, les travaux futurs pourraient évaluer le knockout Bmal1 et la fonction microgliale traitée par SR9011 et la cognition chez la souris dans différentes conditions, telles que les défis liés à l'HFD, l'inflammation systémique, le vieillissement et les maladies neurodégénératives liées au vieillissement - maladie d'Alzheimer (MA), maladie de Parkinson (PD), et la sclérose en plaques (SEP).

Summary (In French)

Résumé

Les microglies sont les macrophages résidents du cerveau dotés de capacités immunomodulatrices et phagocytaires. Les microglis phagocytosent les cellules apoptotiques, les débris cellulaires, les synapses indésirables et les agents pathogènes, et libèrent des cytokines inflammatoires et des facteurs neurotrophiques pour optimiser le microenvironnement environnant et façonner les circuits neuronaux. La perturbation de la fonction microgliale entraîne des déficits de la cognition et de l'équilibre énergétique qui sont principalement contrôlés par l'hippocampe et l'hypothalamus, respectivement. De plus, l'activité immunitaire microgliale et la capacité phagocytaire suivent une variation circadienne. La fonction d'horloge circadienne endogène joue un rôle crucial dans le contrôle du métabolisme cellulaire qui affecte par la suite les fonctions physiologiques globales.

Cette thèse vise à comprendre si l'horloge interne de la microglie dépendante de Bmal1 est impliquée dans le contrôle de l'équilibre énergétique et la formation de la mémoire chez la souris, et comment la dérégulation de cette horloge par la délétion spécifique de Bmal1 dans la microglie affecte les fonctions microgliales dans différentes situations.

Nous avons constaté que les gènes d'horloge montrent une expression rythmique dans la cellule microgliale isolée de souris C57BL/6J adultes en 24 h. Pour clarifier l'impact du facteur Bmal1 microglial dans l'homéostasie de l'énergie systémique et les processus d'apprentissage et de mémoire *in vivo*, nous avons généré des souris knockdown Bmal1 spécifiquement dans la microglie (microglia$^{Bmal1\text{-KD}}$). Nous avons observé que la carence en Bmal1 améliore considérablement la capacité phagocytaire microgliale dans des conditions HFD et pendant les processus cognitifs chez la souris. Cette amélioration est associée à une perte réduite des neurones POMC dans l'hypothalamus lorsque les souris sont nourries avec un HFD, et favorise également la formation d'épines dendritiques plus mature dans l'hippocampe pendant le processus d'apprentissage. En conséquence, non seulement les souris dont les microglies sont dépourvues de Bmal1 présentent une moindre hyperphagie et un moindre gain de poids corporel lorsqu'elles sotn soumises à des conditions HFD, mais elles présentent également une consolidation et une rétention améliorées de la mémoire à long terme, comparé aux souris WT.

Nous avons également observé que les cytokines inflammatoires, l'utilisation des nutriments et l'effet antioxydant montrent une rythmicité quotidienne dans la cellule microgliale isolée de souris C57BL/6J adultes en 24 h. Pour évaluer l'effet de Bmal1 sur le métabolisme cellulaire microglial et la réponse immunitaire dans des conditions normales et inflammatoires, nous avons utilisé des souris knock-out Bmal1 globales et des cellules BV-2 knockdown Bmal1 pour

étudier l'expression des gènes de l'horloge, des gènes liés à l'inflammation et des gènes du métabolisme cellulaire. Nous avons observé que la perte de Bmal1 microgliale diminue l'expression des gènes des cytokines pro-inflammatoires et augmente l'expression des gènes des facteurs antioxydants et anti-inflammatoires dans la microglie. Ces changements protègent les cellules microgliales BV-2 du LPS et de l'inflammation induite par l'acide palmitique. De plus, le manque de Bmal1 facilite l'ajustement des cellules microgliales BV-2 pour l'utilisation des nutriments en fonction de l'augmentation de la demande d'énergie.

PhD Portfolio

Xiaolan Wang

PhD period: October 2016 – May 2021

Publications

1. **Xiao-Lan Wang**, Sander Kooijman, Yuanqing Gao, Laura Tzeplaeff, Brigitte Cosquer, Irina Milanova, Samantha E.C. Wolff, Nikita Korpel, Marie-France Champy, Benoit Petit-Demoulière, Isabelle Goncalves Da Cruz, Tania Sorg-Guss, Patrick C.N. Rensen, Jean-Christophe Cassel, Andries Kalsbeek, Anne-Laurence Boutillier, Chun-Xia Yi. Microglia-specific knock-down of Bmal1 improves memory and protects mice from high fat diet-induced obesity. Accepted by *Molecular Psychiatry*.
2. **Xiao-Lan Wang**, Samantha E.C. Wolff, Nikita Korpel, Irina Milanova, Patrick C.N. Rensen, Sander Kooijman, Jean-Christophe Cassel, Andries Kalsbeek, Anne-Laurence Boutillier, Chun-Xia Yi. Deficiency of the circadian clock gene Bmal1 reduces microglial immunometabolism. *Front. Immunol*. 11:586399. doi: 10.3389/fimmu.2020.586399. 08 Dec 2020.
3. Samantha E.C. Wolff, **Xiao-Lan Wang**, Han Jiao, Jia Sun, Andries Kalsbeek, Chun-Xia Yi, Yuanqing Gao. The effect of Rev-erbα agonist SR9011 on microglial immunometabolism. *Front. Immunol*. 11:550145. doi: 10.3389/fimmu.2020.550145. 25 Sep 2020.
4. Milanova IV, Kalsbeek MJT, **Wang XL**, Korpel NL, Stenvers DJ, Wolff SEC, de Goede P, Heijboer AC, Fliers E, la Fleur SE, Kalsbeek A, Yi CX. Diet-Induced Obesity Disturbs Microglial Immunometabolism in a Time-of-Day Manner. *Front Endocrinol*. 10:424. doi: 10.3389/fendo.2019.00424. 26 Jun 2019.
5. Schueller E, Paiva I, Blanc F, **Wang XL**, Cassel JC, Boutillier AL, Bousiges O. Dysregulation of histone acetylation pathways in hippocampus and frontal cortex of Alzheimer's disease patients. *Eur Neuropsychopharmacol*. doi: 10.1016/j.euroneuro.2020.01.015. 11 Feb 2020.

PhD training

Courses

Electrophysiology School of Strasbourg (Feb 6th-11th, 2017)
Animal courses (2017, Strasbourg, France)
Basic and clinical aspects of neurobiology of rhythms Summer School (Aug 30th- Sep 1st, 2017)
Animal courses (April 9th -20th, 2018, the Netherlands)

Oral presentation

1. NeuroTime Meeting, April 10th &11th, 2017, Amsterdam
Oral presentation title: Cleanup at the right time: a common mechanism underlies the molecular clock of microglia and neuronal activity in metabolic and memory control
Authors: **Xiao-Lan Wang**, B. Cosquer, CX. Yi, AL. Boutillier

2. AG&M PhD-students Retreat, April 5th &6th, 2018, Garderen, the Netherlands
Oral presentation title: Cleanup at the right time: a common mechanism underlies the molecular clock of microglia and neuronal activity in metabolic and memory control
Authors: **Xiao-Lan Wang**, L. Tzeplaeff, B. Cosquer, CX. Yi, AL. Boutillier

3. Dutch Neuroscience Meeting, June 7th &8th, 2018, Lunteren, the Netherlands
Oral presentation title: The molecular clock of microglia and the hypothalamic neuronal activity in metabolic control
Authors: **Xiao-Lan Wang**, L. Tzeplaeff, B. Cosquer, I. Milanova, N. Korpel, CX. Yi, AL. Boutillier

4. AG&M PhD-students Retreat, April 4th &5th, 2019, Garderen, the Netherlands
Oral presentation title: Cleanup at the right time: metabolic control by the molecular clock of microglia
Authors: **Xiao-Lan Wang**, S. Kooijman, L. Tzeplaeff, B. Cosquer, I. Milanova, N. Korpel, MF.Champy, BP. Demoulière, GC. Isabelle, TS. Guss, JC. Cassel, A. Kalsbeek, AL. Boutillier*, CX. Yi*

Conferences/Seminars/Workshops

- European Biological Rhythms Society XV Congress, July 30th -August 3rd, 2017, Academic Medical Center, Amsterdam
- Lab Tour on sleep, September 6th & 7th, 2017, Basel-Freiburg-Strasbourg
- The arcuate nucleus: sensor of time and metabolism, May 31st & June 1st, 2018, Strasbourg
- LNCA research meeting (weekly), 2016-2017, Strasbourg
- INCI seminars (1-2/month), 2016-2017, Strasbourg
- AG&M obesity symposium, 2018, Amsterdam
- The Netherlands Institute for Neuroscience seminars (weekly), 2018-2019, Amsterdam
- AG&M Target lecture (monthly), 2018-2019, Amsterdam UMC, Amsterdam
- Endocrinology research meeting (weekly), 2018-2019, Amsterdam

Université de Strasbourg

Xiao-Lan Wang

Cleanup at the right time: a common mechanism underlies the molecular clock of microglia and neuronal activity in metabolic and memory control

Résumé

Les microglies sont les macrophages résidents du cerveau dotées de capacités immunomodulatrices et phagocytaires. EIles optimisent le microenvironnement et façonnent les circuits neuronaux. La perturbation de la fonction microgliale entraîne des déficits de cognition et d'équilibre énergétique. De plus, la fonction microgliale est contrôlée par un rythme circadien intrinsèque. Cette thèse vise à comprendre si la perte du facteur de contrôle de l'horloge-Bmal1 affecterait les fonctions microgliales. Nous avons constaté que la microglie déficiente en Bmal1 présentait une meilleure capacité phagocytaire dans l'hypothalamus après avoir reçu HFD et dans l'hippocampe après avoir appris une tâche de mémoire spatiale. Les souris knock-out Bmal1 spécifiques microgliales ont été protégées contre l'obésité induite par HFD et ont présenté une performance de mémoire accrue. De plus, la carence en Bmal1 diminue l'expression des gènes des cytokines pro-inflammatoires et augmente l'expression des gènes des facteurs antioxydants et anti-inflammatoires dans la microglie. Nos données suggèrent que l'horloge moléculaire dans les cellules microgliales pourrait être une nouvelle cible pour traiter les troubles métaboliques et cognitifs et les maladies neuro-inflammatoires.

Mots-clés: apprentissage et mémoire, homéostasie énergétique, microglie, horloge circadienne

Summary

Microglia are the brain's resident macrophages with immune-modulating and phagocytic capabilities. They optimize the surrounding microenvironment and shape the neural circuits. Disruption of microglial function results in deficits in cognition and energy balance. Moreover, the microglial function is controlled by an intrinsic circadian rhythm. This thesis aimed to understand whether lacking the core clock gene *Bmal1* would affect microglial functions. We found that *Bmal1* deficient microglia showed better phagocytic capacity in the hypothalamus after receiving HFD and in the hippocampus after learning. Microglial specific *Bmal1* knockout mice were protected from HFD-induced obesity and presented increased memory performance. Moreover, *Bmal1* deficiency decreased gene expression of pro-inflammatory cytokines and increased gene expression of anti-oxidative and anti-inflammatory factors in microglia. Our data suggest that the molecular clock in microglial cells could be a new target to treat metabolic and cognitive disorders, as well as neuron-inflammatory diseases.

Keywords: learning and memory, energy homeostasis, microglia, circadian clock

Acknowledgements

The work presented in this thesis would have not been accomplished without the support and help from many people around me. I would like to thank everyone who assisted me these past almost five years.

First and foremost, I would like to sincerely thank my supervisors, Dr. Anne-Laurence Boutillier, Dr. Chun-Xia Yi, and Dr. Andries Kalsbeek for giving me the opportunity to be part of this exciting work, for the guidance, support, encouragements, thoughtful care in this work, and also understanding and help in personal aspects. Your passion and dedication to science made a strong impression on me and I have always carried positive memories with me. I have learned a lot from working and discussing with you. Without your assistance and dedicated involvement throughout the process, this thesis would have never been accomplished.

I would like to show gratitude to the committee members of my thesis, Dr. David Blum, Dr. Aniko Korosi, Dr. Luc Dupuis, Dr. Chantal Mathis, and Dr. Suzanne La Fleur, for taking the time to read and evaluate my thesis.

Thank Dr. Paul Pevet and Dr. Domitille Boudard for creating the Neurotime program and provide a great platform for us to have so many different experiences. I appreciate your administrative support and efforts.

Thanks to all the lab members in Luc Dupuis's lab for all the support while working there, especially Gina and Sylvie.

Thanks to Sylvie Raison who is my thesis monitoring committee member, for all your suggestions. Thanks to Cristina Gabriela Sandu and Marie-Paule Felder-Schmittbuhl for all the help while working in INCI.

Thanks to all the members of LNCA for accepting, helping, support, and tolerate me. You made my work and life more interesting!

Dr. Jean-Christophe Cassel, the director of LNCA, thank you for your kindness and help in all scientific and administrative issues.

Laura Tzeplaeff, thank you for working together with me in the middle of the night so many times. It's an unforgettable experience! Thank you for all the help, support, scientific discussing, and non-scientific talks. I had a lot of fun together with you.

Brigitte Cosquer, thank you for helping and support me with so many different experiments! Merci beaucoup!

Thanks to my office neighbors Isabel Paiva, Iris Grgurina, and Olivier Bousiges for being so friendly to talk,

discuss, and help me in so many different ways.

Thanks to Catherine Krieger for your kindly administrative help.

Thanks to Rafael Alcala-Vida, Ali Awada, Aminé Isik, and former PhD students Estelle Schuler, Caroine Lotz Tavernier, Marie-Muguet Klein, and Amélie Gressier for all the help and friendly support.

Thanks also to Anne Pereira de Vasconcelos, Karine Mérienne, Karine Herbeaux-Geiger, Olivier Bildstein, Romain Bourdy, Sylvie Bulot, Katia Befort, Celine Heraud, Laura Durieux, Christopher Borcuk, Emanuela Rizzello, Gaelle Awad, and Caroline Correia, for being so nice and kind to me and sharing your knowledge with me. Talking to you is always a pleasure.

Thanks to all the members of the Endocrinology Department at the AUMC for accepting and help me whenever I needed it.

Thanks to Eric, Anita, Unga, Khalid, Olga, Leslie, and Nikita for all the administrative and technical support.

Thanks to Yuanqing Gao, Nikita Korpel, Irina Milanova, Martin Kalsbeek, Shanshan Guo, Clarissa Maya Monteiro, Samantha E.C. Wolff, for all the help and support.

Thanks to Paul de Goede, Fernando Cazarez Marquez, Anayanci Masis Vargas, Lamis Saad, Yalan Hu and for all the suggestions and help.

I am also deeply grateful to all the members and friends of the NIN for all the help, nice talks, and fun together. Thanks to Lin Zhang, Yuting Hu, Yi Qin, Dick Swaab, Bart Fisser, Dorien.

Special thanks to Joop van Heerikhuize who kindly taught me how to use the confocal microscopes and showed great technical support. Thank you also for the funny talks.

Thanks as well to Patrick C.N. Rensen and Sander Kooijman who are from Leiden University for their support and useful comments.

Thanks to my friends Haoyi Liu, Muzeyyen Ugur, Linxi Bai, Jiaming Xiu, Jiae Kim, and Jiaohao Ye, for all your happy talks, suggestions, support, and fun times we spent together. You made my daily life more interesting!

Finally, I must express my very profound gratitude to my parents and my husband Lianjian Li for their unfailing support, continuous encouragement, and most importantly your love, patience, and understanding throughout this journey. This accomplishment would not have been possible without you. Thank you for everything! Thanks for the love of my sister. Thanks to the memory of my grandparents, whose love and insight always inspire me. I have tried to live up to your expectations. Thanks to all members of my family for your support!